AN ACTIVE LOWER-EXTREMITY EXOSKELETON FOR SYNCHRONOUS MOBILITY ASSISTANCE IN LIFTING AND CARRYING MANUAL HANDLING TASK

SADO FATAI

FACULTY OF ENGINEERING
UNIVERSITY OF MALAYA
KUALA LUMPUR

2019

AN ACTIVE LOWER-EXTREMITY EXOSKELETON FOR SYNCHRONOUS MOBILITY ASSISTANCE IN LIFTING AND CARRYING MANUAL HANDLING TASK

SADO FATAI

THESIS SUBMITTED IN FULFILMENT OF THE REQUIREMENTS FOR THE DEGREE OF DOCTOR OF PHILOSOPHY

FACULTY OF ENGINEERING
UNIVERSITY OF MALAYA
KUALA LUMPUR

2019

UNIVERSITY OF MALAYA

ORIGINAL LITERARY WORK DECLARATION

Name of Candidate: SADO FATAI

Matric No: KHA150059

Name of Degree: DOCTOR OF PHILOSOPHY

Title of Project Paper/Research Report/Dissertation/Thesis ("this Work"):

AN ACTIVE LOWER-EXTREMITY EXOSKELETON FOR SYNCHRONOUS MOBILITY ASSISTANCE IN LIFTING AND CARRYING MANUAL HANDLING TASK

Field of Study:

AUTOMATION, CONTROL & ROBOTICS

I do solemnly and sincerely declare that:

(1) I am the sole author/writer of this Work;
(2) This Work is original;
(3) Any use of any work in which copyright exists was done by way of fair dealing and for permitted purposes and any excerpt or extract from, or reference to or reproduction of any copyright work has been disclosed expressly and sufficiently and the title of the Work and its authorship have been acknowledged in this Work;
(4) I do not have any actual knowledge nor do I ought reasonably to know that the making of this work constitutes an infringement of any copyright work;
(5) I hereby assign all and every rights in the copyright to this Work to the University of Malaya ("UM"), who henceforth shall be owner of the copyright in this Work and that any reproduction or use in any form or by any means whatsoever is prohibited without the written consent of UM having been first had and obtained;
(6) I am fully aware that if in the course of making this Work I have infringed any copyright whether intentionally or otherwise, I may be subject to legal action or any other action as may be determined by UM.

Candidate's Signature Date:

Subscribed and solemnly declared before,

Witness's Signature Date:

Name:

Designation:

ABSTRACT

Lifting and carrying manual handling (MH) works are among the leading causes of occupational injuries worldwide. These works involve frequent postural and dynamic movements like repetitive squatting, lowering, and walking (under load) which are risk factors for the pathogenesis and progression of several cumulative trauma or repetitive motion/strain disorders of the lower extremities and lumbar spine such as knee/hip osteoarthritis, meniscal knee damage, and low back pain. These disorders are degenerative, affect workers productivity, and can lead to lifelong immobility for affected workers. Currently, therapies to address this problem have not been sufficient. Active exoskeletons for human performance augmentation (EHPA) are promising alternative intervention which have potentials to augment workers efficiency and capacity to overcome the causal biomechanical risk factors (e.g. fatigue, weak muscle, etc.) of injuries in lifting/carrying works. However, several stumbling blocks pertaining to design and control technologies currently limit a practical adoption. One prominent challenge has to do with how to effectively control the EHPA to achieve synchronous smooth movement assistance/augmentation for its pilot to have adequate assistive benefit, given diversity in movement biomechanics (i.e. squatting/walking) and movement transitions (i.e. squatting-to-standing-to-walking, etc.) in actual lifting/carrying work situation. In this study, a new 12-DOF lower extremity EHPA called UMExoLEA (Universiti Malaya Exoskeleton for Lower Extremity Augmentation) with 4-active bi-directional brushless DC motor actuation and a novel synchronous mobility control algorithm are developed to provide smooth lower-extremity mobility augmentation in lifting/carrying MH works. The control system can assist wearers' movement by a new synergy of three controller algorithms: a dual unscented Kalman filter (DUKF) for trajectory estimation and model update, an impedance controller for generation of assistive torque, and a new supervisory control algorithm for pilot movement detection and synchronization with the exoskeleton.

Experiments are conducted on 15 participants recruited to perform two industrial MH tasks: a mimicked repetitive lifting of 9.5kg box of loads and repetitive lifting and carrying of the same load in two different modes: with and without exoskeleton assistance. EMG signals taken at three muscles: Vastus Medialis, Rectus Femoris, and Gastrocnemius of the right leg, as well as feedback questionnaires and kinetic/kinematic data were used to evaluate the performance of the exoskeleton. Overall, participants muscular effort and maximum exerted force were reduced from 30% to 60% in both tasks. Participants' perceived assistance from UMExoLEA was 73.1% (mean score) which also corresponds to their perceived effort reduction. The mean rating of subjective fatigue (on the lower extremity and low back) was significantly higher between 13.6% (**SD**: 15.0%) to 20.4% (**SD**: 17.8%) without exoskeleton assistance, whereas with assistance, participants' rating was virtually zero. Furthermore, movement detection and synchronization received more than 99% success rate in all the repetitive motion tasks.

Keywords: Lifting and carrying, manual handling, repetitive motion/strain disorders, EHPA, dual unscented Kalman filter

ABSTRAK

Kerja pengendalian manual (MH) mengangkat dan membawa adalah antara punca utama kecederaan semasa bekerja di seluruh dunia. Kerja-kerja ini melibatkan pergerakan postural dan dinamik yang kerap seperti pergerakan mencangkung, menurunkan, dan berjalan (dengan beban) secara berulang, yang merupakan faktor risiko bagi patogenesis dan perkembangan beberapa trauma kumulatif atau gangguan gerakan/terikan yang berulang pada bahagian bawah badan dan tulang belakang lumbar seperti osteoarthritis lutut/pinggul, kerosakan meniscus lutut, dan sakit belakang. Gangguan-gangguan ini adalah bersifat degeneratif, menjejaskan produktiviti pekerja, dan boleh membawa kepada kehilangan mobiliti seumur hidup untuk pekerja yang terbabit. Pada masa ini, terapi untuk menangani masalah ini masih belum mencukupi. Exoskeleton untuk peningkatan prestasi manusia (EHPA) aktif merupakan intervensi alternatif yang mempunyai potensi untuk meningkatkan kecekapan dan kemampuan pekerja bagi mengatasi faktor-faktor risiko biomekanik (seperti keletihan, kelemahan otot, dan sebagainya) yang membawa kepada kecederaan dalam tugas mengangkat/membawa beban. Walau bagaimanapun, beberapa halangan yang berkaitan dengan teknologi reka bentuk dan kawalan mengehadkan penggunaannya secara praktikal pada masa ini. Satu cabaran yang besar adalah berkaitan dengan cara untuk mengawal EHPA secara berkesan untuk memberi bantuan/augmentasi pergerakan yang lancar dan seragam kepada pengemudi untuk mendapat faedah bantuan yang mencukupi, dengan kepelbagaian dalam pergerakan biomekanik (mencangkung/berjalan) dan pergerakan transisi (mencangkung-ke-berdiri-ke-berjalan dan lain-lain) dalam situasi sebenar mengangkat/membawa beban. Dalam kajian ini, EHPA bahagian bawah badan dengan 12 darjah kebebasan (12-DOF) yang dikenali sebagai UMExoLEA dengan aktuasi empat motor DC tanpa berus dwi-arah aktif dan algoritma kawalan pergerakan segerak yang baharu telah dibangunkan untuk menyediakan bantuan pergerakan bahagian bawah badan yang lancar dalam tugas-tugas

MH mengangkat/membawa beban. Sistem kawalan tersebut dapat memberi bantuan pergerakan kepada pemakai dengan sinergi baharu yang terdiri daripada tiga algoritma kawalan: *dual unscented Kalman filter* (DUKF) untuk penganggaran trajektori dan pengemaskinian model, pengawal impedans untuk penjanaan tork bantuan, dan algoritma kawalan penyeliaan yang baharu untuk pengesanan pergerakan pengemudi dan penyegerakan dengan exoskeleton.

Eksperimen dijalankan ke atas 15 orang peserta yang direkrut untuk melaksanakan dua tugas MH industri: tugas mengangkat kotak yang berisi beban seberat 9.5kg secara berulang dan tugas membawa beban yang sama secara berulang dalam dua mod yang berbeza: dengan bantuan dan tanpa bantuan exoskeleton. Isyarat EMG yang diambil pada tiga otot: *Vastus Medialis*, *Rectus Femoris*, dan *Gastrocnemius* kaki kanan, beserta soal selidik maklum balas dan data kinetik/kinematik telah digunakan untuk menilai prestasi exoskeleton tersebut. Secara keseluruhan, tenaga otot dan daya maksimum peserta berkurang sebanyak 30% hingga 60% bagi kedua-dua tugas. Persepsi peserta terhadap bantuan yang diterima dari UMExoLEA adalah 73.1% (markah purata) yang juga selaras dengan persepsi mereka terhadap pengurangan usaha. Penilaian purata keletihan secara subjektif (di bahagian bawah badan dan belakang) jauh lebih tinggi, iaitu antara 13.6% (**SD**: 15.0%) hingga 20.4% (**SD**: 17.8%) tanpa bantuan exoskeleton, manakala dengan bantuan, penilaian peserta adalah hampir sifar. Selain itu, pengesanan dan penyegerakan pergerakan menerima kadar kejayaan lebih daripada 99% dalam semua tugas pergerakan berulang.

Kata kunci: Mengangkat dan membawa, pengendalian manual, gangguan gerakan/terikan berulang, EHPA, *dual unscented Kalman filter*

ACKNOWLEDGEMENTS

First, my utmost gratitude to the Almighty who has helped me, enabled me, and granted me leave and good health to bring this work to a successful completion. No amount of words can articulate this gratitude.

My profound gratitude also goes to my amiable supervisors, Dr. Raja Ariffin bin Raja Ghazilla for his whole-hearted support, thoughtful suggestions, thesis correction, advice, patience, and hours of constant dedication to my research; and Dr. Yap Hwa Jen for his absolute support, thesis correction, patience, advice, thoughtful suggestions and dedication to my research. To Dr. Raja, I remain indebted to the countless hours of treatment to lunch and a cup of tea enriched with an atmosphere of supportive discussions and advice; and to Dr. Yap, I will also be indebted to his ever-timely support and assistance.

My special gratitude also goes to my family members: to my late father for his vision and wise counsel; and my mother for her constant prayers, encouragements, and unremitting moral support; to my wife Zeniat Olere for her patience, support and encouragements, and my kids for their patience and hours of missing their father; to my siblings for their prayers and support; and particularly to my brother Suraj for the countless timely financial support. My gratitude also goes to my friends; most importantly to Dr. Mahdi Ahmad for his supportive prayers and timely financial support, to Mr. Shawgi Younis for his countless financial support, and to Mr. Maidul Islam for his support.

Thank you all.

TABLE OF CONTENTS

LIST OF FIGURES

LIST OF TABLES

LIST OF SYMBOLS AND ABBREVIATIONS

M	:	Mass matrix
C	:	Centripetal and Coriolis vector
m_{tor}	:	Torso mass
m_S	:	Mass of exoskeleton shank
m_T	:	Mass of exoskeleton thigh
m_F	:	Mass of exoskeleton foot
G	:	Gravitational torque
τ_a	:	Actuating torque
τ_2	:	Knee actuating torque
τ_3	:	Hip actuating torque
τ_h	:	Human torque
τ_f	:	Joint frictional torque
μ	:	Coefficient of friction
q	:	Joint variables
θ	:	Joint angles
F	:	3x1 vector of ground reaction forces
F_1	:	Ground force measured at the heel
F_2	:	Ground force measured at the ball of foot
l_t	:	Length of the thigh
l_s	:	Length of the shank
l_f	:	Length of the foot
l_{HAT}	:	Length of the torso/HAT
M	:	Subject with mass

h	:	Subject height
J	:	Jacobian
b_1	:	coefficient of the coulomb or kinetic friction torque
b_2	:	Coefficient of the damping friction torque
b_0	:	Static friction torque
b_3	:	Stiffness torque
$\mathbf{F}$	:	State transition function
$\mathbf{H}$	:	Observation function
k	:	Discrete time
$\mathbf{x}_k$	:	Unobserved states
$\mathbf{y}_k$	:	Noisy position observation from sensors
$\mathbf{w}$	:	Model parameters
$\mathbf{v}$	:	Process noise
$\mathbf{n}$	:	Measurement noise
$\mathbf{P}_{\boldsymbol{n}}$	:	Measurement noise covariance matrix
$\mathbf{P}_{\mathbf{v}}$	:	Process noise covariance matrix
$\mathcal{K}_{\boldsymbol{k}}$	:	Optimal Kalman gain
$\mathbf{I}$	:	3x3 identity matrix
L	:	The dimension of the state vector
$\mathbf{r}_k$	:	Process noise for model parameter estimate
$\mathbf{P}_{\mathbf{r}_k}$	:	Process noise covariance
$\mathbf{d}_k$	:	nonlinear observation on $\mathbf{w}$
$\mathbf{e}_k$	:	Error in the nonlinear model
$\mathbf{P}_{\mathbf{e_k}}$	:	Estimation error covariance
$\mathbb{E}$	:	Expectation

λ	:	Composite scaling parameter
κ	:	kappa
α	:	Alpha
β	:	Statistical power
α	:	Significance level
μ_x	:	Mean for treatment x
σ^2	:	Variance
W_{xx}	:	Between-subject variance
ν	:	Sequence effect
ρ	:	Period effect
λ_x	:	Carryover effects of treatments x
M_r	:	Inertia parameter
B_r	:	Viscous damping parameter
K_r	:	Stiffness parameter
q_d	:	Reference joint position
$\dot{q}_d$	:	Reference joint velocity
$\ddot{q}_d$	:	Reference joint acceleration
ε	:	Ground reaction force sensor offset value
τ_c	:	Computed torque output
$u_{a,q}$	:	Outer loop control output
σ_j	:	Supervisory control output
MH	:	Manual Handling
EHPA	:	Exoskeletons for Human Performance Augmentation
UMExoLEA	:	Universiti Malaya Exoskeleton for Lower Extremity Augmentation
DUKF	:	Dual Unscented Kalman Filter

SD	:	Standard Deviation
LE	:	Lower Extremity
ISO	:	International Standard Organization
MSD	:	Musculoskeletal Disorders
HSE	:	Health and Safety Executive
NIOSH	:	National Institute for Occupational Safety and Health
LBP	:	Lower Back Pain
HR	:	Hazard Ratio
OR	:	Old Ratio
CI	:	Confidence Interval
CLBP	:	Chronic Low Back Pain
RR	:	Risk Ratio
OA	:	Osteoarthritis
PAR	:	Population Attributable Risk
IRR	:	Incidence Rate Ratio
VM	:	Vastus Medialis
RF	:	Rectus Femoris
GA	:	Gastrocnemius
GM	:	Gluteus maximus
UMREC	:	University of Malaya Research Ethics Committee
RMSA	:	Root mean square average
MVC	:	Maximum voluntary contraction
SAC	:	Sensitivity amplification controller
FSM	:	Finite state machine
DOF	:	Degree of freedom
ZMP	:	Zero-moment point

EMG	:	Electromyogram
DMP	:	Dynamic Movement Primitive
AFO	:	Adaptive frequency oscillator
GM	:	Gluteus maximus

LIST OF APPENDICES

CHAPTER 1: INTRODUCTION

1.1 Background

Research on active exoskeletons for human performance augmentation (EHPA) have recently intensified towards assisting industry workers in lifting and carrying manual handling (MH) works (de Looze et al., 2016). Lifting and carrying activities are performed in several industries including production, construction, health care, agriculture, logistics, military, rescue service, fire service, hotels and retails service. These activities pose significant health hazards to workers in these industries and are notable causes of cumulative disorders or repetitive motion or strain injuries due to the gradual and cumulative deterioration of the musculoskeletal system from continuous handling (Gatchel et al., 2014; Nunes & Bush, 2012; Schneider et al., 2010).

Despite automation, mechanization, and workplace design changes, the annual incidence of injuries due to lifting and carrying manual handling activities has been significantly high. Statistics show that activities of lifting/carrying are difficult to eliminate in many workplaces, or low income industries, or developing countries (de Looze et al., 2016; Yang et al., 2017). Reports from the U.S Bureau of Labor Statistics in 2016 revealed that musculoskeletal disorder such as sprains and strains resulting from overexertion in lifting (or moving of patients) accounted for 31% of the total cases of musculoskeletal disorders (MSD) for all workers in 2015 (Bureau of Labor Statistics, 2016) with about 80% of the cases occurring in the private industries. These figures remained essentially the same in their recent statistics in 2018, see Figure 1.1.

In Great Britain, the annual incidence is similar. The national statistics from the Health and Safety Executive (HSE) in 2016/17 revealed that handling, lifting, and carrying accounted for about 22% of all non-fatal injuries in the workplace which caused over seven days absence from work (Health and Safety Executive, 2017). This figure was only slightly lower by 1% in the latest HSE report in 2018, see Figure 1.2. This shows evidence of significant presence of handling, lifting and carrying despite mechanization and automation or workplace design changes in the UK.

Data from developing countries are hard to find, but the figures are expected to be even higher due to the relatively low level of automation or mechanization. In Malaysia, a cross-sectional study conducted in a processed food manufacturing industry in 2010 revealed a heavy activity of lifting and carrying which accounted for a high prevalence of back pain (45%) and low back pain (80%) with mean of 2 days per month absence from work despite existing workplace intervention (Deros et al., 2010). More recent data and statistics from other industrial sectors in Malaysia are hard to find.

Lifting and carrying technically involve a combination of postural and dynamic body activities. This process engages virtually all parts of the human musculoskeletal system and are accompanied by biomechanical stress and strain on different regions of the musculoskeletal system. Commonly reported debilitating injuries/disorders or symptomatic health conditions caused by manual lifting/carrying are low back pain (LBP) which occur on the lumbar spine region (P. Coenen, Gouttebarge, et al., 2014); knee osteoarthritis, hip osteoarthritis and meniscal knee damage which occur on the lower limb (Reid et al., 2010). Currently, existing interventions such as trainings and education on correct posture, personal protective equipment and mechanical assistance have not been sufficient to tackle these disorders (McWilliams et al., 2011; Runhaar & Zhang, 2018).

The commonly identified biomechanical causation of this disorders in lifting/carrying activities are weakness/fatigue of the lower extremity muscles due to overuse of muscles in cumulative, frequent or repetitive heavy lifting/carrying task. These biomechanical factors have been shown to influence joint stability, load distribution across the joint, and wear and tear of the articular (hyaline) cartilage of the synovial knee and hip joint (Amin et al., 2008; K. L. Bennell et al., 2013; Reid et al., 2010; Sasaki et al., 2008; Trafimow et al., 1993).

Active exoskeletons for human performance augmentation (EHPA) are promising alternative intervention for assisting workers in lifting and carrying manual handling activities. They have potentials to address the biomechanical causation of injuries/disorders in these activities for primary prevention purpose. When worn, they can augment the lower extremity for mobility, agility, and weight bearing, minimizing the biomechanical stress/load on joints, strain on muscles, fatigue and other repetitive motion effect on the lower extremity and lumbar spine.

Despite their potentials, the state-of-the-art reveals that EPHAs' technology is still evolving. More work is still required to surmount the current challenges to accelerate EHPAs technology for application in lifting and carrying manual handling works (de Looze et al., 2016). In terms of design, a number of EHPA devices are still bulky, not user-friendly, adding extra weight on the user, having heavy actuation system with low power-to-mass ratio, and having fewer number of DOFs to allow sufficient movement. With regards to control, many EHPAs are still under-controlled given several degrees of freedom, design limitations, and diverse tasks operations (Yang et al., 2017; Young & Ferris, 2017). There is still a huge challenge in controlling and coordinating the exoskeleton system naturally or synchronously to achieve maximum assistive gain, given the diversity of work, body movements, and body biomechanics in lifting/carrying works

(de Looze et al., 2016; Young & Ferris, 2017). Overall, there is need for an appropriate understanding of an EHPA system, its intended application purpose, and its biomechanical effect on the body to pave way for new design improvements.

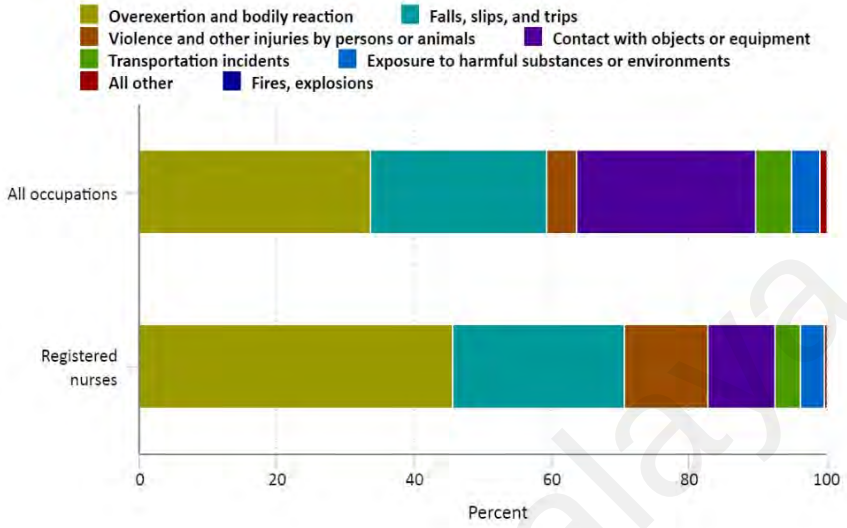

Figure 1.1: Percent distribution of nonfatal occupational injury and illness cases, by event or exposure, private industry, 2016

(Michelle et al., 2018)

Figure 1.2: Non-fatal injuries to employees by main accident kinds (as reported by employers), 2017/18

1.2 Problem Statement

Lifting and carrying manual handling works are responsible for several cumulative trauma or repetitive motion or strain disorders of the lower extremity and lumbar spine such as knee/hip osteoarthritis, meniscal tear, and low back pain affecting a large workforce population. These disorders are degenerative and can lead to frequent absenteeism from work and eventually permanent disabilities for affected workers. Existing workplace interventions for prevention of these disorders include trainings and education on correct posture, the use of personal protective equipment, mechanical assistance and automation. Current statistics however show that these interventions are not adequate to tackle these disorders. The identified biomechanical causations of these disorders are lower extremity muscular weakness/fatigue or poor activation from prolong or frequent overuse (in lifting and carrying works). These have been shown to influence joint stability, load distribution across joint, wear and tear of the articular cartilage of the synovial knee/hip joint, tissue breakdown and micro-fracturing of the lumbar disk (Amin et al., 2008; K. L. Bennell et al., 2013; Reid et al., 2010; Sasaki et al., 2008; Trafimow et al., 1993). An intervention addressing the biomechanical causation of these disorders in lifting and carrying works for long term prevention of lower extremity mobility disabilities or joints failure should therefore prove invaluable.

Active EHPAs are promising alternative intervention which portend numerous benefits in improving workers efficiency and eliminating the causal biomechanical factors in lifting and carrying activities. However, several technological challenges currently limit their practical deployment for lower extremity mobility augmentation. There are numerous design issues for EHPAs and currently control is a weakness in many designs (Young & Ferris, 2017). There is the challenge on how to effectively control and coordinate the movement of the exoskeleton smoothly and synchronously with the pilot

movement to achieve high positive assistive gain from the exoskeleton. Given actual lifting and carrying work that involve movement diversity, different body biomechanics, and movement transitions (squatting-to-standing-to-walking, etc.), this challenge is not trivial. Moreover, if EHPAs are not controlled effectively, they may actually work against the objective for which they are created. There is thus the need to intensify research effort in the design and control of effective EHPAs to facilitate their adoption in manual lifting and carrying industrial activities for lower extremity movement augmentation.

1.3 Research Objective

The main objective of the research is to develop an exoskeleton assistive framework to provide lower extremity (LE) mobility augmentation in lifting and carrying MH tasks. The framework is motivated for long term primary prevention of cumulative trauma or repetitive motion/strain injuries of the lower limbs and lumbar spine. The assistive control framework would have capabilities to allow voluntary and smooth synchronous movement assistance/augmentation in dynamic lifting (involving squatting) and carrying (involving walking) manual handling activities, as well as allow seamless movement transitions within these activities.

The specific objectives are:

1. To develop a dynamic model of the EHPA based on analysis of lower extremity biomechanics in lifting and carrying MH task.
2. To develop a synchronous mobility control algorithm to enable smooth lower extremity mobility augmentation and movement transitions in lifting/carrying MH activities.
3. To develop a prototype lower extremity exoskeleton for mobility assistance in lifting and carrying MH task.
4. To evaluate the assistive-ness of the prototype exoskeleton system.

1.4 Scope of Research

Exoskeleton research is broad and can be categorized into three research directions: medical rehabilitation exoskeletons, assistive exoskeletons for daily living, and exoskeletons for human performance augmentation (EHPA). The scope of this research is on EHPA applied for lifting and/or carrying industrial manual handling task. The research is further narrowed to address the mechanical causation of lower extremity musculoskeletal disorders in lifting and carrying manual handling works which can lead to long term immobility or disabilities of the lower extremity. Thus, the research is focused on developing an EHPA to provide lower extremity mobility augmentation in lifting and carrying manual handling task to address the mechanical causation of lower extremity disorders.

1.5 Thesis Structure

The thesis is composed of seven chapters. The current chapter is **Chapter 1** which presents the background of the research. This chapter gives a brief statistic of prevalence of lifting and carrying manual handling, the prominent disorders or health hazards caused by this activity, some current interventions, and the potentials and limitation in the adoption of exoskeleton technology. The chapter also present the problem statement of the research, the objective of the research and the research scope. The rest of chapters are organized as follows.

Chapter 2 presents the literature review on lifting and carrying manual handling, the state of art in active performance augmentation exoskeleton for lifting and carrying manual handling task, and an overview of current technological limitations.

Chapter 3 presents the methodology of the research. It describes the literature review method, the design method, and the study method.

Chapter 4 presents the UMExoLEA design and Modelling. It details the main concept of design, biomechanical analysis of movements in lifting and carrying activities, system modelling and controller design.

Chapter 5 presents the simulation studies. It details the DUKF robustness simulation studies as well as the impedance control performance test for trajectory following and torque generation.

Chapter 6 presents the UMExoLEA prototyping and system identification studies. It details design of various sub-module of UMExoLEA as well as the segment parameters and frictional torque identification studies.

Chapter 7 presents the quantitative results of experiments conducted to evaluate the performance of the exoskeleton design and control technique. It also presents the qualitative results from the questionnaires.

Chapter 8 presents the conclusion and recommendations

CHAPTER 2: LITERATURE REVIEW

2.1 Introduction

Work-related injuries remain commonplace in several industries where lifting and carrying manual handling activities are routinely performed. Injuries account for a significant number of workers' absenteeism, disabilities, and cost burden on the employers of labor. Currently, there are ongoing interventions in the workplace to assist lifting and carrying works to prevent injury occurrence and progression, however there is no indication that these measures are sufficiently reliable. Exoskeleton for human performance augmentation (EHPA) is a renewed focus in these ongoing efforts. This chapter presents a comprehensive (systematic) review on this subject. It covers two aspects to satisfy the objective of the current study. The first is a review on lifting and carrying manual handling activities to uncover the disorders related to these activities, to identify their biomechanical causations, and to assess the state of existing intervention effort. The second is a comprehensive review on the state of art of active EHPA technologies developed as intervention for lifting and carrying manual handling purpose. This part of review examines critical aspect of EHPA design, control strategies, performance, targeted injury to prevent, and challenges in actualizing these objectives. The search criteria and topics can be found in Appendix A

2.2 Lifting and Carrying Manual Handling

2.2.1 Definitions

In the first international standard on manual handling named "ISO 11228-1", the International Standard Organization (ISO) defines manual lifting as "moving an object from its initial position upwards without mechanical assistance". It defines manual carrying as "carrying when an object remains lifted and is moved horizontally by human force". In addition, it defines manual lowering as "moving an object from its initial

position downwards without mechanical assistance" (ISO 11228-1, 2003). The object can be a person or animal.

Lifting and carrying are usually impossible to separate in many workplace situations. In some reports, lifting and carrying activities are implied when reference is made to manual lifting activity or in general to manual materials handling (Cheung et al., 2007; Health Council of the Netherlands, 2012).

2.2.2 Regulations in Lifting and Carrying

In recognition of the health burden of Lifting and carrying MH on the workforce, there had been efforts to make regulations regarding the mass of objects to be lifted, the working postures and frequency and duration of handling which is reasonable for workers. The two worldwide regulatory bodies, ISO and NIOSH have stipulated possible exposure limits especially for lifting, however there is no clear consensus on these limits. The International Standard Organization (ISO) recommended guidelines for manual lifting and carrying while considering, respectively, the intensity, the frequency and the duration of the task (ISO 11228-1, 2003). For potential risk, it considers limits for lifting of objects of mass 3kg or more; it determines the exposure limits for lifting combined with walking at moderate speeds, i.e. 0.5m/s to 1.0m/s on a horizontal level surface, given 8 h working day shift. However, ISO standard does not consider the combinational effect of tasks in a shift during a day.

The NIOSH applies the traditional NIOSH equation which has been widely adopted in the US and many European countries (Waters et al., 1993). The revised NIOSH equation sets the weight an employee can safely lift manually between 5kg and 23kg for maximum of 8 hours without causing an undue burden to the back. The maximum weight of 23kg (revised from 40kg) is applicable only under the most optimal circumstances, i.e. given the best lifting posture, angulation, load vertical height, horizontal distance from the body, and other psycho-social factors of the worker like age, sex, physical condition etc. For

example, the maximum weight an employee may lift from the floor onto a table of height 75cm once per minute, for 8 hours, is 10kg, provided that the person is standing straight in front of the table. If the person needs to rotate the object over a 90-degree angulation, the recommended weight limit is 7kg, or 8kg if the employee does it for less than 2 hours per day (Health Council of the Netherlands, 2012; Waters et al., 1993).

2.2.3 Health Impact of Lifting and Carrying

There is a modest documentation of epidemiological and biomechanical studies on the health impact of occupational lifting and carrying. Epidemiological studies give account of the exposure rate, incidence and prevalence as well as possible control of the injuries (Gatchel et al., 2014; Manchikanti, 2000). The biomechanical studies on the other hand applies the principles of mechanics to explore the physical or physiological causation of injuries to the human body (Antwi-Afari et al., 2017; Foege et al., 1985; Radwin et al., 2001). See Appendix B for table of summary

2.2.3.1 Biomechanical Studies

Epidemiological researches are useful in the identification of physical risk factors as well as personal and psychosocial factors responsible for regional body disorders, but often, the depth of information from these findings is not of the quality that would be sufficient to control the risk, or in understanding the underlying causal mechanism of the risk (Reid et al., 2010). Biomechanical researches on the other hand can offer direct causal mechanism to the physical causation of regional body disorders (Radwin et al., 2001).

This section presents analysis of biomechanical causation of injuries (to the lower back, lower limb, and upper limb) during lifting/carrying manual handling activities.

(a) ***Lower Back Pain***

With respect to low back pain, biomechanical research has established a more consistent relation between spinal loading (or cumulative low back loading) and low back

pain. Biomechanical loading of the spine occurs in three-dimensional space during lifting or carrying, trunk flexion, rapid or repetitive trunk bending, see Figure 2.1. The loading can be compressional, shear, or torsional, and are derived from all the forces and moment acting on the spine (W. J. E. Marras, 2000; McGill, 2015). Spinal loading provides a more direct relationship with tissue breakdown and thus LBP (P. Coenen, Kingma, et al., 2014); W. J. E. Marras (2000); (McGill, 2015). W. J. E. Marras (2000) showed how excessive loading generated from both within and outside the body can lead to micro-fracturing of the lumbar spine (vertebral end plates) if loading exceeds the end plate tolerance. See Figure 2.2 for the spinal column. Low back pain follows as a result of obstruction of nutrient supplies when scar tissues form on the microfractures during healing. Lotz et al. (1998), the 1998 Volvo Award Winners in Biomechanical Studies, also demonstrated how static compressive disc loading (using a mouse tail intervertebral discs) can initiate pain in a dose-dependent way, lending credence to the harmful effect and association of compressive load on the spine. Ogata et al. (2018), Graham and Brown (2012) and Vakos et al. (1994) showed that compressive load at the spine doubles with speed of lifting which could potentially lead to low back injury. Pieter Coenen et al. (2013) also showed a strong association between cumulative lumbar load and low back pain which could be attributed to accumulation of microdamage or fatigue. The authors found a lumbar dose of 2.0MNm for a work week to be harmful. Thus, for a daily spinal dose of 200Nm in a moderate lifting task, hazardous level occurs after 50 lifting/carrying ($2.000.000/200^2$) in a work week.

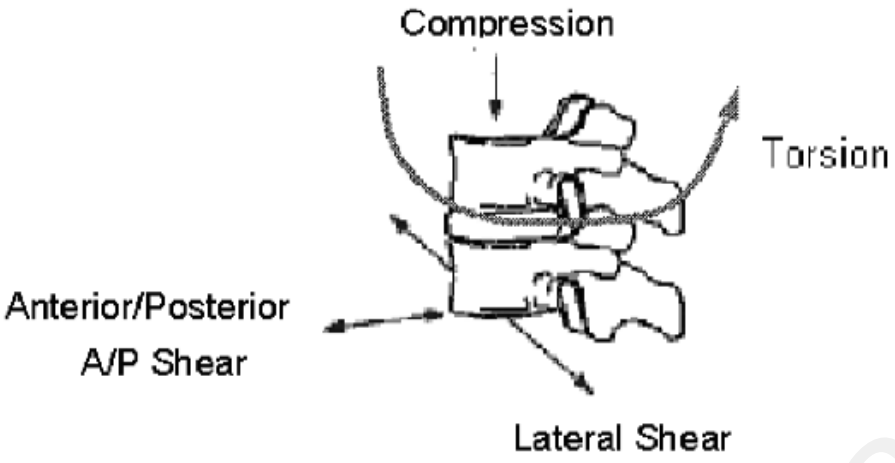

Figure 2.1: Three-dimensional loading of the spine

(W. J. E. Marras, 2000)

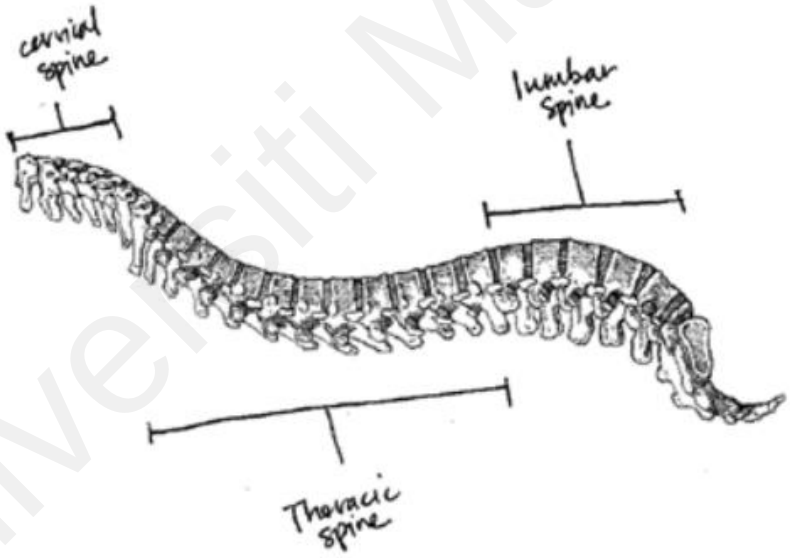

Figure 2.2: Spinal column

(Gatchel et al., 2014)

Biomechanical studies have also established a causal link between fatigue of the lower extremity musculature and lumbar loading. An inverse relationship has been shown between the counterforce of the knees and the counterforce of the lumbar region during lifting (Bejjani et al., 1984). Fatigue on the quadriceps femoris (and other supportive

muscles) as result of repetitive lifting or carrying lowers the counterforce of the knee joint, hip joint and body trunk, and increases the counterforce of the low back muscles which increases the spinal load (Mehta et al., 2014; Sparto et al., 1998). This helps to explain why activity of knee extensor muscles is limited in chronic low back pain patients with easily fatigued lumbar muscles (Suter & Lindsay, 2001). The quadriceps femoris regulates the mode of lifting, and plays an important role in squat lifting, which is mainly based on knee extension (Sasaki et al., 2008; Trafimow et al., 1993). Sasaki et al. (2008) examine the influence of Quadriceps femoris fatigue on the low back load during lifting of loads at different distances from the toes. They found that at 50% fatigue subjects lifted with the same squat technique as they did at 0% fatigue, but the myoelectrical activity of the lumbar muscle increased inversely as the myoelectrical activity of the quadriceps femoris decreased from the start of muscular activity to the time when the heavy object was lifted off the floor. Ground reaction forces also significantly changed. They also found that at lower level of fatigue (25%) subjects changed their squatting techniques towards stooping tending to compensate the load on the low back, which was not possible at high fatigue level. Another study by Trafimow et al. (1993) showed that participants changed their squatting technique from an upright squat to a flexed lumbar spine after fatigue of the quadriceps, increasing the stress on the lumbar region.

(b) ***Lower Limb Disorders***

Based on epidemiological research findings, the commonly reported lower limb disorders associated with occupational lifting/carrying activities are knee osteoarthritis (OA), meniscal tear of the knee, and hip osteoarthritis (OA), see Appendix B for table of summary.

i Knee OA

For knee OA (reputed as the most common joint disorder) (Gatchel et al., 2014), the biomechanical causation of this disease has been linked to excessive loading across the knee, muscle deficit (i.e. poor muscle strength, activation, and proprioception), fatigue particularly of the quadriceps femoris, and speed of movement of the joint (Amin et al., 2008; K. L. Bennell et al., 2013; Reid et al., 2010; Schoenfeld, 2010). Peculiarity of the disease is loss of mobility or knee failure. At the knee joint, the external knee joint loading experienced during human movement is derived primarily from the ground reaction forces and inertial properties of the lower limb, which results in a total tibiofemoral joint force approaching three times body weight (Shelburne et al., 2006; Taylor et al., 2004). To maintain equilibrium of motion and joint stability, all external forces and moments acting on the knee joint must be counteracted by internal forces (derived primarily from muscles, tendons, and ligaments) and moments equal in magnitude, but opposite in direction (K. L. Bennell et al., 2013). The ability to counteract these forces particularly the external adduction moment applied about the knee is believed to influence the initiation (Amin et al., 2004), severity (Sharma et al., 1998), and progression (Kim L Bennell et al., 2011; Miyazaki et al., 2002) of knee OA. Fatigue, muscle weakness, or muscle deficit due to muscle overuse, overexertion, or prolong/repetitive task (e.g. repetitive squatting, walking, lifting/carrying) can weaken the ability of the lower-limb musculature to provide this counteractive force.

The speed of movement of the joint has also been shown to increase compressive forces at the knee. Hattin et al. (1989) demonstrated that performing repetitive half-squat lasting 1 seconds and 2 seconds increases anteroposterior shear and compressive forces at the knee by 50% and 28% respectively, which also showed a positive trend towards increase mediolateral shear. Similar results were reported by Vincent et al. (2012) and

Schoenfeld (2010) of increased in tibiofemoral joint forces at higher speed of joint movements.

Another biomechanical cause of degenerative changes to the knee joint result from malalignment of the knee about the medial compartment. The joint connects the femur to the tibia and fibula in the proper alignment through series of muscles and thick ligaments to stabilize and reinforce its structure, see Figure 2.3. In a normally aligned knee, 60-70% of weight-bearing load is transmitted through the medial compartment (Arden & Cooper, 2005; Dulay et al., 2015). The mechanical alignment of the knee influences the distribution of load across the articular surfaces. Any malalignment or shift in either a valgus or varus direction affects load distribution which can lead to degenerative changes (Dulay et al., 2015).

Figure 2.3: Knee joint

(Gatchel et al., 2014)

Another influence on the knee load balance comes from the hip muscles which are responsible for stabilizing the pelvis on the weight-bearing lower limbs especially during walking/carrying (K. L. Bennell et al., 2013). Their influence is synergistic. Weak hip abductor muscle strength can lead to a contralateral pelvic drop which can theoretically

shift the body's center of mass away from the stance limb toward the swing limb (Perry & Davids, 1992). This increases the distance between the ground reaction force vectors and knee joint center of rotation, thus increasing the knee adduction moment, and consequently the risk of knee OA. The conditions are particularly exacerbated if walking is combined with load carrying or transporting.

ii Meniscal tear and hip OA

Meniscal lesion develop from heavy stress on the knee joint and builds up over time (Reid et al., 2010). P. Baker et al. (2003) showed that standing up from a knee or squat position is an important risk factor due to the enormous stresses that are put on the knee during such type of movement. Thus, lifting while standing up from a squat position is particularly a more dangerous activity for meniscal tear.

With respect to hip OA, very limited studies can be found establishing its biomechanical relationship with occupational lifting and carrying activities (Gatchel et al., 2014; Harris & Coggon, 2015). Degenerative effect or break down of the hyaline (articular) cartilage due to overuse, stress, impact, or heavy loading from occupational activities, accidents, or sports can lead to hip OA (Buckwalter et al., 2013; Harris & Coggon, 2015; Man et al., 2014). Documented occupational risk factors for Hip OA are heavy lifting (Allen et al., 2010; Harris & Coggon, 2015).

(c) ***Upper Limb Disorders***

The most frequently reported symptomatic region of the upper limb in lifting/carrying works is the shoulder joint (often jointly reported with the neck), followed by the wrist/hand, the elbow is the least frequent site of pain (Buckle & Devereux, 2002; Gatchel et al., 2014). Reported biomechanical causality for the upper limb injuries are repetitive forceful works (including repetitive heavy load lifting or carrying manual material

handling) and awkward or sustained positions (such as working with hands above the shoulder level) (Bongers et al., 2002; Gatchel et al., 2014).

Repetitive forceful work exerts significant mechanical stress and strain on the upper limb musculature which can lead to tears, or microtears, and consequently pain. Repetitive forceful exertion is also believed to induce fatigue on the upper-limb muscles due to the frequency and shorter time for muscles recuperation. This fatigue induces metabolic changes that could, in turn, lead to injury and inflammation and pain (Zakaria et al., 2002). Mayer et al. (2012) reported strong evidence of shoulder disorders among workers engaged in manual material handling which involved lifting and carrying works.

Awkward posture on the other hand put increased mechanical stress on muscles and tendons of the upper limb since the limbs are placed in a biomechanical positions that are not optimal to perform the work (Gatchel et al., 2014). Mayer et al. (2012) found working with hands above the shoulder to be strongly associated with shoulder disorders in a longitudinal study involving manual laborers. Sustained awkward position can reduce blood flow or increase pressure on tendons, blood vessels, or nerves and may impede normal metabolism which can lead to pain (Zakaria et al., 2002). see Appendix B for table of summary

2.2.4 Summary of Health Impact

Over all, strong association between lifting/carrying activities and injuries to the low back, upper-limbs, and lower-limbs have been found from both epidemiological and biomechanical research studies. The most prevalent of these injuries are LBP, hip/knee osteoarthritis, meniscal tear, and shoulder/neck disorders, see Appendix B for summary tables. The most commonly reported of these disorders are low back pain, knee OA, and meniscal lesions. Osteoarthritis of the knee is however the most common joint disease which can lead to joint failure and permanent disability (Blalock et al., 2015; Bruchal,

1995; Gatchel et al., 2014). There is currently no cure for this disease (Runhaar & Zhang, 2018).

The biomechanical causation of these disorders in lifting and carrying activities are muscular fatigue, muscle deficit, frequent squatting, frequent walking, heavy lifting/carrying, frequent trunk bending, and speed of movement of joints see Appendix B.

Lower limb muscular weaknesses or fatigue particularly of the quadriceps femoris due to overuse of muscles in repetitive, heavy, or prolong lifting/carrying task have been shown to influence stability, load distribution on the knee joint, and the counteractive de-loading effect on the lumbar (low back) region. Lower-limb muscular weakness, muscle deficit, or fatigue are known pathogenesis for onset, severity and progression of knee/hip osteoarthritis as well as low back pain (Amin et al., 2008; K. L. Bennell et al., 2013; Reid et al., 2010).

Frequent or repetitive squatting and walking in lifting and carrying operations can have symptomatic effect on joint and muscle through series of wear and tear of the articular (hyaline) cartilage which is particularly common in the synovial knee and hip joint; and through repeated overuse of muscle. The lack of sufficient time for muscle recuperation (after series or wear and tear) in repetitive task is the major causative factor of symptomatic conditions. Frequent squatting and walking are strongly correlated with onset and progression of knee osteoarthritis and moderately correlated with low back pain. Deep knee squatting is particularly associated with meniscus tear of the knee.

Heavy lifting/carrying is accompanied with high mechanical loading, stress, and strain on the low back, knee/hip joint, and shoulder region leading to symptomatic conditions.

Cumulative or repetitive effect of lifting and carrying have also been strongly correlated with debilitating disorders in these body regions.

Frequent or sustained trunk bending performed in stoop lifting activities weaken the tolerance limit of the spine and are directly correlated with low back pain. Although manual handling regulation recommends squat lifting to minimize trunk bending, repetitive squat lifting can also lead to symptomatic conditions of the knee and/or low back pain.

2.3 Interventions for Lifting and Carrying Manual Handling Hazards

The most common workplace interventions for minimizing or preventing musculoskeletal injuries caused by manual handling are classified as behavioral/personal intervention, administrative interventions, and engineering interventions, (Curbano, 2018). The interventions mainly try to minimize or prevent injury occurrence (primary prevention) and progression (secondary prevention) in the presence of sustained or continuous exposure to the hazardous handling (Runhaar & Zhang, 2018). This section presents a review of the interventions adopted for the prevention of injuries related to lifting and carrying activities. The inclusion criteria for this section are literatures which investigated interventions for activities such as load lifting, carrying, moving, patient transfer, squatting, walking, and trunk bending movements that pertains to lifting and carrying.

2.3.1 Personal and Behavioral Intervention

Personal and behavioral intervention implies an attempt to reduce the hazardous effects of a risk factor by training on correct handling technique (back school), or by exercise/fitness programs to improve the capacity of the worker to withstand the hazard. It also involve the use of personal protective equipment like wrist splints, back belts, knee

brace, or padded gloves by an individual worker to minimize or create a barrier to the hazard (Curbano, 2018). There is a preponderance of studies on this type of interventions probably because of the ease of study setup.

Training on correct handling technique may be delivered as a short presentation or a comprehensive program giving guidelines to workers on how to properly perform manual handling works. The content may include knowledge of human anatomy, risk factors, correct posture, and proper lifting technique for example training on using upright squat-lifting as against trunk bending or stoop lifting. Exercise or fitness program on the other hand maybe a work-based stretching or stress management therapy. It could be supervised, group-based or home-based exercise interventions.

With respect to Training, there is currently no positive indication from studies that it has led to a diminished occurrence of musculoskeletal disorder or absenteeism or productivity amongst workers. In the study of Verbeek et al. (2012), nine high quality randomized controlled trials (involving 20101 employees) and nine cohort studies (involving 1280 employees) were analyzed for the impact of educational training on back pain prevention. Some of the studies compared training to no intervention, or to other interventions like professional education, a video show, the use of a back-belt and exercise. Other studies compared training plus lifting aids to no intervention and to training only. The studies were conducted among several occupations which include healthcare workers exposed to lifting/moving patients, baggage handlers exposed to lifting and carrying, construction workers exposed to several manual handlings including lifting and carrying, postal workers handling mail and workers in a distribution center. All exposures were sufficient to elicit back pain; and all interventions applied an educational model that ensured that the information provided in the intervention would lead to a change in knowledge, attitude or skills for the workers. However, from all the

studies, there was no evidence of a preventive effect of training on back pain despite increased knowledge in safe manual handling technique. In some studies, there were evidence of no change in workers behavior or adherence despite increased knowledge of back pain. The use of back-belt as personal preventive equipment was not seen to have any preventive effect against low back pain. These results also reconciled with the recent review by Steffens et al. (2016) who found moderate to very low-quality evidence of no effect of education on LBP or sick leave. They also found no significant evidence of protective effect of back-belts and shoe insoles on episodes of LBP or sick leave. Studies could hardly be found examining the effect of educational training on minimizing other regional musculoskeletal disorders such as hip or knee OA and shoulder/neck disorders (Curbano, 2018).

With respect to exercise program, a number of the studies could be found especially examining its impact on sedentary hip/knee OA and low back pain subjects. A randomized controlled trial by Chopp-Hurley et al. (2017) studied the effectiveness of a 12-week workplace exercise program on work ability, performance, and symptoms of knee and/or hip osteoarthritis among sedentary university employees. Their jobs require them to stand or walk for less than one-third of their work day. Twenty-four of the participants with clinical hip and/or knee osteoarthritis were randomized to exercise or no exercise groups. Significant improvements in work ability, pain, function, and depressive symptoms were found in the exercise group. No improvements were detected in the no exercise group. The review by Vignon et al. (2006) also found exercises and other structured activities in the workplace pursued with a goal of health improvement to have a favorable effect on pain and functional ability in the sedentary knee OA patients. Similar results of increased work ability were found by Jakobsen et al. (2015) in a study among 200 female healthcare workers in Danish hospital after 10 weeks of work exercise therapy; and Filiz et al. (2005) among lumbar disc surgery outpatient in Istanbul after

comprehensive exercises therapy compared to a control group. Whether these findings apply to other non-sedentary workers in other industries who are engaged in rigorous work requires further studies.

2.3.2 Administrative Intervention

Administrative intervention involves changing the system of work: the job design, the pace and flow of the work, and the shift length (Curbano, 2018; Samani et al., 2012). Employers may alter the system of work by job assignment changes or rotation or break scheduling. For example, assigning a team handling for carrying heavy loads to reduce the burden on a single worker, introducing frequent short breaks, and job pacing.

As with engineering interventions, some of these policies may be effective in reducing the risk (to a given worker), but there currently exist conflicting reports. With respect to team lifting policy, Dennis and Barrett (2002) reports a 20% reduction in compressive lumbar spine load when lifting is performed with a team lift compared to an individual lifting. In support, W. Marras et al. (1999) also showed that team lift thus minimize spine compression particularly when lifting is done in sagittal symmetric conditions, however, on the contrary, they found lateral shear to be much greater for two-person lifts under asymmetric lifting conditions. Also, in contrast, Dutta et al. (2012) found that two caregivers working together with a floor lift did not reduce spinal loads on the primary caregiver compared to the single-caregiver case, probably due to the differences in trunk kinematics (W. Marras et al., 1999). Overall, there is the notion that by adopting a team lift or having a co-worker perform the task, the risk may still be present not eliminated and may accrue to another worker (Curbano, 2018).

With respect to frequent short break policy, Genaidy et al. (1995) showed that a period of four weeks of active microbreaks led to a statistically significant reduction in perceived discomfort among twenty-eight workers at a meatpacking plant during the course of the

working day, although there was no investigation on injury incidence. Henning et al. (1997) also found reduction in discomfort rating when microbreaks were combined with stretching exercise, but did not find any improvement in productivity or well-being at one site in a period of 4-6 weeks of introduction of microbreaks. Dababneh et al. (2001) studied two breaks scheduling policy on production rate and discomfort as well as stress ratings among 30 workers in a meat processing site. They found no significant effect of short breaks on productivity, except for the later hours of the workday when workers were given frequent rest breaks. Also, they found discomfort ratings in the leg area to improve better only when the longer hourly breaks were given. However, one of the shortcomings was an increase in task interruptions when break time are fragmented into shorter and more frequent resting periods, which prompted negative reaction among workers.

2.3.3 Engineering Intervention

Engineering interventions involve physical manipulations of hazards or the routes of exposure to hazards (Curbano, 2018). This may involve the use of simple or sophisticated mechanical aids to minimize the intensity of the hazard or may involve reorganizing the layout of the workplace/workstation to minimize exposure to the hazard (Arezes et al., 2010; Pavlovic-Veselinovic et al., 2016). Reported examples of engineering mechanical aids for minimizing workplace hazards (in manual lifting or carrying activities) include lift tables, vacuum lifts or hoists, transfer belts, cranes, and pulleys. Example of workplace layout change include introducing adjustable work levels and enlarging the workspace. Several, hazards could be prevented by this means. For example, installing lift tables, can prevent lifting from the ground level; providing some adjustable work levels could reduce bending movements and postures in some workplaces (Curbano, 2018); reducing the weight of the physical load could reduce the biomechanical loading on the low back, shoulder, neck, hip, and knee. Making sure of enough space for task to

be done in an upright posture with the load close to the body of the workers can help to reduce awkward postures.

Although numerous benefits could be derived through these means, conflicting reports exist for their actual efficacy in the workplace. Smedley et al. (2003) examined the impact of a primary engineering intervention program meant to reduce lifting of loads on a prospective cohort of 1239 hospital nurses in southern England, United Kingdom. The nurses were dichotomized into two group: the intervention group and the control group. Both groups had educational training on appropriate lifting and patient handling techniques, however the intervention group were additionally provided with mechanical lifting aids (including lifting devices, hoists, transfer belts, and sliding sheets). After 32 months of follow up, Smedley et al. (2003) found no marked difference between the two groups. Instead, the prevalence rate of LBP in the intervention group was seen to increase slightly from 27% to 30%, whereas the rate in the control group remain 27%. Suggesting that the change in risk factors due to the intervention was insufficient to produce a substantial reduction in back pain. Similar results were obtained by L. D. Jensen et al. (2006) and Hartvigsen et al. (2005) after introduction of mechanical aid for reduced lifting. However, the study by Yassi et al. (2001) found decreased frequency of manual patient handling or lifting, and improvement on self-perceived work fatigue, back and shoulder pain, safety, and frequency/intensity of physical discomfort among 346 hospital nurses on the intervention group (within 6-12 months of follow up on the use of mechanical aids). The engineering intervention adopted consist of total body lifts, sit-stand lifts, and a set of sliding devices. Musculoskeletal injury rates were however not significantly altered.

The systematic review by Burdorf et al. (2013) examining several observational and experimental studies on the impact of mechanical lifting devices found a moderate

reduction in LBP prevalence from 41.9% to 40.5% and a moderate reduction in MSD injury claims from 5.8 to 5.6 per 100 work-years, in the best scenario. In contrast, however, an earlier systematic review by Bigos et al. (2009) where high-quality prospective cohort studies were examined, found no sufficient evidence for the preventive effect of the applied engineering intervention on low back pain.

With respect to lower extremity disorders (e.g. osteoarthritis, meniscal tear), there is a paucity of studies examining the use of mechanical intervention for their prevention (primary or secondary) (Runhaar & Zhang, 2018). The preponderance of reported studies on mechanical intervention pertains to low back pain (especially among caregivers).

2.3.4 Combined Intervention

In workplace scenarios, interventions are usually combined for improved work practices and risk prevention. Moderate evidence exist that such a multifaceted approach leads to better outcome. Zadvinskis and Salsbury (2010) examined the effectiveness of a multifaceted minimal-lift environment on reported equipment use, musculoskeletal injury rates, and workers' compensation costs. The intervention consists of engineering (minimal-lift equipment), administrative (nursing policy), and behavioral (peer coach program) controls. The control group received only engineering intervention. The outcome showed that nursing staff employed in the multifaceted lift environment increased the use of lift equipment and experienced less injury, with reduced worker's compensation costs compared to the control group. Guthrie et al. (2004) similarly found moderate evidence for a combinational preventive effect in a two-week pilot study which introduced a new mechanical lifting equipment (engineering) combined with a back school (behavioral) and a lift team administrative policy in two units in Minnesota hospital. The lift team averaged 80 lifts per day and 95% of the nursing staff attended the back school. The number of injuries were found to decrease from 21 to 9 injuries for the

two units with corresponding decrease in the salary and work replacement. In contrast, the study of van der Molen et al. (2010) evaluating the effects of combinational intervention on the occurrence of low back complaints among gypsum bricklayers, found no effect on productivity, total work time, duration of tasks, duration of carrying, energetics, or biomechanical workload. Instead, they found that the duration and frequency of working between knee and hip height increased during a working day by 25% and 15%, respectively, due to the ergonomic measures.

2.4 Summary on Existing Interventions

Conflicting outcomes are found in a number of studies examining the effectiveness of existing interventions, which currently limits a consensus. Overall, no single intervention has been found sufficiently reliable for the prevention of occurrence (primary prevention) and progression (secondary prevention) of injuries related to lifting and carrying works. There are far more studies showing little or no effectiveness of training for example training on proper lifting techniques and posture, and personal protective equipment use such as back belts for MSD prevention (Curbano, 2018).

For primary prevention, engineering interventions appear amidst conflicting reports to have marginal effect in minimizing exposure to risk factors more than other interventions but more studies, well designed, are still required to be conducted on a reasonably large number of workers and industries to determine their overall effectiveness (Curbano, 2018). Also, few mechanical aids could be found in studies that are evaluated for their preventive effect. The few are also mainly applied for LBP prevention. There is hardly a mechanical aid evaluated for the primary prevention of hip/knee OA (Runhaar & Zhang, 2018).

For secondary prevention, there is some, but limited, evidence for the effectiveness of exercise and knee braces for reduction of pain associated with knee OA. There is however

no known cure currently for OA (Runhaar & Zhang, 2018). More commonly found indicator for determining the effectiveness of an exercise program is the improvement in workers' capacity to withstand the risk through improvements in muscular strength/function, work ability, and reduction in pain and depressive symptoms. These indicators have been shown to delay occurrence and progression of the diseases (Runhaar & Zhang, 2018). For secondary prevention, there are also indications that engineering and administrative interventions are effective in delaying disease progression, but, in all, a multifaceted approach combining engineering, administrative changes, education and exercise in conjunction with managed care have (so far) given the best outcomes (Guthrie et al., 2004; Zadvinskis & Salsbury, 2010). Table 2.1 presents summary of the existing industrial interventions.

Table 2.1: Summary of existing industrial interventions

Industrial Interventions	Description
Engineering	Use of mechanical aids: lift tables, vacuum lifts or hoists, transfer belts, cranes, and pulleys, etc.
	Work layout change: adjustable work levels, enlarging the workspace, etc
Administrative	Change of system of work: the job design, the pace and flow of the work, the shift length, job assignment changes or rotation or break scheduling etc.
Personal and Behavioral	Training (back school)
	Exercise/fitness programs
	personal protective equipment:

	wrist splints, back belts, knee brace, or padded gloves, etc.
Combined intervention	Engineering
	Administrative
	Personal and Behavioral

2.5 Active EHPA for Lifting and Carrying Manual Handling

2.5.1 State of the Art

Active exoskeletons for performance augmentation (EHPA) represent a new alternative solution for assisting workers in manual handling jobs (de Looze et al., 2015). They can be grouped in the category of engineering interventions. There are several potential benefits in their use for discomfort management, work productivity, prevention of work-related musculoskeletal injuries, and also, their ability to act on several risk co-founders at the same time. Active exoskeleton suits can (or have potentials to) increase the human capacity to work, lower the effort required to lift or carry a load, increase endurance, efficiency, productivity, and eliminate or reduce onset of fatigue in repetitive tasks.

By definition, exoskeletons are anthropomorphic devices equipped with several degrees of freedom to provide physical assistance to the wearer (de Looze et al., 2016). They can be designed with flexibility and intelligence to work cooperatively with humans, or in concert with human movements (de Looze et al., 2015), giving the possibility of combining human superior intelligence with machine power for accelerate productivity (Yang et al., 2017). Depending on the body segment, they can be defined as lower-limb exoskeletons - extending from the hip to the foot; or upper-limb exoskeleton - extending from the proximal to the distal part of the human arm; or full bodied exoskeleton -

extending over the entire human body (de Looze et al., 2015). Exoskeletons can also be described as active or passive. Active exoskeletons are actuated by electric motors, hydraulics, or pneumatic drives, etc. Passive exoskeleton, on the other hand, are driven by springs and damper systems or energy harvesters. A considerable literature on passive exoskeleton exist with significant differences in mechanism which detracts from the focus of this study.

Although, exoskeletons have been around over 40 years ago, the last two decades have witnessed a significant development of exoskeletons and their enabling technologies (Anam & Al-Jumaily, 2012). Exoskeleton research and development has consequently emerged in three broad directions. One direction is for medical rehabilitation purposes which aim at assisting or resisting patients' movements to achieve therapeutic gains (Young & Ferris, 2017). Patients' affected limbs or muscles are trained by therapeutic exoskeletons to help regain functional motor ability, or to correct abnormal gait. Example of lower extremity exoskeletons in this category are the Lokomat treadmill gait trainer (Jezernik et al., 2003), the ANdROS gait rehabilitation system (Unluhisarcikli et al., 2011), the WalkTrainer gait re-education system (Bouri et al., 2006), the Lower extremity powered system (LOPES) for patients' gait re-learning (Veneman et al., 2007), and ALEX robotic system (Banala et al., 2009).

Another direction of exoskeleton research is focused on assisting impaired population like the frail elderly or subjects who suffered neurological impairments or muscular disorder following spinal cord injury (Young & Ferris, 2017). Research in this category seek to develop assistive exoskeletons that can help subjects to complete desired movements of daily living which are difficult on their own, such as walking, sit-to-stand, drinking, etc. Examples in this category are the ReWalk exoskeleton developed by ReWalk Robotic Inc., HAL-3 from Tsukuba University (Grüneberg et al., 2018; Hayashi et al., 2005) , Ekso exoskeleton from Ekso Bionic (Bionics, 2015), Honda Exoskeleton

(Buesing et al., 2015), Indego exoskeleton (Tefertiller et al., 2017), and REX Personal (Bogue, 2015).

The third category is exoskeleton for human performance augmentation (EHPA) which aimed at increasing the strength, endurance, and other physical capabilities of able-bodied individuals (Young & Ferris, 2017). This is the focus of this study. The following subsection presents a review of the state of art on active EHPA technology for lifting and carrying manual handling activities. Key aspects of EHPAs technology reviewed are hardware technology (i.e. DOFs, design, etc.), control methods, performance evaluation, and specific domain of application (i.e. work activities, affective region, injury prevention, etc.). Overall summary of EHPAs is presented in Table C1 in Appendix C.

2.5.1.1 Full-body EHPAs

i The Hardiman

EHPA research dates back from 1960 following the initiative of the US Defense Advanced Research Projects Agency (DARPA) to develop a performance augmentation device that could assist military personnel in heavy lifting and carrying under difficult situations. Logistics and support soldiers, on average, are believed to lift about 16,000 pounds of loads a day which pose a significant health concern (Army Technology, 2018). DARPA funded the research development with General Electric Company which resulted in the development of the Hardiman (Figure D1, Appendix D), the first practical EHPA (Fick & Makinson, 1971). Hardiman was hydraulically powered and full-bodied with self-weight of 680kg and total power consumption of 45kW.

It featured 30 active joints and had the ability to manipulate a 340-kg payload with one arm using a master-slave control concept. There were several design and control challenges to overcome for the Hardiman. Upper-body functionality of the Hardiman had significant success, however, the operation of the leg system for operator mobility was

less extensive and unsuccessful. Simultaneous operation of both legs of the Hardiman for operator walking resulted in violent and uncontrollable motion by the machine (Fick & Makinson, 1971). Also, a tested performance of the Hardiman in single support phase resulted in the operator grounding the master to the slave and rotating about the point of contact. The Hardiman project remained incomplete at the time of its termination (Fick & Makinson, 1971; Z. Q. Li et al., 2014). Similar challenges were also faced by contemporary researchers at the time of the Hardiman (Z. Q. Li et al., 2014; Vukobratovic et al., 1972). After failure of Hardiman project, research on EHPA slowed for over two decades. One of the important recommendations advanced by the Hardiman team is the need for improvement of the control logic of the leg system or possibly deactivation of certain joint servos to prevent a condition of over control and conflicting movements.

ii Hybrid Assistive Leg (HAL)

In Japan, the research on EHPA started about the same timeframe as DARPA funded exoskeletons (Z. Q. Li et al., 2014). The most prominent of these was the robot suit hybrid assistive limb (HAL) which was developed by Kawamoto et al. (2003), in Tsukuba University, Japan (Figure D2, Appendix D). HAL featured three prototype versions: an earlier lower-limb version (HAL-1) designed to enhance wearer's walking ability by amplifying wearers' own joint torque. Two later versions, full body, namely HAL-3 and HAL-5, designed to provide support for several daily activities like sit-to-stand and walking (Sankai, 2010). HAL primarily targeted elderly and disabled population in his earlier prototypes. The latest version, HAL-5, is conceived for lifting and carrying objects for application in the industries. Although, no performance evaluation data has been reported, HAL-5 prototype has been shown to have capability to hold and lift loads up to 70kg, with just a system mass of 23kg (Sankai, 2010). The investigators claimed that a

user wearing HAL can carry up to 40kg on the arm with increase in user's "leg press" capability from 100 to 180kg.

HAL is battery operated, and electrically actuated unlike the hydraulically driven DARPA funded exoskeletons. To provide physical support and mobility assistance, HAL uses two complementary controls: the *cybernic* voluntary control which rely on bioelectrical signal to estimate users' intention and to compute assistive joint torques; and the *cybernic* autonomous control which rely on sensors' measurements and centre of gravity (COG) shift to detect users' movements intention for tracking control. HAL uses the *cybernic* voluntary control for able-bodied personnel assistance and the *cybernic* autonomous control with reference tracking control for users in different health conditions especially patients with gait disorders (e.g. paraplegia) or with weak muscular power who have no bioelectric signal on their affected limbs. HAL's technique for synchronizing with the wearer's leg is by tracking control based on reference patterns obtained from healthy patient's walk. Development, testing and commercialisation of HAL for medical and assistive application has been largely successful, although performance data are limited (Young & Ferris, 2017). HAL is one of the few robotic exoskeletons to have received the FDA approval mainly for medical assistive purpose. For industrial purpose, HAL's performance testing are still required.

iii Nurse Power Assisting Suit

The Kanagawa Power Assisting Suit is one of the earliest EHPA from the same region and time as HAL. It is developed at the Kanagawa Institute of Technology in Japan to assist nurses in lifting patients and preventing back injuries (Yamamoto et al., 2003). It is a full-bodied exoskeleton intentionally designed to have no mechanical component on the front of the wearer to allow nurses to have direct physical contact while lifting or carrying a patient (Figure D3, Appendix D). The suit consists of shoulders, arms, back, waist and

legs units. The arms, waist and legs are actuated by direct-drive pneumatic rotary actuators to allow flexion and extension movements. The exoskeleton is made fully portable with air pressure supplied from micro air pumps mounted directly on each actuator and powered by portable Ni-Cd batteries. Muscle forces are sensed by a muscle hardness sensor utilizing a sensing tip mounted on a force sensing film device. For control, an embedded microcomputer combines the measured muscle forces with calculated joint torques (using joint angle measurements) to maintain pose and allow movements.

The suit was tested on the ability to aid a wearer in lifting a weight of 60kg up and down repeatedly, off-ground. It was shown that each unit of the suit could transmit assistive torque directly to each joint, however the biomechanical effect of the suit on the pilot or the effect on the lower back were not reported (K. Yamamoto et al., 2004).

iv Wearable Agri-Robot

Wearable Agri-Robot is another Japanese EHPA under development at the Tokyo University of Agriculture and Technology, Japan (Shigeki Toyama & Gohei Yamamoto, 2009). It is intended for agricultural purposes such as harvesting of Japanese radishes, cucumber, and fruit tree pruning (Shigeki Toyama & Gohei Yamamoto, 2009). Radish harvesting involves a repetition of certain movement pattern involving hand manipulation, squatting, etc. Wearable Agri-Robot is a full-bodied exoskeleton with a total of ten joints consisting of the shoulder, elbow, hip, knee, and ankle joints (Figure D4, Appendix D). The total weight of the device is placed at 30kg. The robot applies two modes of control. One is a "follow-up" PID control to drive motors attached at each joint. Sensors acquire joints angles information under this mode and generate target reference trajectory for each joint tracking PID controller. The authors indicated that Wearable Agri-Robot does not reduce body load under this control scheme (S. Toyama & G.

Yamamoto, 2009). The second mode memorizes the users' movement pattern and reproduce these patterns on the exoskeleton. This method is applied when there is predetermined movement pattern.

Performance evaluation of the exoskeleton was conducted for normal walking assistance which indicated that the exoskeleton could move with a delay of about 20ms to 120ms depending on which actuation systems is used. In the study, DC motor and supersonic wave motor actuation was compared and concluding remarks indicated that the supersonic actuation is better. The performance of the device with respect to metabolic consumption and the muscle activity reduction on a healthy subject was not reported.

v *The Panasonic Suits*

Another prominent EHPA from Japan is the Power Assist Suit developed by the Panasonic Activelink robot development arm of Panasonic for assisting workers in manual handling works (Brown, 2013). The company featured three versions of its prototypes. One is a huge robot exoskeleton suit called the Power Loader (Figure D5(a), Appendix D) which is equipped with 18 electromagnetic motors and intended for heavy lifting of loads up to 100 kilograms with little effort and stress on the lower-back (Brown, 2013). The second is a smaller hip prototype version known as the Power Assist Suit AWN-03 equipped with automatic assist mechanism (Russon, 2016), see Figure D5(b), Appendix D. The third version is known as the "Ninja" exoskeleton suite designed for workers and sportsmen who need to trek up steep, and uneven terrain like mountain trails (Russon, 2016). The "Ninja" exoskeleton suite features shoe sensors and two motors at the lower back to provide walking support (Figure D5(c), Appendix D). Media demonstration have been presented to showcase the performance of Panasonic power assist suites. There is evidence of limitations in the lower-limb mobility functionalities

however detailed system design, control functionalities, and performance data are not available in literatures to allow proper assessment.

vi The Body Extender

In the eurozone, research on EHPA have equally been ongoing (Stadler et al., 2014). The Body Extender (BE) exoskeleton from the Perceptual Robotics (PERCRO) laboratory of Scuola Superiore Sant'Anne, Italy, is one of the recent EHPA from the region (Fontana et al., 2014). It is a full body exoskeleton like DARPA's Hardiman and Panasonic's Power Loader (Figure D6, Appendix D). The Body Extender is electrically actuated with 22 modularly powered active DOFs (6-DOFs for each leg and 5-DoFs for each arm) and a weight of approximately 160kg. BE is reported to have capability of lifting 50kg of load and for potentially transporting loads up to 100kg at a walking speed of 0.5m/s. The functionalities of the BE include full body motion while standing (i.e. squatting, torso rotation, and arm movements), weight lifting/handling, and walking. The arm, torso, and lifted foot of BE are controlled with a simple tracking force controller with an inner (PI) velocity loop at the joints level that seeks to minimize the interaction forces at the physical interfaces between the human and machine (i.e. at the handles, backpack, snowboard bindings, etc.). The closing of the gripper is also force controlled via a closed-loop scheme that enable the operator to feel a fraction of the grasping force that the BE exerts on the manipulated object. For walking control, BE is equipped with a multistate (machine) architecture where states are managed with smooth transition phases implemented via weighted functions. Irrespective of the machine state, a feedforward component of gravity compensation of the self-weight of the machine is always introduced.

Performance functionality of the Body Extender was conducted for walking at low speed, squatting with no load, and lifting an object with one arm. The test showed users'

torque profile and power consumption data of the machine (Fontana et al., 2014). A maximum peak power consumption of approximately 750 W was reported during walking specifically during foot rising. No data for the biomechanical effect of BE on the user was reported (i.e. muscle activity reduction, metabolic cost, etc.). Like other full-body EHPA systems, the overall functionalities of BE are still underexploited. The machine currently presents several limitations. The user is solely responsible for the equilibrium of the machine. The speed of operation is practically slow even to accomplish basic task of walking, squatting, lifting, etc. Development of BE is still in progress.

2.5.1.2 Lower-Extremity Exoskeleton

i Human-powered Augmentation Lower Exoskeleton

A recent EHPA from China, under development at the School of Automation, Center of Robotics, University of Electronic Science and Technology of China, Chengdu, China is the Human-powered Augmentation Lower Exoskeleton (HUALEX). HUALEX system is described as an ergonomic and lightweight system for lower limb power augmentation and walking assistance (R. Huang, Cheng, Guo, Chen, et al., 2016). No specific application scenario is indicated. As shown in Figure E1, Appendix E, the HUALEX system has two active joints on the hip and knee joints of each leg which are actuated by DC servo motors. The authors described the ankle joint of HUALEX as energy storage systems with capability to store energy during stance phase of walking and release it during the swing phase. HUALEX system uses a hierarchical Interactive Learning (HIL) strategy for motion trajectory generation and control which suggest a way to reduce the need for sensory system. The motion trajectories are modeled with dynamic movement primitives (DMPs) and learned with locally weighted regression (LWR) method, in the high-level hierarchy, and in the lower hierarchy, reinforcement learning (RL) is applied to learn the model-based controller sensitivity factor to reduce the interaction forces – which is an improvement upon the SAC algorithm used in BLEEX (Rui Huang et al.,

2018). The performance of HUALEX was demonstrated by walking experiment which showed that the system could adapt to different pilots' motion after one gait cycle's correction. The system was also indicated to perform better at lower speed compared to high speeds. Reduction in metabolic cost of walking, or muscle activity, or other performance metrics have not been reported.

ii Quasi-active exoskeleton

In Korea, a quasi-active lower body exoskeleton for heavy load-carrying task has been under development at the Hanyang University, Seoul (W.-s. Kim et al., 2009; W. Kim et al., 2013). The exoskeleton is intended for carrying payloads (on the back) while walking on a level ground or climbing stairs. It features on each side of the lower limb, a quasi-active joint at the hip, an active joint on the knee joint, and another quasi-active joint on the ankle (Figure E2, Appendix E). It uses rotary actuator for the knee joint actuation and insole force sensor to detect the gait phase. Controls for the different gait phases are configured using the insole sensors. Overall system is 4DOF. To operate the system with a user, the degree of expansion of the muscles were determine by a proposed muscle stiffness sensor (MSS) (W.-s. Kim et al., 2009) or muscle volume sensor (MVC) (W. Kim et al., 2013), and combined with the human knee joint angle kinematics to compute a desired reference signal for a cascaded inner-loop PID controller used for driving the knee actuator. The authors concluded that the exoskeleton could carry a payload of 20kg while walking on flat ground or stairs and could decrease the wearer's muscle activity at the rectus femoris, vastus medialis, biceps femoris and gastrocnemius muscle group (W.-s. Kim et al., 2009). Additional reports show a decrease in maximum voluntary isomeric contraction (MVIC) at the Quadriceps and Gastrocnemius by an average of 40.5% while walking on a level ground and 12.5% when walking upstairs (W. Kim et al., 2013).

2.5.1.3 Upper Limb EHPAs

i Tokyo University of Science Muscle Suit

In Tokyo University of Science, Japan, Kobayashi et al. (2009) proposed an upper limb EHPA powered by McKibben artificial muscle to enable factory workers in lifting and carrying tasks (Figure F1, Appendix F). The introduction of artificial muscles renders the device lightweight; however, control of the muscle suit remains unresolved. In preliminary testing, the suit was found to decrease muscle power by 40% at the sacroiliac in a testing at an automobile factory, although subjects were restricted by the exoskeleton to perform squatting movements (hunker down), even though personnel in the automobile assembling factory must squat to do their job.

ii Tokyo Institute of Technology Power-Assist Robot Arm

Another upper limb EHPA using pneumatic artificial rubber muscles (PARMs) was proposed by Kadota et al. (2009) in Tokyo Institute of Technology, Japan (Figure F2, Appendix F). The EHPA was intended to assist motions related to load lifting. The robot arm uses three PARMs and a PI control (Proportional Integral control), which is based on the pressure value from a balloon sensor, for power-assist motion. To evaluate the effectiveness of the device, the authors measured EMG signals at the brachioradialis and biceps brachii of the arm from a subject performing lifting of a 10-kg object from the floor and back to the ground and, with a followed-up questionnaire, found noticeable decrease in the EMG signal amplitude however numerical values were not presented.

iii Hyundai Wearable Robot

In Korea, Ryu et al. (2012) proposed an upper-limb EHPA developed at Hyundai Rotem Company to unburden or lessen the human effort in handling heavy objects. The

exoskeleton applies a closed chain mechanism and a load distribution algorithm for load sharing between the robot and the human (Figure F3, Appendix F). The authors present an appealing design and simulation however real hardware implementation of the exoskeleton is currently unavailable: it is planned for future work.

iv Hanyang University Upper Extremity Exoskeleton

Another upper limb EHPA from Korea has been proposed by Lee et al. (2012) of the Hanyang University for lifting and handling purposes (Figure F4, Appendix F). The exoskeleton is designed as a 6-DOF upper limb mechanism and controlled by a human-robot cooperative controller using mechanical impedance and inverse dynamic torque controller. Motion following-performance experiment and muscle-strength-assisting effect experiment were conducted for the exoskeleton. Although the suit is still under laboratory research, the authors showed that the exoskeleton robot could follow the wearer's arm motions and decreased muscle activity at the biceps brachii, triceps brachii, deltoid posterior and deltoid anterior muscle of the arm while handling weight of 10kg.

v IKO

At the IKERLAN Technological Research Center, in Spain, a 5 DOF actuated upper-limb EHPA has also been proposed by Martinez et al. (2008) for human force amplification during routine workplace manual activities (which should include lifting and carrying) (Figure F5, Appendix F). Actuation of the exoskeleton is achieved by electrical motors and pneumatic muscles. The system is still under laboratory development and there is currently no reported human testing.

2.5.1.4 Single-Joint EHPAs

i Waist Power-Assisted Suit

Waist Power-Assisted Suit is a single joint EHPA under development at the Kogakuin University, Japan (Tsuzura et al., 2013), see Figure G1, Appendix G. The suite is designed to assist a caregiver waist against strain when performing nursing care of lifting patients. The prototype is actuated by a combination of direct drive motors and passive torsion springs. It is indicated to generate a considerably large torque that can reduce physical strain when lifting heavy weights. A total torque of up to 200Nm has been reported for the passive torsion spring version. Performance evaluation of the exoskeleton on the muscle activation level of the erector spinae muscle of the back were mentioned however no data were reported in support (Tsuzura et al., 2013).

ii RobotKnee

RobotKnee is a single joint (lower body) exoskeleton developed by Yobotics Inc. at the time of BLEEX and Sarcos-Raytheon (J. E. Pratt et al., 2004). It is designed to augment the knee power during walking and squatting. The device applies torque across the knee to allow the user's quadriceps muscles to relax. User intent is determined through the knee joint angle and ground reaction forces. It is indicated to enable a user to perform deep knee bend while carrying a significant load in a backpack (Jerry E Pratt et al., 2004). The device is actuated by a linear series elastic actuator (SEA) connected to the upper and lower portions of the knee brace (Figure G2, Appendix G). By implication, it can augment the power to the knee joint while at the same time exhibit a physically low-impedance interface to the wearer for safe usage. Performance evaluation of the device shows that a user was able to do one-legged deep knee bends with a 60 kg backpack load filled with sand without getting tired. However, the metabolic cost and the muscle activity reduction

metrics are not reported. One of the drawbacks of the RobotKnee is that it takes about 10mins to wear. Also, a user cannot sit when wearing it.

2.5.2 State of the Art in Active EHPA Control

Generally acknowledged requirement for EHPA control is that the control system must allow the wearer to be in charge of all movements activities while the EHPA should follow and assist this movement just like a biological extension of the wearer's limb (Stadler et al., 2014). This section presents a review of control methods currently adopted in active EHPA system for activities involving lifting and/or carrying. A summary of findings is organized in Table C2 in Appendix C.

2.5.2.1 Master-Slave Control

The master-slave control of exoskeleton robots implies a concept of control where one device known as the master has complete control over the movement and pose of another device called the slave. The operator must wear the master exoskeleton device suit which is equipped with measurement sensors to continuously capture the movement information and pose of the operator. The operator movement information is used as reference input signal for controlling the slave exoskeleton whose purpose is to carry the payload. The control modality ensures that each joint angle reference input from the master maps a corresponding joint on the slave exoskeleton thus tracking the movement of the human operator. Under this control scheme, the slave exoskeleton does not actually support or augment the movement of the pilot but follows it. In fact, the best master-slave design effectively ensures that the movement of the slave device does not collide with that of the master. The assistive principle is therefore achieved by having the slave do the job of carrying the payload to relieve the pilot, not physically augmenting the pilot's limb. The Hardiman is one of the earliest exoskeleton to apply the master-slave control method (Fick & Makinson, 1971). The internal exoskeleton of the Hardiman is the "master"

which is equipped with sensors and worn by the operator. The movement of the operator is thus captured and used (as reference signals) to command the external "slave" exoskeleton, giving the same physical sense as riding a bicycle (Fick & Makinson, 1971). The Nanyang Technological University exoskeleton suit is another EHPA that applied the master-slave control method to copy the human walking movement while load carrying (Low et al., 2006). The Hercule from RB3D also applied the master-slave control concept for walking and running in different terrains (B. Baker, 2012).

Perhaps, one of the limitations of a master-slave control concept is the complexity of the system design. A significant amount of design and control effort is required to ensure that the slave exoskeleton operate within the activity space of the master exoskeleton without colliding (Yang et al., 2017). Furthermore, how much muscular effort is reduced by this means still requires clarification to justify the complexity and the approach.

2.5.2.2 Force Feedback Control

In human-EHPA coupled systems, the critical forces/torques of interest are usually the forces or torques exerted on the exoskeleton by the pilot (i.e. human-robot interaction forces) which should be kept as small as possible to minimize energy expended by the user in driving the exoskeleton, or to such an extent that the pilot feels less the presence of the exoskeleton. By means of a force feedback control, it is possible to maintain these interaction forces at desired level relying on force/torque measurement from sensors or determination of forces from the physical characteristics of interaction like stiffness or mechanical impedance (Yang et al., 2017). Force feedback control may also be achieved indirectly by an inner position loop which computes a torque or force value (Yang et al., 2017).

Fontana et al. (2014) adopted a direct force tracking controller with inner PI velocity loop for the arm, torso, and lifted foot of the Body Extender (BE) exoskeleton that seeks

to minimize the interaction forces at the physical interfaces (see Section 2.5.1.1). They used force/torque sensors installed at the feet, trunk, and hand gripper to measure the interaction forces/torques. These are consequently converted to inner loop velocity references to drive the BE leaving the operator the possibility of feeling a fraction of the forces that the BE exerts on the payload. J. E. Pratt et al. (2004) applied a positive force feedback controller for the RobotKnee exoskeleton to decrease the effort of the quadriceps muscles and provide a physically low impedance across the users knee joint. The feedback force is derived from the ground reaction forces on the foot. Cao et al. (2009) also applied a direct force feedback controller on the knee of ELEBOT to decrease the human foot pressure with feedback force sensor located at the end of an hydraulic piston rod. Kadota et al. (2009) of the Tokyo Institute of Technology, Japan applied a force feedback with inner-loop pressure controller for the robot arm driven by pneumatic artificial rubber muscle (PARM). Force conversion to pressure was achieved by a balloon sensor. Lee et al. (2012) of the Hanyang university, Korea on the other hand applied an indirect torque feedback controller with a virtual mechanical impedance interface to generate reference motion and an inner-loop inverse dynamic controller to produce joint torque for the arm of a 6-DOF upper-limb exoskeleton robot (Section 2.5.1.3). Sensors acquire user's movement data with no reference trajectory specified. Shigeki Toyama and Gohei Yamamoto (2009) also applied an indirect force control with an inner-loop "follow-up" PID controller to drive motors attached at each joint of the Wearable Agri-robot.

A limitation of direct force feedback control approach is the need for expensive sensors to determine the pilot input forces or torques which can also increase size or complexity of the system design. Another limitation is the placement location for the sensors. In practice, it is difficult to place sensors in certain parts of human body which limits the possibility of obtaining interaction forces at those locations. The relative merit of the

indirect force feedback control with inner-loop position or impedance control can be investigated to simplify design.

2.5.2.3 Sensitivity amplification control

The sensitivity amplification control (SAC) was proposed by H. Kazerooni et al. (2005) at UC Berkeley for the control of BLEEX. SAC algorithm enabled a pilot wearing BLEEX to carry a payload while walking on level ground (Hami Kazerooni et al., 2005). A variant of the control has also been implemented by R. Huang et al. (2015) for the control of the HUALEX system. SAC is a form of indirect force feedback control. Theoretically, the principle of SAC is to specify a sensitivity factor that minimizes all the interaction forces and torques between the user and the exoskeleton to the extent that the exoskeleton shadows (or synchronizes with) the user's movement. The sensitivity factor is derived as a transfer function of the pilot's input torques to the exoskeleton angular velocities in a positive closed-loop feedback system. By adopting a positive feedback, SAC derails from the conventional negative feedback closed-loop control to become more sensitive and at the same time highly unstable to slight parameter variation or input disturbance forces. A potential advantage of the SAC method is that it removes the need for expensive sensors to measure the user's input torques or myoelectric signal for control, but determination of joint kinematic states of the exoskeleton is still needed (H. Kazerooni et al., 2005). The main limitations of SAC are the need for an accurate dynamic model of the exoskeleton and the high sensitivity of the control system to parameter variation. The controller could also amplify external disturbance forces (or torques) with no mechanism for distinguishing between these forces (or torques).

2.5.2.4 Gravity compensation control

The gravity compensation control is a classical approach to control which prescribes a torque term on a feedforward loop to cancel or compensate the effect of gravity on the

robotic mechanism (Babič et al., 2006). In human-exoskeleton systems, it can be used to compensate the weight of the pilot and the device, given kinematics and inertia informations. Petric et al. (2013) applied the gravity compensation control strategy on a knee exoskeleton to study the influence of noninvasive control methods on repetitive squatting motion of able-bodied human subjects. Overall, the device was found to augment the knee power of the subjects while reducing their musculoskeletal torque, however, the controller was seen attempting to always extend the knee, even when the wearer is trying to perform a squat. The mechanism was found to comply only when the subjects pushes down with its weight and muscles to override the motor torque.

2.5.2.5 Myoelectric Control

Myoelectric control is a technique of control which is concerned with the detection, processing, classification, and application of myoelectric signals from the human muscles to control the assisting robots (Oskoei et al., 2007). An important aspect of myoelectric control is its useful application in movement intention driven systems. The human central nervous system sends signals to change the surface muscle electrical signal which often precede muscular contraction or limb movements. This fact enables prompt detection of human movement intention and adequate time to process and compute exoskeleton control signal to synchronize with the machine. One of the most successful exoskeleton projects that have applied myoelectricity control for is the Japanese HAL. Kawamoto et al. (2003) reports the application of myoelectricity to control a HAL-3 robot to provide direct joint torque assistance for walking corresponding to the operator's intention. In conjunction with a feedback controller, they could adjust the assist torque. Sawicki and Ferris (2008) also employed the proportional myoelectric control on a pneumatically powered ankle exoskeleton to provide ankle joint assistance with the aim to reduce metabolic cost of walking.

The application of myoelectricity however presents some shortcomings. There is the inconsistencies problem of estimated EMG signals from different subjects or from a particular subject under different motion trials which would demand a recalibration of the control system each time a subject or session has changed (Kiguchi et al., 2001). And, since many muscles are involved in a motion, it is still difficult to predict accurately the actual movement intended by the user (Cao et al., 2006; Kiguchi et al., 2001). Furthermore, under prolong working conditions or strenuous exercises, the quality of EMG signal can also be affected seriously by sweat or fatigue. The sensor can fall off or shift from its placement which would affect the signal quality. Noise, placement of electrodes, user skin condition, muscle mass, etc. affects signal quality. Another shortcoming is that the sensor needs to be attached to the users' body which may not be convenient in actual work situation.

2.5.2.6 Dynamic Movement Primitive

DMPs are a set of nonlinear dynamic systems for generating discrete and periodic movement behaviors (Ijspeert et al., 2013; Kimura et al., 2006). They are considered building blocks like motor pattern generator (MPG) in neurobiology (Marder, 2000; Selverston, 1980) that can be modulated in real time by a learning signal or forcing signal (e.g. sensor signals etc.) to generate or reproduce complex trajectories, control signals, or movements. Dynamic movement primitive suggests a general notion that kinematic representation of complex movement behavior is more advantageous than direct motor command since it allows independent workspace planning (although it is possible to apply DMPs for direct motor commands). DMPs have been applied for imitation learning with humanoid robots (Ijspeert et al., 2002). In active EHPAs application, R. Huang, Cheng, Guo, Chen, et al. (2016) and the team at the University of Electronic Science and Technology, China, applied DMPs on HUALEX system (see Section 2.5.1.2) to learn and predict in real time the natural walking gait of a wearer; and applied a locally weighted

regression (LWR) to update the DMP incrementally. The HUALEX system was shown to follow pilot's motion after one gait cycle's correction. Kamali et al. (2016) also applied DMP as a trajectory generator for the standing up movement using a library of training data and initial joint angles as input to predict the wearer's standing up trajectory. They applied a low-level impedance controller to drive the exoskeleton using the predicted trajectory. Using the control strategy, Kamali et al. (2016) showed that the system could decrease the user's average muscle activity.

One of the limitations of DMP is its robustness to generate accurate movements in dynamic interaction situation or constraint environment (Gams et al., 2014; R. Huang, Cheng, Guo, Lin, et al., 2016). An effective learning framework (e.g. LWR, reinforcement learning, etc.) to deal with variable interaction dynamics from different wearers, or the same wearer in different walking patterns is often required (Gams et al., 2014). Another limitation is the difficulty in formulating an appropriate -starting point- control policy (i.e. sets of nonlinear dynamic equations) that fit a particular movement behavior, which may require expertise (Ijspeert et al., 2013).

2.5.2.7 Adaptive Frequency Oscillator

Adaptive frequency oscillator (AFO) is a nonlinear oscillator introduced by Righetti et al. (2006) for reproducing periodic movements. It is basically a unique DMP with limit cycle attractor landscape capable of synchronizing with a periodic signal and extracting its features (like frequency, amplitude, envelop, etc.) in dedicated states variables (Righetti et al., 2006; Ronsse, Lenzi, et al., 2011). AFOs work as predictive state observers. They have capabilities of predicting future walking pattern (joint positions) of a subject based on patterns learned during preceding cycles. Robotic assistance is then provided by attracting the subject's joints to this future positions using either a force field (Ronsse, Koopman, et al., 2011), or a position controller (Ronsse et al., 2012). Lenzi et

al. (2013) applied AFOs in ALEX II exoskeleton to assist the human hip during walking and showed that the system could reduce both hip and ankle muscle activation of the users. Ronsse, Koopman, et al. (2011) applied AFO on LOPES treadmill to assist participants in a walking task and showed a significant decrease in energy expenditure (4.2~5W/kg). Ronsse et al. (2012) also applied AFOs to infer temporal derivatives - velocity and acceleration- of human walking gait from noisy position signal derived from a user wearing LOPES lower-limb exoskeleton. Petric et al. (2013) applied AFO combined with an adaptive Fourier series on a testbed knee exoskeleton device to augment wearers' knee torque in repetitive squatting motion and showed the feasibility of the approach for movement adaptation and synchronization.

A potential limitation of traditional AFOs is that they are effective for predicting only uniform periodic movements, which makes them less attractive for complex movement behaviors atypical in industrial work situation. Matsubara et al. (2012) suggested, in a simulation study, an improvement to the traditional AFOs by separating the gait pattern adaptation into style and phase parameters to account for the diversity (style) in human walking.

2.5.2.8 FSM Based Control

A finite state machine (FSM) or finite state automaton is a mathematical model of computation that can be implemented with hardware or software to simulate sequential logic or to drive discrete events systems (Hopcroft et al., 2001). A hybrid automaton version models a mixed discrete and continuous system. FSM can change from one state to another in response to some external inputs. The change from one state to another is called a transition. An FSM is defined by several states, a default transition state (initial state), events, and conditions for state transitions. Finite state machines can be used to model problems in many fields including mathematics, artificial intelligence, games, and

linguistics. A system where some inputs cause some changes in state can be represented using finite state machines. Fontana et al. (2014) applied multistate finite state machine to the Body Extender for walking control. The authors managed smooth states transition via weighted functions. L. H. Huang et al. (2005) applied a hardware implemented state machine to transit between stance, swing, heel-strike, and toe-off of BLEEX for walking assistance. To decide which state each leg is in, two sets of digital pressure activated footswitches are used to provide information to the controller about the foot status of each leg.

2.5.2.9 Hybrid Control

L. H. Huang et al. (2005) applied the hybrid control approach to control the walking gait cycle of a pilot wearing BLEEX and showed that the control system added robustness to the changing BLEEX payload. Under the control scheme, the walking gait cycle was divided into stance control and swing control phases. Position control was used for the BLEEX leg in stance phase (including the torso and backpack) and a sensitivity amplification controller was used for the swing leg. The hybrid controller did not require a good model of the BLEEX torso and payload, which was a disadvantage in earlier implementation of BLEEX with SAC. However, one of the shortcomings of the proposed hybrid approach was the need for the human to wear seven inclinometers to measure human limb and torso angles in order to effectively implement the position control mode. These sensors require careful design and setup time. Fontana et al. (2014) also applied hybrid control for the Body Extender: a direct force control for the lifted arm, torso, and foot, and a multistate finite state machine to control walking motion. No specific advantage was reported for the hybrid structure.

2.5.3 Highlights of Design and Control Challenges in Active EHPA for Lifting and Carrying

2.5.3.1 Design Limitations

Hardware design may not be considered complete or satisfactory without addressing concerns such as weight, size, cost, design complexity, ease of movement, flexibility of use, and the ability to decrease the load burden on the user. Majority of the reviewed EHPAs still require considerable improvements in one or more of these aspects.

With respect to flexibility and ease of movement, some of the EHPA have used a fewer amount of DOFs which can affect the execution of certain movements. The human arm has 7 degrees of freedom: 3-DOF at the shoulder ball and socket joint, 1-DOF at the elbow joint, and another 3-DOF at the wrist (Sturman, 1992). The human leg also has a total of 7-DOF: 3-DOF at the hip ball and socket joint, 1-DOF at the knee hinge joint, and 3-DOF at the ankle joint. To move flexibly with the human limbs, the exoskeleton is required to permit similar degree of freedom as the human limbs. Some design mechanisms have been seen to restrict certain movement like the ability to sit or squat (see Table C2 in Appendix C).

Weight is still a major issue in many designs. Attempt to minimize weight would influence other design considerations. For example, there is a proportional relationship between the maximum torque output of actuators and their weight which influences the overall weight of exoskeleton design. To maintain lightweight design, a dilemma is created that necessitate a tradeoff of needed actuating torque/power for weight reduction or heavy weight for high actuating torque. Another tradeoff exists for the cost and choice of material in deciding the strength/weight of the needed material (to withstand payload). Aluminum and carbon fiber have been more popular in this regard to meet certain design requirements.

Design intuitiveness for weight reduction is required. For virtually all the upper limb EHPAs covered, the weight of the exoskeleton and load is borne entirely by the wearer without any mechanism for diverting the weight to the ground. This is a critical design issue that would rather put workers at increased risk of MSD of the lower extremities. A mechanism to divert this weight would be beneficial, or the use of lighter materials/actuators with significant power output like pneumatic muscles may also benefit researches in this direction.

Design for specific application is also required. For example, military type exoskeleton that uses a back support to carry loads may be impractical for industrial manual handling or caregiving task were lifting and carrying work are mainly performed over short distances with the use of the hand.

2.5.3.2 Controller Limitations

Controller is a weakness in many of the EHPAs. Currently, many of the control implementation cannot be considered satisfactory to meet the requirement for industrial application. An effective control method for industrial EHPAs should enable the exoskeleton to augment the wearers' musculoskeletal power to decrease muscular effort or muscle activation, while following or synchronizing with the users' entire movement (like a biological extension of the limb). In some of the reviewed EHPA systems, the control actions can be found to restrict certain users' movement (Kobayashi et al., 2009), or movements of some body segments (Gui et al., 2007; Yang et al., 2009) (Table C2 in Appendix C). Some controller actions can be found to overextend the user's limb or impose undesired movements (Petric et al., 2013), whereas some are highly unstable to parameter variation and disturbance forces (H. Kazerooni et al., 2005). Many of the EHPAs still suffer from slow controller response rate due to the lag in the communication

protocols and some can be found to result in very slow movement of the exoskeleton in performing even simple basic task (Fontana et al., 2014).

In some EHPA, the control mechanisms do not actually lead to a physical augmentation of the users' limb but ensures that the exoskeleton follows the user's motion, e.g. the master-slave control system. For such controllers, the pilot must perform movements that drives the exoskeleton (while wearing a master exoskeleton suit). How much energy the pilot expends by this action still need to be clarified.

Virtually all EPHAs covered have not been applied or tested for multiple industry tasks or a complete workflow operation of lifting and carrying that involves combination of squatting under load, lowering, standing, walking, sit-to-stand, and stand-to-sit, etc. Some EHPAs have featured on media show demonstrating important feat but with no scientific documentation. Perhaps a next step would be to test EHPA controllers for a completely simulated work operation to ascertain their effectiveness and usefulness, task-based, and to study their weaknesses for further improvements.

Hybrid control technique has proven useful in combining different controller strength in one control architecture. For example, using a force feedback controller for the exoskeleton lifted arm and an FSM based controller for lower limb walking assistance; or using force feedback for stance phase of walking and a position controller for swing. However, a few EHPA studies have applied this concept. It is still unclear which control action results in the best performance. Switching problems and other control modalities are important issues with hybrid system which have not been fully resolved.

2.5.3.3 Performance Reporting

One of the major limitations in the progress of EHPA developments and control is the paucity of performance data as well as the weaknesses in some of the approaches to

performance reporting. Many studies covered have reported only feasibility studies which is currently not sufficient for overall assessment of their proposed technology (Young & Ferris, 2017). Some EHPAs have also been shown in the media with several ecstatic features and some demonstrated performance feat but with no performance data in support. The absence of scientific documentation for current EHPAs performance is a hindrance to progress in future EHPAs development.

2.6 Literature Review Summary

This chapter has systematically reviewed existing literatures (within the scope of study) on lifting and carrying manual handling activities in the industries and has unveiled the health hazards/disorders related to these activities through epidemiological and biomechanical studies. The most dominant injuries/disorders that are found related to lifting and carrying activities are knee/hip osteoarthritis (OA), meniscal knee damage and low back pain (LBP). More consistent biomechanical causal factors of these injuries are weaknesses, muscle deficit, or fatigue of the lower extremity muscles (particularly the Quadricep femoris) due to overuse of muscles in frequent or repetitive squatting and walking movements, lifting/carrying, or heavy lifting/carrying task. These biomechanical factors influence stability; load distribution on the knee, hip, and low back; the wear and tear of the articular (hyaline) joint cartilage; and the counteractive loading effect on the lumbar region which are pathogenesis for onset, severity and progression of the disorders (Amin et al., 2008; K. L. Bennell et al., 2013; Reid et al., 2010).

Existing workplace interventions to curb these disorders such as trainings and education on correct posture, the use of personal protective equipment, pacing of work, introduction of microbreaks, exercise therapy, mechanical assistance and automation have not been enough to tackle these disorders. An effective intervention directly addressing the biomechanical causation of these disorders is required.

This chapter also reviewed the state of art in EHPA technology developed as interventions to assist lifting/carrying manual handling activities with focus on technologies for performance efficiency and technologies tailored to address injuries/disorders related to these activities. Several design and control challenges are currently a limitation in EHPA research that requires attention before a functional EHPA can reach the workplace. Lack of performance data or performance reporting is also a big stumbling block in evaluating the technology of some EHPAs or judging their potency for industry. Currently, there is no EHPA that is certified to have met all requirement for intervention in the industry. Moreover, there is hardly evidence of technological focus in many of the EHPAs researches targeted specifically for primary prevention of severe workplace injuries like knee/hip OA, and meniscal tear which can lead to lifelong immobility for workers (Appendix C).

Overall, the following are summary of the important findings, or gaps in EHPA research for lifting and carrying manual handling activities based on the comprehensive literature review:

1. There is urgent need for intervention in manual lifting and carrying activities to prevent long term mobility disability or lower limb joints' failure especially of the knee.
2. There is need for more effective EHPAs (as workplace intervention) for lower extremity augmentation directly addressing the biomechanical causation of disorders in manual lifting and carrying activities.
3. There is need for design improvement of EHPAs to achieve lightweight for decrease burden on wearer; and the need for EHPAs with sufficient degrees of freedom on the lower extremities to permit ease of movement.

4. There is the need for control improvements in current EHPA technology to permit synchronous or smooth movement assistance for lifting and carrying manual handling activities.
5. There is also need for improved EHPA design and control for accurate detection and synchronization of wearers movement (for prompt assistance) in diverse manual handling activities such as in multiple industry tasks or a complete workflow operation of lifting and carrying that involves combination of squatting, lowering, standing, and walking movement transitions.
6. Lastly, there is need for improved performance reporting of EHPA to facilitate technological improvement.

Based on these findings, this study will seek to resolve the following questions:

1. Given the complexity of lower extremity biomechanics and motion transitions (i.e. squatting-to-standing-to-walking, etc.) in lifting and carrying MH task and given the knowledge of the biomechanical factors in injury causation, how can a suitable dynamic model of an EHPA be developed to accommodate the dynamics of this task?
2. Given a suitable model of an EHPA for the lifting and carrying MH task, what effective control algorithm can be developed for the EHPA to enable synchronous smooth movement assistance/augmentation for its pilot with maximal assistive benefit?
3. Finally, what appropriate design specifications can be applied in the development of an actual lightweight lower extremity EHPA prototype to enable efficient utilization of the control algorithm for lifting and carrying MH task?

CHAPTER 3: METHODOLOGY

3.1 Introduction

This chapter presents the methodology of study. It is organized in three parts. The first part (Section 3.2) highlights the literature review method adopted in the study. The second part gives highlight of the design method (Section 3.3). The last part (Section 3.4) gives an overview of the study design which include the study setup, study population, procedure, and data analysis. The overall overview of the research methodology in this chapter is depicted in the flow chart in Figure 3.1.

3.2 Design Method

The design of the EHPA is based on cues from literature review. The design is motivated to augment the lower extremity for squat-lifting, walking and carrying manual handling. To facilitate the design, the biomechanics of the human movements in activities of lifting and carrying (involving squatting and walking) are analyzed (Section 4.2) primarily to determine design requirements such as motor torque, mechanical power, and range of motion (ROM) as well as to facilitate the development of the modality of control. This is followed by development of the EHPA CAD model in SolidWorks IDE environment (Section 4.3.1). The dynamic model of the EHPA is derived based on the CAD model plus analysis of the human biomechanics (Section 4.3.2). This model is applied for the controller design (Section 4.3.3). Prototyping of the EHPA follows a simulated evaluation of the controller performances and derivation of operating parameters. The block diagram in Figure 3.2 gives a simplified flow of the design method. More details in Chapter 4.

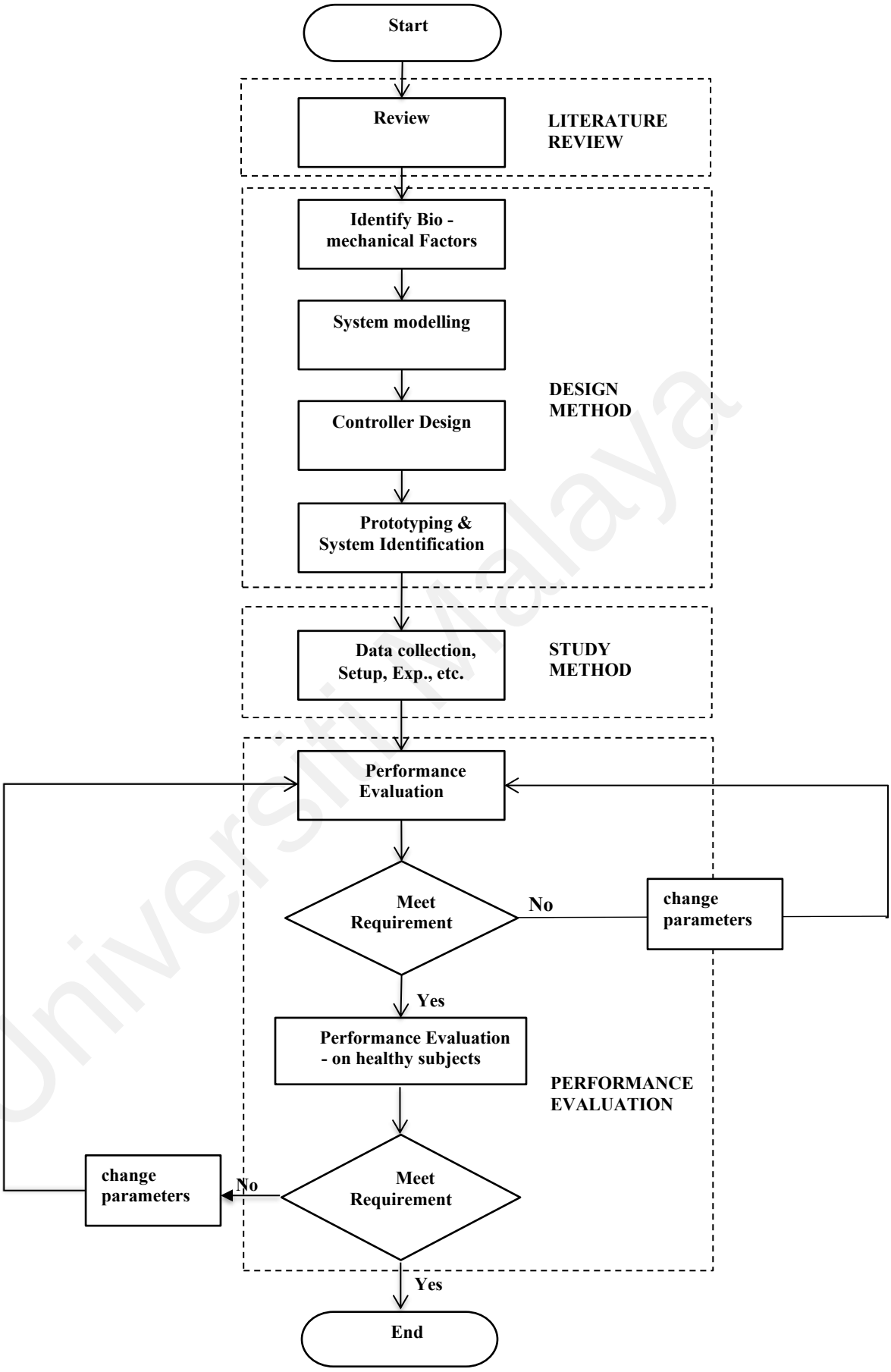

Figure 3.1: Research Methodology Flowchart

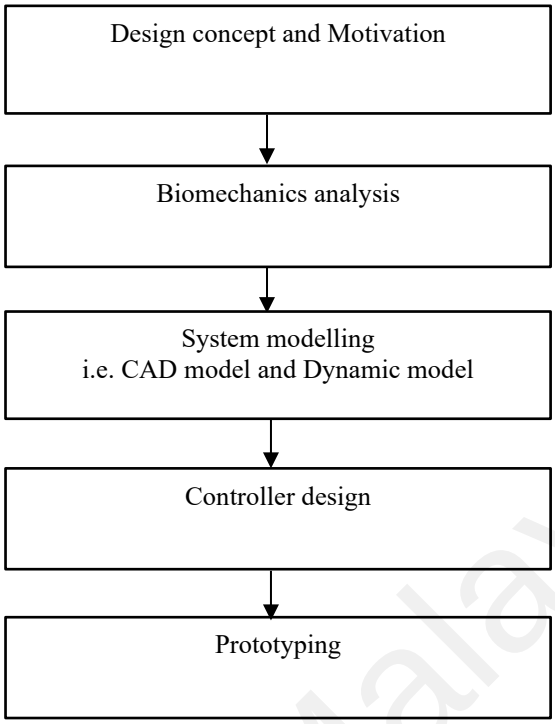

Figure 3.2: Design method

3.3 Study Method

As detailed in the following sequel, this section presents the method, protocol, and design of study for data collection, experiment, and data analysis in testing the biomechanical effect, wearers perception, and kinematic/kinetic performance of the prototype EHPA (UMExoLEA).

3.3.1 Study Design

The approach to experiment, data collection and data analysis in testing the biomechanical effect and wearers perception is an experimental crossover design approach. A crossover design is a repeated measurements design whereby each eligible participant in the study receives different treatments/intervention during different time periods, and crossover from one treatment (for example, no-exoskeleton assist) to another treatment (for example, exoskeleton assist) during the course of the trials (Piantadosi, 2017). In this way, each patient serves as his own matched control and the outcome can

thus be monitored appropriately during/after each period of treatment or intervention. To minimize the possibility of bias in a crossover design, a "wash out" period of treatment is introduced between treatments to eliminate any carry over effect that may result from a treatment (Coggon et al., 2009).

A crossover design is particularly useful when outcome of an intervention is measured by reports of subjective symptoms (for example, pain, discomfort, or fatigue), or when the effects of treatment are short lived (for example, pain relief or assistance effect from the use of an intervention) (Coggon et al., 2009). Another important reason for a crossover design is that it can yield a more efficient comparison of treatment outcome with fewer number of subjects to attain the same level of statistical power or precision as compared to the parallel controlled trials (on different participants) without crossover (Coggon et al., 2009).

The order of treatment/intervention administration in a crossover experiment is called a sequence and the time of a treatment/intervention administration is called a period, see Table 3.1. The treatments/interventions are usually designated with capital letters, such as A (e.g. no exoskeleton intervention), B (e.g. with exoskeleton intervention). For the randomized crossover design, the order of treatment/intervention is normally randomized, potentially, so that different patients receive treatment/intervention in different sequence, and often the sequences are determined beforehand and the participants randomized to sequences (Piantadosi, 2017). The most popular crossover design is the 2-sequence, 2-period, 2-treatment crossover design, with sequences AB and BA, sometimes called the 2×2 crossover design as shown in Table 3.1. Participants that are randomized to the AB sequence receive treatment A in the first period and treatment B in the second period, whereas participants that are randomized to the BA sequence receive treatment B in the first period and treatment A in the second period.

Table 3.1: Crossover design

Study Design	Period 1 (No Exo)	Period 2 (Exo)
Sequence AB	A	B
Sequence BA	B	A

In the current study, two treatments are performed on study participants to test the biomechanical effects and wearers perception of the EHPA intervention. These are labelled A – no exoskeleton assistance/intervention, and B – exoskeleton intervention/assistance. Consequently, three outcomes are evaluated after every treatment sequence namely: (1) the reduction in muscle effort/activation on the lower extremity due to exoskeleton torque assistance; (2) the subjective rating of perceived effort reduction and perceived assistance from UMExoLEA and (3) the subjective rating of fatigue/discomfort on the lower extremity musculature and lumbar spine. More discussion is given in the following subsections. Other performance outcome includes tracking of motor torque, and supervisory control: i.e. movement detection, and movement synchronization which are determined from kinematic/kinetic sensor data during exoskeleton assisted movements (treatment B) – details of these are presented in Chapter 6.

3.3.2 Sample Size Determination

Sample size determination is crucial in experimental studies that require testing the effect of an intervention on sampled populations. The determination of sample size is influenced by the need for precision (for example, the need to attain 95% confidence interval for mean within $\pm\delta$units) or statistical power (for example, 0.80 or 0.90 statistical power (1-β) for a hypothesis test). Validity and unbiasedness is not necessarily considered related to sample size(B. Jones & Kenward, 2014; C.-S. Li & Davis, 2016).

For a 2 × 2 crossover design AB|BA, the total sample size, n, required for a two-sided, α significance level test with 100(1 − β) % statistical power and effect size $\mu_A - \mu_B$ is given as (Chow et al., 2017)

$$n = \left(z_{1-\alpha/2} + z_{1-\beta}\right)^2 \sigma^2 / (\mu_A - \mu_B)^2 \quad (3.1)$$

where μ_A and μ_B represent means for the direct effects of treatments A and B, respectively. This formula involves percentiles, z , from the standard normal distribution. The percentiles of interest for the two-sided hypothesis test with significance level α and statistical power (1 − β) are $z_{(1-\alpha/2)}$ and $z_{(1-\beta)}$. For a one-sided hypothesis test, $z_{(1-\alpha)}$ is used instead. The common choices for α are 0.05 and 0.01, and for β are 0.20 and 0.10, so the percentiles of interest are usually determined as:

$$z_{0.995} = 2.58, z_{0.99} = 2.33, z_{0.975} = 1.96, z_{0.95} = 1.65, z_{0.90} = 1.28, z_{0.80} = 0.84$$

Figure 3.3 shows an example of the 2.5th percentile and the 97.5th percentile on the normal distribution graph.

In (3.1), σ^2 denotes variance which is given as

$$\sigma^2 = 1.0(W_{AA} + W_{BB}) - 2.0(W_{AB}) + (\sigma_{AA} + \sigma_{BB}) \quad (3.2)$$

where W_{AA} represent between-subject variance for treatment A (no Exo) and W_{BB} represent between-subject variance for treatment B (with Exo). W_{AB} represent between-subject covariance between treatments A and B; σ_{AA} represent within-subject variance for treatment A; and σ_{BB} represent within subject variance for treatment B.

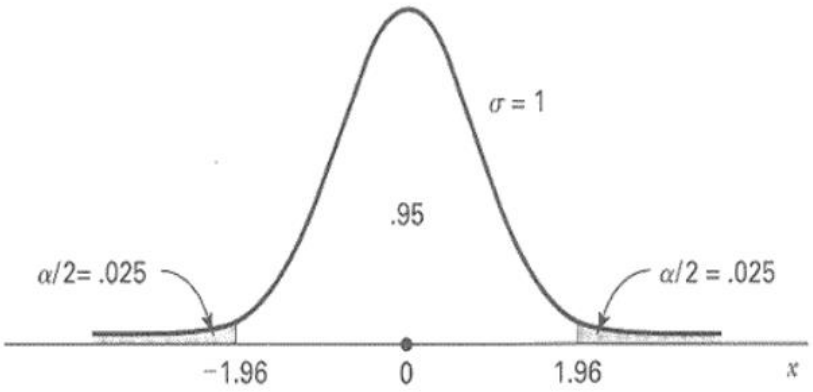

Figure 3.3: The 2.5th percentile and the 97.5th percentile on the normal distribution graph

Thus, to apply a 0.05 significance level test with 90% statistical power for detecting the effect size of $\mu_A - \mu_B = 1$, from published results, if the investigator assumes that:

$W_{AA} = W_{BB} = W_{AB} = x$, and

$\sigma_{AA} = \sigma_{BB} = 0.75$

The sample size is therefore n = 16 (from Equation (3.1))

3.3.3 Statistical Analysis

The common statistical analyses tools for a 2×2 crossover trial are the A two-way analysis of variance (ANOVA) test with repeated measures (Gueorguieva & Krystal, 2004), or the two-sample t test (Senn & Senn, 2002), or a Wilcoxon rank sum test (Senn & Senn, 2002). The estimated differences in treatment means (i.e. $\mu_A - \mu_B$) in two-period, two-treatment designs are usually the primary interest of statistical analysis. It may also be necessary to estimate the variance of the treatment mean, that is, between-subjects variability (i.e. W_{AA}, W_{BB}, W_{AB}, etc.) and within-subject variability (σ_{AA} , σ_{BB}, etc.). Where between-subject variability accounts for the dispersion in measurements from one subject to another, within-subject variability accounts for the dispersion in measurements from one time point to another for a given subject. In the current study, the

primary interest of study is the difference in estimated means between treatment A (i.e. no Exoskeleton assist) and treatment B (i.e. Exoskeleton assist).

Given a normally-distributed data from a 2 × 2 crossover trial, the statistical analysis is relatively straightforward if statistical bias or nuisance effect are assumed minimal or can be eliminated. Nuisance effect include period, sequence, or carryover effect. For example, in Table 3.2, if the nuisance effects for sequence, period, and first-order carryover are included, then the statistical model can be written thus:

Table 3.2: Crossover design with nuisance effect

Study Design	**Period 1**	**Period 2**
Sequence AB	$\mu_A + \nu + \rho$	$\mu_B + \nu - \rho + \lambda_A$
Sequence BA	$\mu_B - \nu + \rho$	$\mu_A + \nu - \rho + \lambda_B$

where ν represents a sequence effect, ρ represents a period effect, and λ_A and λ_B represent carryover effects of treatments A and B, respectively.

The difference in the treatment means for a given subject in the AB sequence is therefore given as:

$$\mu_{AB} = \mu_A - \mu_B + 2\rho + \lambda_A \quad (3.3)$$

And the difference for a subject in the BA sequence is given as:

$$\mu_{BA} = \mu_B - \mu_A + 2\rho + \lambda_B \quad (3.4)$$

If the wash-out periods are of adequate length, the carryover effects may be assumed equal or negligible, i.e. $\lambda_A = \lambda_B = \lambda$. Therefore, the mean differences in treatment for every subject (across periods) can be computed and compared between the two sequences using the two-way ANOVA test, the two-sample t test, or a Wilcoxon rank sum test with repeated measures.

The analysis test for the hypothesis:

H_0: $\mu_{AB} - \mu_{BA} = 0$

Since the expression: $\mu_{AB} - \mu_{BA} = 2(\mu_A - \mu_B)$ where $\lambda_A = \lambda_B = \lambda$, testing the null hypothesis H_0: $\mu_{AB} - \mu_{BA} = 0$, is equivalent to testing:

H_0: $\mu_A - \mu_B = 0$.

Thus, in this study, the statistical analysis is designed to reject the null hypothesis that $\mu_A - \mu_B = 0$ since we expect significant difference in the *within-subject* treatment mean between exoskeleton assistance and no exoskeleton assistance.

3.3.4 Study Setup and Protocol

This section highlights the procedure for data collection in the study.

3.3.4.1 Data Collection

Three types of data are collected in this study: (1) biomechanical data from EMG sensors; (2) quantitative data from questionnaires; and (3) kinematic/kinetic data from potentiometer, ground reaction force sensors, and torque sensors. The biomechanical data and questionnaire data are obtained in controlled crossover experiments (already explained). Kinetic/kinematic data are obtained in the exoskeleton assisted period (Treatment B) to test the supervisory control: i.e. movement detection and synchronization (detailed in Chapter 7). The biomechanical data include muscle activity determined from EMG data. EMG sensors from Shimmer Sensing Technology are used to collect these data. Figure 3.4 shows the setup of the EMG sensors. Three of the sensors are firmly attached at the location of the right Vastus Medialis (VM), right Rectus Femoris (RF), and the right Gastrocnemius (GA) on each participant. These muscles are key contributors to motion during squatting and walking. Rectus femoris is one of the

Quadriceps muscles for hip flexion and knee extension. Vastus Medialis is another Quadriceps muscle primarily for knee extension; while GA is a two-headed muscle at the back of calf for plantar flexion of the ankle/foot and knee flexion. The choice of Vastus Medialis over Vastus Lateralis (another Quadriceps muscle) in this study is strictly informed by placement convenience. Previous studies report no difference between vastus medialis and vastus lateralis activations during lower body resistance training (Escamilla, 2001; Signorile et al., 1994).

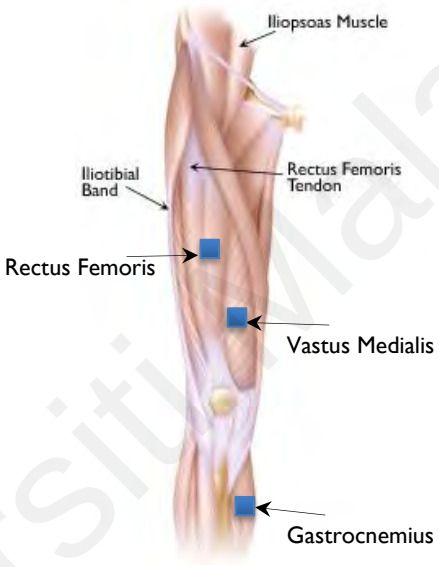

Figure 3.4: Position of placement of the EMG sensors.

3.3.4.2 Study Population

The initial number of participants recruited for the experimental study are fifteen (15) male subjects with mean age of 25 ± 7 years, mean height of 175 ± 7cm, and mean weight of 77 ± 5kg (Table 3.3). These participants are drawn randomly from different research units, manufacturing centers, and workshops across the main campus of University of Malaya. To be eligible, the physiological features of the participant such as height (>175cm) and weight (70-85kg) are considered in the selection to ensure fitness with the exoskeleton suite. Typically, participants are excluded from the study if they (are obese or) had suffered any neurological or musculoskeletal disorders that could affect their

capacity to perform lifting, squatting, carrying, or walking activities; and if they had sustained injury to the lower or upper limbs, or to the back region which required treatment within the last 12 months prior to study; or if they had engaged in prolong strenuous work/exercise that caused significant muscular fatigue on the muscles a day prior to experiment.

The ethics clearance for the experimental study is granted by the University of Malaya Research Ethics Committee (UMREC). In compliance with the ethics regulation, all the participants are required to give written informed consent prior to experiment.

Table 3.3: Study population

Population	**Data**
Initially recruited	20
Participants	15
Age	25 - 37 years
Height	175 – 180 cm
Gender	Male
Weight	70 – 81 kg
BMI	22.85 – 25kg/m^2
Industry	CPDM, Mechanical Engineering Workshop, Concrete Lab, Civil Eng. Lab,

3.3.4.3 Procedure

Foremost, to ensure safety and smooth experiment, the experimental protocol demands that participants are guided on the functionalities of the wearable EHPA suit and how to use the power-down switch to shut-down the system for safety in case of severe discomfort/pain and emergency. Preliminary tests are also included to acquaint the participants with the operation of the exoskeleton.

The experiments performed in the study are repetitive load lifting and load lifting/carrying industrial manual handling task. Load lifting task in the experiment involved squatting movements whereas load carrying involved walking movements. The weight of the object (lifted/carried) in the study is 9.5kg which can be considered moderate in a typical industrial scenario. Two periods of experiment are performed for each task, see Figure 3.5. The first period involves lifting or lifting/carrying experiments without wearing the suite, and the second period involve same experiments with active support from the EHPA suite. In all, the experiments are split into three tasks (as presented in the following subsections) stretched over 2 hours per day for each participant. A maximum of two participants could perform experiments in a day, however in some days only one or none is available extending the data collection period to two months.

(a) ***Task 1***

The first task is a lifting task which involve lifting a box weighing 9.5kg from the ground by upright squatting method without performing walking motion. This is repeated three times and would be considered one trial. Muscle activity data are recorded on selected muscles throughout the trial. The maximum voluntary contraction (MVC) and the root mean square average (RMSA) of the EMG signal are estimated across repeated trials. In this task, a total of three trials is to be performed by each participant (see Figure 3.5) with approximately 2mins resting interval (wash-over) between each trial to allow muscles to recuperate, minimize fatigue or possible cofounder. The task is performed in two crossover periods: A – no exoskeleton suite and B – active support from exoskeleton suite (Figure 3.5). Between period wash over is 5mins. This period is also used to administer the trial-by-trial based questionnaire to obtain quantitative wearer's responses to perceived discomfort/fatigue or assistance of the exoskeleton during the trials. See Appendix H for a sample of the Questionnaire. Kinematic/kinetic data are recorded from

the exoskeleton in period B. The donning on and off time for the EHPA at start and finish is approximately 3mins.

(b) ***Task 2***

The second task is a lifting and carrying experiment. It involves lifting the 9.5kg load (box) from the ground by squatting motion, walking a short distance within 3m on level ground, squatting again to drop the load on the ground before returning to the starting position to lift another load. This operation thus involves both walking and squatting movements. Two back and forth movements is considered one trial and each participant is also requested to perform three trials in two different periods (A – no Exo and B – with Exo) with approximately 5mins resting interval between periods, as in Task 1, see Figure 3.5. The maximum voluntary contraction (MVC) and EMG RMSA are estimated across repeated trials. The trial-by-trial based questionnaire are also administered in resting wash over period and kinematic/kinetic data are recorded from the exoskeleton in period B.

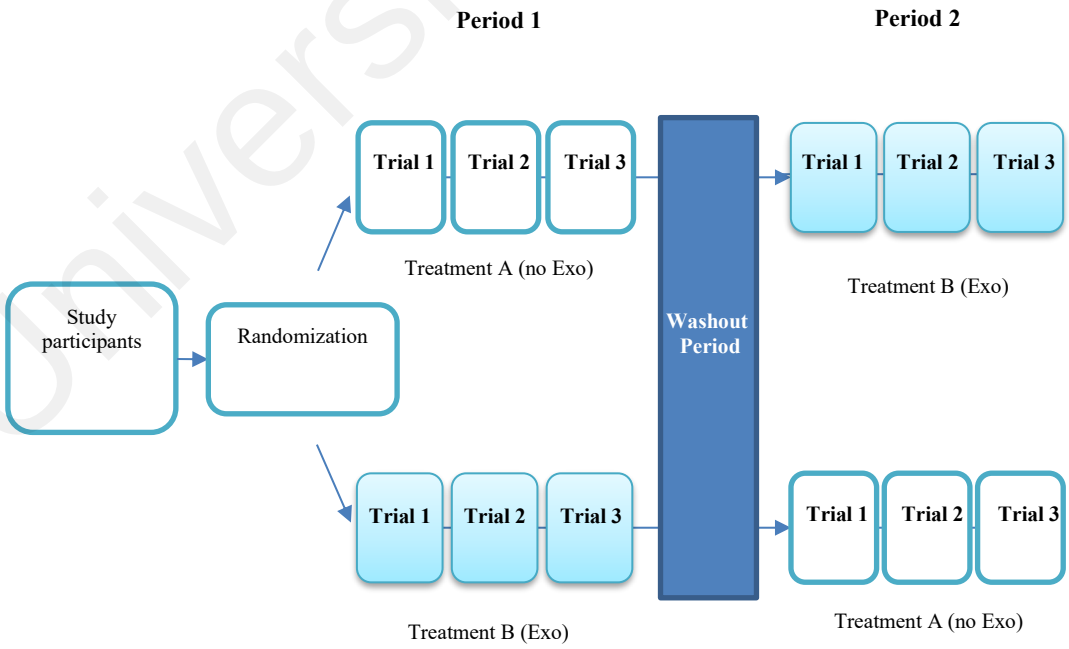

Figure 3.5: The general experiment protocol for task 1 and task 2. Task 1 involves lifting experiment and task 2 involves lifting and carrying experiment.

(c) ***Task 3***

This task is a comparison task; to compare the performance of the exoskeleton controller with another state-of-art controller namely the sensitivity amplification control (SAC). Only five participants are recruited in this task. The task involves same lifting and lifting/carrying experiment in Task 1 and Task 2 but performed in two exoskeleton assisted mode – (1) with proposed controller and (2) with sensitivity amplification controller (SAC). Kinematic/kinetic data are recorded from the exoskeleton to determine the wearers' interaction torque for comparison of controllers. Detail of experiment in Chapter 7.

3.3.5 Data Analysis

Offline EMG data processing from each participant including rectification, low pass filtering, computation of linear envelopes, normalization, and other data plotting are achieved in MATLAB software environment. A developed MATLAB GUI is used for the real-time computer-side data capturing and recording via a Bluetooth communication channel from the EMG sensors. Starting from the raw EMG data, linear envelopes are computed by full-wave rectification of the band-passed EMG signals (third-order Butterworth filter, cut-off 20-512Hz) and low-pass filtered by a third order Butterworth filter (cut-off, 5Hz). The EMG signals are further divided into traces for each task. Lifting/squatting task is divided per squat- lifting cycle (i.e. squat-descent and ascent) and carrying/walking task is divided per stride (i.e. heel-off to heel strike). Information from the in-sole ground reaction force sensor is applied to define proper intervals between traces. For each subject, the root mean square amplitude (RMSA) of the EMG signals and the peaks or Maximum voluntary contraction (MVC) are then computed per each trace and trial in both experiments. And for each activity, the EMG signal from each participant muscle is normalized by the average of the peaks or Maximum voluntary contraction (MVC) in the corresponding free movement task (i.e. task under Treatment A) for

uniformity of comparison. RMSA gives the measure of the level of the muscle activation and effort over a stride duration whereas MVC indicates the maximum level of muscle activation during the movement cycle.

Statistical analyses are accomplished using SPSS 23.0 (SPSS Inc., Chicago, IL, USA). Each dependent measure (i.e. EMG data from VM, RF, and GA) is calculated for a trial and then averaged over trials for a given treatment period. Repeated measure ANOVA with one independent factor (Intervention/Treatment) at two levels (A – no Exo assist, and B - Exo assist) is run on each of the dependent measures. Alpha is set at 0.05 and at 95% confidence interval, and significant effect is compared using a sequential Bonferroni post-hoc multiple tests procedure where appropriate. The administered Questionnaires were also analyzed in SPSS. Since the quantitative data from questionnaire are ordinal, ranked in the range of 0 – 10, the nonparametric Wilcoxon Signed-Rank Test is applied to assess the mean rank difference of perceived regional discomfort/fatigue on the lower extremity and low-back and perceived effort/assistance between the two treatments (no-Exo assist, Exo assist).

3.4 Summary

This chapter has presented the methodology of the current study, that is, the literature research method, the design method, and the study method. The method applied for literature review is systematic, designed to investigate some critical aspect of industrial manual lifting and carrying activity and to assess the state of art in active EHPA technology with the aim to derive the necessary information for effective design and control of the EHPA. The design method on the other hand highlights details of conceptualization of study to the stage of prototyping and experiment setup. The design is motivated to augment the hip and knee for squat-lifting, walking and carrying manual handling. Lastly, the study method gives highlights of the procedure for data collection,

experiments and data analysis which are necessary for the evaluation and experimental verifications (presented in Chapter 7) of the prototype EHPA. The approach is an experimental crossover design where each participant serves as his own matched control.

CHAPTER 4: UMEXOLEA DESIGN AND MODELLING

4.1 Introduction

This chapter presents the design and modelling of UMExoLEA. It details the design concept and motivation, the analysis of the movement biomechanics, the modelling, controller design, and stability analysis.

4.2 Design Concept and Motivation

UMExoLEA design is motivated to augment the hip extension/flexion muscles (gluteus maximus, rectus femoris, hamstring, etc.), and the knee extension/flexion muscles (Quadriceps femoris, hamstring, Gastrocnemius) of the lower extremity which are used for power generation, support, load distribution and stability in squat-lifting and walking/carrying manual handling activities. The overall expectation of the design is therefore to decrease repetitive strain and stress on the lower extremities musculature such that the wearer will have more capacity to withstand load during repeated tasks.

The identified biomechanical risk factors in lifting and carrying activities from epidemiological and biomechanical studies are the important considerations in the design of UMExoLEA (Table 4.1). Figure 4.1 show the flowchart of the EHPA system modelling. Upper-limb power augmentation capability for load lifting/carrying are not included in the current design due to the scope of study. Furthermore, the use of back support to carry loads on the back as commonly adopted in military-type exoskeleton are not conceived in the current design since this may not be applicable in several manual handling industries where loads are supported by the hand.

4.3 Biomechanics Analysis of Movements in Lifting and Carrying

The understanding of the biomechanics of the lower extremity musculature for squat-lifting and walking/carrying motion has been useful to facilitate the design of

UMExoLEA since the current study seeks to augment the knee, hip, and ankle flexors/extensors.

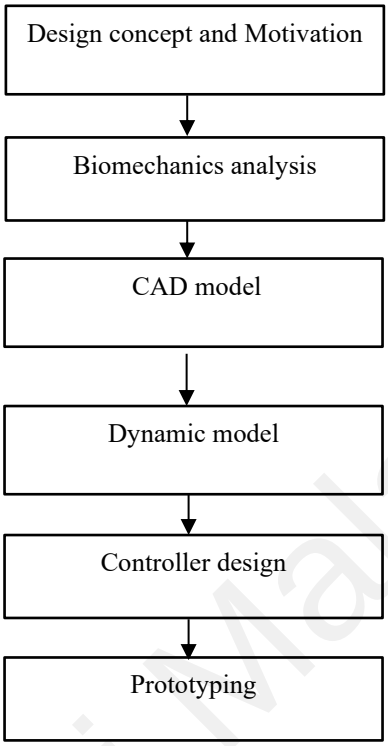

Figure 4.1: Flowchart on system modelling

4.3.1 Biomechanics of Squat-Lifting

Squat-lifting involves coordinated interaction of numerous muscle groups of the human body (Schoenfeld, 2010). Squats can be performed in a variety of depths measured generally by the degree of flexion of the knee (Schoenfeld, 2010). Three classifications of squat are possible: partial squats (40^{o} Knee angle), half squats (70^{o} to 100^{o}), and deep squats (greater than 100^{o}). Refer to Figure 4.2 for illustration of an upright squat-lifting motion. A dynamic squat begins with the torso in an upright position, and the knees and hips fully extended. Squat is then performed by flexing at the hip, knee, and ankle joints to a desired depth. This process dynamically engages the lower-body musculature, including the quadriceps femoris, hip extensors, hip adductors, hip abductors, and the calf or triceps' muscles (Nisell, 1986) to coordinate the movements of the ankle, knee, hip, and spinal joints. Some other isomeric activities which involve a wide range of supporting

muscles of the upper body are also involved to facilitate postural stabilization of the torso (Solomonow et al., 1987).

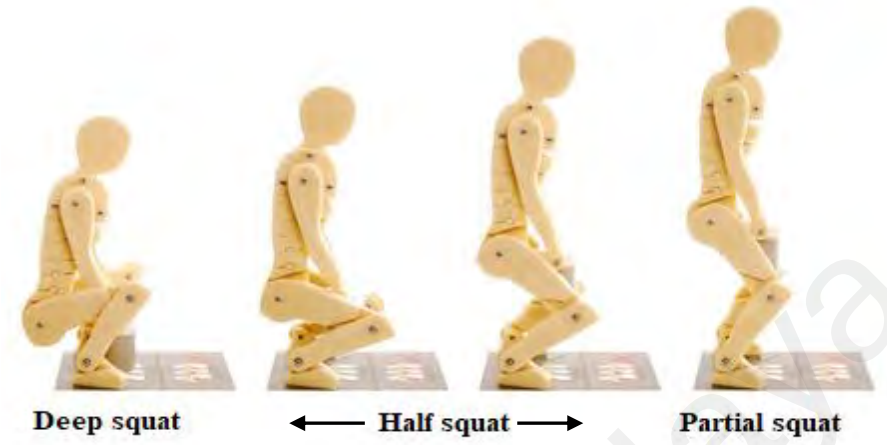

Figure 4.2: Biomechanics of squatting movement

4.3.1.1 The ankle

The ankle joint contributes significantly to the lower body support and power generation during squat performance (Hung et al., 1999). It is comprised mainly of the talocrural (articulation of the tibia and fibula with the talus) joint which enables dorsiflexion and plantar flexion, and the subtalar joint which maintains postural stability and prevent eversion/inversion movement of the foot (Signorile et al., 1995). The gastrocnemius and soleus muscles (collectively referred to as the triceps surae) attached at the shank enable the ankle movement by contracting concentrically during plantar flexion and eccentrically during dorsiflexion (Potvin et al., 1991; Signorile et al., 1994). The common range of motion of the talocrural joint during dorsiflexion is 20 degrees and 50 degrees during plantar flexion. Eversion/inversion range of the subtalar is approximately 5 degrees without movement of the forefoot (Clarkson, 2000) (Table 4.1). The contractions of the gastrocnemius, soleus, and tibialis anterior or tibialis posterior generate torques at the ankle at different phases of the squatting or squat-lifting

movements. Peak ankle moments of 50-300Nm have been reported in some studies during squatting (R. F. Escamilla et al., 2001)

4.3.1.2 The Knee

The knee consists of the tibiofemoral (tibia and femur) which enables sagittal plane movements during squatting in a range of motion from 0 to approximately 160 degrees of flexion (G. Li et al., 2004). Small amount of axial rotation is also present at the knee joint during dynamic movement, with the femur rotating laterally during flexion and medially during extension with respect to the tibia. Knee forces/torque are generated by the quadriceps femoris (vastus lateralis, vastus medialis, vastus intermedius, and rectus femoris) which contract to enable concentric knee extension as well as eccentrically resisting knee flexion. In contrast, the antagonistic hamstrings muscles (biceps femoris, semitendinosus, semimembranosus) co-contract to oppose the knee extensor moments. They exerts a counter-regulatory pull on the tibia to neutralize the anterior tibiofemoral shear impacted by the quadriceps (R. F. J. M. Escamilla et al., 2001). This synergy enhances the integrity of the knee joint during squatting. Highest values of tibiofemoral compressive forces reaching 8000N at 130 degrees (deep knee squat) have been reported among powerlifters lifting 2.5 times bodyweight (Nagura et al., 2002). Mean peak shear forces during squatting have been reported to exceed 2,700 N (Donnelly et al., 2006).

The flexion/extension driving torque of the quadriceps femoris and the restraining effect of the hamstring muscle and other ligaments suggests the use of back-drivable actuators to allow both knee flexion/extension and some passive restraining elements (or active impedance control technique) to limit/regulate the motion for compliance and joint integrity. Maximum tibiofemoral compressive forces have been correlated with knee flexion angle and forces at the quadriceps tendon (Nagura et al., 2002), thus, for EHPA

design, incorporating a mechanically high supporting torque when standing-up from deep squat can significantly alleviate compressive forces on the knee.

4.3.1.3 The Hip

At the hip joint, the gluteus maximus (GM), rectus femoris (RF), and the hamstrings act eccentrically to control squat descent and concentrically to overcome external resistance on the ascent. Hip torques increases with increase in hip flexion up to a maximum at full squat (Nagura et al., 2002). Mean hip flexion range of motion have been estimated to about 95 $\pm$ 27 degrees (Hemmerich et al., 2006). The biomechanics of the hip in sagittal motion suggest the use of a similar actuation mechanism as suggested for the knee joint in EHPA design.

4.3.2 Biomechanics of Walking/Carrying

The human walking is commonly divided into two phases: the stance and the swing phase based on the duration between one heel-strike (foot-strike) to the next heel-strike (Figure 4.3). The stance phase (foot-in-contact with ground duration) dominates the walking by 62% whereas the swing phase (the foot-off ground duration) takes the remaining 38%. The stance phase is also commonly divided into three stages (Rose, 1994): (1) *initial double limb support* (i.e. foot strike to opposite foot-off), (2) *single limb support* (opposite foot-off to opposite foot-off), and (3) *second double limb support* (opposite foot strike to foot-off). In some literature, a *mid-stance* (Guo & Jiang, 2015) is considered which may require a laboratory procedure to determine because of its short duration. The swing phase on the other hand is sub-divided into three phases: 1) *initial swing* (foot-off to foot clearance) 2) *mid-swing* (foot clearance to tibia vertical) and 3) *terminal swing phase*, (tibia clearance to foot-strike).

Table 4.1: Summary of lower extremity biomechanics during sagittal squat-lifting movements

Joint/DOF	Muscles	Torque Generation (*Typical range*)	Joint Movement Effect (*Typical range of motion*)	Stabilization/ Torque Dissipation
Ankle DOF = 3	Gastrocnemius	Concentric and eccentric contraction (ankle moment: 50-300Nm)	Ankle plantar flexion (~50°) and dorsiflexion (~20°)	
Knee DOF = 1 (with small axial and lateral displacement)	Quadriceps	Concentric and eccentric contraction	Knee extension and flexion respectively (0~160°)	eccentric contraction to oppose the knee extensor moments
	Hamstrings muscle	Co-contraction	counter-regulatory pull on the tibia	Neutralize/limit anterior tibiofemoral shear
	Gastrocnemius	Concentric and eccentric contraction	1. Offset knee valgus moments 2. Limit posterior tibial translation	
Hip DOF = 3	gluteus maximus (GM)	eccentric and concentric contraction	Squat descent and external resistance on squat ascent respectively (Mean hip flexion 95 ± 27°)	
	Rectus Femoris	Hip flexor and knee extensor	Not dominant when knee is extended or when hip is fully flexed	Direct antagonist to the hamstring

At early stance, the hip extensors (hamstring muscle group etc.) contract to stabilize the hip while the quadriceps and tibialis anterior contracts eccentrically to support the heel strike. The ankle also dorsiflexes (tibialis anterior) eccentrically to control plantar flexion moment while the quadriceps contract to stabilize the knee and counteract the flexion moment. At late stance, the toe flexors, the tibialis posterior, and the hip flexors

(rectus femoris, sartorius, etc.) contract to propel the advancing limb. For the swing movement, the hip flexors contract concentrically to advance the swinging leg. This is followed by ankle dorsiflexion to ensure foot clearance (at mid-swing). Finally, in late swing, the hamstring muscles decelerate forward motion of the thigh preventing the leg from over-extending. These facts are crucial in developing exoskeleton control algorithms for human walking assistance.

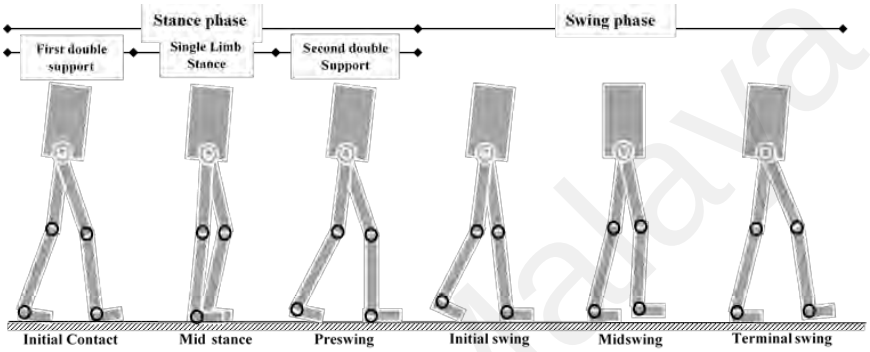

Figure 4.3: The Walking phases

4.3.2.1 Joint Kinematics and Kinetics

Walking predominantly takes place on the sagittal plane of the human body and has a cyclic nature on this plane as can be seen in different motion studies (Vaughan et al., 1999; Winter, 2009). The angular displacement of the hip, knee, and ankle joints thus vary in quasi-sinusoidal manner during walking and/or load carrying. From a peak at heel strike (0% of gait cycle), a low at about mid-way (50%) of the cycle, to another peak at the next heel strike (100%). The flexion and extension range of motion of the hip joint on the sagittal plane can reach about 40 degrees for a normal adult male during level or load carrying walking. The knee joint may extend up to 60 degrees, while the ankle dorsiflexes and plantarflexes over a relatively small range of about 29 degrees on the sagittal plane. Table 4.2 presents a summary of the human walking data.

The torque/power profile on the hip, knee, and ankle are also quasi sinusoidal during level walking (Winter, 2009). The three joints exhibit unique kinetic properties for

synergy in walking. Hip torque power (about ≈ 0.6Nm/kg peak on sagittal plane) is positive in the stance support phase as the hip support the stance leg and propel the leg forward (Ryder et al., 2013; Winter, 2009). It goes negative, at terminal swing, as the tendons and muscles stretch to absorb energy, decelerating the leg prior to heel strike. The hip power exhibit both positive and negative peaks, but the average power transfer is found positive (Han et al., 2010; Ryder et al., 2013). This fact suggests the prescription of bi-directional, back-drivable actuators when designing exoskeleton to assist hip sagittal motion.

The knee joint also exhibits positive energy phase (for torque generation) and a negative dissipative phase (for energy absorption). The average knee power (about ≈ 0.2Nm/kg peak torque on sagittal plane) is however negative which indicates that the knee function more as a shock absorber dissipating energy during the walking cycle (Kirkwood et al., 2007). The behavior of the knee joint suggests the use of back-drivable actuators in conjunction with passive elements such as springs and dampers (or software implemented impedance control) when designing knee joint of exoskeletons for walking or load carrying assistance.

The ankle joint also exhibit (large) positive and negative power transfer phase (Han et al., 2010; Winter, 2009) which suggest that the ankle functions as a source of energy for walking as well as dissipative absorbing energy at some point during the walking stance (Han et al., 2010; Winter, 2009). Under loaded walking or load carrying, however, the ankle can generate more driving torque extending the phase of positive torque. For exoskeleton design, passive devices (spring and damper etc.) absorbing energy during negative power transfer and releasing it for positive work may be beneficial for ankle design of exoskeletons for walking assistance.

Table 4.2: Summary of relevant lower extremity biomechanics during horizontal walking on sagittal plane

Joint	Plane (movement)	Range of Motion	Peak Driving Torque	Main Driving Muscles
Hip	Sagittal (Flexion. /Extension)	$0^o \sim 40^o$	≈ 0.6 Nm/kg	Gluteus maximus (GM), rectus femoris, psoas major, Iliacus, biceps femoris, etc.
Knee	Sagittal (Extension/Flexion)	$0^o \sim 60^o$	≈ 0.2Nm/kg peak	**Flexion:** Quadriceps femoris and sartorius **Extension:** hamstring muscles (e.g. biceps femoris, semitendinosus, and semimembranosus muscles)
Ankle	Sagittal (Dorsi. /Plantar flexion)	$0^o \sim 29^o$	-	Gastrocnemius and soleus

4.4 System Modelling

4.4.1 Design Model

Based on ongoing discussions, the proposed lower-limb EHPA system is modeled as a 12 degree of freedom lower extremity exoskeleton in SolidWorks IDE environment. Figure 4.4 shows the overall kinematic configuration of the exoskeleton. Each leg of the exoskeleton is modelled as six degrees of freedom (DOF): 2-DOFs at the hip joint (one active and one passive), 2-DOFs at the knee joint (one active and one passive), and 2 passive DOFs at the ankle. The active hip DOF is modelled to allow flexion and extension movement on the sagittal plane and the passive counterpart to allow abduction/adduction on the frontal plane for some comfortable movement. The third DOF of the hip for Internal rotation and external rotation on the transverse plane is unmodeled however this DOF is unhindered. Similarly, the active knee DOF is designed to allow flexion and extension movement on the sagittal plane while its passive DOF to permit some axial and lateral translation/rotation. The passive ankle joint is modelled to permit 2 DOFs

movement i.e. dorsiflexion and plantarflexion on the sagittal plane, internal/external (abduction/adduction) rotation on the transverse plane. The ankle model also allows unhindered eversion/inversion on the frontal plane. Each link of the exoskeleton is dimensioned considering the body figures of a section of the Malaysian mixed ethnic workforce with heights ranging from 170 to 180 cm (Lim & Ding, 2000). See Table 4.2 for the EHPA link parameters.

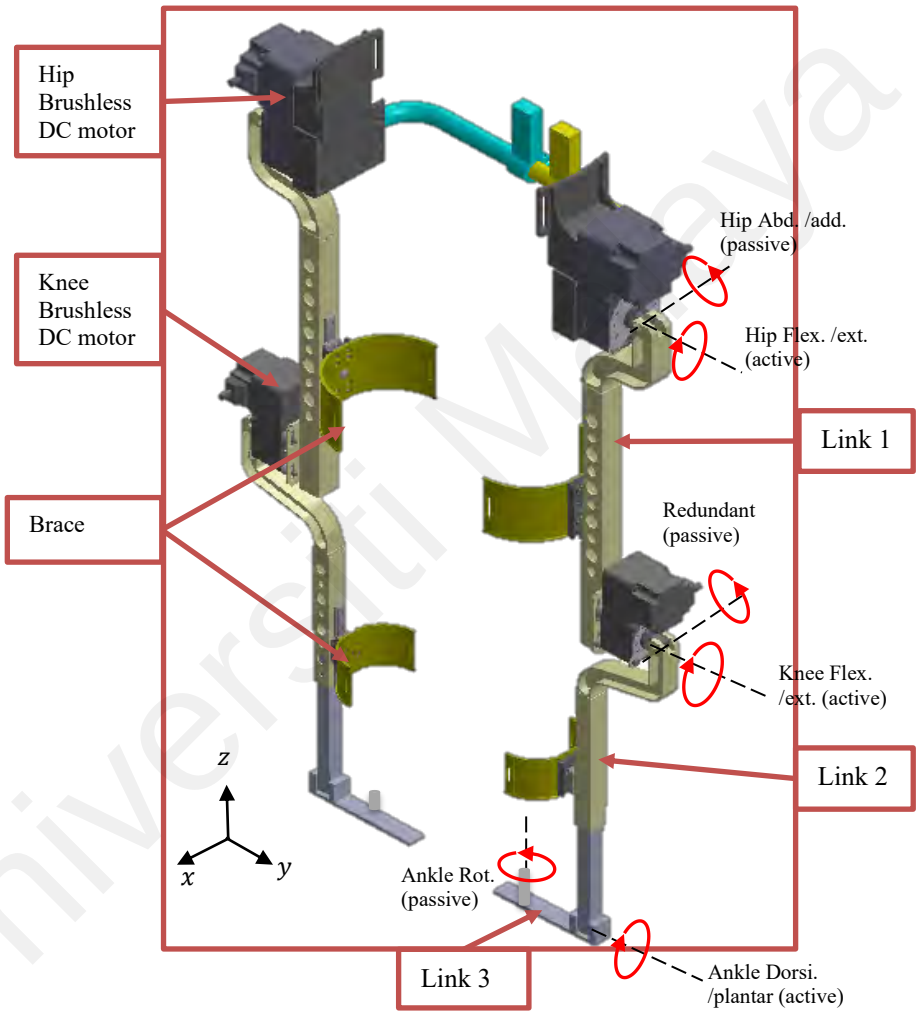

Figure 4.4: A Solid Work model of the prototype exoskeleton system.

Table 4.3: Exoskeleton Segment Parameters

Segment (Left and Right)	Length (m)	Inertia (kg/m^2)	COM (m)
Link 1	0.465	0.0423	0.085
Link 2	0.330	0.0051	0.170
Link 3	0.150	0.010	0.150

4.4.2 The Dynamic Model

This section presents the dynamic model of the lower limb EHPA system for squatting and walking movements while the user is lifting and carrying the payload on both hands. The dynamic model is thereafter applied in Section 4.4.3 for the controller design.

The dynamic model of the EHPA is derived by analyzing the kinematic/kinetic configuration of a single leg in each phase of motion, see Figure 4.5. For squatting while lifting, the lower limb EHPA can be modeled as a triple inverted pendulum with three segments (shank, thigh, and torso) articulated around the hip, knee, and pivoted at the ankle joint as shown in Figure 4.5(a) (Babič et al., 2006; Huo et al., 2016; Petric et al., 2013). For walking while carrying, specifically at stance, the EHPA can be similarly modeled by a three-segment triple inverted pendulum articulated at same joints (Figure 4.5(b)), whereas the swing phase model can be achieved by a three-segment or 3-DOF serial link manipulator model pivoted at the hip joint (Ghan et al., 2006; L. H. Huang et al., 2005; Racine, 2003), see Figure 4.5(c).

Overall, some assumptions are made to obtain the partial model of the exoskeleton system. The mass of the torso which carries the bag-pack and the control unit have been modelled with some uncertainties. Both the pilot and exoskeleton are rigidly connected at the torso and waist thus the exoskeleton bears some of the weight of the pilot. This weight is included in the torso mass as an uncertainty. The pilot and the exoskeleton also make contacts at the thigh and shank brace as well as the foot. These contacts are complaint and periodic and are modelled as interaction forces between the human and the

exoskeleton. The effect of interaction is felt at the joints thus the interaction forces are modelled as human input torque at the joints. The overall goal of this section is to find only an approximate dynamic model of the EHPA for both motions (i.e. squatting and walking) to be used for the controller design, especially since the proposed controller based on dual unscented Kalman filter does not require a good model of the exoskeleton. More details are discussed as follows.

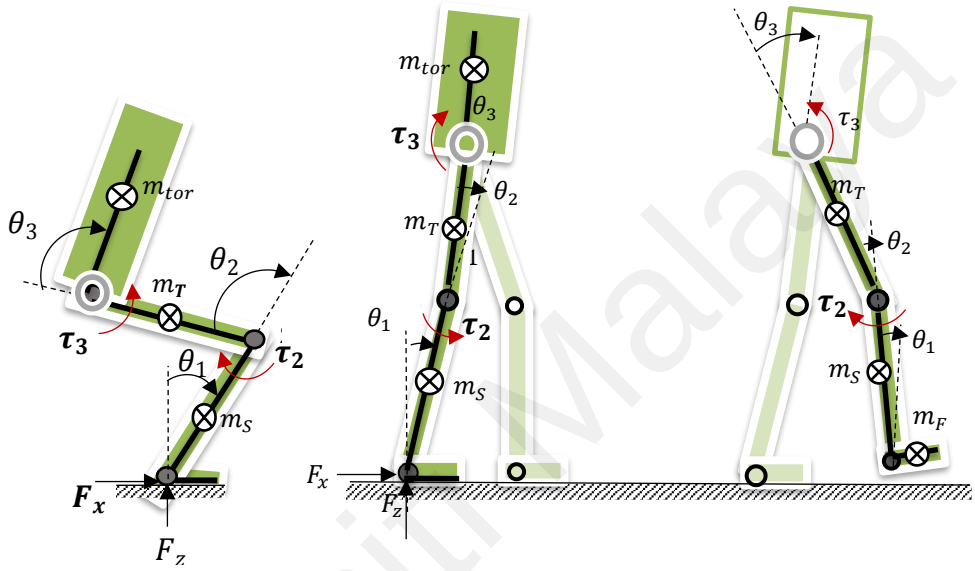

(a) Squatting – all stance **(b) Walking-stance** **(c) Walking-swing**

Legend: θ_3 – hip angle, θ_2 – knee angle, θ_1 – ankle angle, τ_1 – hip torque, τ_2 – hip torque, m_{tor} – torso mass, m_T – thigh mass, m_S – shank mass, and m_F – foot mass

Figure 4.5: Three DOF serial-link manipulator configuration for squatting and walking motion while lifting and carrying a payload on the sagittal plane.

4.4.2.1 Squatting and Walking-Stance Phase

Consider the exoskeleton system in Figure 4.5 (green shades indicate human body segments while the black bold lines indicate the exoskeleton link segments), a single leg performing squatting movement (Figure 4.5(a)) or undergoing walking-stance (Figure 4.5(b)) is approximated by the general Euler-Lagrange dynamic equation of a 3-DOF serial-link manipulator pivoted at the ankle joint:

$$M(q)\ddot{q} + C(q,\dot{q})\dot{q} + G(q) + \tau_f(q,\dot{q}) = \tau_a + \tau_h - J^T F \quad (4.1)$$

where $q = [\theta_1,\ \theta_2, \theta_3]^T$ are the joint angles as shown in Figure 4.5, and M is a 3 x 3 inertia matrix of the exoskeleton system in stance phase. C is a centripetal and Coriolis matrix and a function of q and $\dot{q}$. G is a 3x 1 vector of gravitational torque and a function of q. τ_f is a vector of joint frictional torque. $\tau_a = [0, \tau_2, \tau_3]^T$ are the joints actuator torque respectively with the first element set to zero since there is no actuation for the ankle joint. τ_h is the 3 x 1 vector of human input torque (felt on the joints). J is the Jacobian matrix and F is the 2x1 vector of ground reaction forces (GRF) with cartesian coordinates: $F_x(= \mu F_1)$, and $F_z(= F_1)$ where μ is the coefficient of friction and F_1 is the ground force measured at the heel (refer to Section 4.4.3.4 (a) for details) . Derivation of (4.1) and the Jacobian, J, are presented in Appendix I.

4.4.2.2 Walking-Swing Phase

The dynamics of the exoskeleton swing leg during walking while can also be written in the general Euler-Lagrange form, considering the model of a 3-DoF serial link manipulator pivoted at the hip joint (and supporting only its weight), as:

$$M(q)\ddot{q} + C(q,\dot{q})\dot{q} + G(q) + \tau_f(q,\dot{q}) = \tau_a + \tau_h \quad (4.2)$$

where all the parameters are as described in (1), however the ground reaction forces $F = 0$ for the swing leg with foot off ground. Furthermore, the weight of the torso exerts no influence on the thigh and shank segments since the swing leg rotates about the hip. Derivation of (4.2) is also presented in Appendix I.

4.4.2.3 The Human Body Segment Parameters

The parameters of each segment of the human body (i.e. moment of inertia, segment masses, length, and centers of mass (COM)) in coupled movement with the exoskeleton system can be estimated from the height, h, and total mass, M, of the human subject (Vaughan et al., 1999; Winter, 2009). Assuming the torso or HAT (Head, Arm, and Trunk) and the lower-body segments to be rigid, and to move on the sagittal plane, the segment parameters of an average healthy adult can be estimated from Winter (2009)

equations, see Table 4.3, where l_t, l_s, l_f and l_{HAT} represents the length of the thigh, shank, foot and torso/HAT segments respectively. The moment of inertias of each segment are calculated for the particular case of a healthy subject with mass, M = 77kg, and height, h = 1.78m.

Table 4.4: Body segment parameters of an adult male adapted from (Winter, 2009)

Segment parameters	Mass (kg)	Moment of Inertia* (kg.m^2)	CoM (m)	Length, l_* (m)	Radius of Gyration (m)
Thigh	0.1057M	0.161	$0.433l_t$	$0.245h$	$0.323l_t$
Shank	0.0465M	0.063	$0.433l_s$	$0.246h$	$0.302l_s$
Foot	0.0145M	0.018	$0.500l_f$	$0.152h$	$0.475l_f$
HAT	0.6780M	30.43	$1.142l_{HAT}$	$0.475h$	$0.903l_{HAT}$
**Moment of Inertia(kg.m^2) = Segment Mass x (Radius of Gyration)^2*					

4.4.2.4 The Joint Friction Model

The estimate of joint friction and stiffness torque $\tau_f(q, \dot{q})$ parameters are achieved by a system identification procedure presented in Chapter 6. This is necessary to minimize uncertainties in the model and to ensure an accurate relationship between the joint torques and motion of the exoskeleton. The friction/stiffness torque model (Ghan et al., 2006; Wu et al., 2016) for each joint is given as

$$\tau_f(q,\dot{q}) = \begin{cases} b_0, & q = 0, \dot{q} = 0 \\ b_1 sgn(\dot{q}) + b_2(\dot{q}), & \dot{q} \neq 0 \\ b_3(q), & q \neq \dot{0}, \dot{q} = 0 \end{cases} \quad (4.3)$$

where b_0 is the static friction torque; b_1 is the coefficient of the coulomb or kinetic friction torque; b_2 is the coefficient of the damping friction torque; and $b_3(q)$ is the stiffness torque which is a function of joint position.

4.4.3 Synchronous Controller Design

4.4.3.1 Concept

The proposed controller in this study is a novel synchronous mobility control technique intended for lower extremity mobility augmentation and smooth movement transitions. It is motivated to assist/augment squatting and walking motions in lifting and carrying task as well as to allow seamless inter-transition between these motions. Since the motions are typically diverse, a means to accurately estimate or predict the human motion trajectories in real time from noisy sensor measurement is crucial. Furthermore, given such diverse movement and interaction situation, parameter variations are expected thus a means to update the model parameters in real time is necessary. These facts motivate the use of a dual unscented Kalman filter (DUKF) for both states/trajectory estimation as well as for online model parameter update. The state estimation mechanism of the DUKF can generate estimate of human joint motion trajectories (spatio-temporal features of the human movement i.e. joint position, velocity, and acceleration) based on the partial model of the coupled human-exoskeleton system and on the current observation from noisy position sensors. The parameter estimation mechanism can update model parameters online to improve the model. The wearer motion trajectory estimate is applied to an impedance based computed torque controller (or inverse dynamic torque controller) to generate torque to assist the wearer's motion. An important feature of the impedance controller is that it uses feed-back of the interaction force and a set of impedance parameters in its control law to ensure compliance while assisting and following the user's movement.

Over all, by this approach to trajectory estimation and control, we adopt the notion of movement primitive which suggests representation of dynamic movement behavior such as walking and squatting using kinematic representation (Ijspeert et al., 2013; Kimura et al., 2006). Kinematic representation of movement primitive is thought to offer more flexibility for workspace planning of complex movements for control than direct motor command for control. This approach is similar to that of the DMPs or AFOs which can predict future estimates of states from current observations (poor or noisy signals from sensors), working fundamentally as state observers, and can attract the exoskeleton to these future states by a force field or controller. The proposed DUKF approach is however different from the traditional AFOs which have capability for generating only uniform/cyclical movements trajectories and DMPs which require reinforcement learning mechanism for parameter update. The proposed DUKF approach have capabilities for estimating/generating dynamic/diverse movement behaviors and online parameter update.

Another important aspect of the proposed control strategy is the application of a novel supervisory controller for prompt human movement detection and synchronization of exoskeleton movement with the wearer. The supervisory controller integrates a sensor fusion algorithm in a hybrid automaton to achieve this purpose. Although EMG sensor-based feedback control is very useful for prompt movement detection and motion control, it has not been used in this study due to its numerous shortcomings which include sensitivity to sweat and electrode placement and recalibration issues. These factors are very important in actual industry manual handling situation where type of work or lengthy hours of work make sweating inevitable and where body movements can affect placement of electrodes and vice versa during work. Details of the proposed controller design is presented in the following sequel.

4.4.3.2 The Dual Unscented Kalman Filter Design Algorithm

The well-known Kalman filter is an optimal estimator for generating maximum-likelihood estimate of states of a linear, discrete-time, dynamic system (Haykin, 2001). It provides a more efficient recursive solution to the states estimation problem in the sense that each updated estimate or prediction of states of a linear system is computed from previous estimate and new observation (i.e. sensor data), without need to compute estimates over an entire past observation data. It optimally combines noisy input observation with predictions from a known dynamic model.

Aside states estimation, an important extension of the Kalman filter is for supervised learning or parameter identification of a partially known dynamic model given noisy observation from sensors. This important feature has motivated several applications in adaptive control (Grewal & Andrews, 2010) involving the dual estimation of states and parameters. The dual estimation method works heuristically by alternating between estimate of states using the model and estimate of the model using the states (Figure 4.6). If the model improves, so do the states. This exceptionally enhances its robustness to states prediction and the overall system to model parameter variations.

The standard Kalman filter is however limited to linear systems. An extension to nonlinear systems necessitated the formulation of the Extended Kalman filter (EKF) (Wan & Nelson, 2001) which involves first-order linearization of the nonlinear dynamic model. The linearization is done at every time step around the most recent estimate of states. The first order linearization and approximation by a Gaussian random variable (GRV) introduces large error in the true posterior mean and covariance of the transformed GRV which sometimes leads to divergence of the filter. A more superior approach to the EKF is the *unscented Kalman filter* (UKF) which solves the linearization problem using a deterministic sampling approach. UKF applies a minimal set of carefully chosen sample points, called sigma points, that completely capture the true posterior mean and

covariance of the Gaussian random variable to a second order accuracy when propagated through the true nonlinear system (Wan & Van Der Merwe, 2000).

The Kalman filter has been largely popular in several fields including aerospace(Grewal & Andrews, 2010), SLAM (Dissanayake et al., 2001) etc. for its accurate states prediction (or generation) in highly nonlinear, partially observed, dynamic systems, using the extended (Wan & Nelson, 2001) or unscented versions (Wan & Van Der Merwe, 2000), and working fundamentally as a state observer, like the DMPs or AFOs, that can predict future estimates of states from current observations (poor or noisy signals from sensors).

(a) ***States Estimation***

Consider the Exoskeleton dynamics given in (4.1) and (4.2), if transformed into stochastic nonlinear states variable representation, the approximate nonlinear state transition equation and measurement equation of the coupled human-exoskeleton system can be written respectively as

$$\mathbf{x}_{k+1} = \mathbf{F}(\mathbf{x}_k, \mathbf{u}_k, \mathbf{w}) + \mathbf{v}_k \tag{4.4}$$

$$\mathbf{y}_k = \mathbf{H}(\mathbf{x}_k, \mathbf{n}_k) \tag{4.5}$$

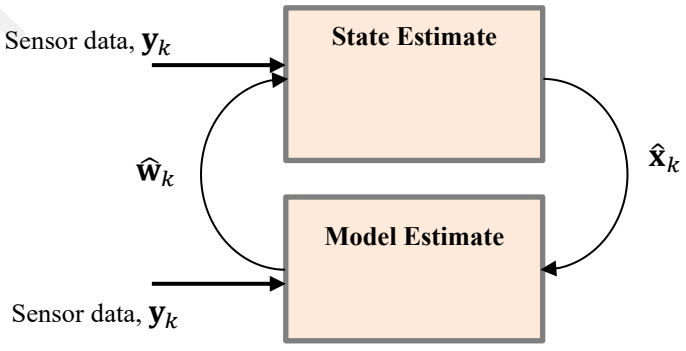

Figure 4.6: Dual estimation

where $\mathbf{x}_k = [q^T \quad \dot{q}^T]^T$ denote the unobserved states of the system, and $k \in [0, 1, 2, \ldots \infty]$ denotes discrete time. $\mathbf{y}_k$ represent the noisy position observation from sensors. $\mathbf{w}$ stands for the system parameters (e.g. link masses). $\mathbf{H}$ is the measurement function given here

as $\mathbf{H} = \mathrm{H}\mathbf{x}_k + \mathbf{n}_k = [1,0,0]\mathbf{x}_k + \mathbf{n}_k$. $\mathbf{v}$ represents the process noise which is assumed additive with covariance matrix given as $\mathbf{P_v}$, and $\mathbf{n}$ denotes the measurement noise, non-additive, with covariance matrix given as $\mathbf{P}_{\boldsymbol{n}}$. Both the process and measurement noise are assumed additive, white and Gaussian, with zero mean ($\boldsymbol{E}[\mathbf{v}] = \boldsymbol{E}[\mathbf{n}] = 0$).

The nonlinear term $\mathbf{F}(\cdot)$ is derived as

$$\mathbf{F}(\cdot) = \begin{bmatrix} \dot{q} \\ -\widehat{M}^{-1}(q, \mathbf{w}) \left\{ \hat{C}(q, \dot{q}, \mathbf{w})\dot{q} + \hat{G}(q, \mathbf{w}) + \hat{\tau}_f \right\} \end{bmatrix} + \begin{bmatrix} 0 * \mathbf{I} \\ -\widehat{M}^{-1}(q, \mathbf{w}) \end{bmatrix} u \qquad (4.6)$$

where $u = \tau_a + \tau_h - J^T F$.

The hat symbol ˆ on the nonlinear terms stands for estimates and $\mathbf{I}$ is a 3x3 identity. In subsequent derivation, we adopt the notations used by Wan and Van Der Merwe (2000).

Given the noisy observation $\mathbf{y}_k$ from sensor, at k^{th} sampling time, our goal is to generate optimal estimates of states, $\mathbf{x}_k$. The UKF does the estimation, much the same way as the EKF, using the following recursion (Wan & Van Der Merwe, 2000):

$$\hat{\mathbf{x}}_k = (\text{prediction of } \mathbf{x}_k) + \mathcal{K}_k[\mathbf{y}_k - (\text{prediction of } \mathbf{y}_k)] \qquad (4.7)$$

where $\hat{\mathbf{x}}_k$ represents the optimal minimum mean-squared error (MMSE) estimate for $\mathbf{x}_k$ assuming that the prior estimate $\hat{\mathbf{x}}_{k-1}$ and the current observation $\mathbf{y}_k$ are Gaussian Random Variables (GRV). If the (optimal) prediction of $\mathbf{x}_k$ is denoted $\hat{\mathbf{x}}_k^-$, and the (optimal) prediction of $\boldsymbol{y}_k$ is denoted $\hat{\mathbf{y}}_k^-$, their expectations can be expressed as:

$$\hat{\mathbf{x}}_k^- = \mathbb{E}[\mathbf{F}(\hat{\mathbf{x}}_{k-1}, \mathbf{v}_{k-1})] \qquad (4.8)$$

$$\hat{\mathbf{y}}_k^- = \mathbb{E}[\mathbf{H}(\hat{\mathbf{x}}_k^-, \mathbf{n}_k)] \qquad (4.9)$$

where $\mathbf{v}_{k-1}$ **(**process noise) and $\mathbf{n}_k$**(**measurement noise) are also random variables (GRV).

The optimal Kalman gain on the other hand is given by

$$\boldsymbol{\mathcal{K}}_k = \mathbf{P}_{\mathbf{x}_k\mathbf{y}_k}\mathbf{P}_{\tilde{\mathbf{y}}_k\tilde{\mathbf{y}}_k}^{-1} \qquad (4.10)$$

It is expressed as a function of the posterior covariance matrices $\mathbf{P}_{\mathbf{x}_k\mathbf{y}_k}$ and $\mathbf{P}_{\tilde{\mathbf{y}}_k\tilde{\mathbf{y}}_k}$ (with $\tilde{\mathbf{y}}_k = \mathbf{y}_k - \hat{\mathbf{y}}_k^-$) which also requires computation of the expectation of a nonlinear function of the prior state estimates.

The UKF computes these expectations or optimal terms ($\hat{\mathbf{x}}_k^-, \hat{\mathbf{y}}_k^-$, and $\mathcal{K}_k$) by generating a set of $2L+1$ *sigma* vectors χ_{k-1} (where L is the dimension of the state vector) symmetrically distributed around the prior (true) mean estimate $\hat{x}_{k-1}$.

$$\chi_{k-1} = \left[\hat{\mathbf{x}}_{k-1},\ \ \hat{\mathbf{x}}_{k-1} + \sqrt{(L+\lambda)\mathbf{p}_{k-1}},\ \ \hat{\mathbf{x}}_{k-1} - \sqrt{(L+\lambda)\mathbf{p}_{k-1}}\right] \tag{4.11}$$

where, $\lambda = \alpha^2(L+\kappa) - L$ is a composite scaling parameter. The constant α determines the spread of sigma points around $\hat{\mathbf{x}}_{k-1}$, and is usually set to a small positive value in the range $1e^{-3}$. The constant κ is a secondary scaling factor, which is usually set to zero (or $3-L$). $\mathbf{p}_{k-1} = \boldsymbol{E}[(\mathbf{x_{k-1}} - \hat{\mathbf{x}}_{\boldsymbol{k-1}})(\mathbf{x_{k-1}} - \hat{\mathbf{x}}_{\boldsymbol{k-1}})^{\boldsymbol{T}}]$ is the state covariance matrix.

The generated sigma points χ_{k-1} are propagated through the nonlinear system in (4.4) and (4.5) (see (4.12), (4.13), and (4.14)), to obtain the optimal predictions $\hat{\mathbf{x}}_k^-$, $\hat{\mathbf{y}}_k^-$, and $\widehat{\mathbf{P}}_k^-$ (prior covariance) for the recursion to a 3rd order accuracy (of the Taylor series expansion) (see (4.15), (4.16), and (4.17)).

$$\chi^*_{(k|k-1)} = \mathbf{F}(\chi_{k-1}, \mathbf{u}_{\mathrm{k-1}}, \mathbf{w}) \tag{4.12}$$

$$\chi_{(k|k-1)} = \left[\chi^*_{(k|k-1)},\ \chi^*_{(0,k|k-1)} + \gamma\sqrt{\mathbf{P_v}},\quad \chi^*_{(0,k|k-1)} - \gamma\sqrt{\mathbf{P_v}}\right] \tag{4.13}$$

$$\mathcal{Y}_{(k|k-1)} = \mathbf{H}(\chi_{(k|k-1)}) \tag{4.14}$$

$$\hat{\mathbf{x}}_k^- = \sum_{i=0}^{2L} W_i^{(m)} \chi^*_{(i,k|k-1)}, \tag{4.15}$$

$$\widehat{\mathbf{P}}_k^- = \sum_{i=0}^{2L} W_i^{(c)} \left(\chi^*_{(i,k|k-1)} - \hat{\mathbf{x}}_k^-\right)\left(\chi^*_{(i,k|k-1)} - \hat{\mathbf{x}}_k^-\right)^T + \mathbf{P_v} \tag{4.16}$$

$$\hat{\mathbf{y}}_k^- = \sum_{i=0}^{2L} W_i^{(m)} \mathcal{Y}_{(i,k|k-1)}, \tag{4.17}$$

where W_i are the generated weights alongside the sigma points given by

$$W_i^{(m)} = W_i^{(c)} = \frac{\lambda}{2(L+\lambda)}, \qquad i = 1, \ldots, 2L \tag{4.18}$$

with initial values, $W_0^{(m)} = \frac{\lambda}{(L+\lambda)}$, and $W_0^{(c)} = \frac{\lambda}{(L+\lambda)} + 1 - \alpha^2 + \beta$. The constant β is used to incorporate prior knowledge of the distribution, for Gaussian distribution, $\beta = 2$ is optimal(Wan & Van Der Merwe, 2000). Notice that the superscripts (m) and (c) implies weighting factors for states and covariances respectively. The terms $\chi^*_{(k|k-1)}$ (augmented as $\chi_{(k|k-1)}$), and $\mathcal{Y}_{(i,k|k-1)}$ denote the posterior (propagated) sigma vectors of the process and observation functions.

The posterior covariances for computing the optimal gain, are thus given as

$$\mathbf{P}_{\tilde{\mathbf{y}}_k\tilde{\mathbf{y}}_k} = \sum_{i=0}^{2L} W_i^{(c)} \left(\mathcal{Y}_{(i,k|k-1)} - \hat{\mathbf{y}}_k^-\right)\left(\mathcal{Y}_{(i,k|k-1)} - \hat{\mathbf{y}}_k^-\right)^T \tag{4.19}$$

$$\mathbf{P}_{\mathbf{x}_k\mathbf{y}_k} = \sum_{i=0}^{2L} W_i^{(c)} \left(\chi_{(i,k|k-1)} - \hat{\mathbf{x}}_k^-\right)\left(\mathcal{Y}_{(i,k|k-1)} - \hat{\mathbf{y}}_k^-\right)^T \tag{4.20}$$

Equation (4.15), (4.17), (4.19), and (4.20)) are used in the recursion (during the measurement update phase) to generate the optimal estimate of states $\mathbf{x}_k$. Details of the UKF procedure for states estimation/generation can be found in (Wan & Van Der Merwe, 2000).

(b) ***Parameter Estimation***

For identification of the parameters of the model in (3.1) and (3.2), we define a new state-space formulation given as

$$\mathbf{w}_{k+1} = \mathbf{w}_k + \mathbf{r}_k \tag{4.21}$$

$$\mathbf{d}_k = \mathbf{Y}(\mathbf{x}_k, \mathbf{w}_k) + \mathbf{e}_k, \tag{4.22}$$

where $\mathbf{w}_k = [m_1^T, m_2^T, m_3^T]^T$ corresponds to the partially known model parameters, represented here as a stationary process with identity state transition matrix, driven by the process noise $\mathbf{r}_k$ with covariance $\mathbb{E}\left[\mathbf{r}_k\, \mathbf{r}_k^{\mathbf{T}}\right] = \mathbf{P}_{\mathbf{r}_k}$. The parameter m_1, m_2, and m_3 represent the link masses. Parameter m_1 denotes mass of shank (m_S) in the stance phase (squatting/walking) whereas it represent the mass of the foot (m_F) in the swing phase of

walking; parameter m_2 represents the mass of thigh (m_T) in the stance phase (squatting/walking) whereas it represent the mass of shank (m_S) in the walking-swing phase; and m_3 represents the mass of torso m_{tor} in the stance phase (walking/squatting) whereas in the walking-swing phase, it represent the mass of thigh. The output $\mathbf{d}_k$ corresponds to a nonlinear observation on $\mathbf{w}_k$ (in this case, a torque output); and $\mathbf{e}_k$ corresponds to the error in the nonlinear model. We define $\mathbf{Y}(\cdot)$ from (4.1) and (4.2) as

$$M(\cdot)\ddot{q} + C(\cdot)\dot{q} + G(\cdot) + \tau_f(\cdot) = \mathbf{Y}(\cdot) \tag{4.23}$$

The UKF also estimates the model parameters $\mathbf{w}_k$ using the recursion given in (4.7) and by propagating a set of generated sigma points. As an optimization approach, the UKF attempt to minimize the prediction error cost on every time step (similar to the EKF) using the cost function given by

$$J(\mathbf{w}) = \sum_{t=1}^{k} [\mathbf{d}_t - \mathbf{Y}(\mathbf{x}_t, \mathbf{w}_k)]^{\mathrm{T}} (\mathbf{P}_{\mathbf{e_k}})^{-1} [\mathbf{d}_t - \mathbf{Y}(\mathbf{x}_t, \mathbf{w})] \tag{4.24}$$

where $\mathbf{P}_{\mathbf{e_k}}$ is the estimation error covariance $\mathbb{E}[\mathbf{e}_k \, \mathbf{e}_k^{\mathbf{T}}]$.

In this study we chose the innovation covariance $\mathbf{P}_{\mathbf{r}_k}$ based on the recursive least square algorithm (Nelson, 2000) define as:

$$\mathbf{P}_{\mathbf{r}_k} = (\boldsymbol{\lambda}_{RLS}^{-1} - 1)\mathbf{P}_{\mathbf{w}_k}, \tag{4.25}$$

where $\lambda_{RLS} \in (0, 1)$ is the forgetting factor. The rate of convergence and tracking performance of the UKF filter is influenced by the innovation covariance $\mathbf{P}_{\mathbf{r}_k}$. The constant λ_{RLS} provides an exponentially weighting on past data which makes it possible to emphasize the most recent data. Notice that this feature is useful to enable tracking of the complex motion dynamics of human squatting and walking.

4.4.3.3 The Impedance Control Algorithm

In this section, we introduce the impedance based inverse dynamic (or computed torque) control law to achieve motion following and torque assistance by the exoskeleton using (as reference input) the estimated/predicted joint kinematics ($\hat{\mathbf{x}}_k$) from the DUKF.

Given the exoskeleton dynamics in (4.1) and (4.2), the impedance based computed torque control law is defined as, τ_c

$$\tau_c = \widehat{M}(q)u_{a,q} + \hat{C}(q,\dot{q})\dot{q} + \hat{G}(q) + \tau_f(q,\dot{q}) + J^T F - \tau_h \quad (4.26)$$

where,

$$u_{a,q} = \ddot{q}_d + M_r{}^{-1}[B_r(\dot{q}_d - \dot{q}) + K_r(q_d - q) - \tau_h] \quad (4.27)$$

The variables q_d, $\dot{q}_d$, and $\ddot{q}_d$ are the reference joint kinematics, i.e. 3x3 vectors of joint position, velocity and acceleration respectively, which are predicted from the DUKF. The constants M_r, B_r,and K_r are the controller impedance parameters (inertia, viscous damping, and stiffness parameters respectively). τ_h is the torque exerted on the exoskeleton by the human, defined earlier in (4.2). All other parameters are as defined in (4.1) and (4.2). F is set to zero when the foot is off the ground.

Equation (4.26) is the inner-loop computed torque control law while (4.27) is the outer-loop impedance control law which can be referred to as the commanded acceleration. To assist and follow the user's movement, the controller produces physical torque commands which attract the exoskeleton to the estimated/predicted trajectory using the inner-loop control law. The outer-loop control law ensures a desired compliance is maintained at the interaction port by means of the stipulated impedance parameters and feedback of the interaction forces τ_h.

4.4.3.4 Supervisory Control Algorithm

This section introduces the development of the higher-level supervisory controller to ensure synchronization of the exoskeleton movement with the wearer's motion, and to ensure that the wearer is in charge of the motion. The supervisory controller implements the human movement detection and movement synchronization in a 7-state hybrid automaton (see Figure 4.7). A hybrid automaton is a dynamic system (or states machine) which can be described by both discrete and continuous dynamic systems, thus, the core

of the supervisory controller is governed by discrete and continuous dynamics. The output of the supervisory controller is either -1, 0, or 1 which is used to regulate the assistive torque output of the impedance controller. More elaboration is presented in subsequent subsections.

(a) ***Discrete Dynamics***

Under the supervisory framework, five (5) events are used to detect the pilot's movement and to enable transitions between squatting and walking movements or motion phases. These events are (1) heel-off, (2) heel-strike, (3) double stance, (4) hip flexion, and (5) knee flexion. The events are captured by means of the insole ground reaction force sensors (GRF) and joint angle sensors. However, for switching the hybrid automaton or for appropriately detecting the events and phases, we compute a fractional index, P, of the ground reaction force for each leg as

$$P = \begin{cases} \dfrac{\alpha_1 F_1 + \alpha_2 F_2}{F_1 + F_2}, & either\ F_1 > \varepsilon\ or\ F_2 > \varepsilon \\ 1, & F_1 + F_2 = 0\ or\ F_1 + F_2 \leq 2\varepsilon \end{cases} \tag{4.28}$$

where, F_1 is the force measure from the insole GRF sensor placed at the heel (rear), and F_2 is the force measure from the sensor placed at the ball of foot (front). The constants α_1 and α_2 are chosen arbitrary to normalize P in the range [-1, 1]. The constant ε is the sensor offset value determine from the manufacturer documentation. Under continuous loading and unloading situation such as squatting descent/ascent or stance and swing, the offset is determined as $\varepsilon \cong 4.5\%$ ($\frac{F_{1,max} + F_{2,max}}{2}$) after each phase to correct the effect of hysteresis.

The computed P value allows classification of the modes (m) or phases of motion thus

$$m = \begin{cases} 0, & P = 1 \\ 1, & P = -1;\ q - q_t > 0 \\ 2, & P = -1;\ q - q_t < 0 \end{cases} \tag{4.29}$$

where $m = 0$ denotes walking-swing phase; $m = 1$ denotes walking-stance; and $m = 2$ denotes squatting (both ascent/descent) motion. The variable q represents the current angular position of the joint (hip or knee joint) while q_t is a set knee angle threshold, see Table 4.4.

Based on the computed P value (for either left or right leg), the 7-state hybrid automaton can be transited to synchronize with the motion state of the left and right leg. Each state enables/allows the assistance for the hips or knees. An approximate positive value of 1 ($P \approx 1$) detects the intention to swing (heel-off) which allows the joints assistance for swing motion. This event also set the mode m to zero for walking enable (4.29). An approximate negative P value (i.e. $P \approx -1$) detects the stance phase (heel-strike or foot-on-ground). Overall, squatting and walking phase is decoded by the fusion of GRF sensors and joint angle sensors. Notice that the squatting mode is generally a double stance phase. This is enabled when both heels or feet are on the ground. Squatting ascent is decoded from slight hip angle extension and flexion respectively; while squatting decent is decoded by slight knee angle flexion. The algorithm further distinguishes the stance phase of walking from squatting mode using the set knee angle threshold q_t. Table 4.5 summarizes the events logic for the detection of the walking and squatting phases and Table 4.6 gives summary states transition logic of the finite hybrid automaton

(b) ***Continuous Dynamics***

For the continuous dynamics, the supervisory controller uses a new modified Gaussian-bell sensor fusion algorithm (4.30) enmeshed in the hybrid automaton machine. This algorithm combines measurement, P, of the ground reaction forces, and the joint position measurement, q, to compute a supervisory control output σ_j given as:

$$\sigma_j = (P + m)\frac{1}{1 + \left|\frac{q - q_c}{a}\right|^{2b}} \tag{4.30}$$

where,

$$q_c = q_0 + \frac{\Delta q_j}{2}, \quad \text{and} \tag{4.31}$$

$$a = \frac{\Delta q_j}{2} \tag{4.32}$$

The subscript, j, stands for the joint identifier (i.e. hip or knee). Δq_j is the pilot's flexion/extension range of motion for each joint during walking or squatting phase derived from the knowledge of the human biomechanics (Table 4.4); q_0 represents the initial position of the joint just before heel-off (for walking mode), or just before squat-decent (or ascent) for the squatting mode, detected by P; q_c is the center of the Gaussian Bell function; b controls the slope of the function; while a controls the spread around q_c. A sample plot of the supervisory control output σ_j with respect to joint position is shown in Figure 4.8. The control output σ_j is combined with the computed torque output of the impedance controller as shown in the overall synchronous control system architecture in Figure 4.9.

The supervisory control algorithm outputs any of the following three values: -1, 0, and 1. It outputs 1 or -1 along the range of motion $q_0 < q < q_0 + \Delta q_j$, and zero outside this range. When the swing phase is enabled, an output of 1 allows the torque assistance to continue for hip or knee flexion (-1 for hip or knee extension) as long as q is within the allowable range of motion and drops-off the torque assistance outside this range. Likewise, when the squatting mode is enabled, the algorithm outputs 1 to allow either hip or knee flexion (or -1 for hip/knee extension). The algorithm ensures synchronous movement assistance and also ensures that the joints do not extend beyond the pilot's normal flexion/extension range of motion, Δq_j. By this means, power consumption can also be saved. The overall control architecture is depicted in Figure 4.9.

Analysis that shows stability of the overall hybrid supervisory control system, including occasions when potentially unsafe events occurs that cause $\sigma_j = 0$, have been provided in Section 4.4.4. In this context, we attempt to address the problem of system stability where healthy users can be forced into unintended movement or towards unsafe posture configuration as a result of the exoskeleton assistance. A similar system stability problem had been encountered in the work of Petric et al. (2013) using gravity compensation control for a knee exoskeleton to assist squatting movement. The exoskeleton had been seen attempting to always extend the user's knee even when the user had intended the reverse movement. Our current supervisory control scheme thus seek to resolve such unsafe situations by ensuring that the exoskeleton follows and assist the user's movement and drop assistance when the assistance tends to move the user or his centre of gravity (COG) outside the safe base of support e.g. when the user's lower-limb reaches the hip/knee extension or flexion limits during squat-ascent or squat-descent (in double stance), or flexion/extension limits during single leg swing or single leg stance. Thus, while ensuring stability within the base of support, the control scheme also attempts to prevent risky situation or unsafe configuration outside the base of support for safety. This scheme may be analogous to the restraining functions of the human tendons and ligaments in preventing over-flexion/extension of the lower-limb joints while also ensuring the stability and integrity of the respective joint. See Section 4.4.4 for the overall control system stability prove.

Table 4.5: Summary of states and transitions

GRF index (P)	**Knee Joint Angle**	**Detection**	**m**	**Mode**	**Δq_j (degree)**
1	n/a	Leg swing	0	Walking (swing)	Hip = 40 Knee =60
-1	$q - q_t > 0$	Stance (heel-strike)	1	Walking (stance)	
-1	$\boldsymbol{q - q_t < 0}$	Stance (squatting)	2	Squatting	Hip = 65 Knee = 65

Table 4.6: Summary of events logics

Movement	Discrete Events		Transition (c)
	Right leg	**Left leg**	
	Default transition	Default transition	c_0
Squatting	Hip-flexion/extension ($P \approx -1, m = 2, \lvert(q - q_0)\rvert_{hip} > 0$)	Hip-flexion/extension ($P \approx -1, m = 2, \lvert(q - q_0)\rvert_{hip} > 0$)	c_1
	Knee-flexion ($P \approx -1, m = 2, (q - q_0)_{knee} > 0$)	Knee-flexion ($P \approx -1, m = 2, (q - q_0)_{knee} > 0$)	c_2
Walking	Heel-off ($P \approx 1, m = 0, (q - q_0)_{hip} > 0$)	Stance ($P \approx -1, m = 1, (q - q_0)_{hip} \approx 0$)	c_3
	Heel-strike ($P \approx -1, m = 1, (q - q_0)_{hip} \approx 0$)	Stance ($P \approx -1, m = 1, (q - q_0)_{hip} \approx 0$)	c_4
	Stance ($P \approx -1, m = 1, (q - q_0)_{hip} \approx 0$)	Heel-off ($P \approx 1, m = 0, (q - q_0)_{hip} > 0$)	c_5
	Stance ($P \approx -1, m = 1, (q - q_0)_{hip} \approx 0$)	Heel-strike ($P \approx -1, m = 1, (q - q_0)_{hip} \approx 0$)	c_6

Table 4.7: Summary of states logics

Movements	States	Continuous Dynamics (σ_j)	Mode	Continuous Dynamics (σ_j)	Mode
		Right Leg	**Right Leg**	**Left Leg**	**Left Leg**
	S1	Default State		Default State	
Squatting	**S2**	Squat descent	($m = 2$)	Squat descent	($m = 2$)
	S3	Squat ascent	($m = 2$)	Squat ascent	($m = 2$)
Walking	**S4**	Right_leg_swing	($m = 0$)	Left_leg_stance (Mid stance)	($m = 1$)
	S5	Right_leg_stance (initial contact)	($m = 1$) Double stance	Left_leg_stance (Pre-swing)	($m = 1$) Double stance
	S6	Right_leg_stance (Mid stance)	($m = 1$)	Left_leg_swing	($m = 0$)
	S7	Right_leg_stance (Pre-swing)	($m = 1$) Double stance	Left_leg_stance (initial contact)	($m = 1$) Double stance

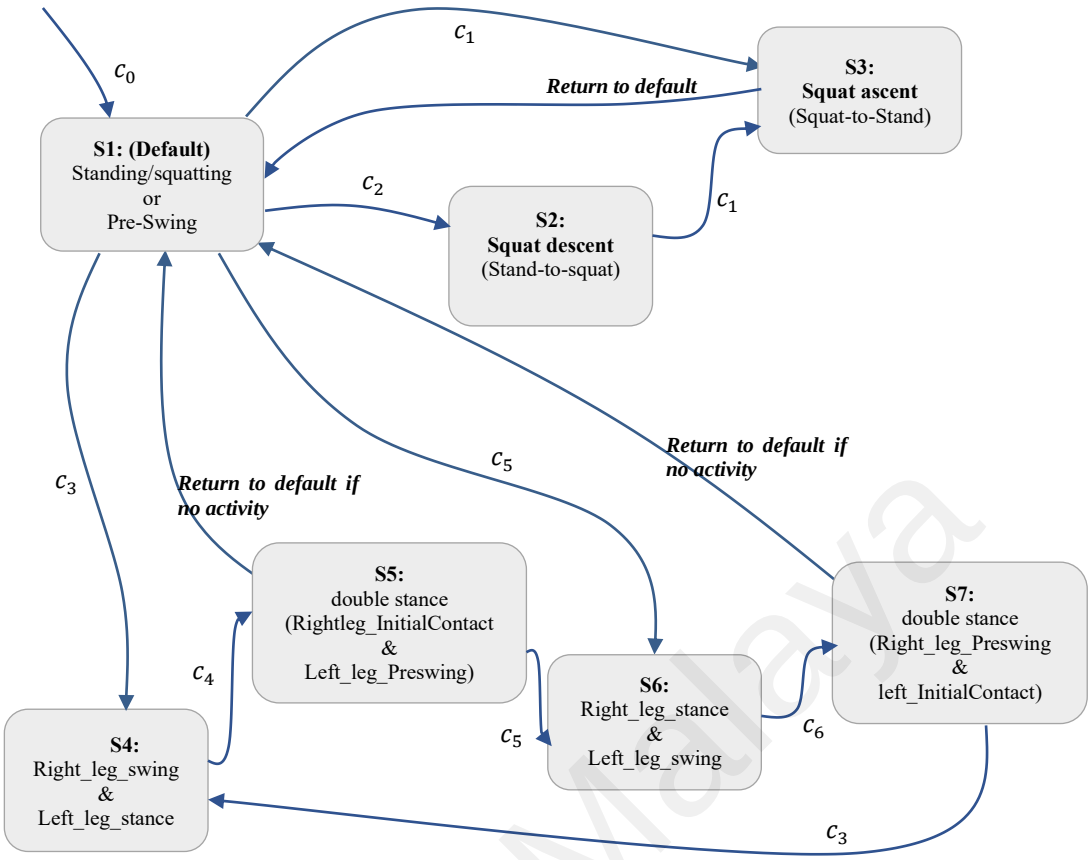

Figure 4.7: Supervisory hybrid automaton architecture

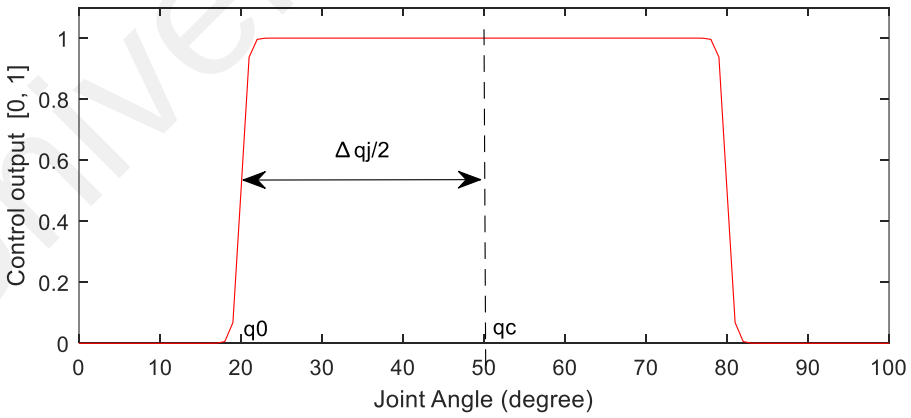

Figure 4.8: Modified Gaussian bell function

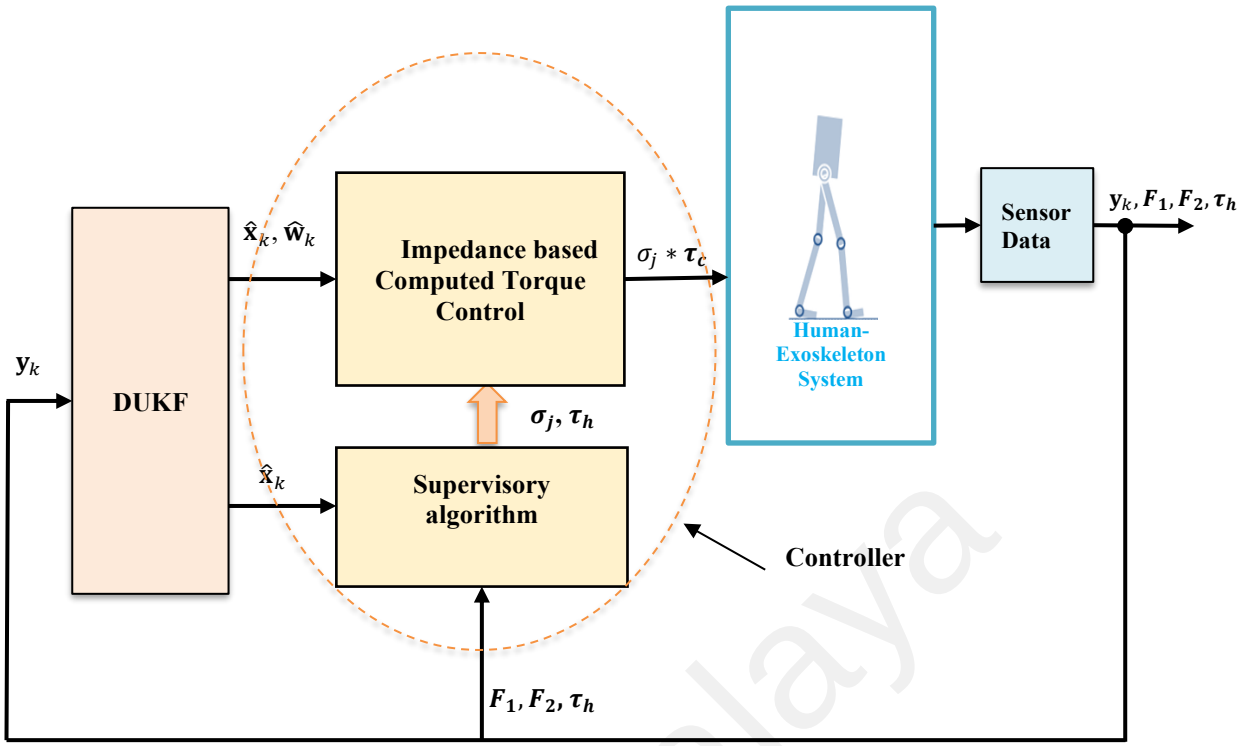

Figure 4.9: The proposed EHPA control architecture

4.4.4 Stability Analysis

4.4.4.1 Closed-loop Impedance Control System

Consider the exoskeleton dynamics given in (4.1) and (4.2), and the impedance based computed torque control law, τ_c given in (4.26) and (4.27), the resulting closed-loop system obtained by equating (4.1) (or (4.2)) and (4.26) (i.e. $\tau_a = \tau_c$) is

$$\ddot{q} = \ddot{q}_d + {M_r}^{-1}[B_r(\dot{q}_d - \dot{q}) + K_r(q_d - q) - \tau_h] \quad (4.33)$$

where parameters are as defined in (4.26).

Let M_r =$diag$ (M_{ri}), B_r =$diag$ (B_{ri}), and K_r =$diag$ (K_{ri}) be positive definite symmetric matrices, where i = 1 to 3. To show stability of the closed-loop system (4.33), the error state space vector is defined as

$$e = [\delta q^T \ \ \delta \dot{q}^T]^T \quad (4.34)$$

where $\delta q = q_d - q$

Thus, the closed-loop system (4.33) can be rewritten in terms of the error dynamics as

$$M_r\,\delta\ddot{q} + B_r\delta\dot{q} + K_r\delta q = \tau_h \tag{4.35}$$

The system can be proven to be globally asymptotically stable by Lyapunov's method.

Consider the candidate Lyapunov function $V(\delta q)$ given as,

$$V(\delta q) = \frac{1}{2}\delta\dot{q}^T M_r\delta\dot{q} + \frac{1}{2}\delta\dot{q}^T K_r\delta q \tag{4.36}$$

Taking the time derivative of $V(\delta q)$ along the trajectories of the closed-loop system (4.35), we get

$$\dot{V}(\delta q) = \delta\dot{q}^T M_r\delta\dot{q} + \delta\dot{q}^T K_r\delta q \tag{4.37}$$

Re-arranged as

$$\dot{V}(\delta q) = \delta\dot{q}^T(M_r\delta\dot{q} + K_r\delta q) \tag{4.38}$$

Solving for $M_r\delta\dot{q} + K_r\delta q$ in (4.35), for the case $\tau_h = 0$, the following negative semi-definite function is obtained

$$\dot{V} = -\delta\dot{q}^T B_r\delta\dot{q} \leq 0 \tag{4.39}$$

which shows that the closed-loop system (4.35) is asymptotically stable for the case $\tau_h = 0$ based on the following theorem:

Theorem. If M_r, B_r, and K_r in the closed loop system are symmetric positive definite, the system is asymptotically stable (Bonitz & Hsia, 1996; Khalil & Grizzle, 1996).

Proof. The proof is given from Lyapunov theory (Bonitz & Hsia, 1996; Khalil & Grizzle, 1996), which says that the system is asymptotically stable if there exist a scalar function $V(\delta q)$ of the error state δq with continuous first order derivatives such that

(a) $V(\delta q)$ is positive definite;

(b) $\lim_{\|\delta q\|\to\infty} V(\delta q) = \infty$; and

(c) $\dot{V}(\delta q) \leq 0$ (i.e. negative definite).

For the case when $\tau_h \neq 0$ (i.e. human exert torque on the exoskeleton), solving for $M_r\delta\dot{q} + K_r\delta q$ in (4.35) yield the following function

$$\dot{V}(\delta q) = \delta\dot{q}^T\tau_h - \delta\dot{q}^T B_r\delta\dot{q} \tag{4.40}$$

In this case, a different robust stability can be found only when B_r is sufficiently large (i.e. $B_r \gg \tau_h$), consistent with the theorem proposed in (Qu et al., 1991) (Theorem 2) which showed that a closed loop error system is stable in the sense that it is uniformly ultimately bounded if a constant gain is chosen to be large enough.

4.4.4.2 Overall Synchronous Controller Stability

The overall synchronous controller can be described as a hybrid feedback system which combines a continuous error dynamic (flow) derived from the impedance controller (4.34) and a discrete flow σ_j (or resetting signal) derived from the supervisory controller (4.30).

Once again, consider the exoskeleton dynamics given in (4.1) and (4.2), the impedance control law, τ_c, given in (4.26) and the supervisory control law, $\sigma_j \in \{-1, 0, 1\}$, given in (4.30); the hybrid feedback closed-loop system is obtained by combining (4.2), (4.26), and (4.30) as

$$\tau_a = \tau'_c \tag{4.41}$$

where

$$\tau'_c \quad = \tau_c|\sigma_j| \quad = \begin{cases} \tau_c, & |\sigma_j| = 1 \ (i.e.\ either\ \sigma_j = -1\ or\ \sigma_j = 1) \\ 0, & |\sigma_j| = 0 \end{cases} \tag{4.42}$$

In our case, $\tau_c|\sigma_j| = |\tau_c|\sigma_j$ since the direction sense of τ_c and σ_j are same.

For the case $|\sigma_j| = 1$, Equation (4.41) becomes $\tau_a = \tau_c$, thus the closed loop system dynamics of the hybrid feedback system is the same as the one given in (4.35). Asymptotic and robust stability of the system by Lyapunov stability analysis also proceeds as presented in (4.36) to (4.40).

For the case $|\sigma_j| = 0$, we have $\tau_a = 0$, and a new closed loop system is formed from (4.41) as

$$M(q)\ddot{q} + C(q,\dot{q})\dot{q} + G(q) + \tau_f(q,\dot{q}) = \tau_h \quad (4.43)$$

Notice that the driving torque is solely derived from the wearer who is also responsible to guarantee stability of the system (4.43). This situation describes two regions: (1) the initial point where $\sigma_j(0) = 0$ and (2) a small range about the limit of hip/knee extension or flexion which is outside the range of allowable motion assistance for safety (i.e. outside $q_0 < q < q_0 + \Delta q_j$) (see Section 4.4.3.4 (b) for detailed explanation).

Stability under this situation can also be established by Lyapunov's method. Consider the following candidate Lyapunov function motivated by the inertia-related and passivity approach in (Dawson et al., 2003):

$$V(q) = \frac{1}{2}\dot{q}^T M(q)\dot{q} + \beta - \int_0^t \dot{q}^T N(q,\dot{q})dt \quad (4.44)$$

where $N(q,\dot{q}) = \tau_h - G(q) - \tau_f(q,\dot{q})$ and β is some positive scalar constant chosen such that $\int_0^t -\dot{q}^T N(q,\dot{q})dt \geq -\beta$ at all times (Dawson et al., 2003).

Taking the time derivative of $V'(q,\dot{q})$ along the trajectories of the system (4.43), we get

$$\dot{V}(q) = \dot{q}^T M(q)\ddot{q} + \frac{1}{2}\dot{q}^T \dot{M}(q)\dot{q} - \dot{q}^T N(q,\dot{q}) \quad (4.45)$$

Substituting $M(q)\ddot{q} = N(q,\dot{q}) - C(q,\dot{q})\dot{q}$ from (4.43) in (4.45) gives

$$\dot{V}(q) = \dot{q}^T N(q,\dot{q}) + \dot{q}^T \left(\frac{1}{2}\dot{M}(q) - C(q,\dot{q})\right)\dot{q} - \dot{q}^T N(q,\dot{q}) \quad (4.46)$$

Applying skew-symmetric property highlighted in (Dawson et al., 2003), it can be shown that $\left(\frac{1}{2}\dot{M}(q) - C(q,\dot{q})\right) = 0$, thus

$$\dot{V}(q) = 0 \tag{4.47}$$

which shows that the system is asymptotically stable for the case $|\sigma_j| = 0$.

(a) ***Transition Stability***

Although stability has been independently established for the closed-loop system (i.e. (4.33) or (4.35)) for the case $\tau_a = \tau_c$ (when $|\sigma_j| = 1$) and $\tau_a = 0$ (when $|\sigma_j| = 0$), the effect of a signal jump (i.e. $\tau_c \to 0$) due to the discrete supervisory control output σ_j can still lead to system instability. Analysis of stability of the hybrid system is thus motivated to guarantee transition stability or stability of the closed-loop system in the presence of a resetting signal (i.e. σ_j) or an event.

Following the procedure highlighted by (Bainov & Simeonov, 1989; Bupp et al., 2000; Haddad et al., 2014), it can be proven that given a dynamic closed loop system ((4.33) or (4.35)) with impulsive effect or a resetting signal (σ_j), local and global asymptotic stability conclusions of an equilibrium point of the system can be provided if a smooth Lyapunov function (positive-definite and at least continuously differentiable) can be constructed for which its time rate of change over the continuous-time dynamics is strictly negative and its difference across the resetting times is negative(Haddad et al., 2014).

Theorem. Suppose there exist a continuously differentiable function $V : \mathbb{R}^n \to [0, \infty)$ satisfying $V(0) = 0, V(q) > 0,\ q \neq 0$, and

$$\langle \nabla V(q), F(q) \rangle \leq 0 \qquad q \in \mathbb{R}^n, \tag{4.48}$$

$$V(q + \rho(q)) - V(q) \leq 0 \qquad q \in \mathbb{R}^n \tag{4.49}$$

Then the zero solution of the system is Lyapunov stable (Bupp et al., 2000; Goebel et al., 2009). Furthermore, if the inequality in (4.48) is strict for all $q \neq 0$, then the zero solution

of the system is asymptotically stable. If, in addition $\lim_{\|q\|\to\infty} V(q) = \infty$, then the zero solution of system is globally asymptotically stable. Detail proof of the theorem can be found in (Bupp et al., 2000).

In (4.48), $F(\delta q)$ represent the flow map given by (4.33) where $|\sigma_j| = 1$. Thus, the Lyapunov stability condition (4.48) is established by the analysis given in (4.36) to (4.40), i.e.

$$\langle \nabla V(q), F(q) \rangle = \big(V(\delta q)\big)_{B_r \gg \tau_h} \leq 0 \tag{4.50}$$

In (4.49), $\rho(q)$ represent a difference equation given by $\delta q = \rho(q)$, which governs the way the states are instantaneously changed when a resetting event occurs. Thus, stability condition (4.49) is established as

$$V(q + \rho(q)) - V(q) = V(\delta q) - V(q) = (\delta \dot{q}^T \tau_h - \delta \dot{q}^T B_r \delta \dot{q}\,)_{B_r \gg \tau_h} \leq 0 \tag{4.51}$$

Since stability condition of (4.48) and (4.49) is established (by an ultimately uniformly bounded constant gain $B_r \gg \tau_h$), the hybrid system's equilibrium point is stable during each jump.

4.5 Summary

This chapter has presented the design and system modelling of UMExoLEA. It details the main concept of design, biomechanical analysis of movements in lifting and carrying activities, and system modelling which involve formulation of the dynamic model, controller design, and stability analysis. UMExoLEA design has been motivated to augment the hip extension/flexion muscles and the knee extension/flexion muscles of the lower extremity in order to decrease the effect of repetitive strain and stress on the lower extremity musculature during repeated lifting/carrying tasks. To achieve this aim, applying knowledge of the biomechanics of the lower extremity and the kinematic/kinetic

configuration of the exoskeleton in squat-lifting and walking/carrying motion has facilitated the formulation of the dynamic model of the exoskeleton which is a requisite for the development of the synchronous mobility controller. Consequently, the developed synchronous mobility controller integrated three main algorithms for estimation/prediction of wearers motion trajectory (i.e. joint position, joint angular velocity, and acceleration), torque assistance, movement detection and synchronization of the exoskeleton with the wearer during squat-lifting and walking/carrying motion. Overall stability analysis has also been presented in this chapter which shows that the system is stable under the synchronous mobility controller.

CHAPTER 5: SIMULATIONS STUDIES

5.1 Introduction

This chapter presents simulation studies to test the robustness of the dual unscented Kalman filter (DUKF) and trajectory performance of the impedance controller.

5.2 DUKF Robustness Analysis

The constructed DUKF was tested, first, by simulation for accuracy in state estimation/generation, and validated for robustness using the extensive Monte Carlo simulations (Lefebvre* et al., 2004; Rubinstein & Kroese, 2016) before being applied to the prototype exoskeleton. These simulations test the variations in the process noise (i.e. human-exoskeleton system disturbances/uncertainties) and measurement noise (i.e. sensor noise) realization, as well as the initial states guesses, and states covariance guesses for validating the accuracy of states estimation/prediction during coupled movement interaction. Generally, the key signal of interest for validation is the residuals (or innovations), $\tilde{\mathbf{y}}_k = \mathbf{y}_k - \hat{\mathbf{y}}_k^-$, which should satisfy three criteria:

(1) Should have small magnitude

(2) Zero mean and

(3) No autocorrelation, except at zero lag.

Prior to validating the robustness of the DUKF for state estimation/generation, we make our initial guess of states and states covariance. For both simulation and experiment, our initial states guess is given by $\mathbf{x}_k = [84, -175, 0, 0, 0, 0]^T$ where the first three elements (joint angles, q^T) are taken experimentally from the position sensor measurement on the hip, knee, and ankle in double stance phase, and the last three elements (joint velocities, $\dot{q}^T$) are arbitrarily assumed zero since the velocities are small

in this phase. Our initial guess of process noise covariance is specified as **v**=**diag** ([0.8, 1, 1, 1, 1, 1]) to account for model inaccuracies and the effect of unknown disturbances on the plant. The higher values of process noise covariance reflect the knowledge that the states are more impacted by modeling errors. We also provided our knowledge (initial guess) of (sensor) measurement noise covariance as **n**=**diag** ([0.8, 0.8, 0.8, 0.8, 0.8, 0.8]). The DUKF generated states using recorded hip and knee gait trajectory as sensors' input to the filter is shown in Figure 5.1. The mean values of the residuals are found to be 0.0229 degrees and -0.4968 degrees for the hip and knee joints respectively, which are small relative to the magnitude of the residuals, indicating no divergence in states estimation, and good filter performance. See Figure 5.2 for a plot of the residuals and the autocorrelation of the residuals. The mean correlations of the residuals are also close to zero (0.0011 for hip and 0.0362 for knee). They are found to be small for all lags except 0 and does not show any significant non-random variations. Ideally, the mean correlation of residuals is also required to be small, zero mean, and uncorrelated with less variance within filter error covariance estimate. These characteristics increase the confidence in filter performance and are indicative of the robustness of the filter. Refer to Table 5.1 for summary of the filter performance.

The error between the estimated states $\hat{\mathbf{x}}_k$ and the true states $\mathbf{x}_k$ (just as with the residuals) is also found to be small and uncorrelated with approximately zero mean, indicating boundedness of the states' estimation errors.

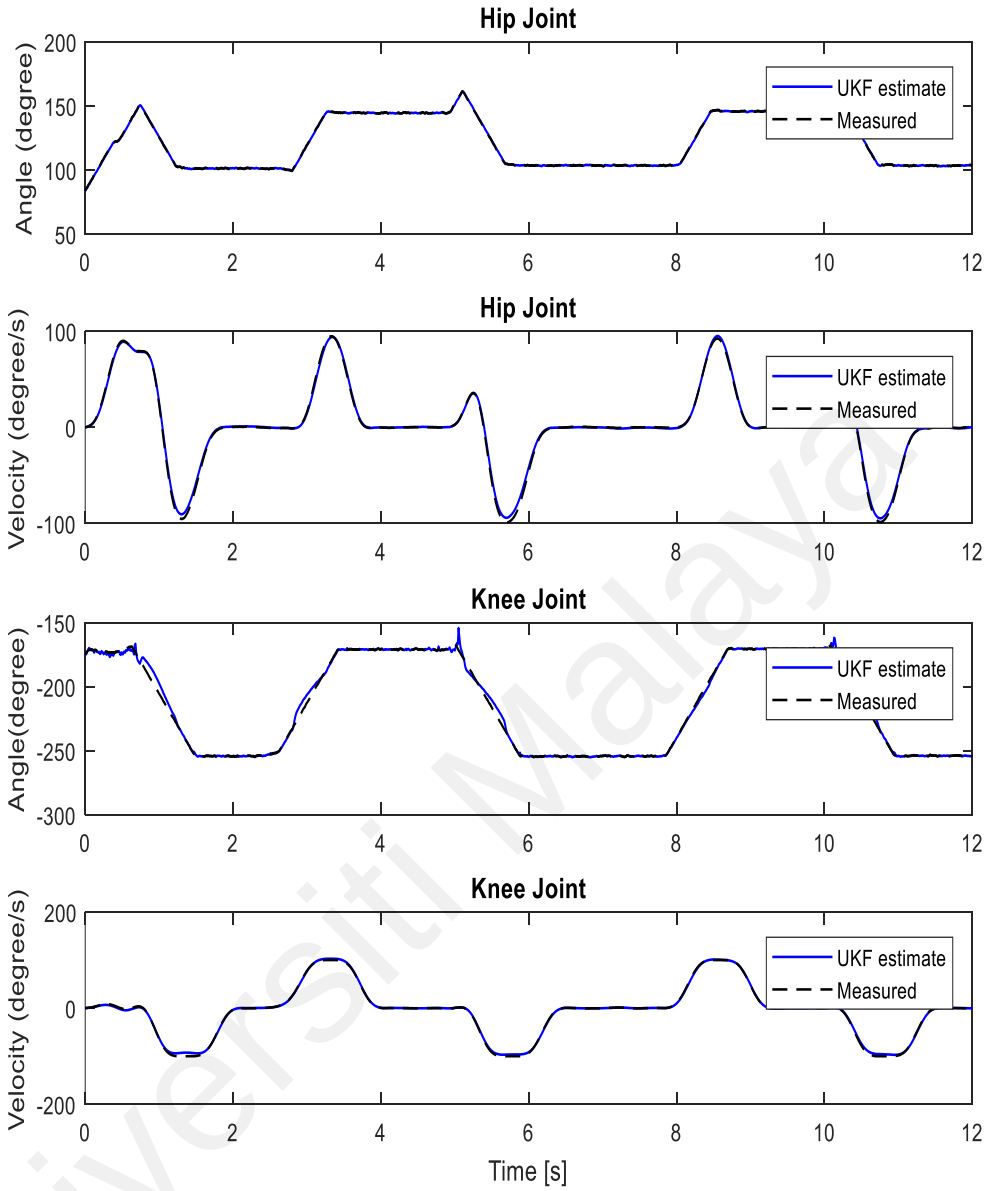

Figure 5.1: UKF simulation performance: comparison between estimated states and measured states

Figure 5.3 shows the states estimation error and the 1-σ uncertainty bounds from the filter error covariance estimate. The σ (sigma) uncertainty bounds indicate the confidence interval around the best estimate. Less than 30% of the errors exceeding the 1-sigma uncertainty bound implies good estimation. The first states estimation (i.e. joint positions) errors for hip and knee exceed the 1-sigma uncertainty bound by approximately

0% and 27.81% (less than 30%) respectively of the time steps which indicate good confidence and robustness in the filter performance. However, the second states estimation (i.e. joint velocities) are slightly higher than 30% (Refer to Table 5.1). Meanwhile, the mean values of the errors are small relative to the value of states which suggest overall confidence in filter performance. Figure 5.4 shows the autocorrelation plot of state estimation error which give little non-random variations for small lag values.

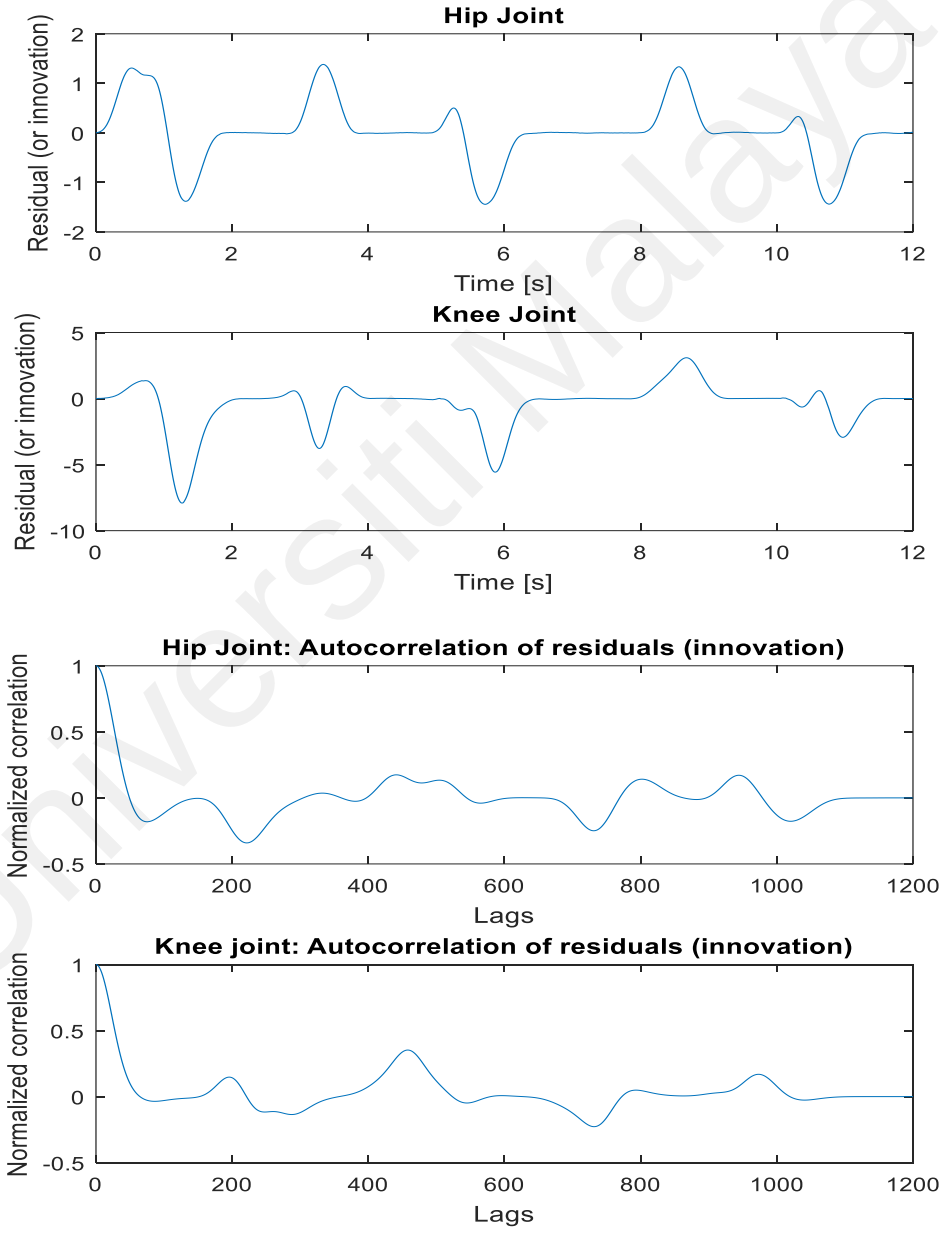

Figure 5.2: The residuals of the innovation and normalized autocorrelation of the residuals

Table 5.1: Summary of DUKF performance

Joint	Mean Value of Residuals (degrees)	Mean correlation of Residuals (degrees)	Mean states estimation error (degrees)	1-sigma uncertainty bounds (%)
Hip	0.0229	0.0011	State 1: -0.7490 State 2: -0.7490	State 1: 0 State 2: 39.72
Knee	-0.4968	0.0362	State 1: -0.5792 State 2: -0.5792	State 1: 27.81 State 2: 46.29

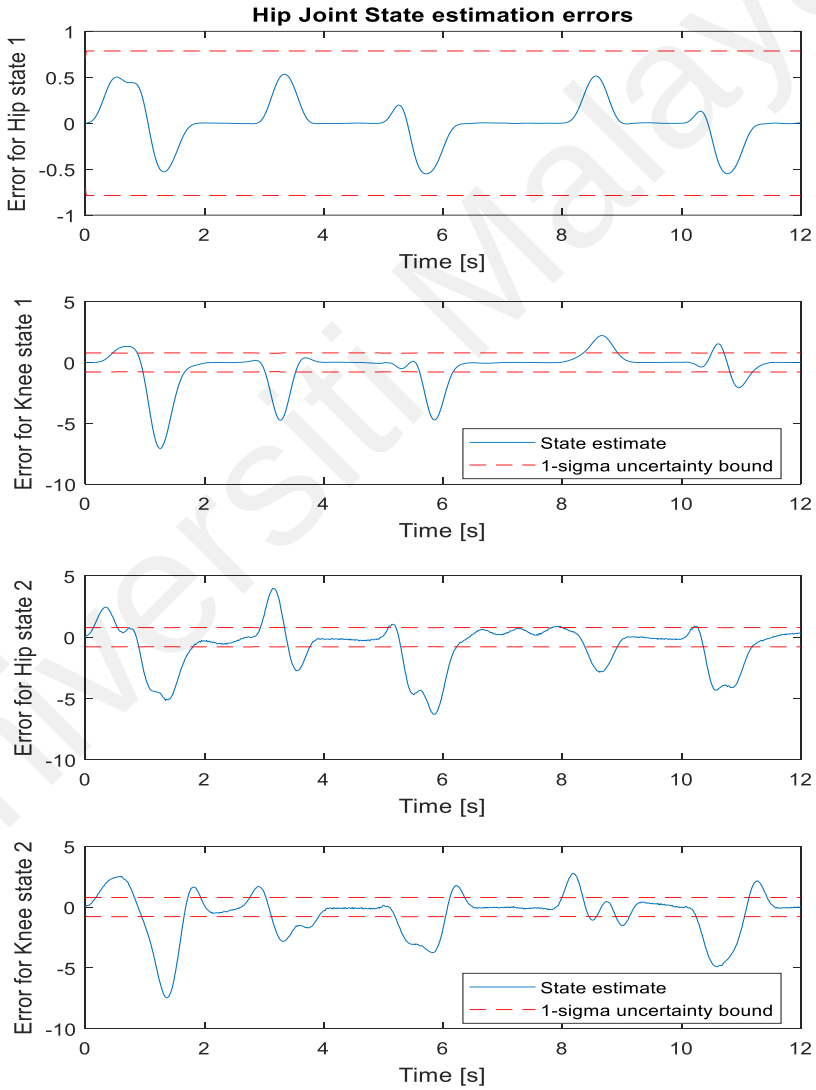

Figure 5.3: The states estimation error and the 1-sigma uncertainty bound from the filter error covariance estimate

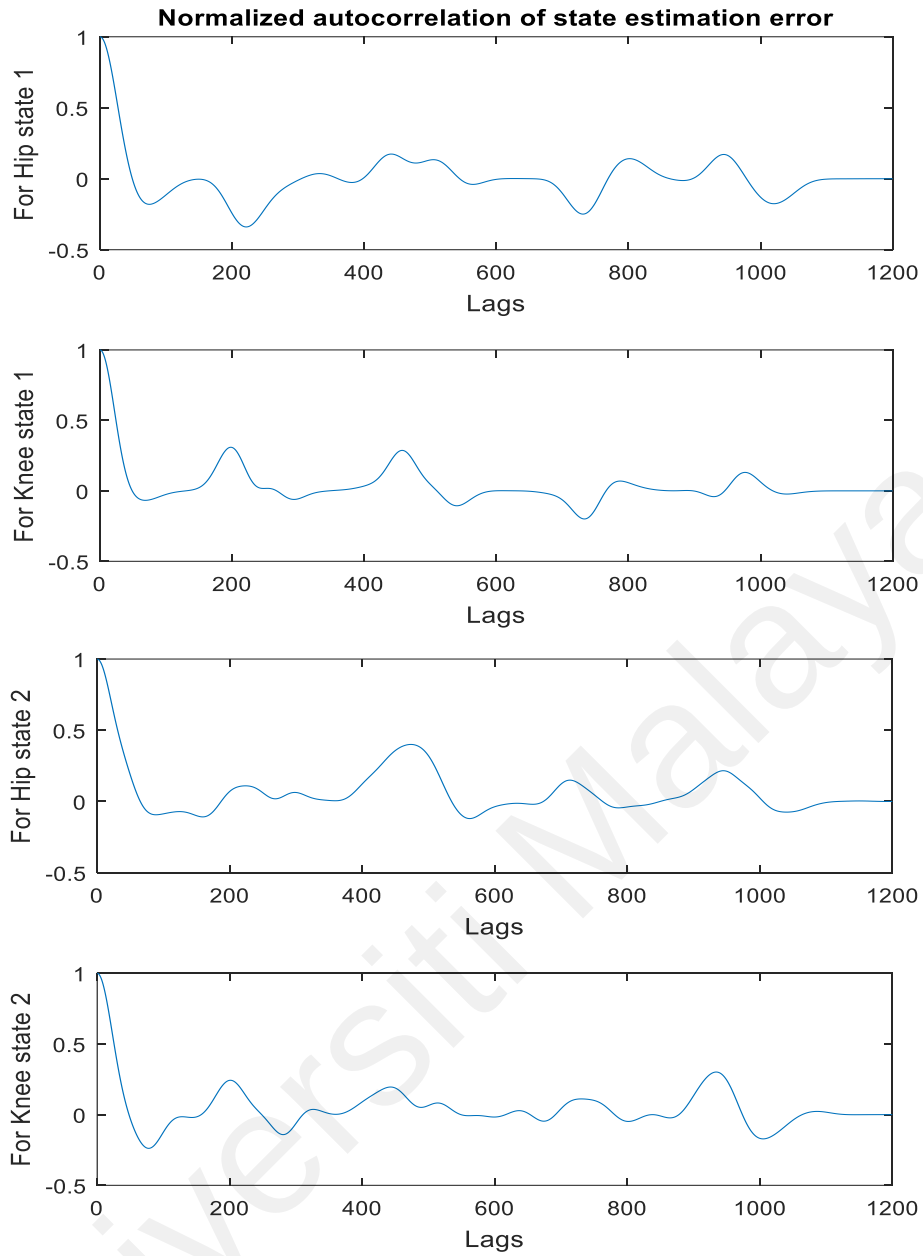

Figure 5.4: The normalized autocorrelation of states estimation error

5.3 Impedance Control Simulation

5.3.1 Trajectory Following

Figure 5.5 and Figure 5.6 show the simulation results of the impedance controller for hip and knee trajectory following respectively. Comparison is made between the estimated trajectory (i.e. joint position and angular velocity) by the DUKF and the actual trajectory feedback from the plant. The plant in this case is the exoskeleton dynamics

given in (4.1) and (4.2) coupled with the motor transfer function given in Table 5.2. See Figure J1 in Appendix J for the Simulink model of plant. Figure 5.5 (a) and Figure 5.5 (b) show position and velocity following performance respectively for the hip joint. Good performance is achieved with impedance parameters selected as $M_r = 1\text{Ns}^2(\text{degree})^{-1}$, $B_r = 260$ Ns(degree)$^{-1}$, and $K_r = 16.9$ kN(degree)$^{-1}$ at natural frequency of $\omega_n = 0.72\pi$rad/s, after heuristic tuning, which produced least tracking root mean squared error of 9.62% and 0.88% for position and angular velocity respectively.

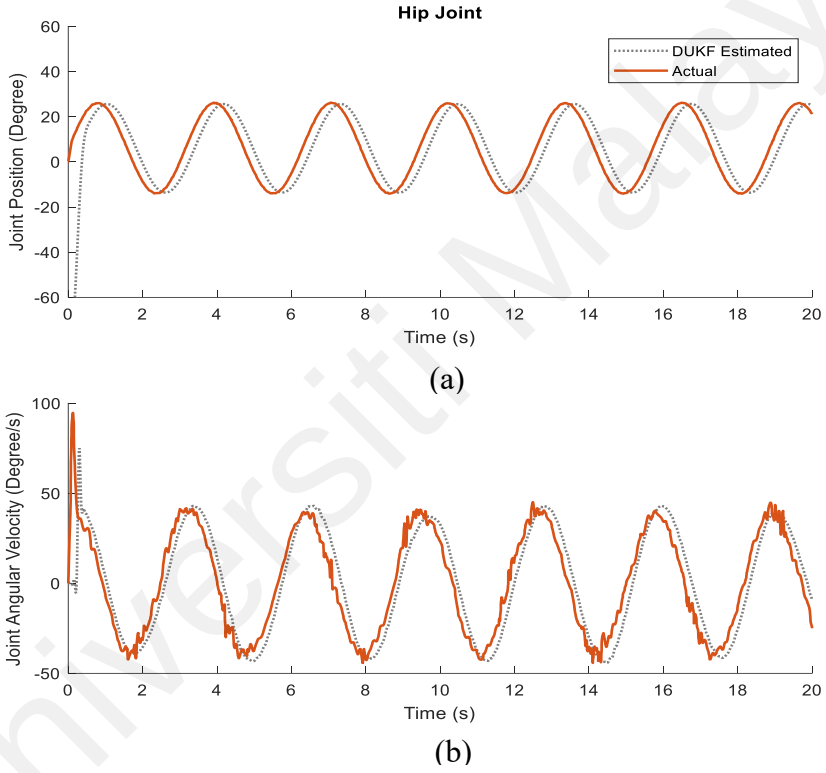

Figure 5.5: Hip joint trajectory following simulation. Comparison is made between DUKF estimated and actual (a) joint position and (b) angular velocity.

For the knee joint, best performance is achieved with the same selected impedance parameters which produced tracking root mean squared error within 3.61% and 2.43% for knee joint position and angular velocity respectively. These parameters are also selected to achieve critical damping $\zeta = 1$ without overshoot.

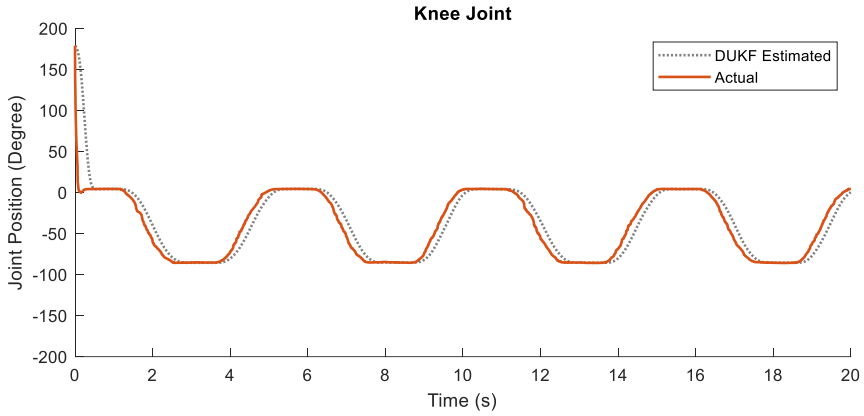

(a)

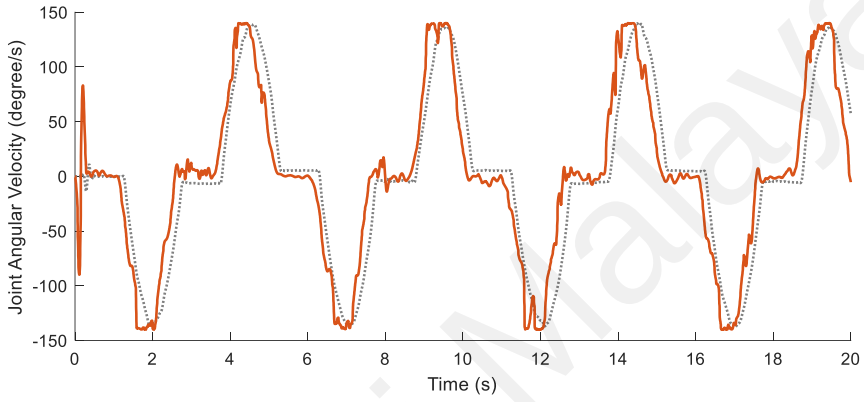

(b)

Figure 5.6: Knee joint trajectory following simulation. Comparison is made between DUKF estimated and actual (a) joint position and (b) angular velocity.

5.3.2 Torque Generation and Motor Torque Tracking

Figure 5.7 show the torque generation by the impedance controller and the motor tracking performance for the hip (Figure 5.7 (a)) and knee joint (Figure 5.7 (b)) respectively. Root mean square error difference between the impedance computed control torque and motor torque is achieved within 0.046% for the hip joint and 3.68% for the knee joint respectively, which indicate good performance.

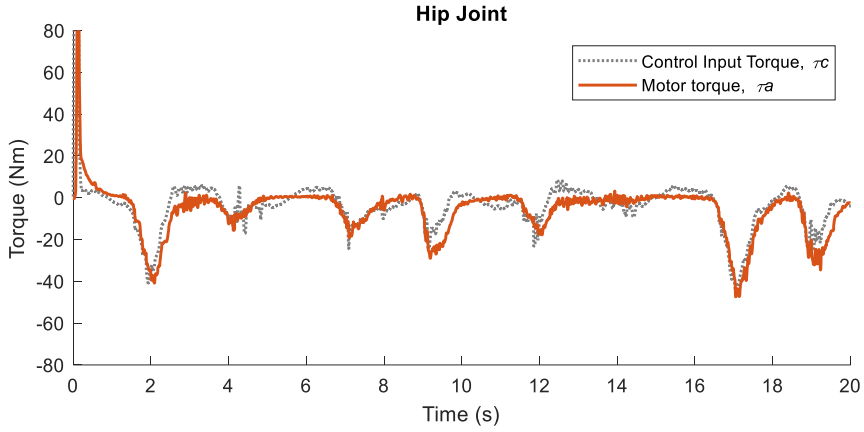

(a)

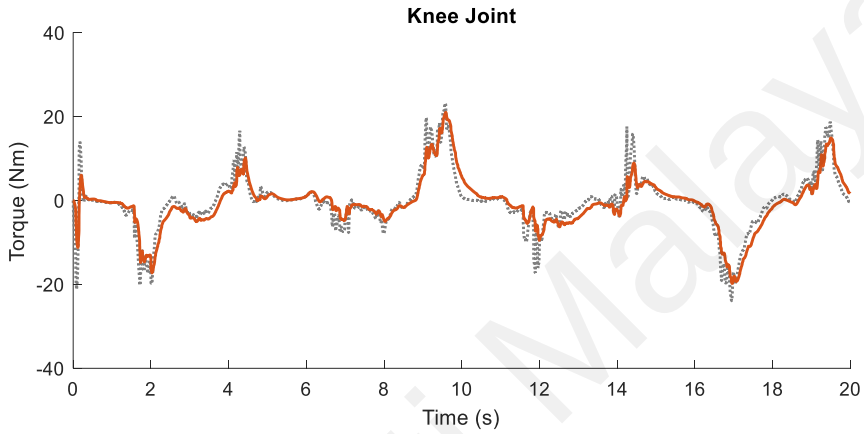

(b)

Figure 5.7: Hip and Knee motor torque tracking simulation. Comparison is made between the computed torque and motor torque.

Table 5.2: Experimentally determined BLDC motor transfer function

Joint	**Motor Transfer Function** $(\frac{i_a}{i_c})$	**Motor Torque Constant** (K)**Nm/A**
Hip	$\frac{-7.469\,s\,-\,5.706}{s^2\,+\,6.859\,s\,+\,0.8224}$	10.97
Knee	$\frac{1.128\,s\,+\,0.5911}{0.3344\,s^2\,+\,2.17\,s\,+\,1}$	8.10

5.4 Summary

This chapter has presented the simulation studies of the robustness of the dual unscented Kalman filter (DUKF) and performance of the impedance controller. The

DUKF robustness has been analyzed using extensive Monte Carlo simulations which test the variations in the process noise (i.e. human-exoskeleton system disturbances/uncertainties) and measurement noise (i.e. sensor noise) for validating the accuracy of the states' estimation/prediction during coupled movement interaction. The mean values of the residuals (the key signal for validation) have been found to be 0.0229 degrees and -0.4968 degrees for the hip and knee joints angles estimate respectively, which are small relative to the magnitude of the residuals, indicating no divergence in states estimation, and good filter performance. The mean correlations of the residuals were also close to zero (i.e. 0.0011 for hip and 0.0362 for knee) for all lags except 0 and does not show any significant non-random variations also indicating good filter performance.

The performance of impedance controller on the other hand have been analyzed by motion tracking and torque generation simulations. For the hip joint, least tracking error (root mean square) of 9.62% and 0.88% for position and angular velocity respectively have been achieved with selected impedance parameters of $M_r = 1\text{Ns}^2(\text{degree})^{-1}$, $B_r = 260\ \text{Ns}(\text{degree})^{-1}$, and $K_r = 16.9\ \text{kN}(\text{degree})^{-1}$ at natural frequency of $\omega_n = 0.72\pi\text{rad/s}$, after heuristic tuning. For the knee joint, root mean squared error were within 3.61% and 2.43% for knee joint position and angular velocity respectively. For torque generation, the root mean square error difference between the impedance computed control torque and motor torque were achieved within 0.046% for the hip joint and 3.68% for the knee joint respectively, which indicated good performance.

CHAPTER 6: PROTOTYPING AND SYSTEM IDENTIFICATION

6.1 Introduction

This chapter presents the prototype design of UMExoLEA and system parameter identification experiments. The system parameter identification involves identification of the exoskeleton actual link parameters and joint frictional torque to further enhance the accuracy and validity of the dynamic model (developed in Chapter 4) for control purpose.

6.2 Prototype design

6.2.1 Exoskeletal Structure and Actuation Module

Based on the biomechanics analysis and the system model in Chapter 4, a prototype 12-DOF active EHPA system is designed. Figure 6.1 shows the overall configuration of the developed exoskeleton with main components. The system is designed as a lower-limb anthropomorphic device with six link segments: the right thigh (RT), the right calf/shank (RC), the right foot (RF), the left thigh (LT), the left calf/shank (LC), and the left foot (LF) links. See Table 6.1 for the exoskeletons link lengths. Two hollow shafts, back-drivable, bi-directional brushless DC motor-types (BLH450KC-200 and BLH230KC-200 from Oriental Motor Inc.) with rated torques 34Nm (power = 50W and weight = 2.4kg) and 17Nm (power = 30W and weight = 1.3kg) are selected for the hip and knee actuation respectively to allow sagittal hip/knee flexion and extension movements (Figure 6.2). See Table 6.2 for details of the joint actuation system. No actuation system is used for the passive ankle joint to minimize energy cost and simplicity of design.

The selection of motor torques for the hip and knee joints were mainly influenced by two factors: the demand for lightweight and the amount of muscle torque needed by an average adult for squatting (hip->0.6Nm/Kg; Knee->0.2Nm/Kg) and walking (hip ->0.6Nm/Kg; Knee- >0.2Nm/Kg) movements under moderate loading conditions (0-10kg) (Escamilla, 2001; Kirkwood et al., 2007; Vaughan et al., 1999). In this design, a

trade-off is applied for the selection of the actuation systems as well as materials (aluminum alloy 8081) to arrive at an approximately 12.5kg overall weight of the lower-limb exoskeleton-without the bag-pack.

The foot module of the exoskeleton is designed into a detachable shoe to allow the possibility of using different sizes of shoes by different users. It also provides a means to channel the exoskeleton's weight to the ground. To ensure firm coupling and compliant movement between the wearer and the exoskeleton, the EHPA is designed with four soft braces attached at the thigh and shank links (Figure 6.1). At the upper-body, a rigid mechanical bar around the hip and a thin harness made of aluminum sheet is used to fasten the backpack (Figure 6.1). Rigidity is thus provided partly by the backpack worn around the shoulder of the operator. The backpack is provided to host the power pack, electronics, and communication unit.

6.2.2 Sensor Module

The exoskeleton suite is equipped with torque sensors, ground reaction force sensors and potentiometers. Four custom made strain gauges, mechanically integrated at the hip and knee joints serve as torque sensors for measurement of the joints rotational torques. Joint angle potentiometers (22.2 mm Multi Turn Wirewound 5kΩ Potentiometer – 534 from Digi-Key Electronics) are also coupled at each joint for position measurements. Table 6.3 shows the allowable EHPA joint range of motion (ROM) for safety. At the foot module, a pair of shoe insole is equipped with two ground reaction force (GRF) sensors each: one sensor installed at the ball of foot and another place at the rear (close to the heel), see Figure 6.3. The insole GRF sensors are custom-made with *flexiforce* force sensing pressure resistor from Tekscan, Inc. They are slightly flexible in design to fit inside different shoes. Based on manufacturer documentation, the sensor drift is within 5%/logarithmic time at constant load, repeatability is within $\pm$2.5%, linearity is within 3% of full scale, and hysteresis is within 4.5% of full scale.

Table 6.1: Exoskeleton Segment Parameters

Segment (Left and Right)	Material	Length (m)	Mass (kg)	Inertia (kg/m2)	COM (m)
Link 1 (thigh)	8081 Aluminum alloy	0.465	2.65	0.0423	0.085
Link 2 (shank)	8081 Aluminum alloy	0.330	0.77	0.0051	0.170
Link 3 (foot)	8081 Aluminum alloy	0.150	0.50	0.010	0.150

Table 6.2: Joints actuation system

Joint	Actuator	Mass (kg)	Power (Watt)	Rated Torque (Nm)	Torque Constant (Nm/A)
Hip	Hollow shaft Brushless dc motor BLH450KC-200	2.4	50	34	10.97
Knee	Hollow shaft Brushless dc motor BLH230KC-200	1.3	30	17	8.10
Ankle	None	N/A	N/A	N/A	N/A

Table 6.3: Exoskeleton joint range of motion

Joint	Plane	Type	Robot ROM
Hip	**Sagittal (Flex. /Ext)**	Active	$0^o \sim 85^o$
	Coronal (Ad./Ab.)	Passive	$-11^o \sim 9^o$
Knee	**Sagittal (Ext./Flex.)**	Active	$0^o \sim 160^o$
Ankle	**Sagittal** (Dorsi. /Plantar.)	Passive	$-21^o \sim 35^o$
	Coronal (Ever. /Inver.)	Passive	$-11^o \sim 10^o$
	Frontal (Int. rot. /Ext. rot)	Passive	$-8^o \sim 9^o$

6.2.3 Communication and Electronic Unit

The exoskeleton communication and electronic unit (CEU) provide the interface between the exoskeleton and the PC. As can be seen in Figure 6.1, the CEU is housed in the backpack to allow ease of movement. Current weight of backpack and CEU is 4kg. Figure K1 in Appendix K shows a minimal electrical schematic of the CEU. The CEU consist of a data acquisition system from National Instrument (DAQ NI USB-6259 with 1.25MS/s analog input sampling frequency and 2.8MS/s analog output sampling frequency) and three brushless DCs motor drivers from MAXON (ESCON 36/3 EC module). Custom-made signal conditioning shields for the insole GRF sensors are also wired in the CEU. The communication protocol between PC and CEU is currently by a Universal Serial Bus which guarantees an effective sampling frequency from the DAQ.

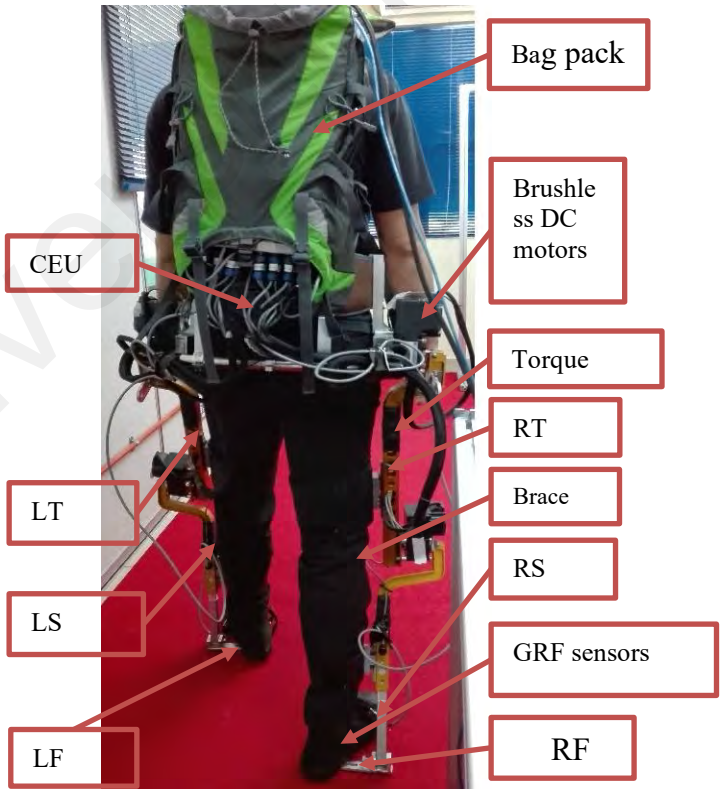

Figure 6.1: Exoskeleton Prototype

(a) (b)

Figure 6.2: (a) Hip and (b) Knee brushless DC motor

Figure 6.3: Insole ground reaction force sensor

6.2.4 Control software unit

The controller software is developed in MATLAB/SIMULINK environment. Figure L1 in Appendix L show screenshots of the graphical controller program in SIMULINK. The program consists of five important units: the Movement Detection Block which host the supervisory controller; the Impedance Controller blocks for trajectory following and torque generation (for left and right legs); DAQ Analog Input ports for retrieving sensor data to the SIMULINK interface via the DAQ system; DAQ Analog Output ports for commanding the EHPA machine; and DAQ Digital Output ports for controlling the

logical states of the DC motor actuators (enable and direction). Figure M1 in Appendix M shows the inner components of the Impedance Controller block which consist of the DUKF trajectory generation/estimation block; the impedance control algorithm block; and the computed torque converter block.

Overall communication from Simulink to the DAQ is established by a universal serial bus (USB) at sampling rate of 0.001s.

6.3 System Identification Experiments

6.3.1 Segment Parameters

Prior to actual lifting/carrying experiment, the actual geometric and inertia features of the exoskeleton which include the link lengths (l_t, l_s, and l_f), links masses (m_t, m_s, and m_f) are verified experimentally (refer to Table 4.2). The actual values are inputted into Solid Work to correct the estimation of the Center of Mass (COM) and the moment of inertias (I_t, I_s, and I_f) along the principal COM axis.

6.3.2 Static and Dynamic Joint Friction

Parameters of static ($\tau_f = b_0,\ q = 0, \dot{q} = 0$) and dynamic joint friction ($\tau_f = b_1 sgn(\dot{q}) + b_2(\dot{q}),\ \dot{q} \neq 0$) torques in (4.3) are estimated experimentally using a combination of static ($\dot{q} = 0, \ddot{q} = 0$) and dynamic ($\dot{q} \neq 0, \ddot{q} \neq 0$) experiments. For analysis, the actual joints angles and torques are measured from joint angle sensors and torque sensor respectively. In the static experiment, the exoskeleton joints (active hip and knee DOF) are controlled to fixed positions. The dynamic friction torque (i.e. kinetic and damping frictions) are thus zero. Each joint is operated in a closed-loop current (or torque) control mode such that the joints can be driven by a reference torque (or current) value. The static friction torques for the hip and knee joint are then estimated by driving a positive and negative ramping signal in the range (0A-0.1A) and locating the threshold

where the joints begins to move. We compute the average of the two signals as the static friction torque. See Figure 6.4 for the left knee joint signal plot. Table 6.5 gives the summary of estimated frictional torque.

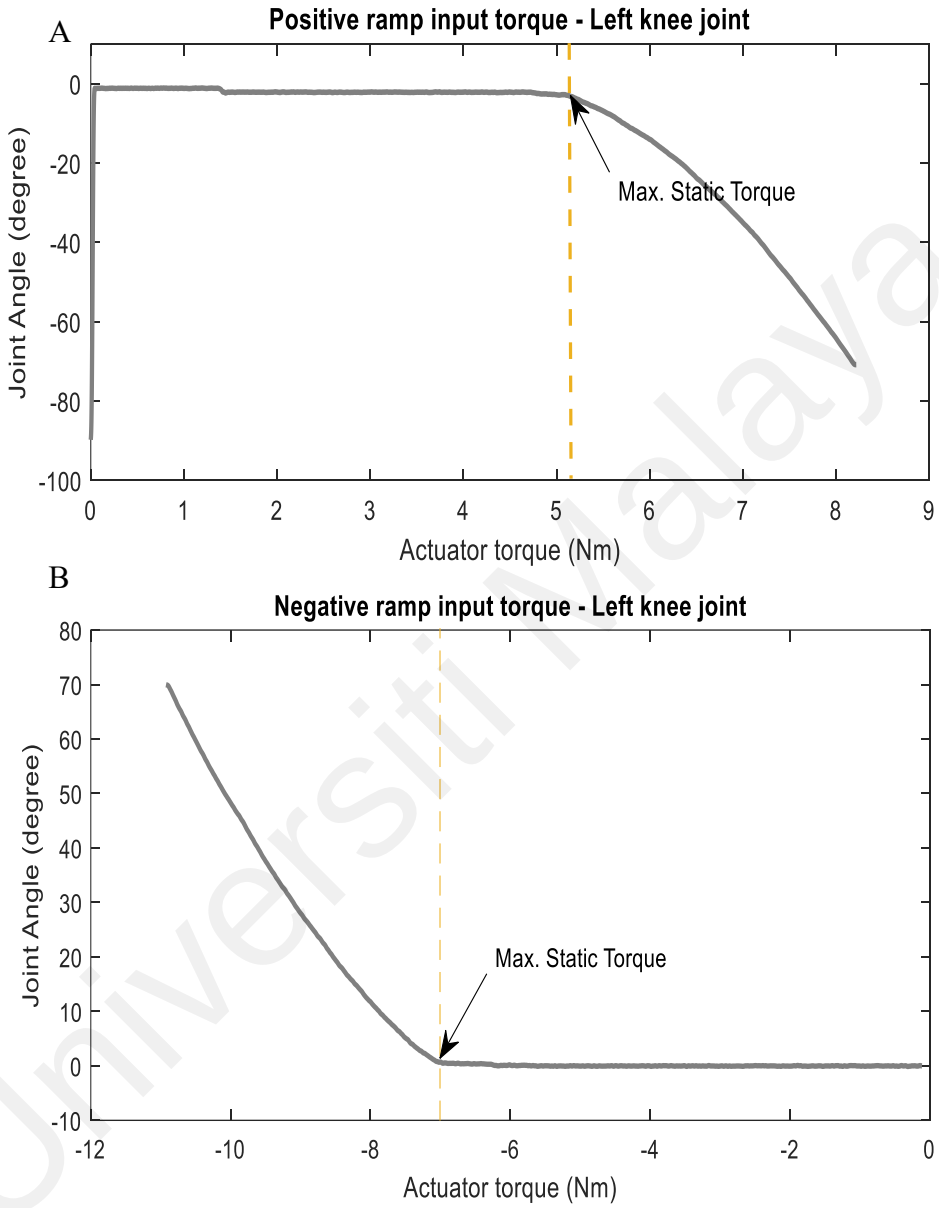

Figure 6.4: (A) Positive and (B) and negative ramp signal for estimating the static friction (Left Leg)

In the dynamic experiment, the joints are driven on a reference trajectory by a simple proportional controller $u = -K_p(q - q_d)$ where u is the voltage sent to the actuators, q_d is the desired joint angles and K_p is the proportional gain. The joint static friction torques are zero in this case. The joint kinetic and damping friction torque are computed by a

regression analysis of actuating torques versus joint positions after subtracting the effect of stiffness and gravitational torques (see Figure 6.5 for the estimation plot for the left knee). Table 6.3 presents summary of all joint stiffness and friction estimates.

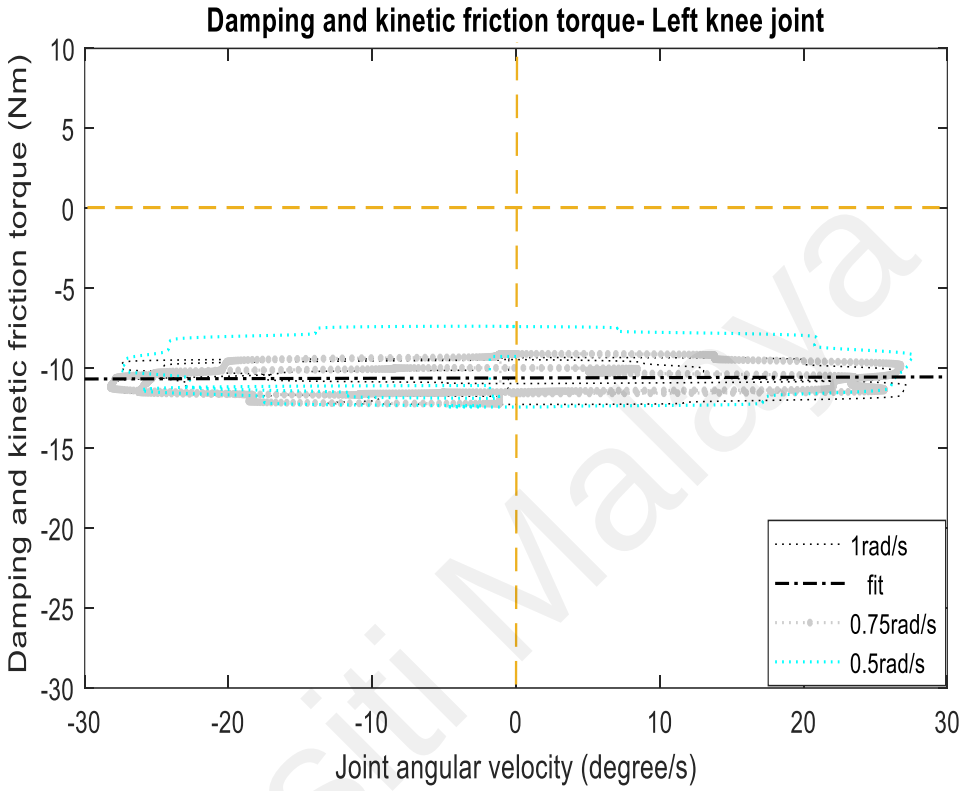

Figure 6.5: Dynamic friction torque estimation (Left Knee joint)

6.3.3 Stiffness Torque Estimation

The joint stiffness torque is a function of joint position as can be seen in (4.3). It is given by $\tau_f = b_3(q)$.

Experimentally, the constants are determined by moving each joint to several static angular positions and recording the joint torque respectively (using a torque sensor). In this procedure, the motors are not actuated. The only friction component after overcoming the static friction is therefore the joint stiffness torque. The parameters of the stiffness torque are then computed from a regression plot of joint torques versus static joint positions, after subtracting the effect of static friction torque and gravitational torque.

Figure 6.6 and Figure 6.7 gives the estimated joint stiffness for the hip and knee joints (right and left respectively).

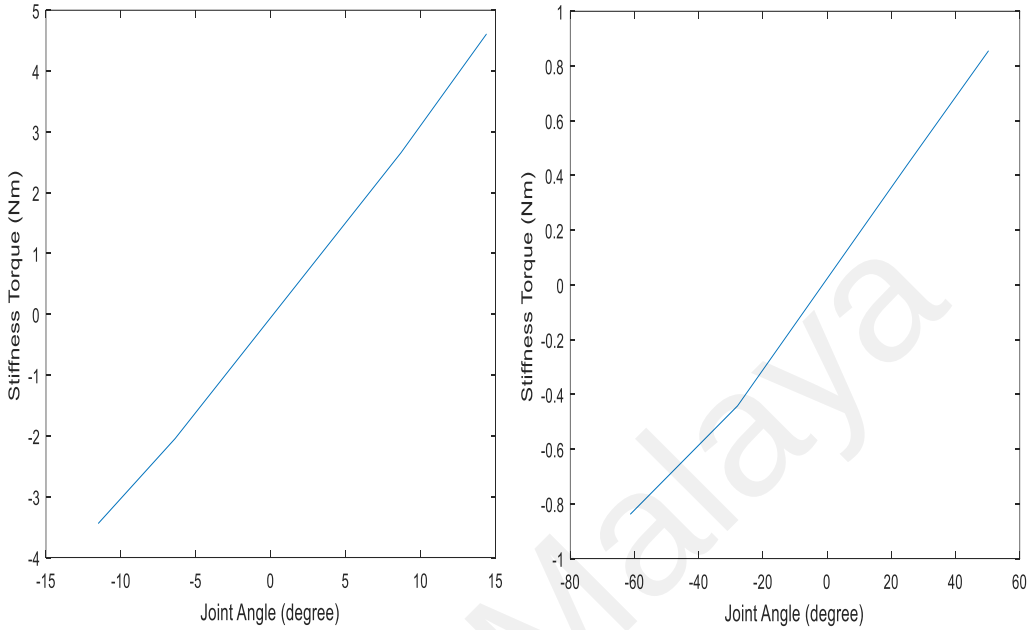

(a) (b)

Figure 6.6: (a) Right hip and (b) right knee stiffness torque

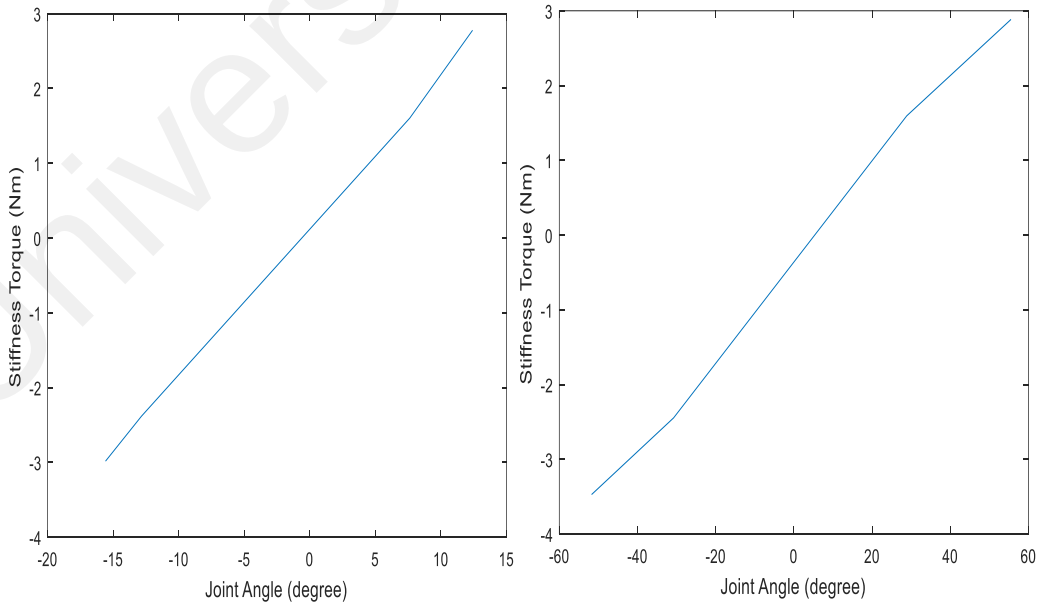

(a) (b)

Figure 6.7: (a) Left hip and (b) left knee stiffness torque

Table 6.4: Summary of joint friction and stiffness torque estimation

Torque	Left Hip Joint (Nm)	Left Knee Joint (Nm)	Right Hip Joint (Nm)	Right Knee Joint (Nm)
Avg. Static Friction	b_0=3.830	b_0=6.035	b_0=2.130	b_0=5.318
Damping/kinetic friction	$b_2(\dot{q}) = (-21.909)\dot{q}$	$b_2(\dot{q}) = (-10.609)\dot{q}$	$b_2(\dot{q}) = (-28.009)\dot{q}$	$b_2(\dot{q}) = (-6.7238)\dot{q}$
Stiffness torque	$b_3(q)$= (0.20Nm/deg)q - 0.18	$b_3(q)$= (0.061Nm/deg)q - 0.39	$b_3(q)$= (0.31Nm/deg)q - 0.042	$b_3(q)$= (0.015Nm/deg)q - 0.058

6.4 Summary

This chapter has presented the prototype design as well as system identification of the EHPA. A prototype 12-DOF active lower-limb EHPA system called UMExoLEA has been designed. Four main modules of the EHPA system which include the exoskeletal structure and actuation module, the sensor module, the communication and electronic unit, and the control software unit have been presented concisely. The selected exoskeleton material is aluminum alloy 8081 and the hip/knee actuation system is by two hollow shafts, back-drivable, bi-directional brushless DC motor-types (BLH450KC-200 and BLH230KC-200) from Oriental Motor Inc. with rated torques 34Nm and 17Nm respectively. The communication and electronic unit has been housed in the bag pack to provide interface with the PC which runs the developed exoskeleton controller in Matlab/Simulink environment. Combined with the sensor module which consist of 2pairs of custom-made torque sensors, 2pairs of custom-made ground reaction force sensors from Tekscan inc. (*flexiforce* force sensing pressure resistor) and 2pairs of 22.2 mm Multi Turn Wirewound 5kΩ Potentiometer from Digi-Key Electronics, an overall exoskeleton weight of approximately 12.5kg has been achieved without the bag pack.

This chapter has also presented the system identification studies for identification of the actual link parameters and joint frictional torque of the exoskeleton to further enhance the accuracy and validity of the dynamic model in Chapter 4. The actual link parameters have been identified accurately. Furthermore, the frictional torques which include the static and dynamic friction (damping and kinetic) as well as the stiffness torque have been estimated and presented in Table 6.3.

CHAPTER 7: EXPERIMENTAL VERIFICATION

7.1 Introduction

This chapter presents the experimental verification of UMExoLEA for assisting wearers' movements in lifting and carrying works. Four important verification aspects have been considered. This include (1) muscle activity/effort reduction at three muscles of the lower extremity (which are used for hip flexion/extension, knee flexion/extension, and ankle plantar flexion/extension); (2) subjective discomfort rating by participants during movement task with and without exoskeleton assistance; (3) the comparison of UMExoLEA controller with other state of the art exoskeleton/control strategy in terms of (a) muscle effort reduction and (b) human interaction torque; (4) and finally the test for synchronous tracking and adaptation to wearers movements during squat-lifting and walking (carrying).

The experimental setup and procedure for these experiments have been highlighted in Chapter 3, Section 3.4. Figure 7.1 shows one of the participants in a lifting and carrying motion with the aid of the exoskeleton.

Figure 7.1: Participant in lifting and carrying experiment.

7.2 Muscle Effort Reduction

7.2.1 Based on Biomechanical data

Of the twenty (20) eligible participants earlier recruited for the experimental study (Section 3.4), fifteen (15) participants performed the experiments for lifting (Task 1); and lifting/carrying (Task 2) movement tasks[1]. For all the participants, the normalized EMG signals taken at the right *Vastus Medialis* (VM) – knee extensor muscle; right *Rectus Femoris* (RF) – hip flexor and knee extensor muscle; and right *Gastrocnemius* (GA) – ankle flexor and knee flexor muscle, of the lower extremity in both Task 1 and Task 2 experiments are shown in Figure 7.2 and Figure 7.3 respectively. The normalized EMG values are averaged in percent of lifting time for Task 1 and in percent of lifting and carrying time (while walking one stride length) for Task 2. Both figures compare the EMG averages at the VM, RF, and GA for treatment A (i.e. no exoskeleton assistance) and treatment B (active assistance from exoskeleton) for all participants. The peaks of the curves show the maximum voluntary contraction (MVC), which is well correlated to the maximum force produced by each muscle. RMSA of the EMG signal, on the other hand, gives an indication of the total effort spent during the task. Table 7.2 presents the statistical summary of the effect of both treatments, that is, the % difference in the muscle EMG RMSA and EMG MVC means between the 'no Exo assist' and the 'Exo assist' conditions for all participants. The bar charts in Figure 7.4 to Figure 7.7 show, graphically, the main comparison of effect based on RMSA and MVC mean and standard deviation. The standard deviation (SD) of the mean show the disparity in the effect of treatment across participants.

[1] . The five participants who did not turn up for the experiments dropped out for different reasons. One of the participants dropped out due to his enormous height that caused pain when donning on the exoskeleton. Another participant terminated the experiment mid-way in response to some urgent call. Three other participants did not turn out for unknown reasons, however they sent words of apology.

Higher muscular activations were recorded when participants performed tasks with no exoskeleton assistance. The envelope profiles of the muscles (Figure 7.2 and Figure 7.3) showed a clear reduction of the peak of activation over the whole lifting time and lifting/carrying time when participants performed task with assistance from exoskeleton. For Task 1 (Figure 7.2), comparing assisted condition (black solid line) to unassisted condition (light grey line), VM RMSA was reduced by 51.43% (**SD** =1.14%), RF RMSA by 30.23% (**SD**=0.5%), GM RMSA by 40.63% (**SD**=0.7%); VM peak by 60.63% (**SD**=6.60%), RF peak by 34.55% (**SD**=1.7%), and GM peak by 40.74% (**SD**=4.4%) (Table 7.1). Participants exerted less muscular effort and less peaks when assisted by the exoskeleton. The most evident effect of assistance occurs at the VM (knee extension muscle) and the least occur at the RF (hip flexion/knee extension muscle) under the assisted condition, which suggests greater UMExoLEA impact on the VM and GA muscle.

For Task 2 (Figure 7.3), comparing assisted condition (black solid line) to unassisted condition (light grey line), VM RMSA was reduced by 43.90% (**SD**=0.70%), RF RMSA by 37.78% (**SD**=0.30%), GM RMSA by 58.00% (**SD**=2.30%); VM peak was reduced by 31.40% (**SD**=2.10%), RF peaks by 31.30% (**SD**=0.00%), and GM peaks by 43.79% (**SD**=2.70%) (Table 7.1). The marked decrease in average EMG RMSAs and MVCs of these muscles indicate that participants exert less muscular force and effort under exoskeleton assistance. The highest muscle activity reduction is recorded on the GA muscles for Task 2 which show the most evident effect of UMExoLEA assistance.

The statistical significance of the effect of assistance is established by a repeated measure ANOVA with independent factors at two levels (i.e. treatment A and B) and dependent factors at three levels (i.e. EMG RMSA/MVC at VM, RF, and GA). We define statistical parameters as: **M** is mean, **MD** is mean difference, **SD** is standard deviation

from the mean, **SE** is standard error of the mean, and ***p*** is the confidence level. The ANOVA rejected the null hypothesis of the test (of the effect) of the independent factors on dependent factors at 95% confidence interval. Post hoc pairwise comparison with Bonferroni's multiple adjustment for main effect further confirm a significant statistical difference (only) between the treatments (i.e. A-no Exo assist and B - Exo assist) based on estimated marginal means, at 95% confidence interval for difference. For Task 1, strong statistical significance difference between the 'no Exo assist' and 'Exo assist' is found for EMG RMSA (**MD**= 0.014mV, **SE** = 0.003mV, ***p*** = 0.00009) and for EMG peaks (MVC) (**MD**= 0.055mV, **SE** = 0.012mV, ***p*** = 0.0004. For Task 2, the difference between treatment is found statistically significant for EMG RMSA (**MD**= 0.021mV, **SE** = 0.003mV, ***p*** = 0.000006) as well as for EMG peaks (MVC) (**MD**= 0.051mV, **SE** = 0.007mV, ***p*** = 0.000005). Table 7.2 provides the overall pair-wise comparison with Bonferroni's adjustment for the treatment means and sequence means for both tasks.

The sequence of treatment administration in the crossover design was not found significant in all movement task. Pairwise comparison with Bonferroni's multiple adjustment did not show any statistical difference between the means of the sequence AB and BA for Task 1 (***p*** = 0.807) and the means of the sequence for Task 2 (***p*** = 0.526) which suggest that the order of administration of treatment has no carryover effect on the treatment itself in the crossover design. Thus, between treatment effect is entirely due to the type of treatment (i.e. presence or absence of exoskeleton assistance).

Table 7.1: Summary of the RMSA and MVC means, standard deviations, and percent differences between the 'no Exo assist' and the 'Exo assist' conditions for all the muscles across all participants and treatment conditions

Task	Measure	Vastus Medialis (VM)			Rectus Femoris (RF)			Gastrocnemius (GA)			Total
		Treatment A (no Exo assist) (mV)	Treatment B (Exo assist) (mV)	% Difference of Means	Treatment A (no Exo assist) (mV)	Treatment B (Exo assist) (mV)	% Difference of Means	Treatment A (no Exo assist) (mV)	Treatment B (Exo assist) (mV)	% Difference of Means	% Difference of Means
Lifting	RMSA (SD)	0.035 (SD=0.018)	0.017 (SD=0.0066)	51.43 (SD=1.14)	0.043 (SD=0.020)	0.030 (SD=0.015)	30.23 (SD=0.50)	0.032 (SD=0.014)	0.019 (SD=0.007)	40.63 (SD=0.70)	40.76
	MVC (SD)	0.127 (SD=0.083)	0.050 (SD=0.017)	60.63 (SD=6.60)	0.136 (SD=0.065)	0.089 (SD=0.048)	34.55 (SD=1.70)	0.108 (SD=0.068)	0.064 (SD=0.024)	40.74 (SD=4.40)	45.31
Lifting & Carrying	RMSA (SD)	0.041 (SD=0.020)	0.023 (SD=0.013)	43.90 (SD=0.70)	0.045 (SD=0.018)	0.028 (SD=0.015)	37.78 (SD=0.30)	0.050 (SD=0.029)	0.021 (SD=0.006)	58.00 (SD=2.30)	46.56
	MVC (SD)	0.121 (SD=0.058)	0.083 (SD=0.037)	31.40 (SD=2.10)	0.131 (SD=0.041)	0.090 (SD=0.041)	31.30 (SD=0.00)	0.169 (SD=0.062)	0.095 (SD=0.035)	43.79 (SD=2.70)	35.50

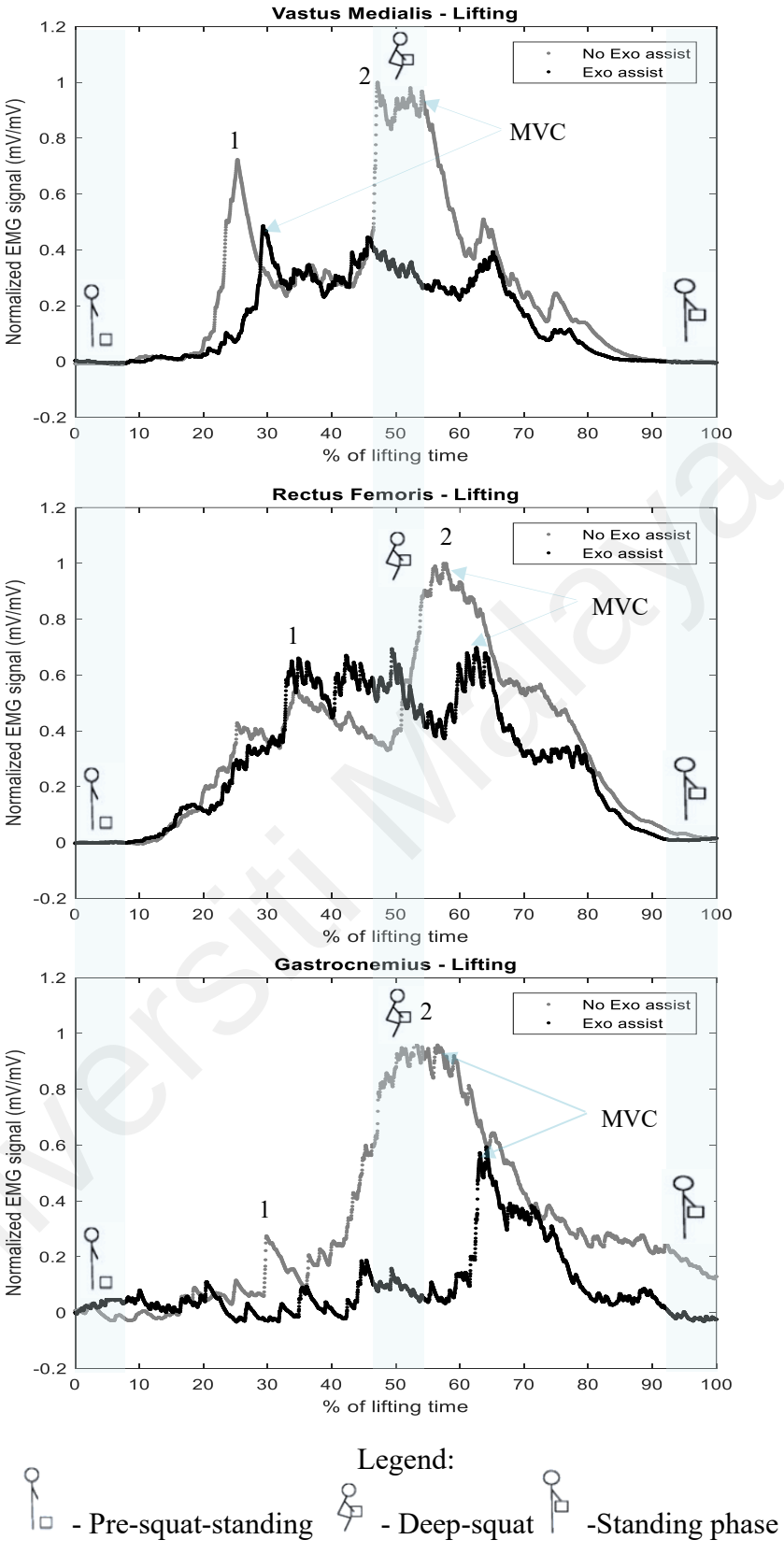

Figure 7.2: EMG ensembled average in percent of lifting time

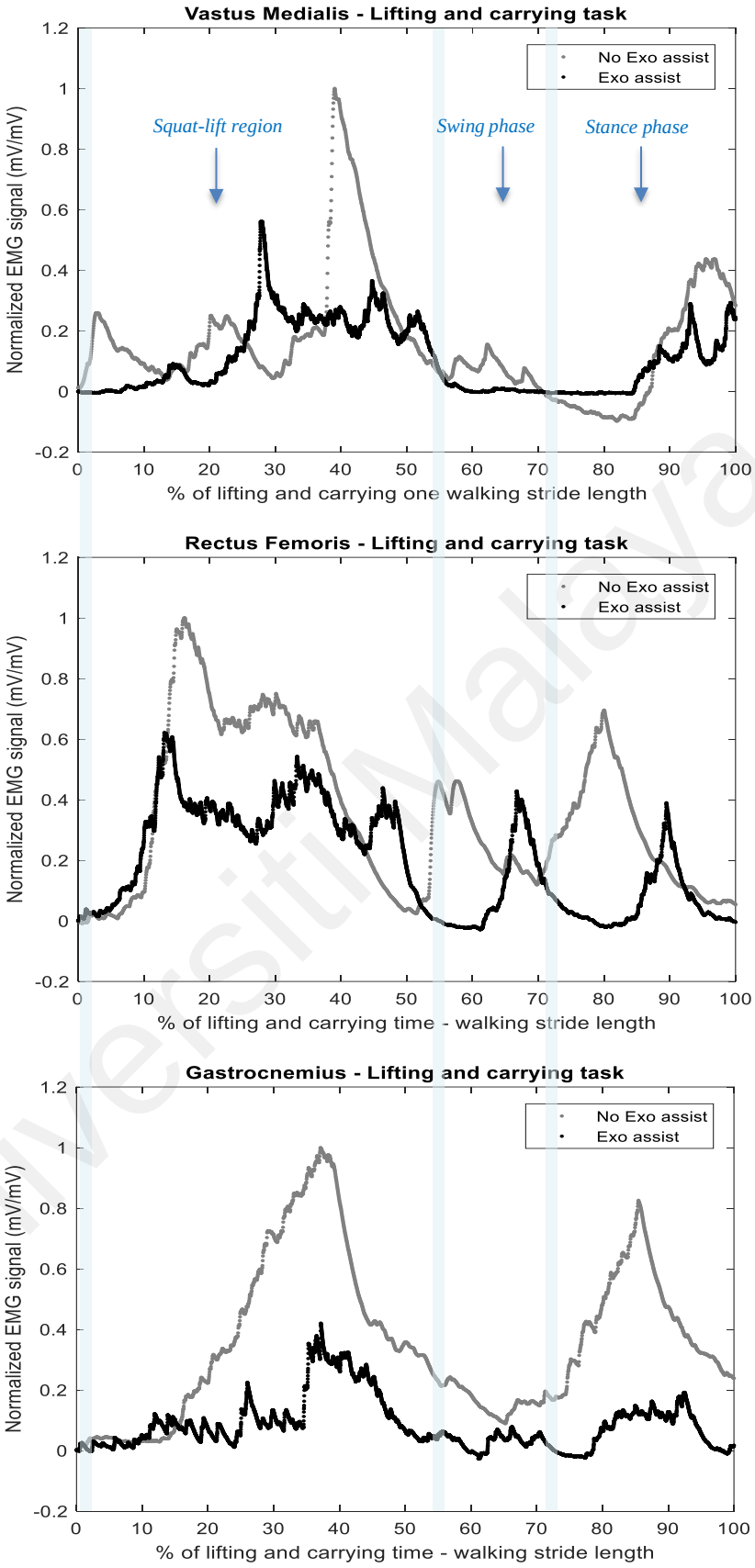

Figure 7.3: EMG ensembled average in percent of lifting and carrying time with walking one stride length

Table 7.2: Pairwise comparisons of mean RMSA across treatments and sequence with Bonferroni adjustment

Task	Treatment Effect		Mean Difference MD (mV)	Standard Error SE (mV)	p [b]
Lifting	A	B	0.055	0.012	0.00009
	B	A	-0.055	0.012	0.00009
	Sequence Effect				
	AB	BA	0.007	0.019	0.714
	BA	AB	-0.007	0.019	0.714
Lifting and carrying	**Treatment Effect**				
	A	B	0.051	0.007	0.000006
	B	A	-0.051	0.007	0.000006
	Sequence Effect				
	AB	BA	0.000	0.015	0.986
	BA	AB	0.000	0.015	0.986

Further analysis of the envelop profile of the EMG signal in Figure 7.2 and Figure 7.3 demonstrates the biomechanical effect of the UMExoLEA on the monitored muscles over the duration of task. For Task 1, the three vertical green shades (is employed to) describe three distinct phases in the lifting task recorded in percent of lifting time (Figure 7.2). First vertical green shade indicates pre-squat (double-support) standing phase in preparation for load lifting, the second shade indicates deep squat-lifting (double-support) phase – i.e. the instant of lifting from deep squat, while the third shade indicates the second double-support standing phase with weight lifted above knee position. Without exoskeleton assistance, VM recruitment show two peaks over the lifting cycle. A lesser peak (labelled '1') during knee flexion between phase 1 and phase 2 following eccentric contraction of the muscle to restrain knee flexion moment; and a higher peak (labelled '2') following concentric contraction of the muscle to extend the knee from deep squat under load (Figure 7.2). With exoskeleton assistance, the VM muscle activity show a

plateaued activation profile exhibiting minimum peaks (~ 61% reduction in exerted muscular force) in both corresponding intervals of the lifting time.

The RF muscle also exhibit two conspicuous peaks without exoskeleton assistance. As a weaker hip flexor muscle and knee extensor muscle, the activity of RF shows a lesser peak (labelled '1') about mid-way between phase 1 and phase 2 following eccentric contraction of the muscle to control hip flexion in squat descent. A higher peak is also seen (labelled '2') following concentric contraction of the muscle to allow knee extension on the ascent. With UMExoLEA assistance, reduction in the peaks of activation (~ 34.6%) are noticeable as the RF EMG envelop plateaus mid-way over the lifting time (Figure 7.2).

Activity of the GA is essentially different showing weak contraction for knee flexion during squat descent (labelled '1') reaching a higher peak to control dorsiflexion movement of the ankle at deep squat (or at the early phase of squat-ascent) (labelled '2') during the lifting time without 'Exo assist'. With assistance, the activity of the GA muscle is hardly noticeable over the lifting time exhibiting very low peak (~ 40.7% reduction) for squat-ascent (Figure 7.2).

For Task 2, the three vertical green shades (is employed to) divide the lifting and carrying time (biomechanically) in three distinct phases: squat-lifting (i.e. squat descent/ascent), swing (walking), and stance (walking) in percent of lifting and carrying time (Figure 7.3). Carrying time is recorded over one stride length of walking. Muscular activity of the VM, RF, and GA in the first phase (i.e. squat-lifting) are recruited in similar fashion to Task 1 (Figure 7.2) as seen by the envelop profile in Figure 7.3, however activity of the muscles for the swing and stance phase of walking (carrying) are noticeably different. Without assistance, VM (knee extensor muscle) activity during the leg swing is seen almost inactive as the knee is partially flexed but peaks at mid or late stance as the

knee is fully extended (Figure 7.3). With UMExoLEA assistance, similar trend is noticeable on the VM EMG envelop but at lesser degree of muscle activation (~ 43.9% average reduction).

RF recruitment peaks during the leg swing phase following eccentric contraction of the muscle to allow hip flexion (Figure 7.3). It exhibits a second higher peak during the stance phase (about early to mid-stance based on recorded EMG envelopes) following concentric contraction of the muscle to control knee extension. Under assisted condition with UMExoLEA, the average muscular activity of the RF is seen minimal over the course of lifting and carrying time. GA muscles on the other hand show very minimal activity during the swing phase in both assisted and un-assisted condition but peaks at mid stance (single leg support) phase following eccentric contraction of the muscle to control ankle dorsiflexion. With UMExoLEA assistance, GA muscular activity are also seen to be minimal (~ 58.0% average reduction) throughout the lifting and carrying time (Figure 7.3).

Overall, as evident in Figure 7.4 to Figure 7.7 and Table 7.1, muscular activity of the VM across participants showed the highest average marginal reduction in Task 1 when UMExoLEA assistance was applied, while GA muscle activity showed the highest in Task 2 under UMExoLEA assistance. The RF muscle derived the least but significant gain from the UMExoLEA. Disparity in the effect of assistance among the participants is noticeable as indicated by the error bars of standard deviation. Significant variability in muscular effort are recorded among the participants when no assistance is applied which may suggest that each participant exerted his utmost strength differently for the tasks. However, with UMExoLEA assistance, there is small disparity about the mean muscle activation (except for the RF) across participants especially for the lifting task (Figure 7.4

and Figure 7.5). This may suggest that each participant received sufficient assistance from UMExoLEA thus contributing less personal effort during performance of task.

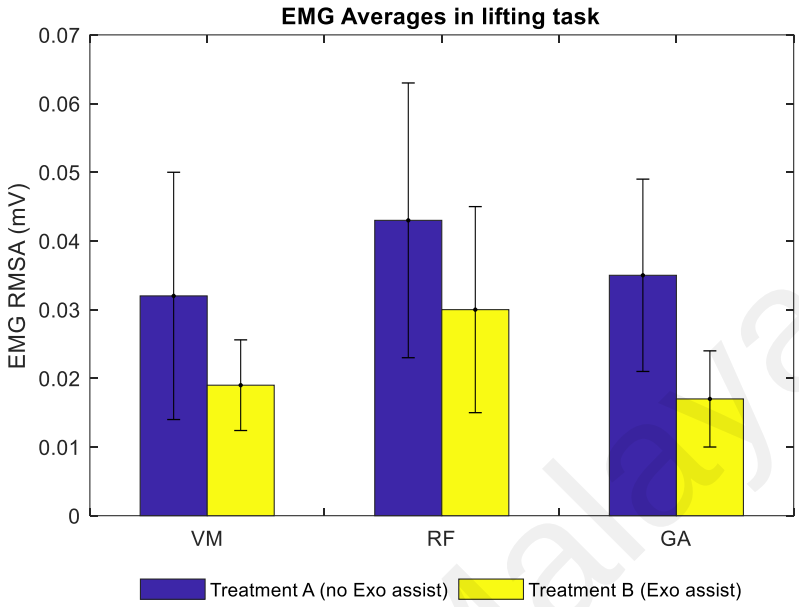

Figure 7.4: EMG root mean square average for all participants in lifting task

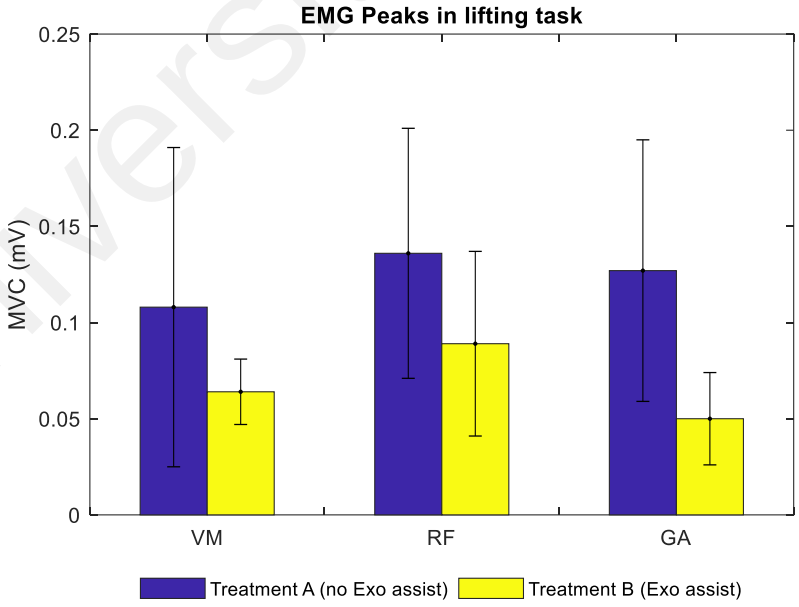

Figure 7.5: Average maximum voluntary contraction for all participants in lifting task

For Task 2, the least subject-to-subject variability in muscle activity with respect to the UMExoLEA assistance occurs at the GA muscle (Figure 7.6 and Figure 7.7), which further suggest that the effect of UMExoLEA assistance is most consistent across participants for this muscle.

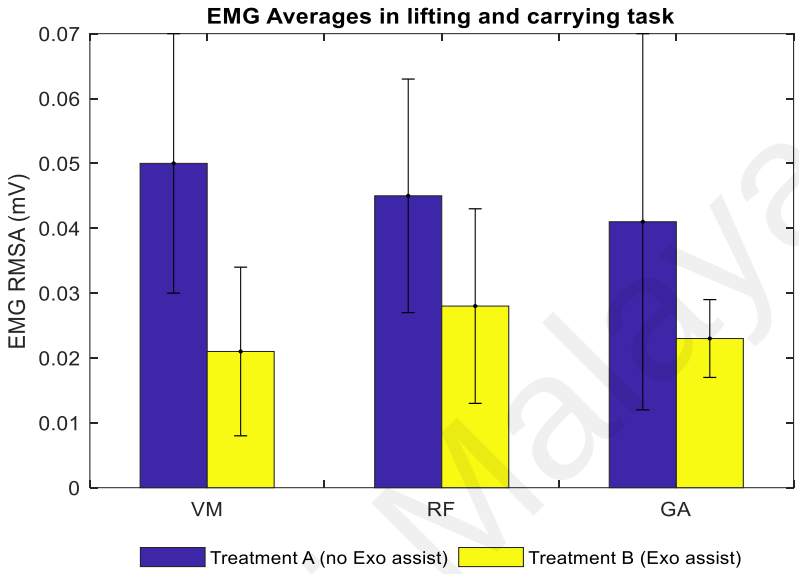

Figure 7.6: EMG root mean square average for all participants in lifting and carrying task

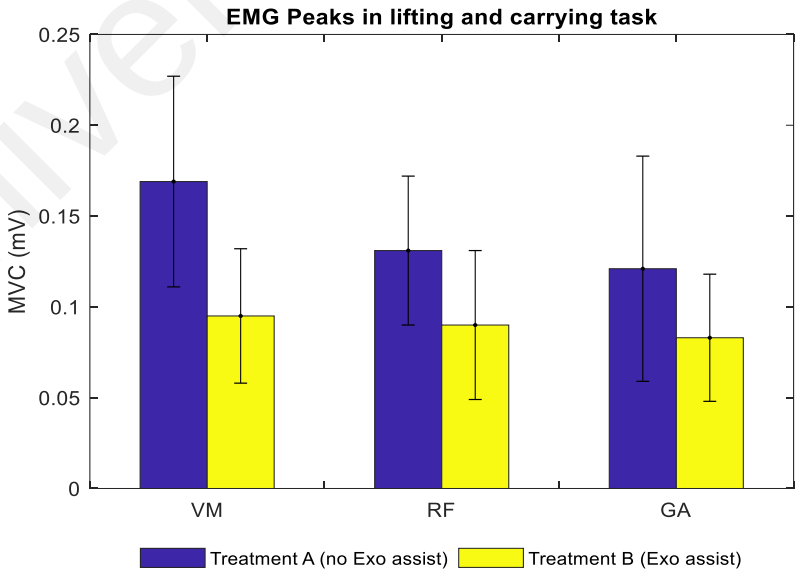

Figure 7.7: Average maximum voluntary contraction for all participants in lifting and carrying task

7.2.2 Based on Subjective Feedback

To determine participants' perception of assistance from UMExoLEA, subjective feedback is obtained from the participants through questionnaires administered on trial by trial basis during performance of tasks. Table 7.3 presents the subjective rating of participants i.e. the mean score, standard deviation, and mean rank of perceived effort from participants and perceived assistance derived from UMExoLEA in both treatments based on the Wilcoxon Signed-Rank (S-R) test. Participants rating are determined on a scale of 0 to 10, where '0' represent 'no effort from participant' or 'no assistance is perceived from UMExoLEA', and '10' represent either 100% of participant effort is utilized or 100% of assistance is derived from UMExoLEA.

For Task 1, all participants reported using less effort to complete the task under treatment B ('Exo assist') compared to Treatment A ('no Exo assist'). The Wilcoxon's pooled (negative) ranking of all differences between the dependent variable rated participants efforts under the 'Exo assist' (mean rank = 8.0) much less than their effort under the 'no Exo assist' (mean rank = 0.0), at significant level, $\mathbf{Z}$ = -3.43, $\boldsymbol{p}$ = 0.001 (Table 6.3). Actual mean score of participants' perceived effort under the 'no Exo assist' is given by (**M** =100.0%, **SD** = 0.0%) and for the 'Exo assist' by (**M** =26.9%, **SD** = 12.2%) which showed ~73.1% mean reduction in participants' effort based on subjective rating when UMExoLEA assistance is applied, see Figure 7.8 and Table 7.3.

For lifting and carrying task, participants also reported exerting less effort when assisted by the exoskeleton (Figure 7.8). The Wilcoxon S-R test based on negative ranking revealed that the participants rated their effort under exoskeleton assistance (mean rank = 8.0) much less than their effort when no exoskeleton assistance is used (mean rank = 0.0) at significant level, $\mathbf{Z}$ = -3.42, $\boldsymbol{p}$ = 0.001 (Table 7.3). Actual mean score of participants' perceived effort under the 'no Exo assist' period is given by (**M** =100.0%,

SD = 0.0%) and under the 'Exo assist' period by (**M** =27.3%, **SD** = 14.8%) which showed similar rating of ~72.7% mean reduction in participants' effort by UMExoLEA (Table 7.3).

On the other hand, subjective rating of UMExoLEA assistance by participants showed that participants perceived UMExoLEA is assisting their movements during performance of the tasks (Figure 7.9 and Table 7.4). For both tasks, the Wilcoxon S-R test ranked participants' perception of UMExoLEA assistance with Mean Rank = 8.0 when compared to a benchmark rating of the participants under the 'no Exo assist' treatment. Interestingly, based on average score, participants perceived that UMExoLEA assisted their movement by (**M** =73.1%, **SD** = 12.2%) in Task 1 and by (**M** =72.8%, **SD** = 14.7%) in Task 2, which correlates well to their perception of effort reduction in Table 7.3.

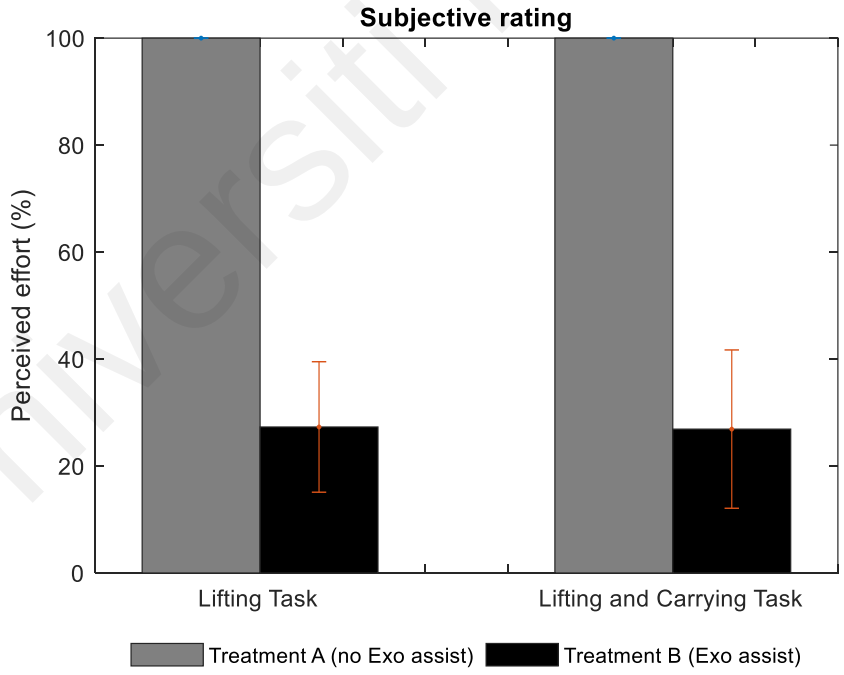

Figure 7.8: Subjective effort rating in both tasks

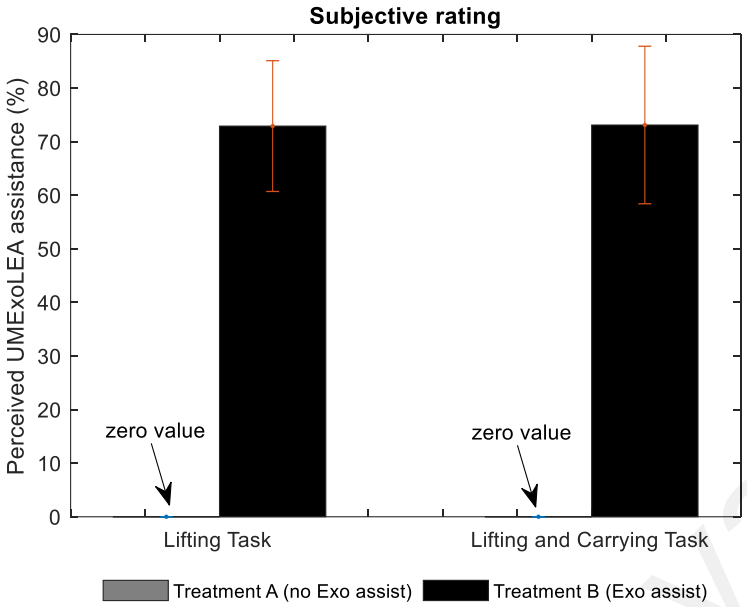

Figure 7.9: Subjective assistance rating in both tasks

Table 7.3: Wilcoxon rank score of treatment effect based on subjective rating-summary of means, standard deviations, and mean rank of perceived user's effort in both treatments

Task	Perceived Effort			Test (Dependent factor = Perceived effort)	Wilcoxon Ranks	
	% Mean (SD) Treatment A (no Exo assist)	% Mean (SD) Treatment B (Exo assist)	Difference of Means		N	Mean Ranks
Lifting	100.0 (0.0)	26.9 (12.2)	73.1%	Treatment A < Treatment B (Negative)	15	8
				Treatment A > Treatment B (Positive)	0	0
				Treatment A = Treatment B (Ties)	0	
				Total	15	
Lifting & Carrying	100.0 (0.0)	27.3 (14.8)	72.7%	Treatment A < Treatment B (Negative)	15	8
				Treatment A > Treatment B (Positive)	0	0
				Treatment A = Treatment B (Ties)	0	
				Total	15	

Table 7.4: Wilcoxon rank score of treatment effect based on subjective rating-summary of means, standard deviations, and mean rank of perceived assistance from UMExoLEA

Task	Perceived Assistance			Test (Dependent factor = Perceived assistance)	Wilcoxon Ranks	
	% Mean (SD) Treatment A (no Exo assist)	% Mean (SD) Treatment B (Exo assist)	Difference of Means		N	Mean Ranks
Lifting	0.0 (0.0)	73.1 (12.2)	73.1%	Treatment A < Treatment B (Negative)	0	0
				Treatment A > Treatment B (Positive)	15	8
				Treatment A = Treatment B (Ties)	0	
				Total	15	
Lifting & Carrying	0.0 (0.0)	72.9 (14.7)	72.9%	Treatment A < Treatment B (Negative)	0	0
				Treatment A > Treatment B (Positive)	15	8
				Treatment A = Treatment B (Ties)	0	
				Total	15	

7.2.3 General Discussion on Muscle Effort Reduction

The current study was designed to evaluate the performance of UMExoLEA in terms of how much muscular effort or force can be minimized by the exoskeleton. Based on myoelectric data from selected muscles, the current experimental verification shows that UMExoLEA is capable of reducing the wearers lower extremity muscular effort and peaks of activation by 30% to 60% in lifting tasks or lifting and carrying task respectively. Subjective feedback from the participants also suggest that UMExoLEA can reduce the wearers effort by ~73.1%.

Although not monitored due to convenience in the placement of EMG electrodes, UMExoLEA is also expected to have similar impact on several other muscles of the Quadricep femoris, hamstring, and calf of the lower extremity which contributes to the

activity of lifting/carrying. For instance, activities of the Vastus Medialis (VM), Vastus Lateralis (VL), and Vastus Intermedius (VI) which contributes to knee extension movement have been suggested in several studies to exhibit similar activation pattern (Schoenfeld, 2010), thus reduction is muscular effort on VL and VI due to UMExoLEA assistance are similarly expected. Likewise, activities of the Soleus which co-activate with the GA to assist ankle dorsi- and plantar flexion movement are expected to be similarly affected by the assistance of UMExoLEA(Di Giulio et al., 2009).

In the current experiment, UMExoLEA appears to have the least impact on the RF muscle compared to the VM and GA. This may be due to the peculiar nature of the RF muscle. The RF, the sartorius, and iliopsoas are the flexors of the thigh at the hip, however the RF is a weaker hip flexor when the knee is fully extended because it is already shortened (Neumann & therapy, 2010). Similarly, the RF is not dominant in knee extension when the hip is flexed since it is already shortened and therefore suffers from active insufficiency. Thus, the activity of extending the knee from deep squat position during lifting is less dominated by the RF which may suggest less benefit from the UMExoLEA. In squat descent, dominant role of RF is expected (Figure 7.2) since the muscle is at an advantage position (i.e. knee not fully extended), but in this phase all muscular activities are normally low which may also suggest less amount of benefit from UMExoLEA.

In all, the impact of UMExoLEA is clearly significant on all the selected muscles and for all the participants. The differences among the wearers (subject-to-subject variability) in terms of muscular effort when assisted by UMExoLEA is minimal (Figure 7.4 – Figure 7.7) which suggest that all the participants benefitted adequately from the exoskeleton.

7.3 Subjective Musculoskeletal Discomfort Rating

One of the objectives of the study is to assess the overall effect of UMExoLEA in minimizing fatigue and/or local discomfort (i.e. sensation of pain, numbness, soreness, tingling, etc.) in repetitive task. By performing lifting task involving repetitive squatting, or by performing lifting and carrying task involving repetitive squatting and walking over the course of three trials (Section 3.4.4.3), the experiment has thus been structured such that participants will experience some degree of fatigue or local discomforts on the lower extremities and lumbar region at some point during performance of task in a single period.

For the lifting task, subjective reports from the participants when task is performed without exoskeleton assistance indicated that 11 of the participants (n=15) experienced some degrees of fatigue at the lower back (LB), 10 participants (n=15) reported some degree of fatigue at the thigh/Quadricep region, and 11 (n=15) reported fatigue at the calf (on the GA, soleus, etc.) region, see Figure 7.10 and Table 7.5. There was no report of subjective discomfort (i.e. pain) on the knee, hip, and ankle joint. Mean score of fatigue at the LB is given as (**M** =13.8%, **SD** = 14.7%), at the thigh/Quadricep region as (**M** =12.7%, **SD** = 13.8%), and at the calf region as (**M** =14.2%, **SD** = 16.4%) (Figure 7.10). There were however no reports of subjective discomfort/fatigue in any region when the same task was performed with the help of exoskeleton assistance except for a mild report of fatigue on the thigh/Quadriceps by one participant (**M** =0.04%, **SD** = 1.72%).

The Wilcoxon S-R test showed that the participants rated fatigue at the LB (Mean rank = 6.0), thigh/Quadriceps region (Mean rank = 5.5), and the calf region (Mean rank = 6) much higher than fatigue on any region when task is performed with exoskeleton assistance (Mean rank = 0.0), at statistical significance level of **Z** = -2.943, ***p*** = 0.003 for LB, **Z** = -2.812, ***p*** = 0.005 for thigh/Quadricep region, and **Z** = -2.941, ***p*** = 0.003 for the calf region respectively (Table 7.5).

Table 7.5: Subjective rating - summary of perceived regional discomfort in lifting task

Task	Body region (Z statistics)	Perceived Discomfort Score (n = 15)		Wilcoxon S-R Test		
		Mean (SD) A (no Exo assist) (%)	Mean (SD) B (Exo assist) (%)	Test	N	Mean Ranks
Lifting	**LB** (Z = -2.943, *p* = 0.003)	13.8 (14.7)	0.0 (0.0)	Negative ranks (A<B)	11	6
				Positive ranks (A>B)	0	0
				Tie (A=B)	4	
	Thigh region (Z = -2.812, *p* = 0.005)	12.7 (13.8)	0.4 (1.7)	Negative ranks (A<B)	10	5.5
				Positive ranks (A>B)	0	0
				Tie (A=B)	5	
	Calf region (Z = -2.941, *p* = 0.003)	14.2 (16.4)	0.0 (0.0)	Negative ranks (A<B)	11	6
				Positive ranks (A>B)	0	0
				Tie (A=B)	4	
	Total	13.6 (15.0)	0.1 (0.0)			

For the lifting and carrying task, there were more reports of fatigue. When task was performed without exoskeleton assistance, 12 participants (n=15) reported fatigue at the lower back (LB) (**M** =20.2%, **SD** = 20.8%). The same number of participants (n=15) also experienced fatigue at the thigh/Quadricep region (**M** =21.8%, **SD** = 15.9%) and calf region (**M** =19.1%, **SD** = 16.8%) (Figure 7.11, Table 7.6). However, no discomfort/fatigue was reported by participants on any region when same task was performed under exoskeleton assistance. The Wilcoxon S-R test showed that participants rated fatigue on the LB (mean rank = 6.5), the thigh/Quadriceps region (Mean rank = 6.5), and the calf region (Mean rank = 6.5) much higher than fatigue on all the regions of the lower extremity during the 'Exo assist' period (Mean rank = 0.0), at statistical

significance level of **Z** = -3.065, ***p*** = 0.002 for LB; **Z** = -3.066, ***p*** = 0.002 for thigh/Quadricep region; and **Z** = -3.066, ***p*** = 0.002 for the calf region (Table 7.6).

Table 7.6: Subjective rating - summary of perceived regional discomfort in lifting and carrying task

Task	**Body region** (Z statistics)	**Perceived Discomfort Score** (n = 15)		**Wilcoxon S-R Test**		
		Mean (SD) A (no Exo assist) (%)	**Mean (SD) B (Exo assist) (%)**	**Test**	**N**	**Mean Ranks**
Lifting and Carrying	**LB** (Z = -3.065, *p* = 0.002)	20.2 (20.8)	0.0 (0.0)	Negative ranks (A<B)	12	6.5
				Positive ranks (A>B)	0	0
				Tie (A=B)	3	
	Thigh region (Z = -3.066, *p* = 0.002)	21.8 (15.9)	0.0 (0.0)	Negative ranks (A<B)	12	6.5
				Positive ranks (A>B)	0	0
				Tie (A=B)	3	
	Calf region (Z = -3.066, *p* = 0.002)	19.1(16.8)	0.0 (0.0)	Negative ranks (A<B)	12	6.5
				Positive ranks (A>B)	0	0
				Tie (A=B)	3	
	Total	20.4 (17.8)	0.0 (0.0)			

Figure 7.10 and Figure 7.11 also reveal the disparity in fatigue rating on the different regions of the lower extremity. Participants reported the highest mean fatigue score on the calf region followed by the low back in the squat-lifting task (Task 1). In the lifting and carrying task, participants rated the thigh with the highest mean fatigue score.

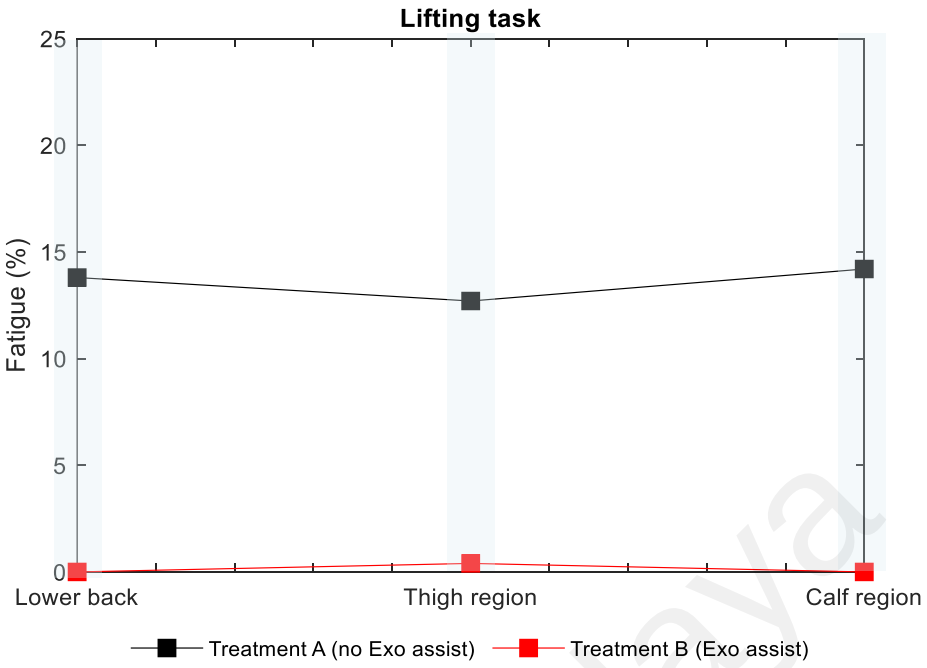

Figure 7.10: Perceived fatigue rating on the lower extremity and lower back in lifting task

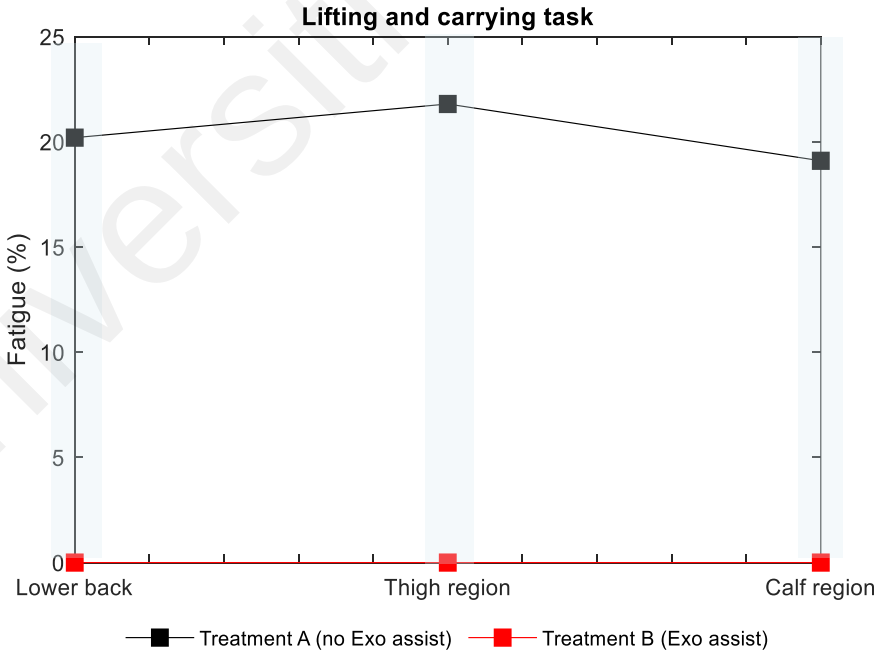

Figure 7.11: Perceived fatigue rating on the lower extremity and lower back in lifting and carrying task

Between-trial variability in mean discomfort/fatigue score is shown in Figure 7.12 and Figure 7.13 for the 'no Exo assist' period. Perceived fatigue generally increased across trials for all participants in the lifting task with most of the participants experiencing fatigue at the third trial. For each of the three regions, fatigue score progress gradually as more trials are performed without exoskeleton assistance. Some participants reported fatigue earlier on, in the first and second trial, while some reported no fatigue throughout the course of the movement task. Participants predisposition to fatigue could be due to the interaction of other cofactors such as lifestyle, sports, or body mass index (BMI).

In the lifting and carrying task, when no assistance is received from UMExoLEA, participants fatigue rating progress most rapidly for the lower back compared to the other two regions of the lower extremity (Figure 7.13).

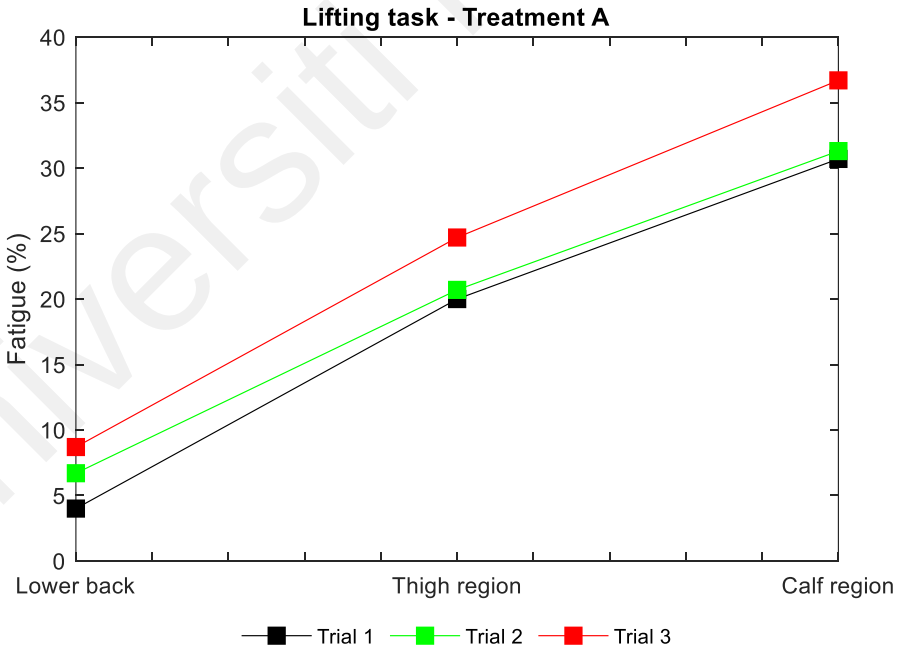

Figure 7.12: Between trials variabilities in perceived regional fatigue rating on the lower extremity and lower back in lifting task.

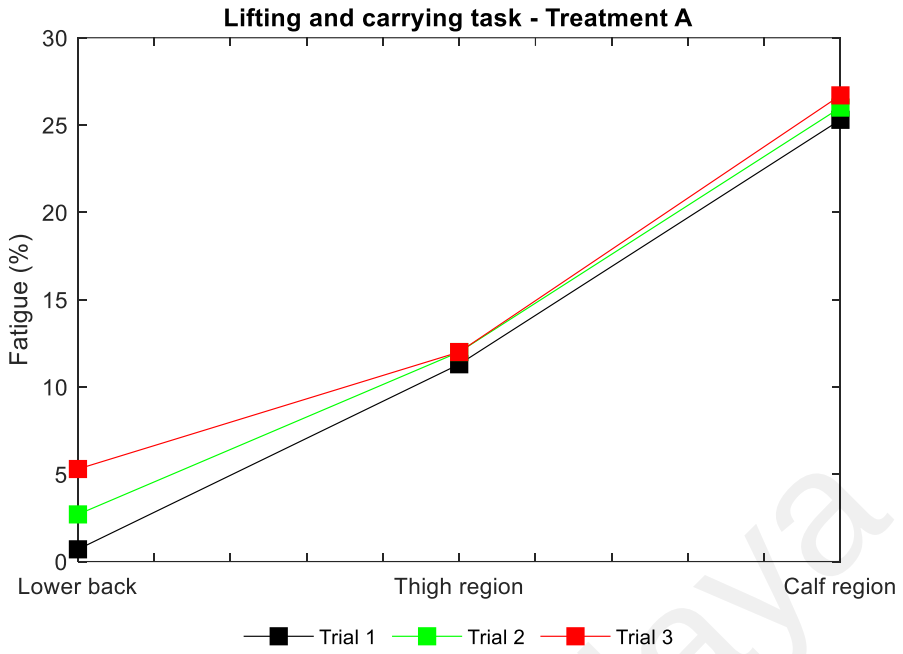

Figure 7.13: Between trials variabilities in perceived fatigue rating on the lower extremity and lower back in lifting and carrying task.

7.3.1 General Discussion on Subjective Discomfort/Fatigue

The above experimental evaluation show that UMExoLEA can minimize lower extremity fatigue and regional discomfort accompanied with repetitive lifting or lifting/carrying MH tasks. Fatigue and regional body discomfort are short-lived and easily detectable under experimental procedure, thus provide a good basis for studying the risk factors to more serious repetitive strain/motion injuries like LBP, meniscal or osteoarthritis of the knee and hip which gestate over long period of time.

In the current experiment, no lower extremity joint pain was reported by participants in both 'Exo assist' and 'no Exo assist' periods. Perhaps more lengthy repetition of task and daily exposures with follow-up periods is needed to determine if pain would occur. Muscular fatigue gestates easily when task is repeated, or muscles are overexerted and thus were reported by more than 70% of the participants in mainly three different regions of the lower extremity: lower back, thigh region, and calf - when the tasks were performed

without exoskeleton assistance. However, with UMExoLEA assistance, virtually none of the participants reported any lower extremity fatigue or muscular weakness. This shows the biomechanical effect of the UMExoLEA to minimize risk factors (i.e. fatigue and muscular weakness) associated with repetitive lifting and carrying activities.

Not included in this study are the extrinsic risk of environmental and psychosocial factors such as temperatures, fear, or intimidation. However, intrinsic risk factors that may influence discomfort levels or fatigue such as past injuries, current health status, and the presence of an active WMSD were eliminated during the screening and recruitment procedure.

7.4 UMExoLEA Performance Comparison

7.4.1 Based on Human Interaction Torque

The performance of EHPA controllers can also be assessed using the human interaction forces as benchmark (H. Kazerooni et al., 2005; Yang et al., 2017). Small values of interaction torques/forces exerted on the exoskeleton by the human implies human exert less effort or torque to drive the exoskeleton. Thus, to further assess the effectiveness of UMExoLEA, the proposed synchronous control scheme is compared with the popular sensitivity amplification control (SAC) proposed by H. Kazerooni et al. (2005) using the exerted human interaction torque as the criterium for comparison. Figure 7.14 to Figure 7.17 shows the performance of both controllers for the same participant in lifting only and lifting/carrying experiments respectively (Task 3) for the left hip and left knee joints. See, Section 3.4.4.3 (c) for details of procedure of Task 3. Table 7.7 present the summary of average human interaction forces at the hip and knee joints for all the participants during the experiments. Table 7.8 gives the percent reduction in exerted human torque/effort measured as a fraction of total joints torques. Total joint torques are determine from torque sensors, whereas the human torques are estimated from the

difference between the total torques and the motor torque. The motor torques are derived from motor current by the product of the torque constants given as $K_t = 10.97$ Nm/A for the hip motor and $K_t = 8.10$ Nm/A for knee motor respectively.

Overall, the system was unstable in virtually all movement tasks under the SAC algorithm. In many unstable situation (under SAC) participants had no means but to forcefully counter the chattering/disturbance movement of the exoskeleton by high torque/effort to ensure stability of the exoskeleton system thus increasing the interaction forces. Figure 7.14 show some regions of instability under SAC. The SAC algorithm works best (with minimal disturbance) under a perfect model which is not assumed in our case. With our current model, the proposed synchronous control algorithm with supervisory logic outperform the SAC algorithm to provide smooth undisturbed lifting (squatting) and lifting/carrying (walking) movements as can be seen in Figure 7.14 to Figure 7.17 (videos of performance of both controllers may be accessed in the YouTube link: https://youtube/Ecg1A11smnE). In all experiments, we have not achieved near zero interaction torques due to the limits on our rated motor torque in the current design (34Nm and 17Nm for the hip and knee joint actuation respectively) which do not fully compensate for the average joint torques of adult workforce participants (>76kg of weight) especially in squat-lifting experiments.

As seen in Table 7.7 and Table 7.8, two sensitivity factors have been applied for SAC. Interaction torques under SAC should decrease with increasing sensitivity factor, however, in this case interaction torques are fairly high even with high sensitivity factor for SAC. This is adduced to the fact that exoskeleton instability also increases with increasing sensitivity factors, making the participants to forcefully provide stability by increasing interaction torques.

Table 7.7: human-robot interaction torque (RMS)

Interaction Torque	Lifting Interaction Torque (RMS)			Lifting and Carrying (RMS) Interaction Torque (RMS)		
	SAC $\boldsymbol{\alpha = 10}$ (Nm)	SAC $\boldsymbol{\alpha = 100}$ (Nm)	Proposed Controller (Nm)	SAC $\boldsymbol{\alpha = 10}$ (Nm)	SAC $\boldsymbol{\alpha = 100}$ (Nm)	Proposed Controller (Nm)
Right Hip Joint	13.93	8.119	11.54	9.02	6.36	3.82
Right Knee Joint	15.25	15.82	12.23	6.19	9.62	4.56
Left Hip Joint	20.01	20.13	13.14	11.11	11.89	5.91
Left Knee Joint	29.36	24.32	12.10	13.94	10.10	6.23

Table 7.8: Percent reduction in human torque

Joint	Lifting Interaction Torque (%)			Lifting and Carrying (RMS) Interaction Torque (%)		
	SAC $\boldsymbol{\alpha = 10}$ %	SAC $\boldsymbol{\alpha = 100}$ %	Proposed Controller %	SAC $\boldsymbol{\alpha = 10}$ %	SAC $\boldsymbol{\alpha = 100}$ %	Proposed Controller %
Right Hip Joint	39.2	64.1	49.2	30.3	46.0	66.0
Right Knee Joint	35.8	33.2	46.4	44.2	30.6	54.5
Left Hip Joint	27.8	26.1	43.2	24.6	24.8	42.7
Left Knee Joint	18.6	21.6	47.7	19.6	29.1	40.6
Average	30.3	36.3	46.6	29.7	32.6	50.9

*Reduction Factor(%) =
$(rmsTotal\_Joint\_Torque - rmsHuman\_Input\_Torque)/rmsTotal\_Joint\_Torque)\ x\ 100$

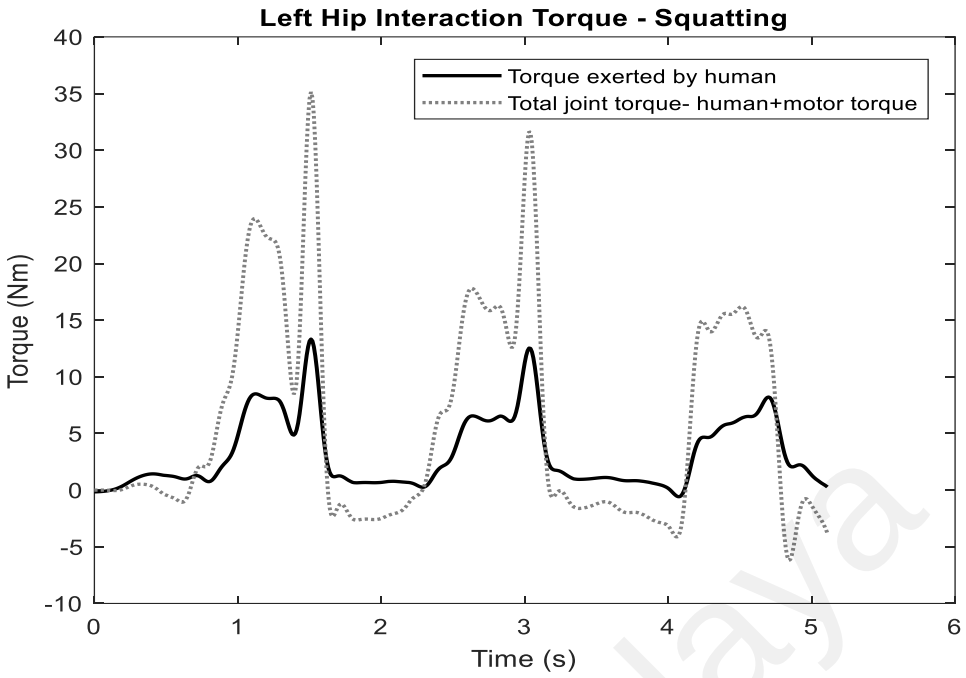

(A)

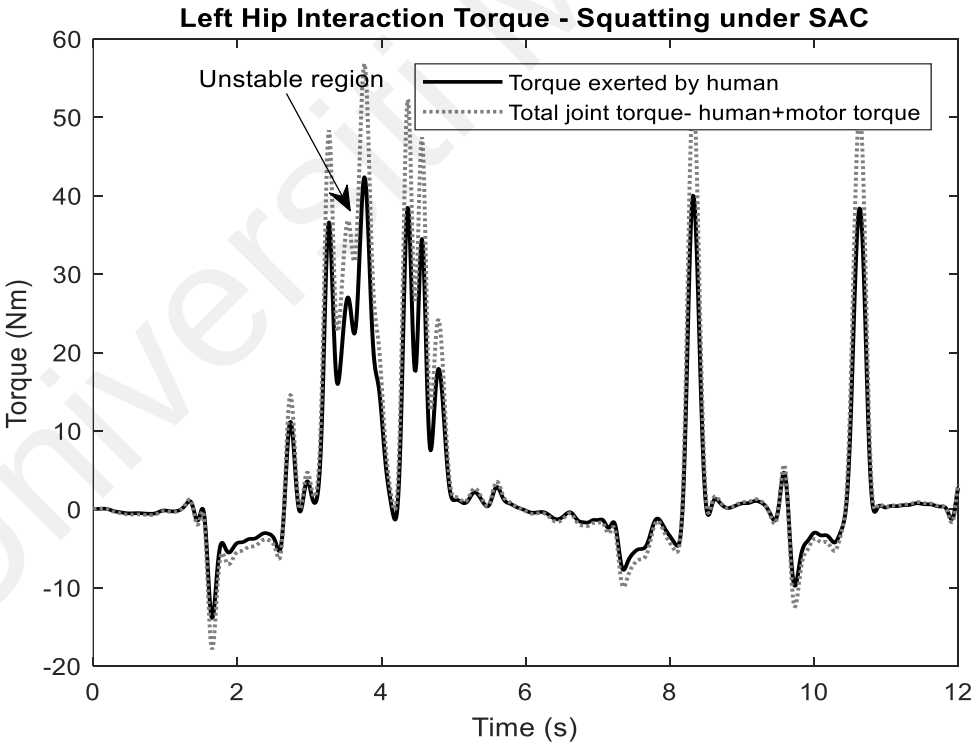

(B)

Figure 7.14: Hip interaction torques in squat-lifting experiment under (A) proposed control algorithm and (B) SAC algorithm (α=10%)

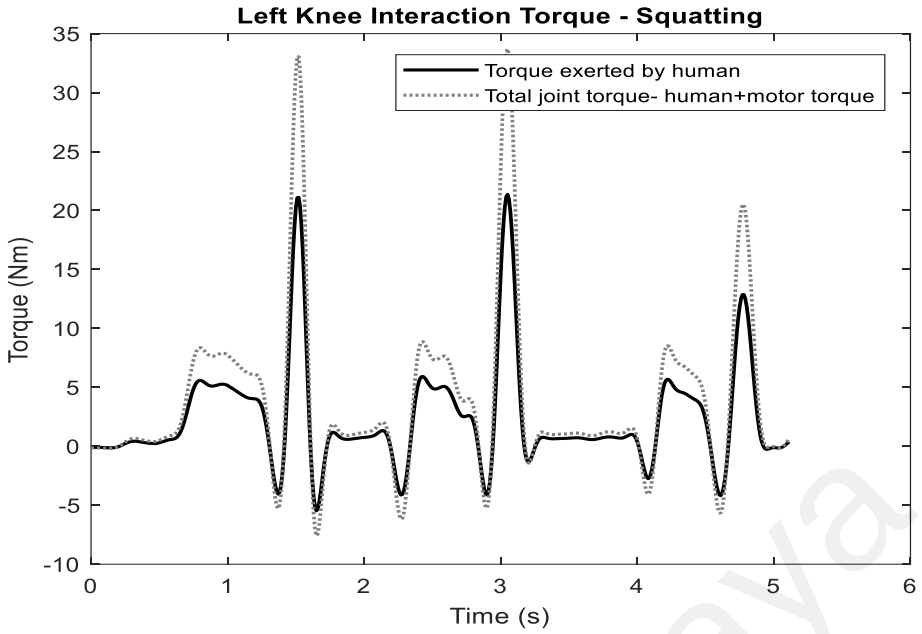

(A)

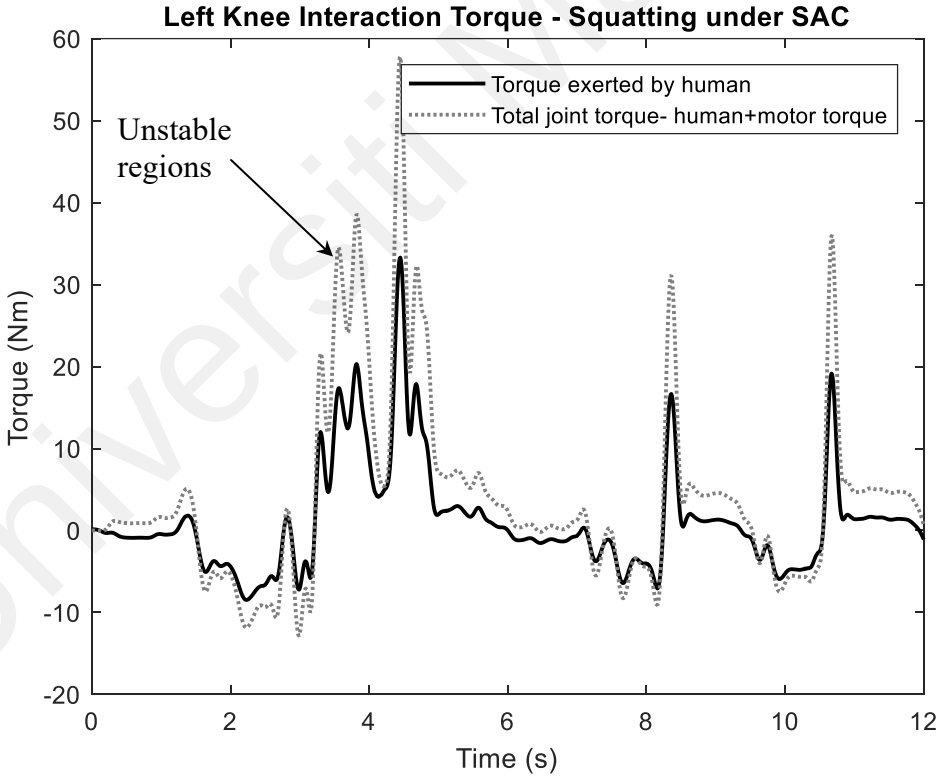

(B)

Figure 7.15: Knee interaction torques in squat-lifting experiment under (A) proposed control algorithm and (B) SAC algorithm (α=10%)

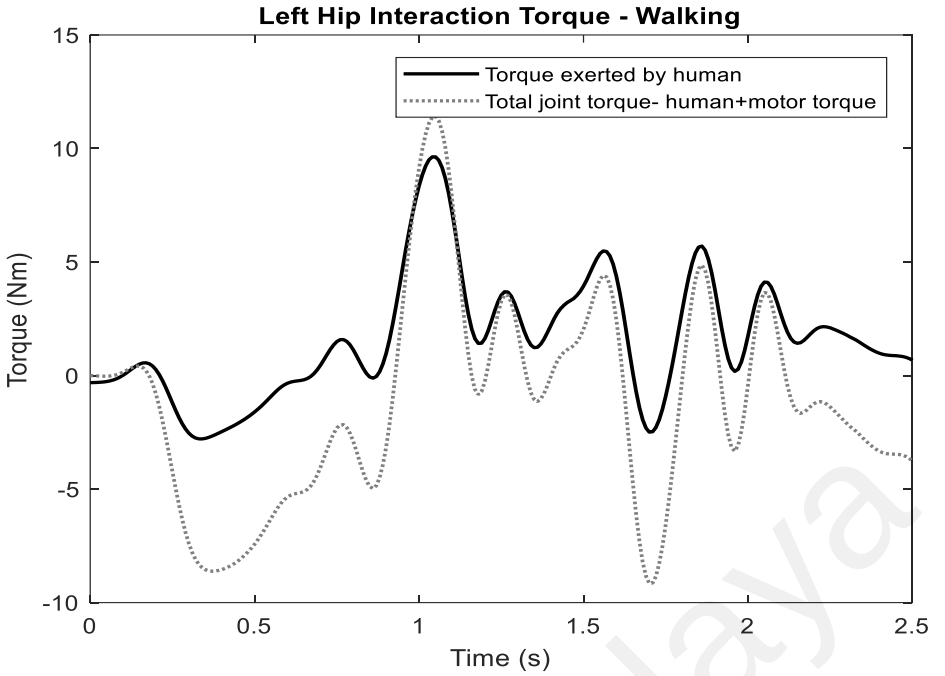

(A)

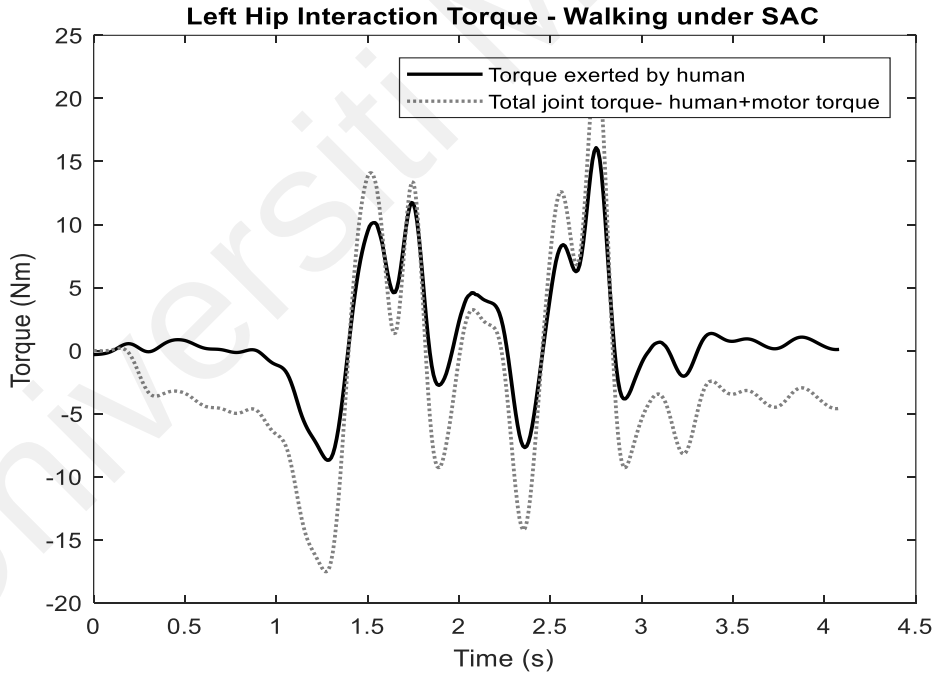

(B)

Figure 7.16: Hip interaction torques in lifting and carrying experiment under (A) proposed control algorithm and (B) SAC algorithm (α=10%)

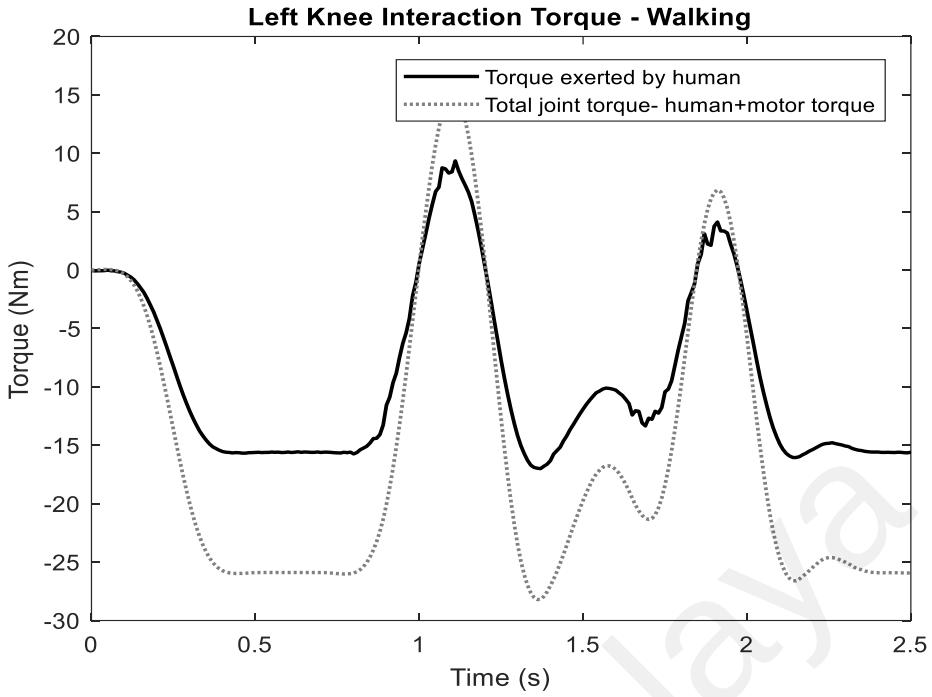

(A)

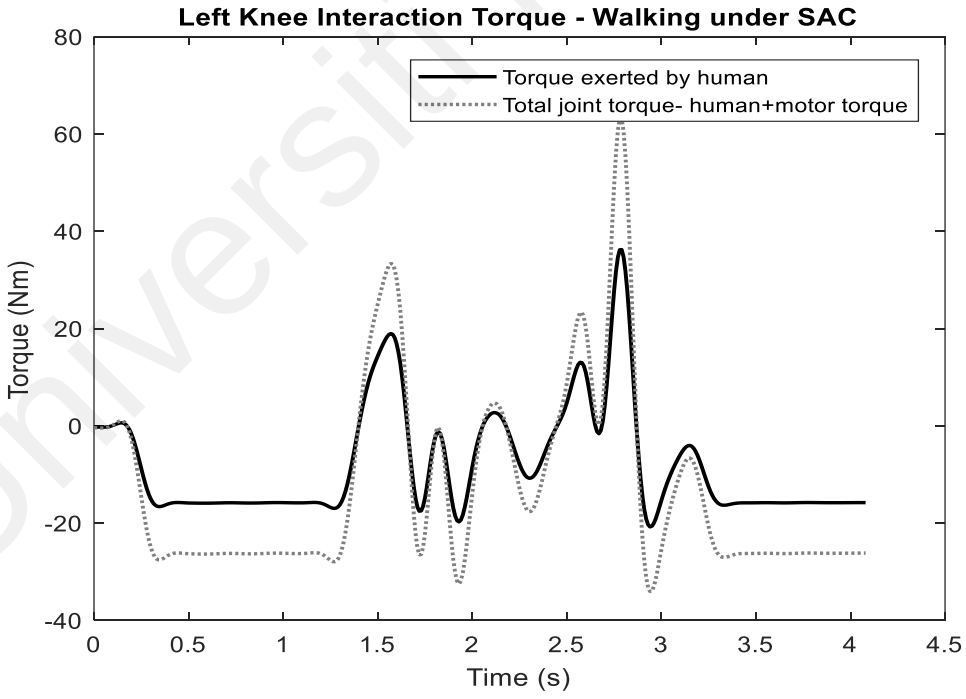

(B)

Figure 7.17: Knee interaction torques in lifting and carrying experiment under (A) proposed control algorithm and (B) SAC algorithm (α=10%)

7.4.2 Based on Muscle Effort Reduction

This section compares UMExoLEA to other state of the art EHPAs based on the % muscle activity reduction (Section 7.2.1). To ensure fair comparison, important factors such as size, weight, and actuation power of the EHPAs are taken into consideration. Table 7.9 present the summary of comparison with respect to three muscle: Vastus Medialis (**VM**), Rectus Femoris (**RF**), and Gastrocnemius (**GA**) of the lower limb musculature. EHPAs which do not provide performance data on one or more of these muscles are generally excluded from the comparison table. This is to ensure proper basis of comparison. Based on the criteria of assessment, five EHPAs could be listed in the comparison table with UMExoLEA. Although, performance data could not be found for some listed EHPAs, UMExoLEA can be seen to be favourably on the high cadre of performance.

7.4.3 General Discussion on UMExoLEA Performance Comparison

Due to lack of performance data and system specification, comparison of UMExoLEA with other state of the art EHPA is difficult. Many EHPAs have not been used on real participants to extract biomechanical data relevant for comparison. Based on human interaction torque, the proposed synchronous mobility control algorithm has been seen to outperform the popular sensitivity amplification control algorithm. SAC algorithm rendered the system unstable due to its heavy reliance on model accuracy. The proposed algorithm however remained stable even in the presence of model uncertainties or external perturbation forces.

Table 7.9: Comparison of the %muscle effort reduction with some selected EHPAs

EHPA	Weight (kg)	Actuating Torque (Nm)	%Muscle Effort Reduction (Squat-lifting)			%Muscle Effort Reduction (Walking/carrying)			Load (kg)
			VM	RF	GA	VM	RF	GA	
UMExoLEA	12.4kg	Electric Motor Hip = 34Nm Knee = 17Nm	51.4%	30.2	40.6	43.9	37.8	58.0%	9.5kg load with two hands 4kg back pack load
Full-body EHPA (H. Kim et al., 2017)	N/A	Hydraulic actuator	N/A	N/A	N/A	36.8	61.5	43.5	45 kg backpack load
Hip joint EHPA (Lenzi et al., 2013)	N/A	N/A	N/A	N/A	N/A	N/A	22.3-38.5%	45-49.4%	0kg
Ankle-foot EHPA (Galle et al., 2013)	0.76kg	pneumatic muscles	N/A	N/A	N/A	N/A	N/A	16%	N/A
H-WEX (waist) (Ko et al., 2018)	4.5kg	Electric motor	N/A	N/A	N/A	N/A	~0%	N/A	15kg
(W. Kim et al., 2013)	N/A	Knee-BLDC motor Hip & ankle – quasi - passive	N/A	N/A	N/A	N/A	40.5%	~32%	20kg

7.5 Synchronous Mobility Control and Movement Adaptation

7.5.1 Torque Assistance and Supervisory Control

Figure 7.18 to Figure 7.21 show the torque generation and motion following plot of the UMExoLEA synchronous mobility controller for lifting (squatting) and carrying (walking) movement assistance respectively. Comparison is made between the computed torque from the impedance controller (black broken lines), the output motor torque (grey dotted lines), and the control torque input (derived as a product of the computed torque and supervisory control output, σ_j). Controller parameters for the impedance controller are selected as $M_r = 1$Ns^2(degree)$^{-1}$, $B_r = 260$ Ns(degree)$^{-1}$, and $K_r = 16.9$kN(degree)$^{-1}$ at natural frequency of $\omega_n = 0.72\pi$rad/s based on simulation studies (Section 5.3). The figures also show plots of the supervisory control output for each phase of movement, plots of the ground reaction forces, and plots of the joint motion trajectory. Notice that the reference input to each motor is the control torque input divided by the motor torque constant whereas the output motor torque is derived as the motor current multiplied by the torque constant. Grey shades in Figure 7.18 to Figure 7.19, represent squatting descent (lowering), and between two grey shades is squatting ascent. First squatting descent (first grey shade) is performed without load, in preparation for load lifting. Between first and second grey is load lifting from deep squat. The second squatting descent (second grey shade) is performed to return the lifted load to the floor. Some unlabeled free body diagrams of the human biomechanics have been used to further the illustration of these activity in Figure 7.18 and Figure 7.19. First two grey shades in Figure 7.20 and Figure 7.21 represent the squat-lifting in Task 2 which is characterized by squatting descent (labelled '1') and squatting ascent (i.e. labelled '2'). Subsequent shades represent stance phase (labelled '4') of walking (carrying). In between these shades is the leg swing phase (labelled '3') (Figure 7.20 and Figure 7.21).

The difference between computed control input torque and the motor torque for all participants in the lifting task is achieved within root mean square error of **RMSE** = 0.030Nm for the hip joint (Figure 7.18(a)) and **RMSE** = 0.065Nm for the knee joint (Figure 7.19(a)). For the lifting and carrying task tracking of the control torque is achieved within **RMSE** = 0.022Nm for the hip joint (Figure 7.20(a)) and **RMSE** = 0.063Nm for the knee joint (Figure 7.21(a)) respectively.

Notice also that the supervisory control output σ_j appropriately detected each phase of movement (i.e. squatting ascent and descent, leg swing, and stance) and allowed exoskeleton assistance to continue as long as the respective joint is within the allowable range of motion (Figure 7.18(b), Figure 7.19(b), Figure 7.20(b), and Figure 7.21(b)). Outside the range of motion, supervisory controller turns off the assistance to prevent the hip or knee from (any possibility of) over-extension or over-flexion. Notice that the computed torque (grey dashed lines) on the other hand, without the supervisory control (especially in Figure 7.20(a) and Figure 7.21 (b)) are sometimes non-zero in this range which could have exerted some torque on the wearer. Notice also that the torque assistance is decreased during squatting descent to accommodate the effect of gravity and increased during squatting ascent to compensate the effect of gravity.

Figure 7.18(c) to Figure 7.21(c) show the ground reaction forces (GRF) at the heels and ball of foot during the movement tasks. Ground forces increased generally during squatting descent and more during squatting ascent. After the first two shades (phases) in Figure 7.18 (c) and Figure 7.19 (c), the participants could be seen to increase the squatting pace and cadence, thus the ground forces increased correspondingly. This phenomenon is supported by existing studies on squat training which show the influence of lifting cadence (Bentley et al., 2010) and squatting depth (Dali et al., 2013) on ground reaction forces. Bentley et al. (2010) demonstrated that while the speed (cadence) of lifting

accentuates ground forces, peak forces developed during the ascent is influenced by the rate of descent, highlighting the importance of the rate of descent on the stretch reflex response. This is expected since the peak forces during the descent phase occurs near the initiation of ascent when the downward velocity of the system was changed quickly to upward velocity (see Figure 7.18 (c) and Figure 7.19 (c)).

Figure 7.18 (c) and Figure 7.19 (c) also show the influence of sensor hysteresis and drift on the measured ground forces. Ground forces could be seen to increase throughout the squatting repetition without returning to their initial values (at start of lifting). Since sensor measurement were taken rapidly, hysteresis effect appears to be the dominant effect which result in significant difference in sensor output response during increased loading (stance) and decreased loading (swing). However, these effects were eliminated in the computation of the fractional P value and were also corrected by the computation of the offset value ε for each phase (see Section 4.4.3.4 (a)). Drift account for difference in sensor output when a constant force is applied over a period of time thus was less dominant in this case.

For Task 2 (Figure 7.20 (c) and Figure 7.21 (c)), ground reaction forces at the lifting time (i.e. first two shades labelled '1' and '2') exhibit similar phenomenon to Task 1; the stretch reflex response phenomenon is generally evident, however force profile during the swing and stance phases are noticeably different. Ground forces dropped momentarily at the initiation of swing in the location marked 'X', expectedly due to temporary unloading of the sensor. Ground forces increased steadily to a peak at the next terminal stance (regions labelled '4'). Despite momentarily drop at the initiation of the next swing (location marked 'Y'), the hysteresis effect can also be seen to influence the peaks of the ground reaction forces. Figure 7.22 show a clearer profile of the ground reaction forces for a single stance phase. This profile is closely similar to the work of (Bouffard et al.,

2011), where **HC** stands for Heel contact, **MWA** for maximum weight acceptance, **MS** for mid-stance, **PO** for push-off, and **TO** for toe-off.

The supervisory control algorithm proposed in this study combines measurement of the ground reaction forces and joint kinematics in a novel gaussian bell function implemented by a hybrid automaton (refer Section 4.4.3.4) to compute the supervisory control output shown in Figure 7.18(b), Figure 7.19(b), Figure 7.20 (b), and Figure 7.21 (b), as mentioned earlier. In Figure 7.18(b) and Figure 7.19(b), the hybrid automaton transit only three states (**S1**, **S2**, and **S3**) to accomplish the squat-lifting movements. In Figure 7.20(b) and Figure 7.21(b), the hybrid automaton transit seven states (**S1**, **S2**, **S3**, **S4**, **S5, S6**, and **S7**) to accomplish the lifting and carrying movement (i.e. squatting and walking motion). A measure of accuracy of identification of each phase by the supervisory algorithm is presented the next section.

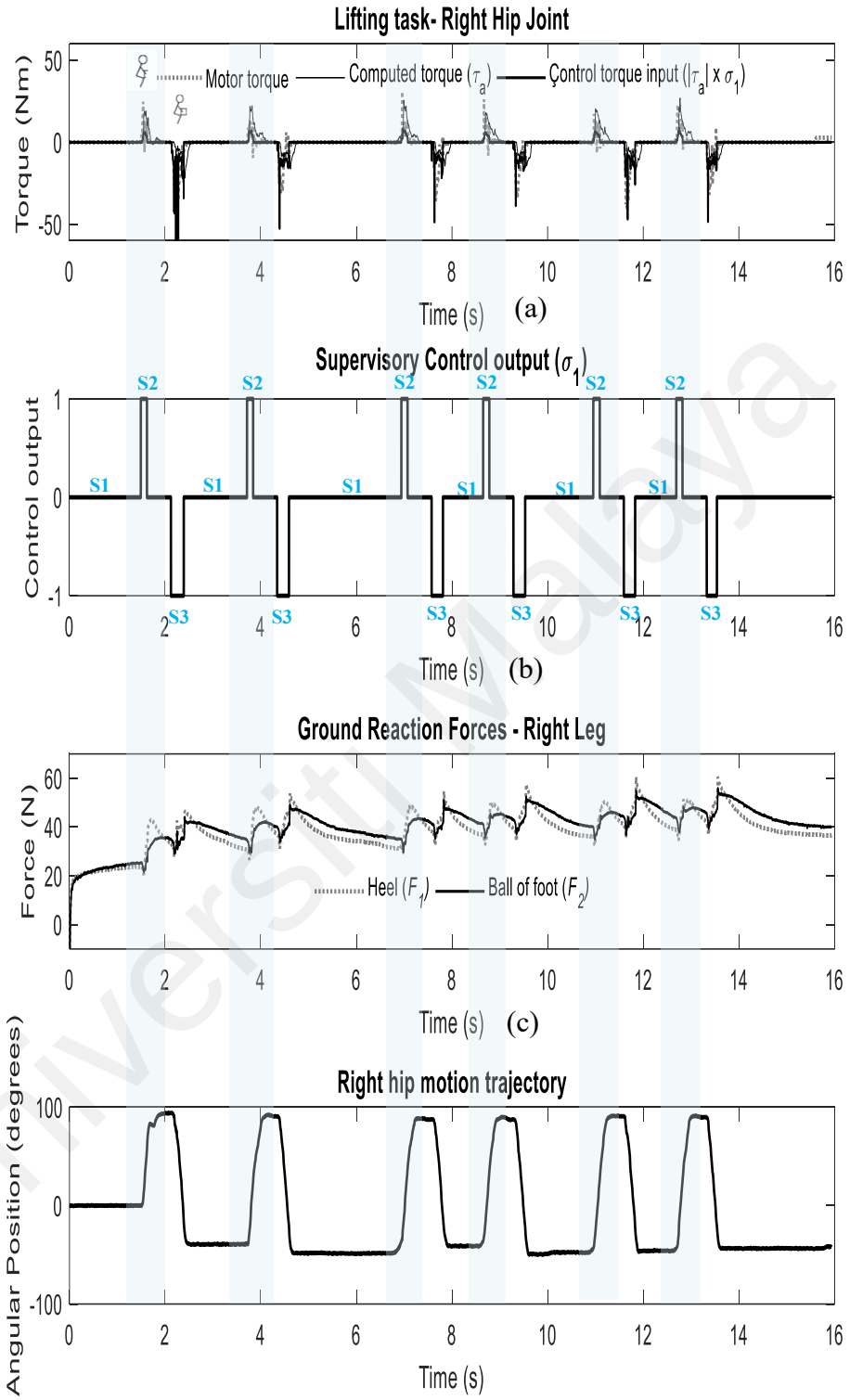

Figure 7.18: Lifting experiment: torque assistance and supervisory control input for right hip

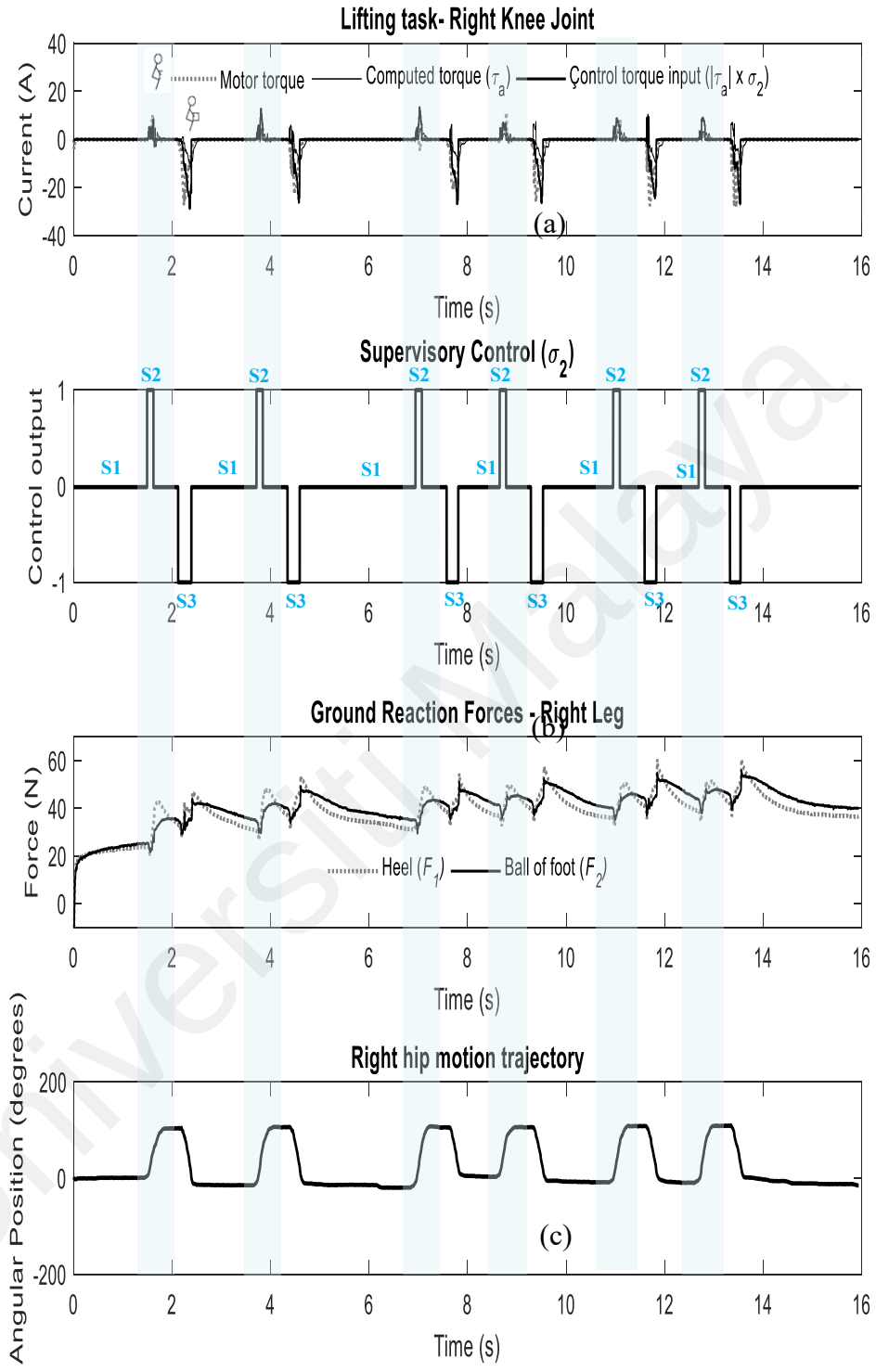

Figure 7.19: Lifting experiment: torque assistance and supervisory control input for right knee

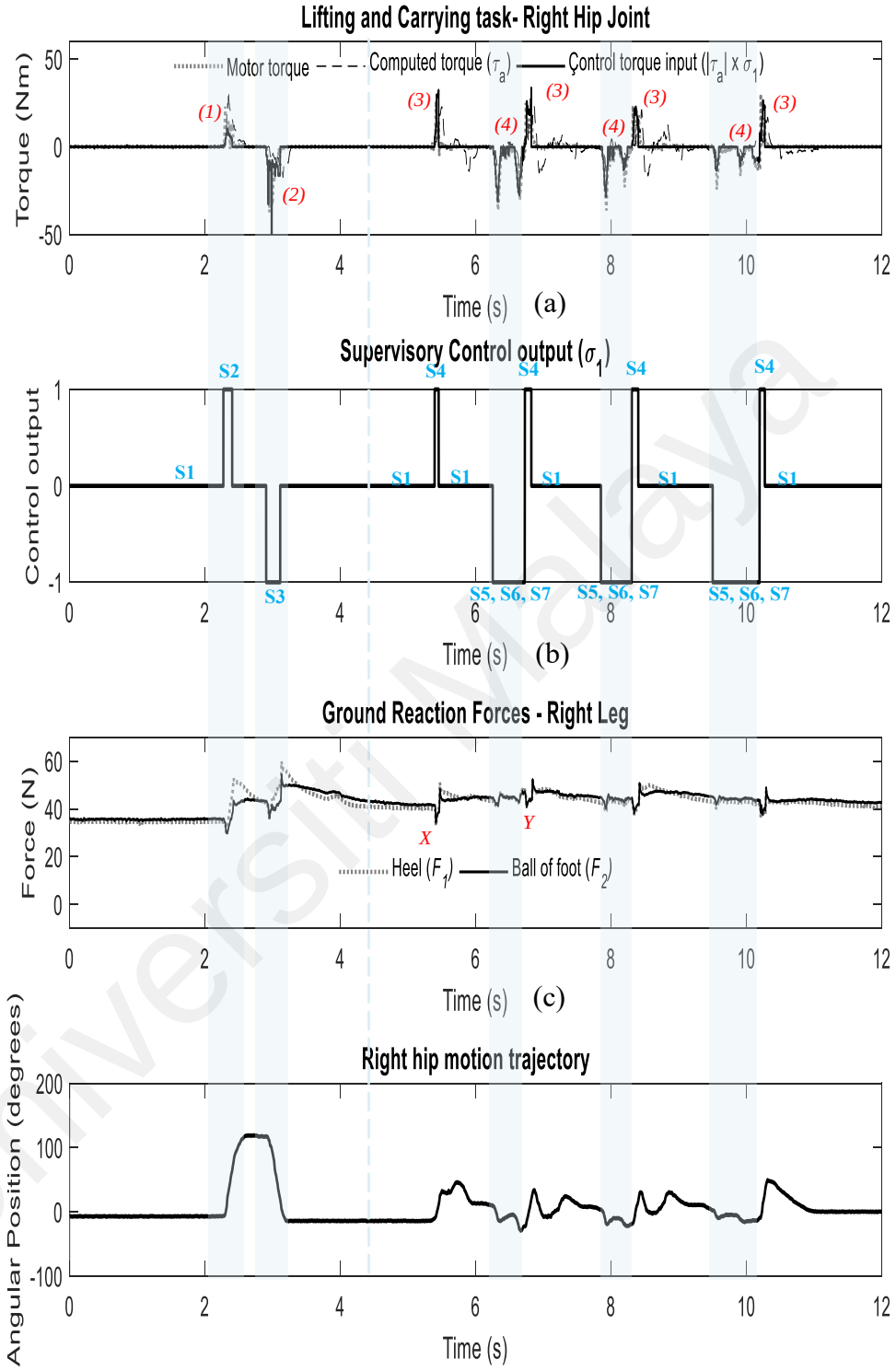

Figure 7.20: Lifting and carrying experiment - torque assistance and supervisory control input for right hip

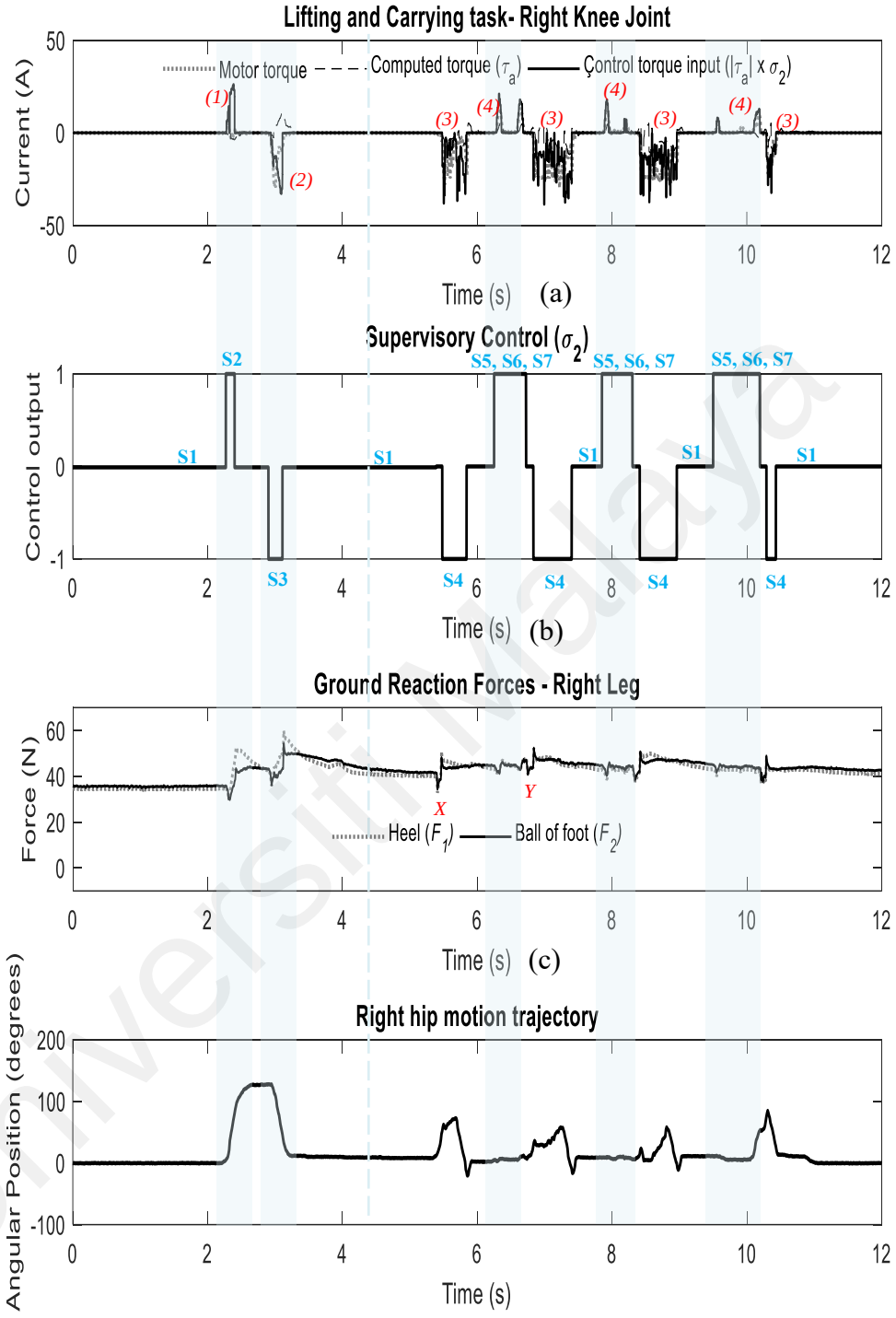

Figure 7.21: Lifting and carrying experiment - torque assistance and supervisory control input for right knee

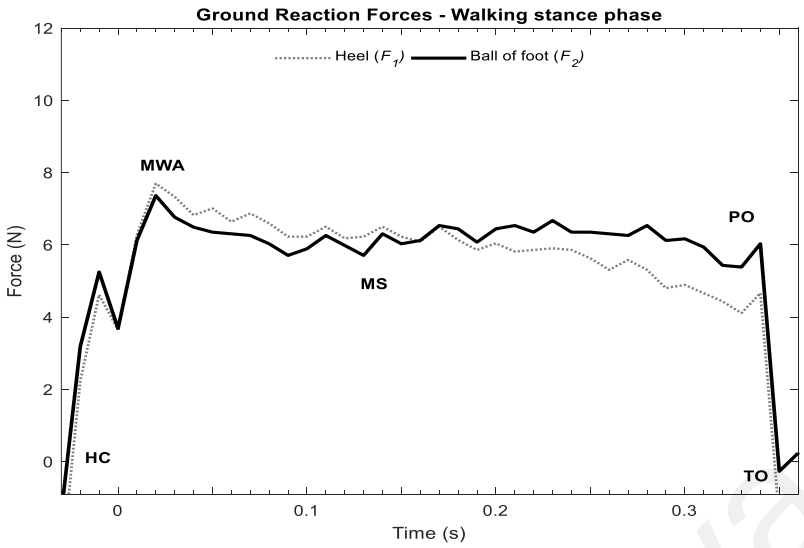

Figure 7.22: Ground reaction forces in a single stance

7.5.2 Movement Detection and Adaptation: Verification by Success Rate Algorithm

The capability of UMExoLEA to detect wearer's squatting phase and walking movements phase during lifting and carrying task is further verified by a success rate algorithm proposed by (Y. D. Li & Hsiao-Wecksler, 2013). The algorithm defined the success rate as the percentage of correctly recognized steps in a movement task.

By extension, the algorithm is expressed as

$$\text{Success Rate} = \frac{\#\ of\ Correctly\ Identified\ Steps}{\#\ of\ Total\ Steps}\ x\ 100\% \tag{7.1}$$

This algorithm provides a basis to assess the overall robustness of the UMExoLEA supervisory control algorithm (Section 4.4.3) (i.e. ability to detect and adapt to wearers' movement). Table 7.10 presents summary of success rate for the 15 participants in Task 1 (squat-lifting movement) and Task 2 (squat-lifting, walking and carrying) movement task. Notice that more than 99% success rate has been achieved for all participants in both movement tasks. One of the very few occasions of incorrectly identified phase can be seen in Figure 7.23. The figure shows a sample plot of an incorrectly identified squatting

ascent phase by one participant during the lifting and carrying task. The consequence was to enable torque assistance in the opposite direction which kept the exoskeleton from assisting the wearer's upward movement. The cause of this particular situation was traced to a broken USB data communication cable which introduced a lag in the squatting descent phase hence an extension of these phase to the squatting ascent phase. Beyond this phase everything returned normal. Other very few similar situations were largely traceable to a communication fault or user error.

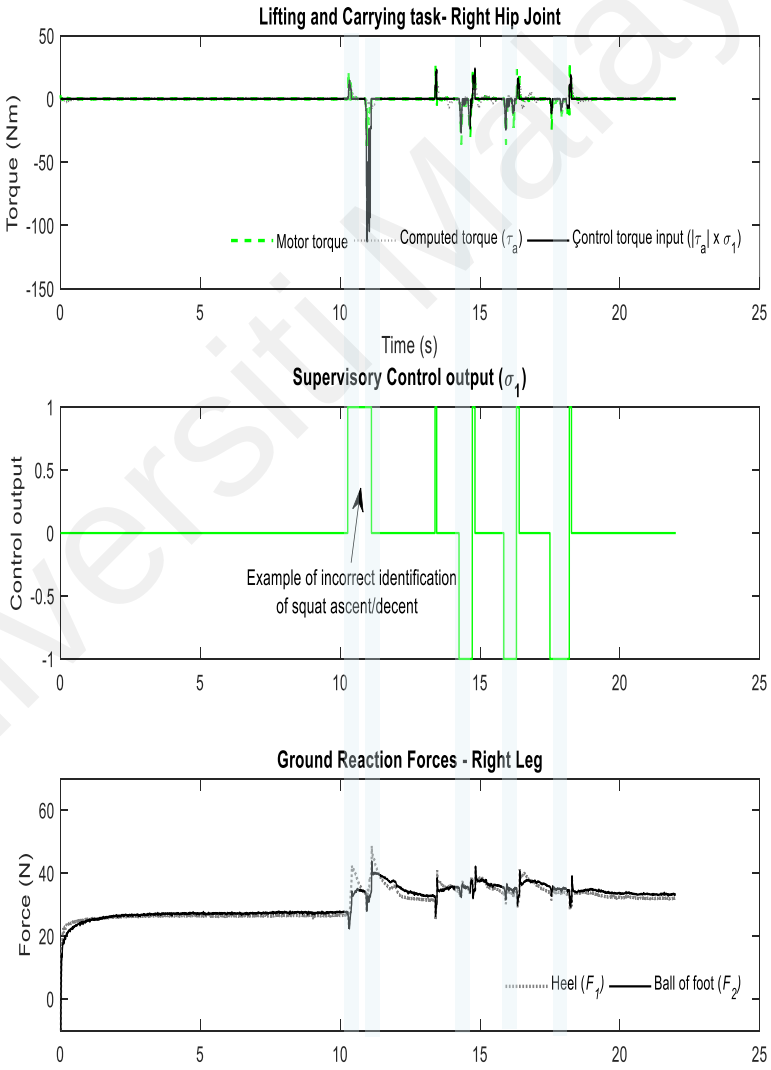

Figure 7.23: Sample plot showing incorrect identification of squatting ascent and descent

Table 7.10: Summary of success rate for the 15 participants in Task 1 and Task 2

Participants	Success Rate (Task 1) (%)				Success Rate (Task 2) (%)			
	Trial 1	Trial 2	Trial 3	Total	Trial 1	Trial 2	Trial 3	Total
S1	100	100	100	100	100	100	100	100
S2	100	100	100	100	100	100	100	100
S3	100	100	100	100	100	100	100	100
S4	100	100	100	100	100	100	100	100
S5	91.7	100	100	97.2	87.5	100	100	95.8
S6	100	100	100	100	100	100	100	100
S7	100	100	100	100	100	100	100	100
S8	91.7	100	100	97.2	100	100	100	100
S9	100	100	100	100	100	100	100	100
S10	100	100	100	100	100	100	100	100
S11	100	100	100	100	100	100	100	100
S12	83.3	100	100	94.4	100	100	100	100
S13	100	100	100	100	100	100	100	100
S14	100	100	100	100	100	100	100	100
S15	100	100	100	100	100	100	100	100
Average	97.8	100	100	99.2	99.2	100	`100	99.7

7.5.3 Model Parameter Update and Switching

Model parameter needs to be updated to ensure appropriate model during walking or squatting-to-walking transition. Two methods to model parameters update are compared experimentally in this study. Conventional approach uses phase-based update mechanism for the model or control parameters. An example has been shown in the hybrid control of BLEEX using sensors placed at the shoe for walking phase detection and consequently for model/parameter and controller switching (H. Kazerooni et al., 2005). In the current scheme, model parameter update has been applied and compared using the conventional

approach as well as the proposed DUKF parameter estimation technique (Section 4.4.3.2 (b)). Conventional switching is achieved by means of the supervisory controller based on different phase detection (see Table 4.4 and (4.30)). Under the DUKF scheme, the initial guess of segment mass parameters, process noise covariance, and measurement noise covariance are given as $w\,(0) = [2, 2.56,\ 0.77\,]^T$, $\mathbf{P}_r = diag([0.8,\ 0.8,\ \ 0.8])$, and $\mathbf{P}_e = diag([0.8,\ 0.8,\ \ 0.8])$ respectively. $w\,(0)$ is chosen for the double stance phase. The noise covariances on the other hand are selected to account for model inaccuracies and the effect of disturbances. The comparison of the model parameter updates by the DUKF and the conventional approach during walking motion are shown in Figure 7.24. Performance of the DUKF model parameter estimation is still near accurate, however interesting results can be found especially for estimate of segment two and three as shown in Figure 7.24 (A) and Figure 7.24 (B) shows the estimated human torque comparison for the two methods of model parameter update. Overall improvements in the filter design for model parameter estimation is planned for future work. It is hoped that this method can serve as a suitable alternative to the conventional switching/update mechanism that relies on sensors' detection of walking phases.

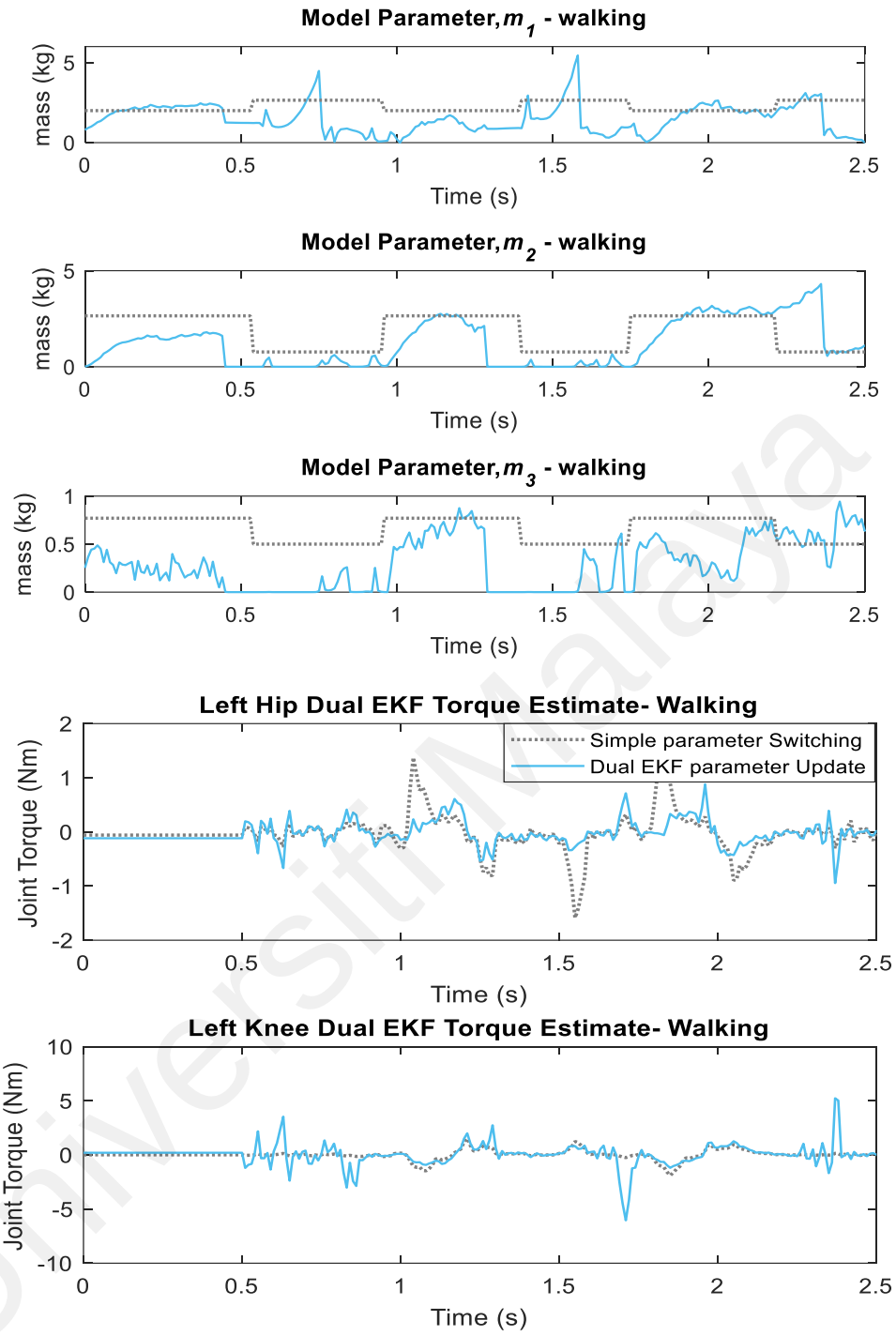

Figure 7.24: (A)model parameter estimates and (B) joint torque estimate compared under the two-update scheme during walking experiment

7.5.4 General Discussion on Synchronous Movement Performance

The proposed synchronous motion assistance controller has shown capability for adequate torque generation, motion following and detection of the different phases of

movement in lifting and carrying MH task. The sensor fusion supervisory algorithm combines the measurement of the GRF sensor and the joint angle sensors to detect, timely, the phases of motion and to compute a supervisory output in the range [-1 1]. This output value coordinates the coupled movement of the wearer and exoskeleton, as well as regulate the assistance provided by the exoskeleton.

Some important observations have been made in this implementation. The estimated ground reaction forces from the GRF sensors (*Flexiforce* sensor) and the phenomenon of stretched reflex response during squatting descent and ascent showed stricken similarity with previous studies. The GRF measurements were also significantly influenced by the effect of hysteresis since loading on the sensor changed rapidly during squatting and walking motion (stance and swing). Based on manufacturer documentation, the sensor drift is within 5%/logarithmic time at constant load, repeatability is within $\pm$2.5%, linearity is within 3% of full scale, and hysteresis is within 4.5% of full scale. The hysteresis effects are more significant when measurements are repeated quickly, typically within 5 – 10min (Ferguson-Pell et al., 2000; Komi et al., 2007; Matute et al., 2017). Nevertheless, the effect was corrected in the supervisory control algorithm.

7.6 Summary

This chapter has presented the experimental verification of the capability of UMExoLEA to enable lower extremity mobility augmentation and smooth movement transitions in lifting/carrying MH activities. UMExoLEA has demonstrated capabilities for lower extremity power augmentation (i.e. torque assistance), muscle effort/activity reduction, fatigue reduction, and synchronous movement with the wearer. Based on extracted EMG data, between 30% to 60% reduction in muscle effort/activity and muscular force at the lower extremity have been achieved; and based on subjective rating, about 73.1% of muscle effort reduction and power assistance from UMExoLEA has been

perceived by participants. In addition, subjective fatigue/discomfort rating has shown that UMExoLEA is able to minimize muscular fatigue in the repetitive tasks during the experiment.

Although comparison of UMExoLEA with other state of the art EHPAs is difficult due to poor performance documentation from other EHPAs, comparison with a few EHPAs with respect to the above capabilities has shown UMExoLEA comparatively better performance. With respect to synchronous mobility control, tracking of motor torques have been achieved within root mean square error (RMSE) of 0.065Nm for the hip and knee joints in both tasks; movement phase (transition) detection and supervisory controller synchronization have been achieved by more than 99% success rate.

CHAPTER 8: CONCLUSION AND RECOMMENDATION

8.1 Conclusions

This study presents the design and implementation of a prototype 12-DOF lower extremity EHPA called UMExoLEA for synchronous lower-extremity mobility augmentation in lifting and carrying MH works. A significant contribution of this work is for long-term prevention of mobility disabilities and disorders such a knee/hip osteoarthritis, LBP, and meniscal injury which are common in repetitive/prolong manual lifting and carrying activities.

To this end, a new synchronous mobility controller has been developed for the prototype EHPA which successfully enabled the exoskeleton to estimate wearers' motion trajectory by means of a dual unscented Kalman filter (DUKF) (via noisy position sensors and an approximate human-exoskeleton model); and to generate torque for movement assistance by means of a computed torque impedance controller. Finally, the prototype is able to promptly detect and synchronize with the wearers movement by means of a novel supervisory controller.

Experimental verification on 15 participants of workforce age shows that UMExoLEA successfully augmented the wearers lower extremity movement by 73.1% (perceived subjectively by participants); decreased their muscular effort and exerted force by 30-60%; and reduced fatigue to nil in the repetitive lifting and carrying tasks. Lifting and carrying MH tasks involve squatting and walking motion, UMExoLEA was also able to assist this motion seamlessly, synchronizing with the wearer's movement by a success rate of more than 99%.

Overall, the following conclusions have been reached in fulfilment of the specific objectives of study:

1. In fulfilment of Objective 1, the dynamic model of the lower extremity EHPA has been developed successfully for lifting and carrying MH task which is a requisite for the development of the synchronous mobility controller. Important lower extremity biomechanics i.e. the analysis of the kinematics and kinetics of squatting and walking motion, with emphasis on torque assistance to the hip and knee joint, were applied to achieve this objective (Section 4.4.2 and Appendix I). Squatting movement is performed in a double support stance phase and walking is performed in stance and swing phase. Understanding of these biomechanics facilitated the simplification of the complex and dynamic movements involved in lifting/carrying activities by two main dynamic equations: (1) Equation (4.1) and (2) Equation (4.2). The first equation models the squatting and walking stance phase for a single leg, and the other models the walking swing phase for a single leg. The form of these equations allowed real time control application and parameter switching. It was also possible to extract the human segment parameters which was applied in the development of the coupled human-exoskeleton (partial) model for the DUKF trajectory estimation.
2. In fulfilment of Objective 2, the synchronous mobility controller has been successfully developed to enable smooth lower extremity mobility augmentation and movement transitions in lifting/carrying MH activities (Section 4.4.3 and Appendix K). In order to achieve this objective, three controller algorithms were integrated: (1) a dual unscented Kalman filter (DUKF) for trajectory estimation and model update, (2) an impedance controller for generation of assistive torque, and (3) a new supervisory control algorithm for pilot movement detection and synchronization with the exoskeleton. The following sequel explains the motivation for these algorithms.

a. The DUKF algorithm was motivated to offer a suitable means for estimation of both uniform and non-uniform motion data (unlike traditional AFOs which are suitable for only uniform motion) i.e. spatial-temporal derivative such as joint position, angular velocity, and acceleration from noisy position sensor input data. This novel implementation of DUKF rely on the powerful robustness capability of the Kalman filter for trajectory estimation and model update/correction which has found tremendous applications in highly nonlinear dynamic scenarios such as aerospace and SLAM.

b. The computed torque impedance control algorithm, on the other hand, was motivated as an indirect force controller to generate assistive torque from users' motion to decrease wearers' exerted effort to a point that wearers feels significantly helped by the exoskeleton. The impedance control algorithm was also motivated to stipulate a desired interaction compliance by means of the impedance parameters and feedback of the interaction forces τ_h. Overall, by this implementation we adopt the notion of movement primitive where complex motion trajectories are estimated (i.e. by DUKF in our case) and a suitable force field or force controller is used to attract the user to this trajectory or to provide torque to assist the user on this trajectory. The indirect force controller approach requires no recalibration of controller parameters for different users as compared to some other torque generation techniques like the myoelectric feedback control where muscle signals are converted to torque assistance with recalibration for different users since different EMG signals are produced.

c. Lastly, the supervisory control algorithm was motivated to provide prompt detection of the wearers' movements/motion phases and synchronization

with the exoskeleton in order to prevent unintended motion or undesirable assistance for the wearer, for example overextension or over-flexion assistance for the wearer's hip or knee; or continued assistance on a forward movement when the wearer has just started an opposite movement. It is also motivated for model parameter updating during the phase transitions to enhance model accuracy for appropriate controller action (i.e. minimize overshoot, instability, etc.).

3. In fulfilment of Objective 3, a prototype 12-DOF lower extremity EHPA weighing 12.5kg (without the bag-pack) has been developed successfully based on completion of Objective 1 and Objective 2. This prototype is called UMExoLEA. The selection of exoskeleton materials (aluminum alloy 8081) and DC motor actuation were mainly influenced by the demand for lightweight, zero backlash, noiseless operation, and the amount of muscle torque needed by an average adult for squatting (hip->0.6Nm/Kg; Knee->0.2Nm/Kg) and walking movements (hip ->0.6Nm/Kg; Knee- >0.2Nm/Kg) under moderate loading conditions (0-10kg).
4. In fulfilment of Objective 4, the assistive-ness of the prototype UMExoLEA has been tested and verified successfully by repetitive lifting and carrying experiment on 15 participants of workforce age. UMExoLEA successfully assisted the participants' lower extremity movement by an average 73.1% based on subjective feedback from participants. Based on extracted myoelectricity data, UMExoLEA decreased participants' muscular effort and exerted force (at the right Vastus Medialis, right Rectus Femoris, and right Gastrocnemius of the Quadriceps femoris and calf) by 30-60%; and reduced fatigue at the lower extremity and low back to zero in the repetitive lifting and carrying tasks. Augmenting the strength of the Quadriceps and the Gastrocnemius, assist force distribution around the knee joint, hip, and lumbar region thus minimizing fatigue and/or regional discomfort

of the lower extremity in repetitive lifting and carrying MH works. Lastly, UMExoLEA also successfully assisted participant motion seamlessly, synchronizing with the wearer's movement by more than 99% success rate.

8.2 Highlights of Contribution/Significance of Study

1. The study has provided fundamental knowledge on the biomechanical causation of injuries in lifting and carrying manual handling works; and the requisite for the development of effective EHPA.
2. The study has also provided a prototype exoskeleton for lower extremity augmentation called UMExoLEA for the benefit of workers in the Malaysian manual handling industries.
3. The prototype can serve as a useful workbench for further research and development of industrial EHPA interventions and can be used for long term prevention of lower extremity disabilities and repetitive strain/motion injuries such as knee/hip osteoarthritis, low back pain, and meniscal injury of the knee.

8.3 Recommendations for Future work

Based on findings from experimental verification and design challenges, the following recommendations can be made:

1. EHPAs should be designed with sufficient degrees of freedom similar to the human lower limbs to allow ease of movement for the wearer. The number of DOFs on the hip and ankle can be increased up to 3-DOFs or more to facilitate some other natural movements such as internal/external motion on the transverse plane for increased flexibilities. Furthermore, the design should be particularly lightweight or equipped with features that drives the weight of the exoskeleton to the ground without burdening the wearer. This should render the exoskeletons more appealing to workers, promoting their adoption in the industries.

2. Hardware or software (control) measures that can ensure stability on the coronal plane will improve functionality of the EHPA. Currently, stability is only considered on the sagittal plane.
3. Typically, frictional forces on the ground allow stability for walking. EHPA designs that modify the contact modality of the shoe and the ground also generally influence stability of the human-exoskeleton system for walking. Thus, for improved stability, EHPA designs should ensure sufficient contact and frictional surfaces of the wearer shoes with the ground.
4. For measurement of grip or ground contact forces, currently, *flexiforce* sensors (pressure resistor) have been demonstrated to show better performance compared to other off-the shelf sensors such as Tekscan Medical Sensor 9811 (matrix-types) and Quantum Tunneling Composite (QTC) pressure sensitive sensor in terms of drift, hysteresis and repeatability. However, these properties still significantly influence force measurement values for walking application since loading (stance) and unloading phase (swing) are typically short time giving less time for sensor values to normalize. Although, these limitations can be corrected by a right choice of algorithm as implemented in this study, if possible, better ground reaction force sensors can be sought in future work to simplify computation time.
5. Currently, the bag pack of UMExoLEA weigh 4kg. This can be reduced in future design to minimize the burden on the wearer.
6. The number of muscles monitored for myoelectric activity can be increased in future experimentation to enhance the results findings.

REFERENCES

Allen, K. D., Chen, J. C., Callahan, L. F., Golightly, Y. M., Helmick, C. G., Renner, J. B., & Jordan, J. M. (2010). Associations of occupational tasks with knee and hip osteoarthritis: the Johnston County Osteoarthritis Project. *Journal of Rheumatology, 37*(4), 842-850. doi:10.3899/jrheum.090302

Amin, S., Goggins, J., Niu, J., Guermazi, A., Grigoryan, M., Hunter, D. J., Genant, H. K., & Felson, D. T. (2008). Occupation-related squatting, kneeling, and heavy lifting and the knee joint: a magnetic resonance imaging-based study in men. *The Journal of rheumatology, 35*(8), 1645-1649.

Amin, S., Luepongsak, N., McGibbon, C. A., LaValley, M. P., Krebs, D. E., Felson, D. T. J. A. c., & research. (2004). Knee adduction moment and development of chronic knee pain in elders. *51*(3), 371-376.

Anam, K., & Al-Jumaily, A. A. (2012). Active exoskeleton control systems: State of the art. *Procedia Engineering, 41*, 988-994.

Andersen, J. H., Frost, P., Thomsen, J. F., Jensen, L. D., & Svendsen, S. W. (2014). 0255 Back Surgery in relation to occupational lifting. A cohort study based on the Musculoskeletal Research Database at the Danish Ramazzini Centre. *Occup Environ Med, 71*(Suppl 1), A33-A33.

Andersen, J. H., Haahr, J. P., & Frost, P. (2007). Risk factors for more severe regional musculoskeletal symptoms: A two-year prospective study of a general working population. *Arthritis & Rheumatism, 56*(4), 1355-1364.

Antwi-Afari, M. F., Li, H., Edwards, D. J., Parn, E. A., Seo, J., & Wong, A. Y. L. (2017). Biomechanical analysis of risk factors for work-related musculoskeletal disorders during repetitive lifting task in construction workers. *Automation in Construction, 83*, 41-47. doi:10.1016/j.autcon.2017.07.007

Arden, N., & Cooper, C. (2005). *Osteoarthritis handbook*: CRC Press.

Arezes, P., Carvalho, D., & Alves, A. C. (2010). *Threats and opportunities for workplace ergonomics in lean environments.* Paper presented at the 17th International Annual EurOMA Conference-Managing Operations in Service Economics.

Army Technology. (2018). Raytheon XOS 2 Exoskeleton, Second-Generation Robotics Suit. https://www.army-technology.com/projects/raytheon-xos-2-exoskeleton-us/

Babič, J., Omrčen, D., & Lenarčič, J. (2006). Balance and control of human inspired jumping robot. *Advances in Robot Kinematics*, 147-156.

Bainov, D. D., & Simeonov, P. S. (1989). Systems with impulse effect: stability, theory and applications.

Baker, B. (2012). France's slender Hercule exoskeleton is no lightweight. Retrieved from https://www.army-technology.com/features/featurefrench-hercule-robotic-exoskeleton/

Baker, P., Reading, I., Cooper, C., & Coggon, D. (2003). Knee disorders in the general population and their relation to occupation. *Occupational and Environmental Medicine, 60*(10), 794-797.

Banala, S. K., Kim, S. H., Agrawal, S. K., & Scholz, J. P. (2009). Robot assisted gait training with active leg exoskeleton (ALEX). *Ieee Transactions on Neural Systems and Rehabilitation Engineering, 17*(1), 2-8.

Bejjani, F., Gross, C., & Pugh, J. J. J. o. b. (1984). Model for static lifting: relationship of loads on the spine and the knee. *17*(4), 281-286.

Bennell, K. L., Bowles, K.-A., Wang, Y., Cicuttini, F., Davies-Tuck, M., & Hinman, R. S. J. A. o. t. r. d. (2011). Higher dynamic medial knee load predicts greater cartilage loss over 12 months in medial knee osteoarthritis. *70*(10), 1770-1774.

Bennell, K. L., Wrigley, T. V., Hunt, M. A., Lim, B. W., & Hinman, R. S. (2013). Update on the role of muscle in the genesis and management of knee osteoarthritis. *Rheum Dis Clin North Am, 39*(1), 145-176. doi:10.1016/j.rdc.2012.11.003

Bentley, J. R., Amonette, W. E., De Witt, J. K., Hagan, R. D. J. T. J. o. S., & Research, C. (2010). Effects of different lifting cadences on ground reaction forces during the squat exercise. *24*(5), 1414-1420.

Bern Hvid, S. H. B., Brauer, Møller, L., Koblauch, Thygesen, Thomsen, Simonsen, Alkjær, Helweg, L., & Mikkelsen. (2013). 338 The risk of musculoskeletal disorders in a cohort of Danish baggage handlers. *Occupational and Environmental Medicine, 70*. doi:http://dx.doi.org/10.1136/oemed-2013-101717.338

Bigos, S. J., Holland, J., Holland, C., Webster, J. S., Battie, M., & Malmgren, J. A. (2009). High-quality controlled trials on preventing episodes of back problems: systematic literature review in working-age adults. *Spine J, 9*(2), 147-168. doi:10.1016/j.spinee.2008.11.001

Bionics, E. (2015). Ekso Bionics. *IEEE Spectrum, 49*(1), 30-32.

Blalock, D., Miller, A., Tilley, M., Wang, J. J. C. M. I. A., & Disorders, M. (2015). Joint instability and osteoarthritis. *8*, CMAMD. S22147.

Bogue, R. (2015). Robotic exoskeletons: a review of recent progress. *Industrial Robot: An International Journal, 42*(1), 5-10.

Bongers, P. M., Kremer, A. M., & Laak, J. t. J. A. j. o. i. m. (2002). Are psychosocial factors, risk factors for symptoms and signs of the shoulder, elbow, or hand/wrist?: A review of the epidemiological literature. *41*(5), 315-342.

Bonitz, R. G., & Hsia, T. C. (1996). Internal force-based impedance control for cooperating manipulators. *Robotics and Automation, IEEE Transactions on, 12*(1), 78-89.

Bouffard, V., Nantel, J., Therrien, M., Vendittoli, P.-A., Lavigne, M., Prince, F. J. R. r., & practice. (2011). Center of mass compensation during gait in hip arthroplasty

patients: comparison between large diameter head total hip arthroplasty and hip resurfacing. *2011*.

Bouri, M., Stauffer, Y., Schmitt, C., Allemand, Y., Gnemmi, S., Clavel, R., Metrailler, P., & Brodard, R. (2006). *The WalkTrainer: a robotic system for walking rehabilitation.* Paper presented at the Robotics and Biomimetics, 2006. ROBIO'06. IEEE International Conference on.

Brown, S. (2013). Movie Tech: Panasonic Creates PowerLoader Exo Skeleton Just Like 'Aliens'. *Health*.

Bruchal, L. (1995). Occupational knee disorders: An overview. *Advances in industrial ergonomics and safety. 7th ed. London: Taylor & Francis*.

Buckle, P. W., & Devereux, J. J. J. A. e. (2002). The nature of work-related neck and upper limb musculoskeletal disorders. *33*(3), 207-217.

Buckwalter, J. A., Anderson, D. D., Brown, T. D., Tochigi, Y., & Martin, J. A. J. C. (2013). The roles of mechanical stresses in the pathogenesis of osteoarthritis: implications for treatment of joint injuries. *4*(4), 286-294.

Buesing, C., Fisch, G., O'Donnell, M., Shahidi, I., Thomas, L., Mummidisetty, C. K., Williams, K. J., Takahashi, H., Rymer, W. Z., & Jayaraman, A. (2015). Effects of a wearable exoskeleton stride management assist system (SMA®) on spatiotemporal gait characteristics in individuals after stroke: a randomized controlled trial. *Journal of Neuroengineering and Rehabilitation, 12*(1), 69.

Bupp, R. T., Bernstein, D. S., Chellaboina, V. S., Haddad, W. M. J. J. o. V., & Control. (2000). Resetting virtual absorbers for vibration control. *6*(1), 61-83.

Burdorf, A., Koppelaar, E., & Evanoff, B. (2013). Assessment of the impact of lifting device use on low back pain and musculoskeletal injury claims among nurses. *Occup Environ Med, 70*(7), 491-497. doi:10.1136/oemed-2012-101210

Bureau of Labor Statistics. (2016). Case and demographic characteristics for work-related injuries and illnesses involving days away from work. In: United States Department of Labor Washington, DC.

Cao, H., Ling, Z., Zhu, J., Wang, Y., & Wang, W. (2009). *Design frame of a leg exoskeleton for load-carrying augmentation.* Paper presented at the 2009 IEEE International Conference on Robotics and Biomimetics, ROBIO 2009.

Cao, H., Yin, Y. H., Du, D., Lin, L. Z., Gu, W. J., & Yang, Z. Y. (2006). Neural-network inverse dynamic online learning control on physical exoskeleton. *Neural Information Processing, Pt 3, Proceedings, 4234*, 702-710.

Cheung, Z., Feletto, M., Galante, J., Waters, T., Control, C. f. D., & Prevention. (2007). Ergonomic guidelines for manual material handling. In *NIOSH Publication*: NIOSH.

Chopp-Hurley, J. N., Brenneman, E. C., Wiebenga, E. G., Bulbrook, B., Keir, P. J., & Maly, M. R. (2017). Randomized Controlled Trial Investigating the Role of

Exercise in the Workplace to Improve Work Ability, Performance, and Patient-Reported Symptoms Among Older Workers With Osteoarthritis. *J Occup Environ Med, 59*(6), 550-556. doi:10.1097/JOM.0000000000001020

Chow, S.-C., Shao, J., Wang, H., & Lokhnygina, Y. (2017). *Sample size calculations in clinical research*: Chapman and Hall/CRC.

Clarkson, H. M. (2000). *Musculoskeletal assessment: joint range of motion and manual muscle strength*: Lippincott Williams & Wilkins.

Coenen, P., Gouttebarge, V., van der Burght, A. S., van Dieen, J. H., Frings-Dresen, M. H., van der Beek, A. J., & Burdorf, A. (2014). The effect of lifting during work on low back pain: a health impact assessment based on a meta-analysis. *Occup Environ Med, 71*(12), 871-877. doi:10.1136/oemed-2014-102346

Coenen, P., Kingma, I., Boot, C. R., Bongers, P. M., & van Dieen, J. H. (2014). Cumulative mechanical low-back load at work is a determinant of low-back pain. *Occup Environ Med, 71*(5), 332-337. doi:10.1136/oemed-2013-101862

Coenen, P., Kingma, I., Boot, C. R., Twisk, J. W., Bongers, P. M., & van Dieën, J. H. (2013). Cumulative Low Back Load at Work as a Risk Factor of Low Back Pain: A Prospective Cohort Study. *Journal of Occupational Rehabilitation, 23*(1), 11-18. doi:http://dx.doi.org/10.1007/s10926-012-9375-z

Coggon, D., Barker, D., & Rose, G. (2009). *Epidemiology for the Uninitiated*: John Wiley & Sons.

Curbano, R. J. P. (2018). *Development of ergonomic intervention in manual material handling to prevent work related musculoskeletal disorder.* Paper presented at the Proceedings of the International Conference on Industrial Engineering and Operations Management.

Dababneh, A. J., Swanson, N., & Shell, R. L. (2001). Impact of added rest breaks on the productivity and well being of workers. *Ergonomics, 44*(2), 164-174.

Dali, S., Justine, M., Ahmad, H., & Othman, Z. (2013). Comparison of ground reaction force during different angle of squatting.

Dawson, D. M., Abdallah, C. T., & Lewis, F. L. (2003). *Robot manipulator control: theory and practice*: CRC Press.

de Looze, M. P., Bosch, T., Krause, F., Stadler, K. S., & O'Sullivan, L. W. (2015). Exoskeletons for industrial application and their potential effects on physical work load. *Ergonomics*, 1-11.

de Looze, M. P., Bosch, T., Krause, F., Stadler, K. S., & O'Sullivan, L. W. (2016). Exoskeletons for industrial application and their potential effects on physical work load. *Ergonomics, 59*(5), 671-681.

Dennis, G., & Barrett, R. (2002). Spinal loads during individual and team lifting. *Ergonomics, 45*(10), 671-681.

Deros, B. M., Daruis, D. D., Ismail, A. R., & Rahim, A. R. (2010). Work posture and back pain evaluation in a Malaysian food manufacturing company. *American Journal of Applied Sciences, 7*(4), 473.

Descatha, A. M. D. P., Teysseyre, D. M. D., Cyr, D. P., Imbernon, E. M. D. P., Chastang, J.-F. P., Plenet, A. M., Bonenfant, S. M., Zins, M. M. D. P., Goldberg, M. M. D. P., Roquelaure, Y. M. D. P., & Leclerc, A. P. (2012). Long-term effects of biomechanical exposure on severe shoulder pain in the Gazel cohort. *Scandinavian journal of work, environment & health, 38*(6), 568-576.

Di Giulio, I., Maganaris, C. N., Baltzopoulos, V., & Loram, I. D. J. T. J. o. p. (2009). The proprioceptive and agonist roles of gastrocnemius, soleus and tibialis anterior muscles in maintaining human upright posture. *587*(10), 2399-2416.

Dissanayake, M. G., Newman, P., Clark, S., Durrant-Whyte, H. F., & Csorba, M. (2001). A solution to the simultaneous localization and map building (SLAM) problem. *IEEE TRANSACTIONS ON ROBOTICS AND AUTOMATION, 17*(3), 229-241.

Donnelly, D. V., Berg, W. P., Fiske, D. M. J. J. o. S., & Research, C. (2006). The effect of the direction of gaze on the kinematics of the squat exercise. *20*(1), 145.

Dulay, G. S., Cooper, C., & Dennison, E. M. (2015). Knee pain, knee injury, knee osteoarthritis & work. *Best Pract Res Clin Rheumatol, 29*(3), 454-461. doi:10.1016/j.berh.2015.05.005

Dutta, T., Holliday, P. J., Gorski, S. M., Baharvandy, M. S., & Fernie, G. R. (2012). A biomechanical assessment of floor and overhead lifts using one or two caregivers for patient transfers. *Applied Ergonomics, 43*(3), 521-531. doi:10.1016/j.apergo.2011.08.006

Eriksen, W., Bruusgaard, D., & Knardahl, S. (2004). Work factors as predictors of intense or disabling low back pain; a prospective study of nurses' aides. *Occupational and Environmental Medicine, 61*(5), 398-404.

Escamilla, R. F. (2001). Knee biomechanics of the dynamic squat exercise. *Medicine & Science in Sports & Exercise, 33*(1), 127-141.

Escamilla, R. F., Fleisig, G. S., Lowry, T. M., Barrentine, S. W., Andrews, J. R. J. M., sports, s. i., & exercise. (2001). A three-dimensional biomechanical analysis of the squat during varying stance widths. *33*(6), 984-998.

Escamilla, R. F. J. M., Sports, S. i., & Exercise. (2001). Knee biomechanics of the dynamic squat exercise. *33*(1), 127-141.

Esquirol, Y., Niezborala, M., Visentin, M., Leguevel, A., Gonzalez, I., & Marquié, J.-C. (2017). Contribution of occupational factors to the incidence and persistence of chronic low back pain among workers: results from the longitudinal VISAT study. *Occupational and Environmental Medicine, 74*(4), 243. doi:http://dx.doi.org/10.1136/oemed-2015-103443

Ferguson-Pell, M., Hagisawa, S., Bain, D. J. M. e., & physics. (2000). Evaluation of a sensor for low interface pressure applications. *22*(9), 657-663.

Feveile, H., Jensen, C., & Burr, H. (2002). Risk factors for neck-shoulder and wrist-hand symptoms in a 5-year follow-up study of 3,990 employees in Denmark. *International Archives of Occupational and Environmental Health, 75*(4), 243-251.

Fick, B., & Makinson, J. (1971). Final report on Hardiman I prototype for machine augmentation of human strength and endurance. *United States Army Project No. IM62410105072, General Electr. Co., New York, DTIC Accession Number: AD0739735*.

Filiz, M., Cakmak, A., & Ozcan, E. (2005). The effectiveness of exercise programmes after lumbar disc surgery: a randomized controlled study. *Clin Rehabil, 19*(1), 4-11. doi:10.1191/0269215505cr836oa

Foege, W., Baker, S., & Davis, J. (1985). Injury biomechanics research and the prevention of impact injury. In *Injury in America* (pp. 48-64): National Academy Press, Washington, DC.

Fontana, M., Vertechy, R., Marcheschi, S., Salsedo, F., & Bergamasco, M. (2014). The body extender: A full-body exoskeleton for the transport and handling of heavy loads. *Ieee Robotics & Automation Magazine, 21*(4), 34-44.

Galle, S., Malcolm, P., Derave, W., & De Clercq, D. (2013). Adaptation to walking with an exoskeleton that assists ankle extension. *Gait & Posture, 38*(3), 495-499. doi:https://doi.org/10.1016/j.gaitpost.2013.01.029

Gams, A., Nemec, B., Ijspeert, A. J., & Ude, A. (2014). Coupling Movement Primitives: Interaction With the Environment and Bimanual Tasks. *Ieee Transactions on Robotics, 30*(4), 816-830. doi:10.1109/tro.2014.2304775

Garg, A., Kapellusch, J., & Hegmann, K. (2017). 0097 Risk factors for occupational low back pain (lbp), medicine use, and seeking care for lbp: results from a prospective cohort study. *Occupational and Environmental Medicine, 74*. doi:http://dx.doi.org/10.1136/oemed-2017-104636.73

Gatchel, R. J., Kishino, N. D., & Strizak, A. M. (2014). Occupational musculoskeletal pain and disability disorders: An overview. In *Handbook of Musculoskeletal Pain and Disability Disorders in the Workplace* (pp. 3-17): Springer.

Genaidy, A., Delgado, E., & Bustos, T. (1995). Active microbreak effects on musculoskeletal comfort ratings in meatpacking plants. *Ergonomics, 38*(2), 326-336.

Ghan, J., Steger, R., & Kazerooni, H. (2006). Control and system identification for the Berkeley lower extremity exoskeleton (BLEEX). *Advanced Robotics, 20*(9), 989-1014. doi:10.1163/156855306778394012

Goebel, R., Sanfelice, R. G., & Teel, A. R. J. I. C. S. M. (2009). Hybrid dynamical systems. *29*(2), 28-93.

Goldblatt, J. P., & Richmond, J. C. J. O. T. i. S. M. (2003). Anatomy and biomechanics of the knee. *11*(3), 172-186.

Graham, R. B., & Brown, S. H. J. J. o. b. (2012). A direct comparison of spine rotational stiffness and dynamic spine stability during repetitive lifting tasks. *45*(9), 1593-1600.

Grewal, M. S., & Andrews, A. P. (2010). Applications of Kalman filtering in aerospace 1960 to the present [historical perspectives]. *IEEE Control Systems, 30*(3), 69-78.

Grüneberg, P., Kadone, H., Kuramoto, N., Ueno, T., Hada, Y., Yamazaki, M., Sankai, Y., & Suzuki, K. (2018). Robot-assisted voluntary initiation reduces control-related difficulties of initiating joint movement: A phenomenal questionnaire study on shaping and compensation of forward gait. *Plos One, 13*(3), e0194214.

Gueorguieva, R., & Krystal, J. H. J. A. o. g. p. (2004). Move over anova: progress in analyzing repeated-measures data andits reflection in papers published in the archives of general psychiatry. *61*(3), 310-317.

Gui, L., Yang, Z., Yang, X., Gu, W., & Zhang, Y. (2007). *Design and control technique research of exoskeleton suit.* Paper presented at the Automation and Logistics, 2007 IEEE International Conference on.

Guo, Q., & Jiang, D. (2015). Method for Walking Gait Identification in a Lower Extremity Exoskeleton based on C4.5 Decision Tree Algorithm. *International Journal of Advanced Robotic Systems, 12*, 11. doi:10.5772/60132

Guthrie, P. F., Westphal, L., Dahlman, B., Berg, M., Behnam, K., & Ferrell, D. (2004). A patient lifting intervention for preventing the work-related injuries of nurses. *Work, 22*(2), 79-88.

Haddad, W. M., Chellaboina, V., & Nersesov, S. G. (2014). *Impulsive and hybrid dynamical systems: stability, dissipativity, and control* (Vol. 49): Princeton University Press.

Han, Y. L., Wang, X. S., & Ieee. (2010). Biomechanics study of Human lower limb walking: implication for design of power-assisted robot. In *Ieee/Rsj 2010 International Conference on Intelligent Robots and Systems* (pp. 3398-3403). New York: Ieee.

Harkness, E., MacFarlane, G. J., Nahit, E., Silman, A., & McBeth, J. (2003). Risk factors for new-onset low back pain amongst cohorts of newly employed workers. *Rheumatology, 42*(8), 959-968.

Harris, E. C., & Coggon, D. (2015). HIP osteoarthritis and work. *Best Practice & Research Clinical Rheumatology, 29*(3), 462-482. doi:http://dx.doi.org/10.1016/j.berh.2015.04.015

Hartvigsen, J., Lauritzen, S., Lings, S., & Lauritzen, T. (2005). Intensive education combined with low tech ergonomic intervention does not prevent low back pain in nurses. *Occupational and Environmental Medicine, 62*(1), 13-17.

Hattin, H. C., Pierrynowski, M. R., Ball, K. A. J. M., sports, s. i., & exercise. (1989). Effect of load, cadence, and fatigue on tibio-femoral joint force during a half squat. *21*(5), 613-618.

Hayashi, T., Kawamoto, H., & Sankai, Y. (2005). *Control method of robot suit HAL working as operator's muscle using biological and dynamical information.* Paper presented at the Intelligent Robots and Systems, 2005.(IROS 2005). 2005 IEEE/RSJ International Conference on.

Haykin, S. S. (2001). *Kalman filtering and neural networks*: Wiley Online Library.

Health and Safety Executive. (2017). Health and safety at work: Summary statistics for Great Britain 2017.

Health Council of the Netherlands. (2012). *Manual lifting during work*. In Vol. 2012/36E. *The Hague: Health Council of the Netherlands*.

Hemmerich, A., Brown, H., Smith, S., Marthandam, S., & Wyss, U. J. J. o. o. r. (2006). Hip, knee, and ankle kinematics of high range of motion activities of daily living. *24*(4), 770-781.

Henning, R. A., Jacques, P., Kissel, G. V., Sullivan, A. B., & Alteras-Webb, S. M. (1997). Frequent short rest breaks from computer work: effects on productivity and well-being at two field sites. *Ergonomics, 40*(1), 78-91.

Herquelot, E., Bodin, J., Petit, A., Ha, C., Leclerc, A., Goldberg, M., Zins, M., Roquelaure, Y., & Descatha, A. (2015). Incidence of Chronic and Other Knee Pain in Relation to Occupational Risk Factors in a Large Working Population. *Ann Occup Hyg, 59*(6), 797-811. doi:10.1093/annhyg/mev010

Heuch, I., Heuch, I., Hagen, K., & John-Anker, Z. (2017). Physical activity level at work and risk of chronic low back pain: A follow-up in the Nord-Trøndelag Health Study. *Plos One, 12*(4). doi:http://dx.doi.org/10.1371/journal.pone.0175086

Hoogendoorn, W., Bongers, P., De Vet, H., Ariens, G., Van Mechelen, W., & Bouter, L. (2002). High physical work load and low job satisfaction increase the risk of sickness absence due to low back pain: results of a prospective cohort study. *Occupational and Environmental Medicine, 59*(5), 323-328.

Hoogendoorn, W. E., Bongers, P. M., de Vet, H. C., Douwes, M., Koes, B. W., Miedema, M. C., Ariëns, G. A., & Bouter, L. M. (2000). Flexion and rotation of the trunk and lifting at work are risk factors for low back pain: results of a prospective cohort study. *Spine, 25*(23), 3087-3092.

Hopcroft, J. E., Motwani, R., & Ullman, J. D. J. A. S. N. (2001). Introduction to automata theory, languages, and computation. *32*(1), 60-65.

Huang, L. H., Steger, J. R., Kazerooni, H., & Asme. (2005). *Hybrid control of the berkeley lower extremity exoskeleton (BLEEX)*. New York: Amer Soc Mechanical Engineers.

Huang, R., Cheng, H., Chen, Q., Tran, H. T., & Lin, X. (2015, Sept. 28 2015-Oct. 2 2015). *Interactive learning for sensitivity factors of a human-powered augmentation lower exoskeleton.* Paper presented at the 2015 Ieee/Rsj International Conference on Intelligent Robots and Systems (Iros).

Huang, R., Cheng, H., Guo, H., Lin, X., Chen, Q., & Sun, F. (2016, 9-14 Oct. 2016). *Learning Cooperative Primitives with physical Human-Robot Interaction for a HUman-powered Lower EXoskeleton.* Paper presented at the 2016 IEEE/RSJ International Conference on Intelligent Robots and Systems (IROS).

Huang, R., Cheng, H., Guo, H., Lin, X., & Zhang, J. J. I. S. (2018). Hierarchical learning control with physical human-exoskeleton interaction. *432*, 584-595.

Huang, R., Cheng, H., Guo, H. L., Chen, Q. M., & Lin, X. C. (2016). Hierarchical Interactive Learning for a Human-Powered Augmentation Lower Exoskeleton. In A. Okamura, A. Menciassi, A. Ude, D. Burschka, D. Lee, F. Arrichiello, H. Liu, H. Moon, J. Neira, K. Sycara, K. Yokoi, P. Martinet, P. Oh, P. Valdastri, & V. Krovi (Eds.), *2016 Ieee International Conference on Robotics and Automation* (pp. 257-263). New York: Ieee.

Hung, Y.-j., Gross, M. T. J. J. o. O., & Therapy, S. P. (1999). Effect of foot position on electromyographic activity of the vastus medialis oblique and vastus lateralis during lower-extremity weight-bearing activities. *29*(2), 93-105.

Huo, W. G., Mohammed, S., Amirat, Y., & Kong, K. (2016). Active Impedance Control of a Lower Limb Exoskeleton to Assist Sit-to-Stand Movement. In A. Okamura, A. Menciassi, A. Ude, D. Burschka, D. Lee, F. Arrichiello, H. Liu, H. Moon, J. Neira, K. Sycara, K. Yokoi, P. Martinet, P. Oh, P. Valdastri, & V. Krovi (Eds.), *2016 Ieee International Conference on Robotics and Automation* (pp. 3530-3536). New York: Ieee.

Ijspeert, A. J., Nakanishi, J., Hoffmann, H., Pastor, P., & Schaal, S. (2013). Dynamical movement primitives: learning attractor models for motor behaviors. *Neural computation, 25*(2), 328-373.

Ijspeert, A. J., Nakanishi, J., & Schaal, S. (2002). *Movement imitation with nonlinear dynamical systems in humanoid robots.* Paper presented at the Robotics and Automation, 2002. Proceedings. ICRA'02. IEEE International Conference on.

ISO 11228-1. (2003). Ergonomics–Manual handling–Part 1: Lifting and carrying. In: ISO Geneva.

Jakobsen, M. D., Sundstrup, E., Brandt, M., Jay, K., Aagaard, P., & Andersen, L. L. (2015). Physical exercise at the workplace prevents deterioration of work ability among healthcare workers: cluster randomized controlled trial. *BMC Public Health, 15*, 1174. doi:10.1186/s12889-015-2448-0

Jansen, J., Morgenstern, H., & Burdorf, A. (2004). Dose-response relations between occupational exposures to physical and psychosocial factors and the risk of low back pain. *Occupational and Environmental Medicine, 61*(12), 972-979.

Jensen, J. C., Haahr, J. P., Frost, P., & Andersen, J. H. (2013). Do work-related factors affect care-seeking in general practice for back pain or upper extremity pain? *International Archives of Occupational and Environmental Health, 86*(7), 799-808. doi:http://dx.doi.org/10.1007/s00420-012-0815-z

Jensen, L. D., Gonge, H., Jørs, E., Ryom, P., Foldspang, A., Christensen, M., Vesterdorf, A., & Bonde, J. P. (2006). Prevention of low back pain in female eldercare workers: randomized controlled work site trial. *Spine, 31*(16), 1761-1769.

Jezernik, S., Colombo, G., Keller, T., Frueh, H., & Morari, M. (2003). Robotic orthosis lokomat: A rehabilitation and research tool. *Neuromodulation: Technology at the neural interface, 6*(2), 108-115.

Jones, B., & Kenward, M. G. (2014). *Design and analysis of cross-over trials*: Chapman and Hall/CRC.

Jones, G. T., Harkness, E. F., Nahit, E. S., McBeth, J., Silman, A. J., & Macfarlane, G. J. (2007). Predicting the onset of knee pain: results from a 2-year prospective study of new workers. *Annals of the rheumatic diseases, 66*(3), 400. doi:http://dx.doi.org/10.1136/ard.2006.057570

Kadota, K., Akai, M., Kawashima, K., & Kagawa, T. (2009). *Development of Power-Assist Robot Arm using pneumatic rubbermuscles with a balloon sensor.* Paper presented at the Robot and Human Interactive Communication, 2009. RO-MAN 2009. The 18th IEEE International Symposium on.

Kamali, K., Akbari, A. A., & Akbarzadeh, A. (2016). Trajectory generation and control of a knee exoskeleton based on dynamic movement primitives for sit-to-stand assistance. *Advanced Robotics, 30*(13), 846-860. doi:10.1080/01691864.2016.1154800

Kawamoto, H., Lee, S., Kanbe, S., & Sankai, Y. (2003). *Power assist method for HAL-3 using EMG-based feedback controller.* Paper presented at the Systems, Man and Cybernetics, 2003. IEEE International Conference on.

Kazerooni, H. (2006). The Berkeley Lower Extremity Exoskeleton. In P. Corke & S. Sukkarieh (Eds.), *Field and Service Robotics* (Vol. 25, pp. 9-15). Berlin: Springer-Verlag Berlin.

Kazerooni, H., Racine, J.-L., Huang, L., & Steger, R. (2005). *On the control of the berkeley lower extremity exoskeleton (BLEEX).* Paper presented at the Proceedings of the 2005 IEEE International Conference on Robotics and Automation.

Kazerooni, H., Racine, J. L., Huang, L. H., & Steger, R. (2005). On the control of the Berkeley Lower Extremity Exoskeleton (BLEEX). In *2005 IEEE International Conference on Robotics and Automation* (pp. 4353-4360). New York: Ieee.

Khalil, H. K., & Grizzle, J. (1996). *Nonlinear systems* (Vol. 3): Prentice hall New Jersey.

Kiguchi, K., Iwami, K., Saza, T., Kariya, S., Watanabe, K., Izumi, K., & Fukuda, T. (2001). *A study of an exoskeletal robot for human shoulder motion support.* Paper presented at the Intelligent Robots and Systems, 2001. Proceedings. 2001 IEEE/RSJ International Conference on.

Kim, H., June Shin, Y., & Kim, J. (2017). Design and locomotion control of a hydraulic lower extremity exoskeleton for mobility augmentation. *Mechatronics, 46*, 32-45. doi:10.1016/j.mechatronics.2017.06.009

Kim, W.-s., Lee, S.-h., Lee, H.-d., Yu, S.-n., Han, J.-s., & Han, C.-s. (2009). *Development of the heavy load transferring task oriented exoskeleton adapted by lower extremity using qausi-active joints.* Paper presented at the ICCAS-SICE, 2009.

Kim, W., Lee, H., Lim, D., Han, C.-S., & Han, J. (2013). Development of a lower extremity exoskeleton system for walking assistance while load carrying. In *Nature-Inspired Mobile Robotics* (pp. 35-42): World Scientific.

Kimura, H., Tsuchiya, K., Ishiguro, A., & Witt, H. (2006). *Adaptive motion of animals and machines*: Springer Science & Business Media.

Kirkwood, R. N., Gomes, H. d. A., Sampaio, R. F., Culham, E., & Costigan, P. (2007). Biomechanical analysis of hip and knee joints during gait in elderly subjects. *Acta Ortopédica Brasileira, 15*(5), 267-271.

Ko, H. K., Lee, S. W., Koo, D. H., Lee, I., & Hyun, D. J. (2018). Waist-assistive exoskeleton powered by a singular actuation mechanism for prevention of back-injury. *Robotics and Autonomous Systems, 107*, 1-9. doi:10.1016/j.robot.2018.05.008

Kobayashi, H., Aida, T., & Hashimoto, T. J. I. J. o. A. T. (2009). Muscle suit development and factory application. *3*(6), 709-715.

Komi, E. R., Roberts, J. R., & Rothberg, S. J. P. o. t. I. o. M. E., Part C: Journal of Mechanical Engineering Science. (2007). Evaluation of thin, flexible sensors for time-resolved grip force measurement. *221*(12), 1687-1699.

Lau, E., Cooper, C., Lam, D., Chan, V., Tsang, K., & Sham, A. (2000). Factors associated with osteoarthritis of the hip and knee in Hong Kong Chinese: obesity, joint injury, and occupational activities. *American journal of epidemiology, 152*(9), 855-862.

Lee, H., Lee, B., Kim, W., Gil, M., Han, J., Han, C. J. I. J. o. P. E., & Manufacturing. (2012). Human-robot cooperative control based on pHRI (Physical Human-Robot Interaction) of exoskeleton robot for a human upper extremity. *13*(6), 985-992.

Lefebvre*, T., Bruyninckx, H., & De Schutter, J. (2004). Kalman filters for non-linear systems: a comparison of performance. *International Journal of Control, 77*(7), 639-653.

Lenzi, T., Carrozza, M. C., & Agrawal, S. K. (2013). Powered hip exoskeletons can reduce the user's hip and ankle muscle activations during walking. *Ieee Transactions on Neural Systems and Rehabilitation Engineering, 21*(6), 938-948.

Li, C.-S., & Davis, C. (2016). Design and analysis of crossover trials. In.

Li, G., Most, E., DeFrate, L., Suggs, J., Gill, T., & Rubash, H. J. J. o. b. (2004). Effect of the posterior cruciate ligament on posterior stability of the knee in high flexion. *37*(5), 779-783.

Li, Y. D., & Hsiao-Wecksler, E. T. (2013). *Gait mode recognition and control for a portable-powered ankle-foot orthosis.* Paper presented at the Rehabilitation robotics (ICORR), 2013 IEEE international conference on.

Li, Z. Q., Xie, H. X., Li, W. L., & Yao, Z. (2014). Proceeding of Human Exoskeleton Technology and Discussions on Future Research. *Chinese Journal of Mechanical Engineering, 27*(3), 437-447. doi:10.3901/Cjme.2014.03.437

Lim, T., & Ding, L. (2000). Distribution of body weight, height and body mass index in a national sample of Malaysian adults. *Medical Journal of Malaysia, 55*(1), 108-128.

Liu, X., & Low, K. (2004). *Development and preliminary study of the NTU lower extremity exoskeleton.* Paper presented at the Cybernetics and Intelligent Systems, 2004 IEEE Conference on.

Lotz, J. C., Colliou, O. K., Chin, J. R., Duncan, N. A., & Liebenberg, E. J. S. (1998). Compression-induced degeneration of the intervertebral disc: an in vivo mouse model and finite-element study. *23*(23), 2493-2506.

Low, K., Liu, X., Goh, C., Yu, H. J. J. o. V., & Control. (2006). Locomotive control of a wearable lower exoskeleton for walking enhancement. *12*(12), 1311-1336.

Macfarlane, G. J., Thomas, E., Papageorgiou, A. C., Croft, P. R., Jayson, M. I., & Silman, A. J. (1997). Employment and physical work activities as predictors of future low back pain. *Spine, 22*(10), 1143-1149.

Man, G., Mologhianu, G. J. J. o. m., & life. (2014). Osteoarthritis pathogenesis–a complex process that involves the entire joint. *7*(1), 37.

Manchikanti, L. (2000). Epidemiology of low back pain. *Pain physician, 3*(2), 167-192.

Marder, E. (2000). Motor pattern generation. *Current opinion in neurobiology, 10*(6), 691-698.

Marras, W., Davis, K., Kirking, B., & Granata, K. (1999). Spine loading and trunk kinematics during team lifting. *Ergonomics, 42*(10), 1258-1273.

Marras, W. J. E. (2000). Occupational low back disorder causation and control. *43*(7), 880-902.

Martinez, F., Retolaza, I., Pujana-Arrese, A., Cenitagoya, A., Basurko, J., & Landaluze, J. (2008). *Design of a five actuated DoF upper limb exoskeleton oriented to workplace help.* Paper presented at the Biomedical Robotics and Biomechatronics, 2008. BioRob 2008. 2nd IEEE RAS & EMBS International Conference on.

Matsubara, T., Uchikata, A., Morimoto, J., Ieee, & Robotics Society of, J. (2012). Full-body Exoskeleton Robot Control for Walking Assistance by Style-phase Adaptive Pattern Generation. In *2012 Ieee/Rsj International Conference on Intelligent Robots and Systems* (pp. 3914-3920). New York: Ieee.

Matute, A., Paredes-Madrid, L., Gutierrez, E., & Vargas, C. A. P. (2017). *Characterization of drift and hysteresis errors in force sensing resistors considering their piezocapacitive effect.* Paper presented at the 2017 IEEE SENSORS.

Mayer, J., Kraus, T., Ochsmann, E. J. I. a. o. o., & health, e. (2012). Longitudinal evidence for the association between work-related physical exposures and neck and/or shoulder complaints: a systematic review. *85*(6), 587-603.

McGill, S. M. (2015). *Low Back Disorders, 3E*: Human Kinetics.

McWilliams, D., Leeb, B., Muthuri, S., Doherty, M., & Zhang, W. (2011). Occupational risk factors for osteoarthritis of the knee: a meta-analysis. *Osteoarthritis and cartilage, 19*(7), 829-839.

Mehta, J. P., Lavender, S. A., & Jagacinski, R. J. J. E. (2014). Physiological and biomechanical responses to a prolonged repetitive asymmetric lifting activity. *57*(4), 575-588.

Michelle, A., Dressner, & Samuel, K. P. (2018). Occupational injuries and illnesses among registered nurses. *Monthly Labor Review*. doi:https://doi.org/10.21916/mlr.2018.27.

Mikkelsen, S., Brauer, C., Ellen Bøtker, P., Alkjær, T., Koblauch, H., Erik Bruun, S., Helweg-Larsen, K., & Lau Caspar, T. (2016). A Cohort Study on Meniscal Lesions among Airport Baggage Handlers. *Plos One, 11*(6). doi:http://dx.doi.org/10.1371/journal.pone.0157336

Miranda, H., Punnett, L., Viikari-Juntura, E., Heliovaara, M., & Knekt, P. (2008). Physical work and chronic shoulder disorder. Results of a prospective population-based study. *Ann Rheum Dis, 67*(2), 218-223. doi:10.1136/ard.2007.069419

Miranda, H., Viikari-Juntura, E., Punnett, L., & Riihimäki, H. (2008). Occupational loading, health behavior and sleep disturbance as predictors of low-back pain. *Scandinavian journal of work, environment & health*, 411-419.

Miyazaki, T., Wada, M., Kawahara, H., Sato, M., Baba, H., & Shimada, S. J. A. o. t. r. d. (2002). Dynamic load at baseline can predict radiographic disease progression in medial compartment knee osteoarthritis. *61*(7), 617-622.

Nagura, T., Dyrby, C. O., Alexander, E. J., & Andriacchi, T. P. J. J. o. O. R. (2002). Mechanical loads at the knee joint during deep flexion. *20*(4), 881-886.

Nelson, A. T. (2000). Nonlinear estimation and modeling of noisy time-series by dual Kalman filtering methods.

Neumann, D. A. J. j. o. o., & therapy, s. p. (2010). Kinesiology of the hip: a focus on muscular actions. *40*(2), 82-94.

Nisell, R. (1986). Joint load during the parallel squat in powerlifting and forces analysis of in vivo bilateral quadriceps tendon rupture. *Scand J. Sports Sci, 8*, 63-70.

Nunes, I. L., & Bush, P. M. (2012). Work-related musculoskeletal disorders assessment and prevention. In *Ergonomics-A Systems Approach*: InTech.

Nuwayhid, I. A., Stewart, W., & Johnson, J. V. (1993). Work activities and the onset of first-time low back pain among New York City fire fighters. *American journal of epidemiology, 137*(5), 539-548.

Ogata, Y., Anan, M., Takahashi, M., Takeda, T., Tanimoto, K., Sawada, T., Shinkoda, K. J. J. o. m., & therapeutics, p. (2018). Relationships Between Trunk Movement Patterns During Lifting Tasks Compared With Unloaded Extension From a Flexed Posture. *41*(3), 189-198.

Oskoei, M. A., Hu, H. J. B. S. P., & Control. (2007). Myoelectric control systems—A survey. *2*(4), 275-294.

Pavlovic-Veselinovic, S., Hedge, A., & Veselinovic, M. (2016). An ergonomic expert system for risk assessment of work-related musculo-skeletal disorders. *International Journal of Industrial Ergonomics, 53*, 130-139.

Pedersen, E. B., Thygesen, L. C., Brauer, C., Møller, K. L., Alkjær, T., Baldvinsson, H. K., Simonsen, E., & Mikkelsen, S. (2016). P200 Knee osteoarthrosis among baggage handlers: an observational cohort study. *Occupational and Environmental Medicine, 73*. doi:http://dx.doi.org/10.1136/oemed-2016-103951.516

Perry, J., & Davids, J. R. J. J. o. P. O. (1992). Gait analysis: normal and pathological function. *12*(6), 815.

Petric, T., Gams, A., Debevec, T., Zlajpah, L., & Babic, J. (2013). Control approaches for robotic knee exoskeleton and their effects on human motion. *Advanced Robotics, 27*(13), 993-1002. doi:10.1080/01691864.2013.804164

Piantadosi, S. (2017). *Clinical trials: a methodologic perspective*: John Wiley & Sons.

Pope, D., Hunt, I., Birrell, F., Silman, A., & MacFarlane, G. J. (2003). Hip pain onset in relation to cumulative workplace and leisure time mechanical load: a population based case-control study. *Annals of the rheumatic diseases, 62*(4), 322-326.

Pope, D. P., Croft, P. R., Pritchard, C. M., Silman, A. J., & Macfarlane, G. J. (1997). Occupational factors related to shoulder pain and disability. *Occupational and Environmental Medicine, 54*(5), 316. doi:http://dx.doi.org/10.1136/oem.54.5.316

Potvin, J., McGill, S., & Norman, R. (1991). Trunk muscle and lumbar ligament contributions to dynamic lifts with varying degrees of trunk flexion. *Spine, 16*(9), 1099-1107.

Pratt, J. E., Krupp, B. T., Morse, C. J., & Collins, S. H. (2004). The RoboKnee: An exoskeleton for enhancing strength and endurance during walking. *2004 Ieee International Conference on Robotics and Automation, Vols 1- 5, Proceedings*, 2430-2435. doi:Doi 10.1109/Robot.2004.1307425

Pratt, J. E., Krupp, B. T., Morse, C. J., & Collins, S. H. (2004). *The RoboKnee: an exoskeleton for enhancing strength and endurance during walking.* Paper presented at the Robotics and Automation, 2004. Proceedings. ICRA'04. 2004 IEEE International Conference on.

Qu, Z., Dorsey, J. F., Zhang, X., Dawson, D. M. J. S., & letters, c. (1991). Robust control of robots by the computed torque law. *16*(1), 25-32.

Racine, J.-L. C. (2003). Control of a lower extremity exoskeleton for human performance amplification.

Radwin, R. G., Marras, W. S., & Lavender, S. A. J. T. I. i. E. S. (2001). Biomechanical aspects of work-related musculoskeletal disorders. *2*(2), 153-217.

Reid, C. R., Bush, P. M., Cummings, N. H., McMullin, D. L., & Durrani, S. K. (2010). A review of occupational knee disorders. *Journal of Occupational Rehabilitation, 20*(4), 489-501.

Righetti, L., Buchli, J., & Ijspeert, A. J. (2006). Dynamic Hebbian learning in adaptive frequency oscillators. *Physica D: Nonlinear Phenomena, 216*(2), 269-281. doi:10.1016/j.physd.2006.02.009

Ronsse, R., De Rossi, S. M. M., Vitiello, N., Lenzi, T., Koopman, B., van der Kooij, H., Carrozza, M. C., & Ijspeert, A. J. (2012). *Real-time estimate of period derivatives using adaptive oscillators: Application to impedance-based walking assistance.* Paper presented at the Intelligent Robots and Systems (IROS), 2012 IEEE/RSJ International Conference on.

Ronsse, R., Koopman, B., Vitiello, N., Lenzi, T., De Rossi, S. M. M., van den Kieboom, J., Van Asseldonk, E., Carrozza, M. C., van der Kooij, H., & Ijspeert, A. J. (2011). *Oscillator-based walking assistance: A model-free approach.* Paper presented at the Rehabilitation Robotics (ICORR), 2011 IEEE International Conference on.

Ronsse, R., Lenzi, T., Vitiello, N., Koopman, B., van Asseldonk, E., De Rossi, S. M. M., van den Kieboom, J., van der Kooij, H., Carrozza, M. C., & Ijspeert, A. J. (2011). Oscillator-based assistance of cyclical movements: model-based and model-free approaches. *Medical & Biological Engineering & Computing, 49*(10), 1173.

Rose, J. (1994). Human walking.

Rubinstein, R. Y., & Kroese, D. P. (2016). *Simulation and the Monte Carlo method* (Vol. 10): John Wiley & Sons.

Runhaar, J., & Zhang, Y. (2018). Can we prevent OA? Epidemiology and public health insights and implications. *Rheumatology (Oxford), 57*(suppl_4), iv3-iv9. doi:10.1093/rheumatology/key014

Russon, M.-A. (2016). Panasonic Assist Suit: Robot exoskeleton aids factory workers, nurses and care workers. Retrieved from https://www.ibtimes.co.uk/panasonic-assist-suit-robot-exoskeleton-aids-factory-workers-nurses-care-workers-1550399

Ryder, M. C., Sup, F., & Ieee. (2013). Leveraging Gait Dynamics to Improve Efficiency and Performance of Powered Hip Exoskeletons. In *2013 Ieee 13th International Conference on Rehabilitation Robotics*. New York: Ieee.

Ryu, H. T., Choi, J. Y., Yi, B.-J., Lee, J., Kim, D. J., & Ko, J. (2012). *Human-robot integrated model of upper-extremity.* Paper presented at the Ubiquitous Robots and Ambient Intelligence (URAI), 2012 9th International Conference on.

Samani, A., Holtermann, A., Søgaard, K., Holtermann, A., & Madeleine, P. (2012). Following ergonomics guidelines decreases physical and cardiovascular workload during cleaning tasks. *Ergonomics, 55*(3), 295-307.

Sankai, Y. (2010). HAL: Hybrid assistive limb based on cybernics. In *Robotics Research* (pp. 25-34): Springer.

Sasaki, M., Horio, A., Wakasa, M., Uemura, S., & Osawa, Y. (2008). Influence of quadriceps femoris fatigue on low back load during lifting of loads at different distances from the toes. *Journal of Physical Therapy Science, 20*(2), 81-89.

Sawicki, G. S., & Ferris, D. P. (2008). Mechanics and energetics of level walking with powered ankle exoskeletons. *Journal of Experimental Biology, 211*(9), 1402-1413.

Schneider, E., Irastorza, X. B., & Copsey, S. (2010). *OSH in figures: Work-related musculoskeletal disorders in the EU-Facts and figures*: Office for Official Publications of the European Communities.

Schoenfeld, B. J. (2010). Squatting kinematics and kinetics and their application to exercise performance. *The Journal of Strength & Conditioning Research, 24*(12), 3497-3506.

Seidler, A., Bolm-Audorff, U., Abolmaali, N., & Elsner, G. (2008). The role of cumulative physical work load in symptomatic knee osteoarthritis–a case-control study in Germany. *Journal of Occupational Medicine and Toxicology, 3*(1), 14.

Seidler, A., Bolm-Audorff, U., Siol, T., Henkel, N., Fuchs, C., Schug, H., Leheta, F., Marquardt, G., Schmitt, E., Ulrich, P. T., Beck, W., Missalla, A., & Elsner, G. (2003). Occupational risk factors for symptomatic lumbar disc herniation; a case-control study. *Occupational and Environmental Medicine, 60*(11), 821. doi:http://dx.doi.org/10.1136/oem.60.11.821

Selverston, A. I. (1980). Are central pattern generators understandable? *Behavioral and Brain Sciences, 3*(4), 535-540.

Senn, S. S., & Senn, S. (2002). *Cross-over trials in clinical research* (Vol. 5): John Wiley & Sons.

Sharma, L., Hurwitz, D. E., Thonar, E. J. M., Sum, J. A., Lenz, M. E., Dunlop, D. D., Schnitzer, T. J., Kirwan-Mellis, G., Andriacchi, T. P. J. A., & Rheumatism. (1998). Knee adduction moment, serum hyaluronan level, and disease severity in medial tibiofemoral osteoarthritis. *41*(7), 1233-1240.

Shelburne, K. B., Torry, M. R., & Pandy, M. G. J. J. o. o. r. (2006). Contributions of muscles, ligaments, and the ground-reaction force to tibiofemoral joint loading during normal gait. *24*(10), 1983-1990.

Signorile, J. F., Kwiatkowski, K., Caruso, J. F., Robertson, B. J. T. J. o. S., & Research, C. (1995). Effect of foot position on the electromyographical activity of the superficial quadriceps muscles during the parallel squat and knee extension. *9*(3), 182-187.

Signorile, J. F., Weber, B., Roll, B., Caruso, J. F., & Lowensteyn, I. (1994). An Electromyographical Comparison of the Squat. *Journal of Strength and Conditioning Research, 8*(3), 178-183.

Smedley, J., Trevelyan, F., Inskip, H., Buckle, P., Cooper, C., & Coggon, D. (2003). Impact of ergonomic intervention on back pain among nurses. *Scandinavian journal of work, environment & health*, 117-123.

Solomonow, M., Baratta, R., Zhou, B., Shoji, H., Bose, W., Beck, C., & D'ambrosia, R. (1987). The synergistic action of the anterior cruciate ligament and thigh muscles in maintaining joint stability. *The American Journal of Sports Medicine, 15*(3), 207-213.

Sparto, P. J., Parnianpour, M., Reinsel, T. E., & Simon, S. J. J. o. s. d. (1998). The effect of lifting belt use on multijoint motion and load bearing during repetitive and asymmetric lifting. *11*(1), 57-64.

Stadler, K., Elspass, W., & Van De Venn, H. (2014). Robo–Mate: Exoskeleton to Enhance Industrial Production : Special Session: Exoskeletons for Emerging Applications. In *Mobile Service Robotics* (pp. 53-60): World Scientific.

Steffens, D., Maher, C. G., Pereira, L. S., Stevens, M. L., Oliveira, V. C., Chapple, M., Teixeira-Salmela, L. F., & Hancock, M. J. (2016). Prevention of low back pain: a systematic review and meta-analysis. *Jama Internal Medicine, 176*(2), 199-208.

Sterud, T., Johannessen, H. A., & Tynes, T. (2014). Work-related psychosocial and mechanical risk factors for neck/shoulder pain: a 3-year follow-up study of the general working population in Norway. *International Archives of Occupational and Environmental Health, 87*(5), 471-481. doi:http://dx.doi.org/10.1007/s00420-013-0886-5

Sterud, T., & Tynes, T. (2013). Work-related psychosocial and mechanical risk factors for low back pain: a 3-year follow-up study of the general working population in Norway. *Occupational and Environmental Medicine, 70*(5), 296. doi:http://dx.doi.org/10.1136/oemed-2012-101116

Sturman, D. J. (1992). *Whole-hand input.* Massachusetts Institute of Technology,

Suter, E., & Lindsay, D. J. S. (2001). Back muscle fatigability is associated with knee extensor inhibition in subjects with low back pain. *26*(16), E361-E366.

Taylor, W. R., Heller, M. O., Bergmann, G., & Duda, G. N. J. J. o. O. R. (2004). Tibio-femoral loading during human gait and stair climbing. *22*(3), 625-632.

Tefertiller, C., Hays, K., Jones, J., Jayaraman, A., Hartigan, C., Bushnik, T., & Forrest, G. F. (2017). Initial Outcomes from a Multicenter Study Utilizing the Indego Powered Exoskeleton in Spinal Cord Injury. *Topics in Spinal Cord Injury Rehabilitation, 24*(1), 78-85.

Toivanen, A. T., Heliövaara, M., Impivaara, O., Arokoski, J. P., Knekt, P., Lauren, H., & Kröger, H. J. R. (2009). Obesity, physically demanding work and traumatic knee injury are major risk factors for knee osteoarthritis—a population-based study with a follow-up of 22 years. *49*(2), 308-314.

Toyama, S., & Yamamoto, G. (2009, 10-15 Oct. 2009). *Development of Wearable-Agri-Robot mechanism for agricultural work.* Paper presented at the 2009 IEEE/RSJ International Conference on Intelligent Robots and Systems.

Toyama, S., & Yamamoto, G. (2009). *Development of Wearable-Agri-Robot～ mechanism for agricultural work～.* Paper presented at the 2009 IEEE/RSJ International Conference on Intelligent Robots and Systems.

Trafimow, J., Schipplein, O., Novak, G., & Andersson, G. (1993). The effects of quadriceps fatigue on the technique of lifting. *Spine, 18*(3), 364-367.

Tsuzura, M., Nakakuki, T., & Misaki, D. (2013). *A mechanism design of waist power assist suit for a caregiver by using torsion springs.* Paper presented at the Control, Automation and Systems (ICCAS), 2013 13th International Conference on.

Tubach, F., Leclerc, A., Landre, M.-F., & Pietri-Taleb, F. (2002). Risk factors for sick leave due to low back pain: a prospective study. *Journal of Occupational and Environmental Medicine, 44*(5), 451-458.

Tüchsen, F., Hannerz, H., Burr, H., Lund, T., Krause, N. J. S. j. o. w., environment, & health. (2003). Risk factors predicting hip pain in a 5-year prospective cohort study. 35-39.

Unluhisarcikli, O., Pietrusinski, M., Weinberg, B., Bonato, P., & Mavroidis, C. (2011). *Design and control of a robotic lower extremity exoskeleton for gait rehabilitation.* Paper presented at the Intelligent Robots and Systems (IROS), 2011 IEEE/RSJ International Conference on.

Vakos, J., Nitz, A., Threlkeld, A., Shapiro, R., & Horn, T. J. S. (1994). Electromyographic activity of selected trunk and hip muscles during a squat lift. Effect of varying the lumbar posture. *19*(6), 687-695.

van der Molen, H. F., Kuijer, P. P., Formanoy, M., Bron, L., Hoozemans, M. J., Visser, B., & Frings-Dresen, M. H. (2010). Evaluation of three ergonomic measures on productivity, physical work demands, and workload in gypsum bricklayers. *Am J Ind Med, 53*(6), 608-614. doi:10.1002/ajim.20793

Van Nieuwenhuyse, A., Somville, P.-R., Crombez, G., Burdorf, A., Verbeke, G., Johannik, K., Van den Bergh, O., Masschelein, R., Mairiaux, P., & Moens, G. (2006). The role of physical workload and pain related fear in the development of low back pain in young workers: evidence from the BelCoBack Study; results

after one year of follow up. *Occupational and Environmental Medicine, 63*(1), 45-52.

Vaughan, C. L., Davis, B. L., & Jeremy, C. (1999). Dynamics of human gait.

Veneman, J. F., Kruidhof, R., Hekman, E. E., Ekkelenkamp, R., Van Asseldonk, E. H., & Van Der Kooij, H. (2007). Design and evaluation of the LOPES exoskeleton robot for interactive gait rehabilitation. *Ieee Transactions on Neural Systems and Rehabilitation Engineering, 15*(3), 379-386.

Verbeek, J., Martimo, K., Karppinen, J., Kuijer, P., Takala, E., & Viikari-Juntura, E. (2012). Manual material handling advice and assistive devices for preventing and treating back pain in workers: a Cochrane Systematic Review. *Occup Environ Med, 69*(1), 79-80.

Vignon, E., Valat, J. P., Rossignol, M., Avouac, B., Rozenberg, S., Thoumie, P., Avouac, J., Nordin, M., & Hilliquin, P. (2006). Osteoarthritis of the knee and hip and activity: a systematic international review and synthesis (OASIS). *Joint Bone Spine, 73*(4), 442-455. doi:10.1016/j.jbspin.2006.03.001

Vincent, K. R., Conrad, B. P., Fregly, B. J., & Vincent, H. K. J. P. (2012). The pathophysiology of osteoarthritis: a mechanical perspective on the knee joint. *4*(5), S3-S9.

Vukobratovic, M., Ciric, V., & Hristic, D. (1972). *Contribution to the study of active exoskeletons.* Paper presented at the Proceedings of the 5th International Federation of Automatic Control Congress.

Wan, E. A., & Nelson, A. T. (2001). Dual extended Kalman filter methods. *Kalman filtering and neural networks*, 123-173.

Wan, E. A., & Van Der Merwe, R. (2000). *The unscented Kalman filter for nonlinear estimation.* Paper presented at the Adaptive Systems for Signal Processing, Communications, and Control Symposium 2000. AS-SPCC. The IEEE 2000.

Waters, T. R., Putz-Anderson, V., Garg, A., & Fine, L. J. J. E. (1993). Revised NIOSH equation for the design and evaluation of manual lifting tasks. *36*(7), 749-776.

Winter, D. A. (2009). *Biomechanics and motor control of human movement*: John Wiley & Sons.

Wu, J., Gao, J., Song, R., Li, R., Li, Y., & Jiang, L. (2016). The design and control of a 3DOF lower limb rehabilitation robot. *Mechatronics, 33*, 13-22. doi:10.1016/j.mechatronics.2015.11.010

Yamamoto, Ishii, M., Hyodo, K., Yoshimitsu, T., & Matsuo, T. (2003). Development of power assisting suit - (Miniaturization of supply system to realize wearable suit). *Jsme International Journal Series C-Mechanical Systems Machine Elements and Manufacturing, 46*(3), 923-930. doi:10.1299/jsmec.46.923

Yamamoto, K., Hyodo, K., Ishii, M., & Matsuo, T. (2002). Development of Power Assisting Suit for Assisting Nurse Labor. *JSME International Journal Series C Mechanical Systems, Machine Elements and Manufacturing, 45*(3), 703-711.

Yamamoto, K., Ishii, M., Hyodo, K., Yoshimitsu, T., & Matsuo, T. (2003). Development of power assisting suit (miniaturization of supply system to realize wearable suit). *JSME International Journal Series C Mechanical Systems, Machine Elements and Manufacturing, 46*(3), 923-930.

Yamamoto, K., Ishii, M., Noborisaka, H., & Hyodo, K. (2004). *Stand alone wearable power assisting suit - Sensing and control systems*. Paper presented at the Ro-Man 2004: 13th Ieee International Workshop on Robot and Human Interactive Communication, Proceedings, New York. <Go to ISI>://WOS:000227715300112

http://ieeexplore.ieee.org/ielx5/9456/30013/01374841.pdf?tp=&arnumber=1374841&isnumber=30013

Yang, Z., Gu, W., Zhang, J., & Gui, L. (2017). *Force Control Theory and Method of Human Load Carrying Exoskeleton Suit*: Springer.

Yang, Z., Zhu, Y., Yang, X., & Zhang, Y. (2009). *Impedance control of exoskeleton suit based on adaptive rbf neural network.* Paper presented at the Intelligent Human-Machine Systems and Cybernetics, 2009. IHMSC'09. International Conference on.

Yassi, A., Cooper, J., Tate, R., Gerlach, S., Muir, M., Trottier, J., & Massey, K. (2001). A randomized controlled trial to prevent patient lift and transfer injuries of health care workers. *Spine, 26*(16), 1739-1746.

Young, A. J., & Ferris, D. P. (2017). State of the Art and Future Directions for Lower Limb Robotic Exoskeletons. *IEEE Trans Neural Syst Rehabil Eng, 25*(2), 171-182. doi:10.1109/TNSRE.2016.2521160

Yu, W., & Rosen, J. (2010). *A novel linear PID controller for an upper limb exoskeleton.* Paper presented at the Decision and Control (CDC), 2010 49th IEEE Conference on.

Zadvinskis, I. M., & Salsbury, S. L. (2010). Effects of a multifaceted minimal-lift environment for nursing staff: pilot results. *West J Nurs Res, 32*(1), 47-63. doi:10.1177/0193945909342878

Zakaria, D., Robertson, J., MacDermid, J., Hartford, K., & Koval, J. J. A. J. o. I. M. (2002). Work-related cumulative trauma disorders of the upper extremity: Navigating the epidemiologic literature. *42*(3), 258-269.